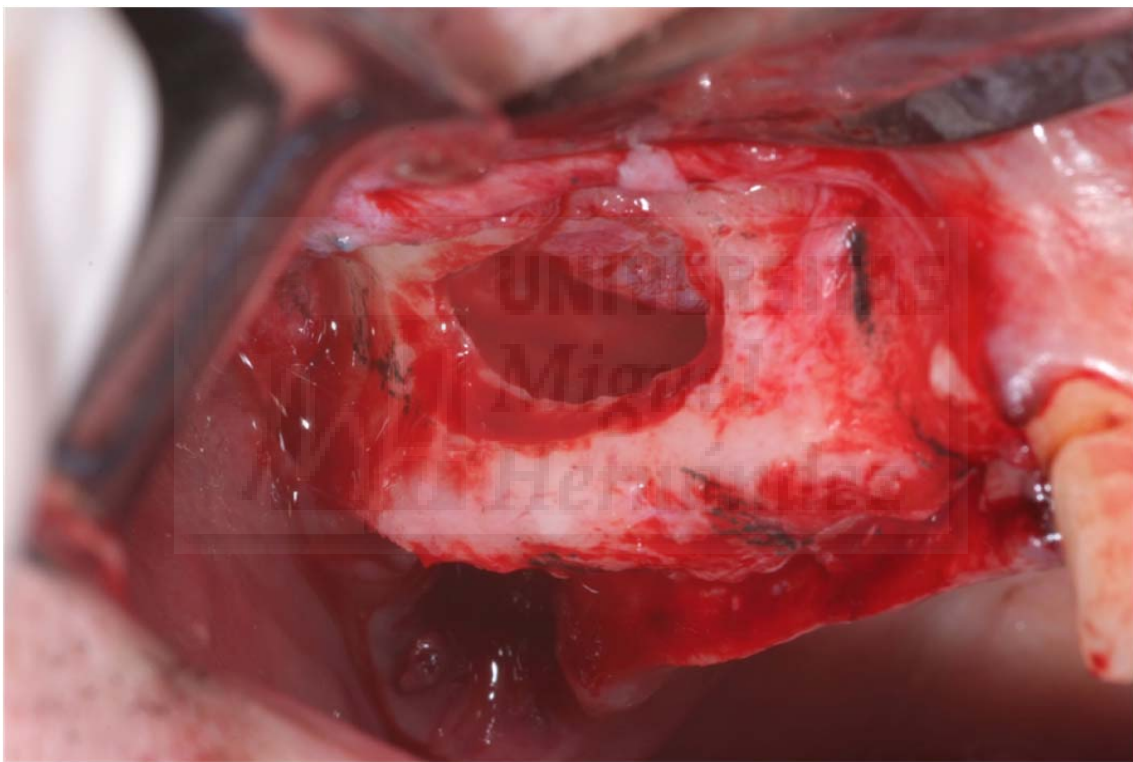


**ESTUDIO COMPARATIVO DE DOS HIDROXIAPATITOS
BIOLOGICOS UTILIZADOS EN PROCESOS DE
ELEVACION DE SENOS MAXILARES**



Memoria presentada por: María Piedad Ramírez Fernández

Directores:

Dra. Piedad N. De Aza Moya

Dr. Jose Luis Calvo Guirado

TESIS DOCTORAL

2017





PIEDAD NIEVES DE AZA MOYA, Catedrática de Universidad de Ciencia de Materiales e Ingeniería Metalúrgica de la Universidad Miguel Hernández de Elche, y

JOSE LUIS CALVO GUIRADO, Catedrático de Investigación en Odontología de la Universidad Católica San Antonio de Murcia.

HACEMOS CONSTAR,

Que el presente trabajo ha sido realizado bajo nuestra dirección y recoge fielmente la labor realizada por Doña María Piedad Ramírez Fernández, Licenciado en Odontología, para optar al grado de Doctor. Las investigaciones reflejadas en esta Tesis se han desarrollado en la Unidad de Biomateriales del Instituto de Bioingeniería, así como en el Área de Ciencia de Materiales e Ingeniería Metalúrgica del Departamento de Ciencia de Materiales, Óptica y Tecnología Electrónica de la Universidad Miguel Hernández de Elche. La parte clínica en humanos se ha realizado en la Universidad de Murcia.

Esta Tesis Doctoral se enmarca dentro del siguiente proyecto:- CICYT MAT2013-48426-C2-2-R “Biomateriales cerámicos multifuncionales con estructuras jerarquizadas para regeneración ósea y/o liberación controlada de agentes bioactivos”

Asi mismo, la alumna ha realizado una estancia de investigación de tres meses en la Universidad de Chieti-Pescara (Italia) en el Departamento de Patología y Medicina Oral de la Escuela Dental, para la obtención de la Mención Europea en el Título de Doctor.

Fdo. Piedad N de Aza Moya

Fdo. Jose Luis Calvo Guirado

Elche, de Mayo de 2017





Eugenio Vilanova Gisbert, Director del Instituto de Bioingeniería de la Universidad Miguel Hernández:

HACE CONSTAR:

Que da su conformidad a la lectura de la tesis doctoral presentada por

Doña **Maria Piedad Ramírez Fernández**, titulada **“ESTUDIO COMPARATIVO DE DOS HIDROXIAPATITOS BIOLÓGICOS UTILIZADOS EN PROCESOS DE ELEVACION DE SENOS MAXILARES**, la cual ha sido desarrollada dentro del Programa de doctorado en Bioingeniería en este Instituto, bajo la dirección de la Dra. Piedad N. de Aza Moya y el Dr. Jose Luis Calvo Guirado

Elche, de Mayo de 2017.

Eugenio Vilanova Gisbert
Catedrático de Toxicología
Director Instituto de Bioingeniería



PREFACIO

Este documento se ha elaborado siguiendo la normativa de la Universidad Miguel Hernández para la “Presentación de Tesis Doctorales con un conjunto de publicaciones”, y se ha dividido en las siguientes partes:

1. **Introducción**, en la que se presenta el tema de la Tesis, los antecedentes del trabajo realizado, y se defienden los objetivos perseguidos
2. **Resumen**, donde se presentan los resultados más relevantes obtenidos.
3. **Conclusiones**, finales derivadas del estudio.
4. **Anexo I**, que contiene los artículos publicados antes del depósito de la Tesis:

- *María Piedad Ramírez Fernández, Patricia Mazón, Sergio Alexander Gehrke, Jose Luis Calvo Guirado, Piedad N. De Aza. "Comparison of two xenograft materials used in sinus lift procedures: Characterization and in vivo behavior." MATERIALS 2017; 10, 623. DOI:10.3390/ma10060623. Factor de Impacto: 2.728. Puesto que ocupa / N° de revistas en el Área de conocimiento de Material Science Multidisciplinary. 63 /271*
- *María Piedad Ramírez Fernández, Sergio Alexander Gehrke, Carlos Pérez Albacete Martinez, Jose Luis Calvo Guirado, Piedad N. de Aza. "SEM-EDX study of the degradation process of two xenograft materials used in sinus lift procedures". MATERIALS 2017; 10, 542. DOI:10.3390/ma10050542. Factor de Impacto: 2.728 Puesto que ocupa / N° de revistas en el Área de conocimiento de Material Science Multidisciplinary. 63 /271*
- *María Piedad Ramírez Fernández, Sergio A. Gehrke, Patricia Mazón, Jose L. Calvo Guirado, Piedad N. de Aza. "Implant stability of biological hydroxyapatites used in dentistry". MATERIALS 2017;10, 644. DOI:10.3390/ma10060644. Factor de Impacto: 2.728. Puesto que ocupa / N° de revistas en el Área de conocimiento de Material Science Multidisciplinary. 63 /271*

Parte de esta tesis se realizó durante una estancia de investigación en la Universidad de Chieti-Pescara (Italia) en el Departamento de Patología y Medicina Oral de la Escuela Dental, lo cual posibilita la obtención de la Mención Internacional en el Título de Doctor al que se opta.

La presente memoria de tesis cumple los requisitos necesarios para la obtención de la Mención Internacional en el Título de Doctor establecidos en la normativa de enseñanzas oficiales de postgrado de la Universidad Miguel Hernández, y el Real Decreto RD1393/2007.



AGRADECIMIENTOS

A los profesores Piedad Nieves de Aza Moya y Jose Luis Calvo Guirado por darme la oportunidad de aprender a investigar, por su labor impecable como directores de esta tesis, por el tiempo que me habéis dedicado y por apoyarme continuamente durante la realización de este trabajo. Gracias de todo corazón

Al profesor y Doctor Honoris Causa Adriano Piatelli, por acogerme en su universidad haciéndome sentir como en casa y enseñarme tantas cosas, es el espejo donde cualquier investigador debe mirarse.

A la profesora Patricia Mazón por su colaboración en la caracterización de los materiales.

Al profesor Sergio Alexander Gehrke por su colaboración en el diseño, análisis e interpretación de los resultados.

A los profesores Jose Eduardo Maté y Carlos Pérez Albacete, amigos y compañeros inseparables, por su colaboración incondicional.

A todos mis compañeros de investigación que de alguna manera formaron parte de esta tesis, Rafa, Jorge, Patri, Nuria, María, etc ...

A mi sobrina Mercedes, por su colaboración en la traducción e interpretación de la tesis.

A mis familia por soportar todas las horas que le dedico a la investigación y respetarme siempre, por eso quiero dedicar esta tesis doctoral a mis hijas.

“Nunca consideres el estudio como una obligación, sino como la oportunidad para penetrar en el bello y maravilloso mundo del saber”

(Albert Eistein)

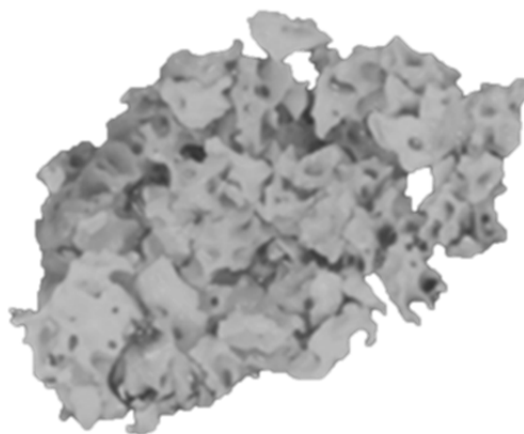


CONTENIDOS	Páginas/Pages
Chapter 1: Introduction	13
Chapter 2: Objectives / Objetivos	27
Chapter 3: Abstract / Resumen	33
Chapter 4: Materials and methods	47
Chapter 5: Results	61
Chapter 6: Discussion	81
Chapter 7: Conclusions / Conclusiones	105
Chapter 8: References	111
Chapter 9: APPENDIX: Published papers	135



UNIVERSITAS
Miguel
Hernández

INTRODUCTION





1. INTRODUCTION

The use of dental implants for the rehabilitation of missing teeth has increased the treatment options for patients. Loss of teeth in the posterior maxillary area can lead to adverse consequences. It is not uncommon, to observe a severe pneumatization of the maxillary sinus, reducing implants prosthetic alternatives for the replacement of missing teeth. The edentulous ridge in the posterior maxilla often presents limited bone volume due to both lack of alveolar bone after ridge remodeling and to maxillary sinus pneumatization. (Sharan et al. 2008)

In this anatomical situation, it can be very difficult to obtain an effective primary stability. Adequate alveolar ridges play a crucial role when it comes to rehabilitation with implants and some augmentation technique will be necessary for patients suffering from alveolar atrophy. (Aghaloo & Moy 2007)

The most predictable and commonly used mean of facilitating implant therapy in the atrophic posterior maxilla has been sinus augmentation. (Corbella et al. 2015) Although alternatives, such as the use of shorter implants, are beginning to be investigated (Felice et al. 2011; Esposito et al. 2015; Nedir et al. 2016), the science evidence that can be found is modest and insufficient to conclude that the success of sinus lift procedures in bone with residual height between 4 and 9 mm will be greater, or not, than when using short implants. (Khouly et al. 2015; Fan et al. 2017)

Augmentation of the maxillary sinus has been shown to be a method of increasing posterior maxillary bone height, making it possible to place dental implants when the residual alveolar ridge is deficient in bone volume. (Berreta et al. 2015)

The sinus augmentation procedure first entered our surgical armamentarium with presentations and publications by Tatum (Tatum 1986) and Boyne and James. (Boyne & James 1980) Multiple modifications to this technique have been published over the years. The original techniques were modified by Wood and Moore (Wood & Moore 1988) in 1988 and by Smiler who reviewed multiple technique variations in 1997. (Smiler 1997)

A wide range of surgical techniques are available for maxillary sinus augmentation the choice of the technique will depend chiefly on the characteristics of the edentulous site,

which will permit or prevent the placement of the implant at the moment of sinus augmentation surgery. (Carreño et al. 2016)

Various treatment modalities, including bone-grafting biomaterials, have been employed to achieve bone augmentation to allow proper implant installation. Grafting the floor of the maxillary sinus has developed into the most common surgical intervention when increasing alveolar bone height before placing endosseous dental implants in posterior maxilla. (Kolerman et al. 2012)

Further, a sinus augmentation procedure without bone grafts has been proposed but the precise mechanisms of this healing pattern are yet unknown. There is a limited amount of studies evaluating long-term results of the sinus membrane elevation technique for bone formation around implants in the maxillary sinus floor without the use of bone graft material. (Sohn et al. 2008; Sohn et al. 2011; Pinchasov & Juodzbaly 2014)

Several factors will influence the results of grafting the floor of the maxillary sinus: specific surgical techniques, simultaneous versus delayed procedure, use of barrier membranes over the lateral window, implant surface characteristics, length and width of the implants and selection of graft material. (Wallace et al. 2003)

Although the surgical techniques of sinus lift are well described, research into which material is the best suited to sinus augmentation in terms of their capacity for bone regeneration, has not reached conclusion, researchers have not come to an agreement about which material is the most suitable to sinus augmentation. (Pjetursson et al. 2008; Tuna et al. 2012; Traini et al. 2015)

Nowadays, there are several types of graft materials used in sinus lift procedures and each has both advantages and disadvantages. Several types of filling biomaterials have been evaluated for bone regeneration and the choice of the biomaterial mostly depends on its features and application site. (Danesh-Sani et al. 2016a)

Sinus elevation with a large variety of different graft materials has been used, there appears to be a correlation between the residual crestal bone height, the graft material, and the survival rate of the implant. (Zinser et al. 2013)

The grafting material is an important determinant of the success or failure of bone augmentation procedures. (Xu et al. 2003) An ideal bone graft material should be

biocompatible (Burg et al. 2000), increase bone volume in the grafted area to promote initial stability at implant sites (Le Geros 2002), and be resorbed with time and replaced by native bone. (Le Geros 1993) The success of scaffold-based bone regeneration approaches strongly depends on the performance of the biomaterial used. Within the efforts of regenerative medicine towards a restitution ad integrum scaffolds should be completely degraded within an adequate period of time. The degradation of bone grafts substitute materials involves both chemical dissolution (physico-chemical degradation) and resorption (cellular degradation by osteoclasts). (Conz et al. 2011)

Based on their physico-chemical properties, the bone-graft material may be either resorbable or non-resorbable, with respect to the extent of dissolution of Ca-P materials. The factors affecting the dissolution properties are similar to those affecting biodegradation or bioresorption. (Fulmer et al. 2002)

The materials should also be fully degradable and this degradation should ideally match with the osteogenic rate. However, no clear insight exists as to the exact relationship between the material properties of these calcium phosphate ceramics and their degradation behavior. (Mate-Sanchez de Val et al. 2016)

The gold standard of bone grafting is harvesting autologous cortical and cancellous bone from the iliac crest. There are both histologic and clinical studies demonstrating that graft maturation times can be reduced when using autogenous bone or composite grafts with autogenous bone as a component. All other forms of bone grafting have disadvantages compared to autograft and as such their use is sub-optimal. (Nkenke & Stelzle 2009) Although the use of autogenous bone may have this advantage, it also has the disadvantage of increased morbidity (Nkenke et al. 2004; Barone et al. 2011) and significant graft resorption (Arasawa et al. 2012), resulting in partial re-pneumatization of the sinus with concomitant loss of graft height (Sbordone et al. 2013). Hard tissue repair also requires high-level mechanical stability, which limits the choice of bone substitute materials. (Jensen et al. 2012)

Search for an ideal bone graft substitute has long been in existence because of the problems associated with the gold-standard autologous bone graft. Therefore, the goal of an ideal scaffold that provides good mechanical support temporarily while maintaining bioactivity, and that can biodegrade later at a tailorable rate. (Chen et al.

2008) There are several grafting materials that have been used for this treatment, but only a few materials are presently considered useful. (Traini et al. 2015)

Synthetic and natural calcium phosphate-based materials may be a suitable alternative for the use of autogenous graft. (Frenken et al. 2010) However, technological evolution along with better understanding of bone-healing biology has led to the development of several bone graft. (Danesh-Sani et al. 2016b) Biomaterials that mimic the structure and composition of bone tissues at nanoscale are important for the development of bone tissue engineering applications. Synthetic hydroxyapatites are the most frequently used (Frenken et al. 2010), but they do not completely match the chemical composition of human bone. (Simunek et al. 2008) After the increased application of synthetic hydroxyapatites during the last decade there has now been a move back to natural hydroxyapatites. (Esposito et al. 2010)

Natural hydroxyapatite ceramics have attracted attention since it may be possible to use them as an alternative to autogenous free bone grafting, due to its chemical composition, biological, and crystallographic similarity with the mineral portion of hard tissues. (Jensen et al. 2012) Hydroxyapatite is the major inorganic component of natural bone and has been applied widely in medical field as bone repair material because of its excellent bioactive and biocompatibility properties. HAs is known for its biocompatible, bioactive, ability of forming a direct chemical bond with surrounding tissues, osteoconductive, nontoxic, no inflammatory, non- immunogenic properties. (Swetha et al. 2010)

Fortunately bones from other species possess a tissue structure similar to that of human bones. In addition, these bones also exhibit osteoinduction and osteoconduction activities, potentially satisfying the requirements of ideal bone graft substitutes. (Tadic & Epple 2004) The information from all reviews does, however, substantiate the finding that implant survival with bone replacement grafts, specially the most rigorously evaluated group (xenografts), are equal to or better that achieved with autogenous bone. (Jensen et al. 2012) These data, coupled with the reduction in patient morbidity realized by eliminating the need for a secondary surgical donor site, appears to position bone replacement grafts as the graft material of choice today. The histologic results with xenografts present a pattern that has been called “bone bridging.” Residual particles of

xenograft are surrounded in part by new vital bone, and through that mechanism they are joined to approximating particles. (Froum et al. 1998)

Bovine bone has practically unlimited availability and great physicochemical and structural similarity to human bone. (Carvalho et al. 2007) For many years now, bovine cortico-spongy bone has been the first choice for buccal and maxillofacial surgery, a number of reports in the literature in which successful regenerative procedures were observed in patients treated with maxillary sinus augmentation using bovine bone. (Orsini et al. 2005; Cordaro et al. 2008; Traini et al. 2007, 2008; Nevins et al. 2011).

However, some studies have pointed out that Bovine bone is not completely reabsorbable, in a sense that it will completely disappear within a year. Moreover, the rate and mechanism of its reabsorption are still unclear. (Jensen et al. 2012) Deproteinized porcine bone mineral was recently developed and commercially available in maxillary sinus grafting, in which demineralized bovine bone mineral was widely used. (Carvalho et al. 2007) Porcine bone has been introduced in the clinical and research fields of dentistry under the banner of prevention of the bovine-specific disease transmission. (Wenz et al. 2001)

Deproteinized porcine bone mineral is one substitute for deproteinized bovine bone mineral, and several researchers already introduced these for clinical dental procedures based on the structural/ physiological similarities of bone tissue between human and swine. (Lee et al. 2016) These xenografts have provoked a great deal of research due to their potential as an adequate bone substitute for maxillary sinus augmentation. (Orsini et al. 2006; Scarano et al. 2011; Barone et al. 2012)

Xenografts usually have bovine or porcine origin and there are constituted by hydroxyapatite similarly to the human bone $[Ca_{10}(PO_4)_6(OH)_2]$. Deproteinized xenografts, primarily constituted of natural apatite's sintered or not, have good physical and physico-chemical properties. Different physicochemical conditions which selectively modulate the tissue response of the host organism. (Conz et al. 2005)

Eliminating the antigens that potentially cause an immune response is a prerequisite for xenogenic bone grafting. It has been shown that deproteinized bones not only lose their immune reactivity but also retain their osteoinduction and osteoconduction activities. (Castro-Cesena et al. 2013)

Deproteinization is an indispensable process for the elimination of antigenicity in xenograft bones. Valid strategies to eliminate the antigenicity of xenograft bones are of vital importance in the development of xenogenic bone graft substitutes. (Barakat et al. 2008) Methods for bone deproteinization have to allow the heterologous deproteinized bone has good biological safety and meets all the demands of scaffold material for tissue engineering. (Lee et al. 2016) Many investigations on HA have centered on a wide range of powder processing techniques, composition and experimental conditions with the aim of determining the most viable synthesis method. (Azran et al. 2004; Kalkura et al. 2004; Herliansyah et al. 2009) Some authors have reported the same observations in reaction to the microscopic structure, in commercial products subjected to thermal processes of deproteinization. The sintering temperature is seen considered as important factors that could alter the HA's characteristics. (Poinern et al. 2011; Kutty et al. 2000; Muralithran & Ramesh 2000; Ashok, et al. 2003) However, effect of sintering temperature to physico-chemical properties of Natural HA (HA from natural source) especially HA from bovine bone has not been fully understood and researches in this area are still wide open. (Kalkura et al. 2004) The most important parameters that can affect the properties of HA are the temperature and duration of heat treatment. (Herliansyah et al. 2009)

On the sintering characteristic of hydroxyapatite (HA), the resulting microstructure and properties are influenced not only by the characteristic and impurities of materials but also are found to be dependent on the thermal history during the fabrication process. (Jensen et al. 2015)

Xenogenous materials have been extensively researched and present a history of results. They have been successfully used to maintain the dimensions of the post-extraction alveolar ridge, in the treatment of alveolar process defects and maxillary sinus lifting. (Mardas et al. 2010)

In clinical practice, the main purpose of the bone augmentation procedures is the formation of bone, where the implants will be positioned to best support the prosthetic rehabilitation. The bone tissue around dental implants must be mechanically competent after the augmentation procedures. Success rates, as determined by the secondary outcome measure of implant survival. (Traini et al. 2015)

Various bone-grafting biomaterials have been employed to achieve bone augmentation to allow proper implant installation. (Browaeys et al. 2007) But it still remains unclear as to which bone grafting material is most suitable for enhancing bone regeneration in the augmented sinus. (Baqain et al. 2012; Zinser et al. 2013) The ultra-structural interface of the graft bone tissue interface as well as the ideal time point of placing the implant have not yet been described. (Danesh-Sani et al. 2016)

Graft consolidation gradient reflects the features of each bone substitute at sites of sinus augmentation. (Busenlechner et al. 2009) According to some studies, the physical and chemical properties of each bone material graft may influence the osteointegration process and this influence may result in shorter healing times from implant placement to restoration. Therefore, not only a deep understanding of the different aspects of biomaterial properties, but also of their relation and influence towards bone healing has proved to be of utmost importance. (Xu et al. 2003)

An undisturbed healing period of at least 3 to 6 months in surgical sites is the generally accepted protocol after implant placement. This may ensure uneventful healing and improve osseointegration between implant and bone. The reason of this approach is based on the fact that functional force around bone-implant interface causes implant micromotion during wound healing, and for its part, implant micromotion may induce fibrous tissue rather than bone contact, resulting in clinical failure. All these concerns related to waiting periods have long been a challenge for both patients and clinicians. Changing trends and demands have made necessary the introduction of early loading techniques as a consequence of the search for faster restoration of dental function using implants. (Gupta et al. 2013)

Physicochemical properties and mechanic strength of deproteinized tissue-engineered bone meet the demands of ideal scaffold materials. In the bioceramics field there remains a need to correlate the chemical and physical composition of hydroxyapatite with cellular interactions. (Liu et al. 2003)

It has been assumed that the difference between filling materials used in sinus elevation procedures may modulate the quality and quantity of newly formed bone. The selection of biomaterials constitutes a key point for the success of tissue regeneration practice.

The mechanisms behind tissue response to hidroxiapatites have not been comprehensively established. (Le Geros 2002)

All aspects of a substitute material must be studied. Some studies have demonstrated that osteointegration and degradation processes are influenced by physical and chemical properties of the material (Blokhuis et al. 2000), including granule size (Carvalho et al. 2007), morphology (Danoux et al. 2016), crystallinity (Yang et al. 2005), porosity (Rosa et al. 2002; Karageorgiou & Kaplan 2005; von Doernberg et al. 2006), surface roughness (Ducheyne & Qiu 1999) and ratio calcium/phosphate in the composition (Ghanaati et al. 2012).

After implantation, biodegradation is critical as this allows for the space to be formed into which the bone and vascular tissues can grow. Biodegradation can be envisioned as an in vivo process by which a material breaks down into simpler components, reducing the complexity of chemical compounds by the action of cells, by simple physical breakdown and/or chemical erosion. (LeGeros 1993)

A completely resorbable ceramic has been the goal of several studies; however, a high rate of resorption or solubilization can interfere with bone formation as the biomaterial may degrade faster than the rate of bone formation. These phenomena lead to a change in the bioceramic's physical structure, which will interfere with cell attachment. (Bertazzo et al. 2010)

Moreover, the release of high concentrations of calcium to the microenvironment results in a change of the pH, promotes a mild inflammatory response and favors fibrous tissue formation (Chou et al. 2005) Furthermore, higher calcium ion levels have been shown to effect osteoclastic activity, varying from its inhibition to its stimulation or no effects (Berger et al. 2001)

Instead the presence of moderate extracellular Ca²⁺ resulting from resorption activity might be involved in the stimulation of osteoblasts. Moderately high extracellular Ca²⁺ is a chemotactic and proliferating signal for osteoblasts and stimulates pre-osteoblast differentiation. (Yang et al. 2005) Some materials, such as autogenous bone, cannot withstand sinus pressure during the first several weeks and lose density and height over time. (Sbordone et al. 2013)

An ideal bone graft material should be biocompatible, increase bone volume in the grafted area to promote initial stability at implant sites, and be resorbed with time and

replaced by native bone. Resorbable calcium phosphate materials are usually unsintered Ca-P materials. (Raynaud et al. 2002) However, the process of bone resorption and the distribution of osteoclasts after deproteinized bone implantation have not been examined in detail, which are relevant to enhance our understanding of the complex role of osteoclasts in bone tissue engineering. (Xu et al. 2004) Further long-term studies are needed to determine whether resorption of deproteinized bone particles proceeds slowly enough to provide sufficient time for bone maturation.

One of the future challenges in bone tissue engineering is to design and to manufacture biodegradable scaffolds with a homogeneous growth rate over their entire volume, using pore size gradients or specific distributions. This requires manufacturing processes with higher resolution and biofabrication capabilities. (Hutmacher et al. 2007)

The level of bone density at the implant site could be of utmost importance as it is related with failure rates and primary stability. When it comes to evaluate primary implant stability in relation with bone density, the implant stability quotient (ISQ), the resonance frequency analysis, can be used. (Iezzi et al. 2015)

Implant stability can be defined as the combination of both mechanical and biological stability. While mechanical stability appears as a consequence of compression of bone tissue during implantation; biological stability is obtained as a result of the formation of new bone cells on the implant surface during the osseointegration process. Hence, implant stability is associated with the quality and quantity of local bone (Sennerby et al. 2008). Nowadays, the most frequently used technique for the detection of implant stability during healing time and in subsequent follow-ups is the non-invasive diagnostic tool known as Resonance frequency analysis (RFA). (Swami et al. 2016; Cehreli et al. 2009) Continuous monitoring in at various time points is important to determine the status of implant stability and to project a long term prognosis for successful therapy. (Atsumi et al. 2007) Evaluate bone density has long been one of the most important parameters to quantify bone quality as it is thought to be a major determinant of primary stability. In other words, primary implant stability is dependent not only on the thickness of the bone into which the implant is placed but also on the bone density. (Lundgren et al. 2017)

There is a strong correlation between primary stability of a dental implant and the absence of mobility in the osseous site after implant insertion, and the quality of the

receptor bone site. Likewise, primary stability is also strictly correlated to the mechanical relationship between the implant surface and the recipient bone. This relationship can determine the outcome of the implant placement by avoiding micromovements at the interface. (Marquezan et al. 2012)

Successful osseointegration is a prerequisite for functional dental implants; an absence of osseointegration was reported for implants with no primary stability. (Lioubavina-Hack et al. 2006)

At present, there is no agreement regarding the advantages of the use of grafting material in maxillary sinus elevation techniques with dental implant insertion as the question whether these techniques and materials may determine implant survival in comparison with pristine bone is still unsolved. (Nasr et al. 2016; Rammelsberg et al. 2012) To find the answer to this question, it was retrospectively examined long term stability up to 20.2 years after the placement of implants both in augmented and non-augmented sites. The results of this retrospective study determined that implants inserted in augmented site were found to have similar implant survival compared to those inserted in non-augmented sites. (Knöfler et al. 2016) Supported by evidence, it can be stated that implants inserted in augmented bone have similar implant survival in comparison with those placed in native bone. (Jensen et al. 2009)

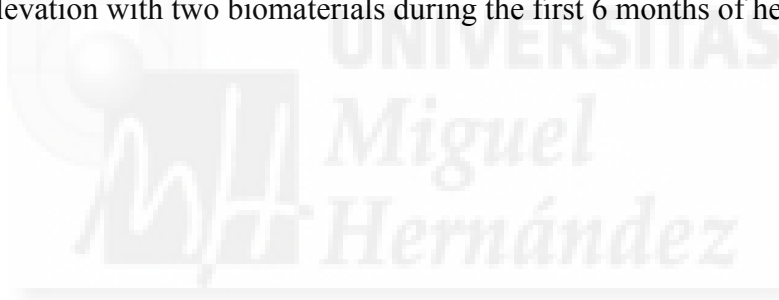
Optimal outcomes in terms of implant survival have been demonstrated for implants placed in the maxillary sinus filled with deproteinized bovine bone mineral, and this material can be considered a safe and predictable graft material for sinus floor augmentation. (Ferreira et al. 2009) However, little is known about the physic-chemical properties of the used grafts and the impact in the bone density and the early implant stability following the use of them.

Part of biological response produced by a biomaterial, is conditioned by their physical and chemical properties. The work reported in this doctoral thesis indicates the great importance of full characterization of the materials being used. The large number of alternatives available in contrast with the few comparative studies leaves the choice of the grafting material to the surgeon's preferences, no always scientifically based. (Habibovic et al. 2008)

However, the use of these materials is sometimes avoided due to lack of information or to contradiction between manufacturers' specifications (clinical indication) and clinical results. The results showed that the hydroxyapatite examined had variable physicochemical properties, which is in disagreement with the manufacturers' specifications. This discrepancy may affect the materials' performance. (Rodrigues et al. 2003)

Many reviews discussed many biomaterials and their manufacturing processes for biodegradable scaffold fabrication, but limited work has been done in order to obtain biomaterials with patient-specific degradation rate. (Conz et al. 2005; Barakat et al. 2008)

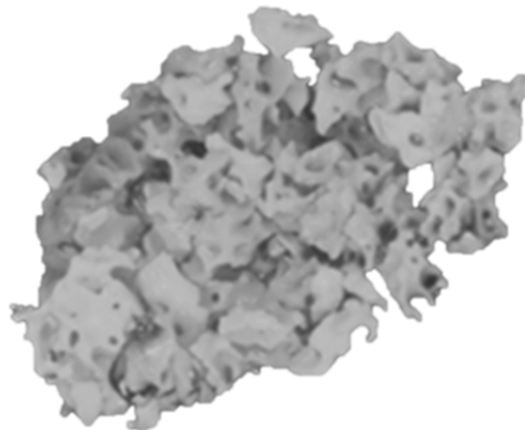
Based on these data, the present study developed a protocol for characterization de xenograft. The objective of this study was to characterize the physicochemical properties of two xenografts deproteinized at different temperature and how the physicochemical properties influence the material performance in vivo and the implant stability after sinus floor elevation with two biomaterials during the first 6 months of healing.





OBJECTIVES

OBJETIVOS





2. OBJETIVES

The main objective of the present study is to investigate the influence of the physico-chemical characteristics of two biological hydroxiapatites, one of porcine origin and the other of bovine origin, and their in vivo behaviour in maxillar sinus lift procedures previous to dental implants placement.

In order to accomplish this objective, a series of specific objectives were contemplated:

- I. Carry out the physical, chemical and mineralogical characterization of two xenografts manufactured on an industrial scale in accordance with a protocol of deproteinization at different temperature.
- II. Study the physico-chemical changes undergone in the materials and determine the degree of resorption of the xenografts after maxillar sinus lift procedure, likewise the biological events that are present in the bone and host-xenograft interface, as well as within them.
- III. Evaluate the quantity and quality of bone regeneration (bone new formation), obtained by using xenografts as filling materials in maxillar sinus lift procedures, and the influence in dental implant stability over the different stages established in the present study.



2. OBJETIVOS

El presente estudio tiene como objetivo principal investigar la influencia de las características físicoquímicas de dos hidroxiapatitos biológicos, uno de origen porcino y otro de origen bovino, en el comportamiento in vivo en procedimientos de elevación de seno maxilar previo a la colocación de implantes dentales.

Para la consecución de dicho objetivo principal se plantea una serie de objetivos concretos:

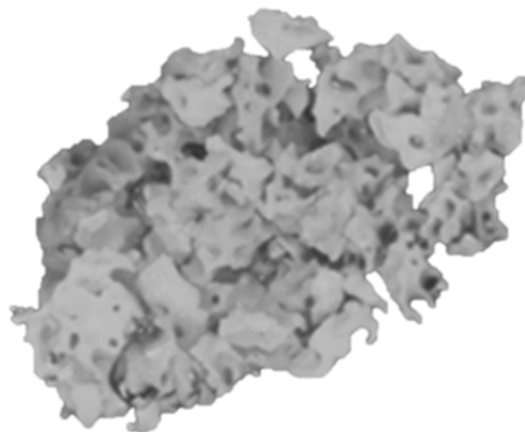
- I. Realizar la caracterización física, química y mineralógica de dos xenoinjertos manufacturados a escala industrial desproteinizados siguiendo un protocolo a diferente temperatura.
- II. Estudiar los cambios físico y químicos experimentados en los materiales y determinar el grado de reabsorción de los xenoinjertos después de la elevación del seno maxilar, así como los acontecimientos biológicos que se presentan tanto en la interfase hueso huésped-xenoinjerto, como en el interior de los mismos.
- III. Evaluar la cantidad y calidad de la regeneración ósea (neoformación ósea), conseguida a través del uso de los xenoinjertos como material de relleno en la elevación de seno maxilar, y su influencia en la estabilidad de los implantes dentales, en los diferentes periodos de estudio establecidos.



UNIVERSITAS
Miguel
Hernández

ABSTRACT

RESUMEN





3. ABSTRACT

Several factors will influence the results of grafting the floor of the maxillary sinus, especially surgical techniques and selection of graft material. Although the surgical techniques of sinus lift are well described, researchers have not come to an agreement about which material is the most suitable to sinus augmentation.

Hydroxyapatite is the major inorganic component of natural bone and has been applied widely in medical field as bone repair material because of its excellent bioactive and biocompatibility properties. Biomaterials that mimic the structure and composition of bone tissues are important for the development of bone tissue engineering applications. Synthetic hydroxyapatites are the most frequently used but they do not completely match the chemical composition of human bone. Fortunately bones from other species possess a tissue structure similar to that of human bones. During the last decade there has now been a move back to natural hydroxyapatites and has been used as reference material in this PhD thesis.

Deproteinization is an indispensable process for the elimination of antigenicity in xenograft bones. The sintering temperature is seen as important factors that could alter the HA's characteristics. The most important parameters that can affect the properties of HA are the temperature of heat treatment. All aspects of a substitute material must be studied. Part of biological response produced by a biomaterial, is conditioned by their physical and chemical properties. The work reported in this PhD thesis indicates the great importance of full characterization of the materials being used. The large number of alternatives available in contrast with the few comparative studies leaves the choice of the grafting material to the surgeon's preferences, no always scientifically based.

Based on these data, the present PhD thesis developed a protocol for characterization the xenograft. The objective of this study was to characterize the physicochemical properties of two xenografts deproteinized at different temperature and how the physicochemical properties influence the material performance in vivo.

Two commercial bone grafts used in dentistry in the form of granules a non-sintered PBM, OsteoBiol® mp3 a natural hydroxyapatite of porcine origin, deproteinized at low temperature (130°C) and a sintered BBM, Endobon® a natural hydroxyapatite of bovine

origin, deproteinized at high temperature (1200°C) were characterized before being used in sinus lift procedures.

Both materials were characterized in terms of crystallinity, morphology, particle size distribution, porosity and pore size, specific surface area, density, and ratio calcium/phosphate in the composition. The hidroxiapatites were characterized thorough powder X-ray diffraction XDR analyses, Fourier transforms infrared spectroscopy FTIR, gas pycnometry, mercury intrusion and scanning electron microscopy SEM. Quantitative analyses were made by an Electronic Dispersive X-ray Spectroscopy (EDX) system.

Ten patients were selected who required bilateral sinus augmentation. The study was performed in two surgical phases. In the first phase, the basic surgical procedure was represented in all patients by maxillary sinus floor elevation via a lateral approach, one material was placed in the right sinus and the other in the left sinus, as determined by randomized choice in a split mouth design. The patients were followed up clinical and radiologically. All patients underwent CBCT after 6 month of surgery as a routine diagnostic approach. The images obtained were processed by Image J software and color thermal graduation was used to observe the changes in radiopacity in the grafted area.

In the second surgical phase the functional implants were placed on each side. Each side received three implants 3i T3® Implante Certain® Tapered placed 6 months after augmentation. A trephine bone core was harvested from the previously elevated maxillary sinus at the moment of implant insertion, 60 bone samples were retrieved and sent for histomorphometric analysis.

The specimens were processed for observation under a scanning electron microscope with backscattered electron imaging (SEM-BSE). Histomorphometric analysis was performed on the bone core samples to determine the vital bone, connective tissue, and residual graft material content. In addition the chemistry of the interphases and the chemical degradation process of the xenograft biomaterials were analyzed using X-ray elemental maps in scanning mode. Additional information was obtained from line scans and elemental maps. Analysis was carried out at a selection of different points, taking different points of interest from the middle and from the periphery of the samples to detect changes in Ca/P ratios. Data were then collected from deliberately targeted sites

of interest within the residual biomaterial (RB), close to and distal from new bone (NB) and at the bone–implant interface if present. A total of more than 900-point analyses were carried out on the sixty biopsies.

After dental implant insertion, the resonance frequency evaluation was performed using the Ostell™ Mentor for measure the primary stability of the implant. The RF value is represented by a quantitative parameter called ISQ. The ISQ values were measured during the surgical procedure (T1- baseline), at 3 months (T2) after surgery and at 6 months (T3) after surgery. The values were recorded for the bucco-lingual (B-L) direction and mesio-distal (M-D) direction.

The results of Characterization of Deproteinized Hydroxyapatite Materials show that X-ray diffraction analysis revealed typical structure of hydroxylapatite for both materials. Both xenograft are porous and exhibit intraparticle pores. Strong differences were observed in term of porosity, cristallinity, density, surface area, and ratio calcium/phosphate composition. PBM has the greatest porosity (59.90%); however, about forty per cent (38.11%) of this porosity corresponds to submicron pore entrances. BBM porosity was (49,13%) but this exhibit a much smaller proportion of submicron pores, only (3.66%). In term of cristallinity the PBM granules exhibit low cristallinity, crystal size is 325 nm, while BBM structure consisted of a highly cristallinity and the crystal size is 732 nm. Higher density was measured for BBM (2.98 g/cm³) respect (2.85 g/cm³) for the PBM. More surface área were observed for the PBM (97.84) (m²/g) compare to the BBM (2.77 m²/g). Statistically significant difference was found between PBM (2.22± 0.08) and BBM (2.31±0.09) ratio calcium/phosphate composition.

Although radiopacity of the augmented volume increased with time for both xenograft materials, the control sites receiving showed a higher density of radiopacity compared with the PBM.

Scanning electron microscopy revealed that newly formed bone had become closely attached to both HAs. Histomorphometric measurements on the bone biopsies showed statistically significant differences. For the PBM, the newly formed bone represented (25.92 ± 1.61%), residual graft material (24.64 ± 0.86%) and connective tissue (49.42 ± 1.62%), while for the BBM newly formed bone (26.83 ± 1.42%), residual graft material (30.80 ± 0.88%) and non-mineralized connective tissue (42.79 ± 2.88%).

In all cases, EDX analysis found a significant a decrease in the percentage of Ca/P ratio was found in the residual biomaterial, with respect to the initial composition while a

gradual increase in the percentages of Ca/P ratio was found at the interface, suggesting an increase in the osteoinductive capacity of the materials and replacement by new bone at its periphery. The PBM showed numerous regions of resorptions, and presented an average Ca/P rate of 1.08 ± 0.32 with respect to the average Ca/P rate 1.85 ± 0.34 of BBM. Statistically significant differences were found too in the interface and in the new bone between the groups. Ca/P ratio in the interface was 1.93 ± 0.18 for the PBM with respect to the 2.14 ± 0.08 of the BBM, and the ratio in the new bone was 1.84 ± 0.14 for the PBM with respect to the 2.00 ± 0.08 of the BBM.

Line Scan show an increase in the porosity inside the material and a faster degradation of PBM in relation with BBM can be observed, fact that it is related with the crystallinity of the material. BSE image showing the resorbed PBM graft in relation to surrounding bone, granular residual material consisting of areas of very few and smaller particles. These indicated the almost complete resorption of the PBM similarly in the middle, and at the periphery of the samples.

According to the elemental X-ray maps and SEM images of the interface between the BBM and PBM implants and the natural bone, the reaction zone was composed of Ca and P phase as well as a short distance away from the reaction zone. There were no obvious morphological differences between the newly formed bone and the old bone into which the implants were inserted.

ISQ (Baseline) averaged values were 63.8 ± 2.97 for a sintered BBM, and 62.6 ± 2.11 for a non-sintered PBM. ISQ (Stage 2) average values were 73.5 ± 4.21 for BBM and 67 ± 4.99 for PBM. ISQ (Stage 3) average values were 74.65 ± 2.93 for BBM and, 72.9 ± 2.63 for PBM; differences were statistically significant in all of stages studied.

As a general conclusion of the work done in this Doctoral Thesis we can say that the data from this study show the effect of sintering temperature on the physico-chemical properties of Natural HAs and the influence in the biological behavior. The differences found in the physic-chemical characteristics of both xenografts justify this distinct in vivo performance. The HAs assessed in the study were shown to be biocompatible and osteoconductive when used for maxillary sinus elevation. A significant difference in resorption time and in the stability of the implants was found in both groups. The PBM non-sintered hydroxiapatite with high porosity, low cristallinity, low density, high surface area and low calcium/phosphate ratio presents high resorption rate but might not

withstand the sinus pressure leading to a repneumatization of the sinus. Whereas the BBM sintered hydroxiapaita with low porosity, high cristallinity, high density, low surface area and high calcium/phosphate ratio presents a slow resorption rate that inhibit the resorption of the newly formed bone, tents the sinus lining, maintains the space, and stablies augmented the maxillary sinus floor increased the early implant stability.

Detailed information about graft material characteristics is crucial to evaluate their clinical outcomes. The influence of physic-chemical properties of the bone graft materials on osseointegration has translated to shorter healing times from implant placement to restoration. A sound understanding of various aspects of biomaterial properties and their relation and influence towards bone healing is of utmost importance.





3. RESUMEN

Son muchos los factores que influyen en el resultado de la elevación de seno maxilar, especialmente la técnica quirúrgica y la selección del material de injerto. Aunque las técnicas de elevación de seno ya han sido ampliamente descritas, los investigadores no han llegado a un acuerdo sobre cuál es el material más apropiado en el uso de esta técnica.

La hidroxiapatita es el principal componente inorgánico del hueso natural y se ha aplicado ampliamente en el campo médico como material sustituto óseo gracias a sus excelentes propiedades de bioactividad y biocompatibilidad. Los biomateriales que imitan la estructura y la composición de los tejidos óseos son cruciales en el desarrollo de la regeneración ósea. Las hidroxiapatitas sintéticas son las más utilizadas; sin embargo, no coinciden completamente con la composición química del hueso humano. Afortunadamente, la estructura del tejido del hueso de otras especies es similar a la del hueso humano, y es por eso por lo que durante la última década se ha producido un retorno hacia la hidroxiapatita natural, el material de referencia en esta Tesis Doctoral.

La desproteínización es un proceso indispensable para la eliminación de antigenicidad en los senoinjertos de hueso. La temperatura de sintetizado se considera un importante factor que puede alterar las características de la hidroxiapatita. Los parámetros más importantes que pueden afectar las propiedades de la hidroxiapatita son la temperatura y el tiempo de precesado. Por ello, deben estudiarse todos los aspectos relacionados con el material sustitutivo. Parte de la respuesta biológica producida por el biomaterial está condicionada por sus propiedades físicas y químicas. El trabajo expuesto en esta Tesis Doctoral muestra la gran importancia que tiene la completa caracterización de los materiales utilizados. El gran número de alternativas disponibles en contraste con los pocos estudios comparativos hace que la elección del material del injerto se lleve a cabo siguiendo las preferencias del cirujano, y estas no siempre se apoyan en una base científica.

Teniendo en cuenta lo anterior, la presente Tesis Doctoral desarrolla un protocolo de caracterización del xenoinjerto y su objetivo es determinar las propiedades fisicoquímicas de dos xenoinjertos desproteínizados a diferente temperatura y cómo estas influyen en el comportamiento in vivo del material.

Se utilizaron dos injertos óseos comerciales utilizados en odontología en forma de gránulos, un material PBM no sinterizado, OsteoBiol® mp3, una hidroxiapatita natural de origen porcino, desproteinizada a baja temperatura (130 °C); y un material BBM sintetizado, Endobon®, una hidroxiapatita natural de origen bovino desproteinizada a alta temperatura (1200 °C) ambas caracterizadas antes de su uso en la técnica de levantamiento de seno.

Ambos materiales fueron caracterizados en términos de cristalinidad, morfología, porosidad y tamaño de los poros, área de superficie específica, densidad ratio calcio/fosfato en la composición. Las hidroxiapatitas fueron caracterizadas a través de difracción de rayos X, espectrofotómetro de transformada de Fourier (FTIR), picnometría de gas He, porosimetría de mercurio y microscopia electrónica de barrido. Los análisis cuantitativos se hicieron con un sistema de fluorescencia de rayos X por energía dispersiva (EDX).

Fueron seleccionados diez pacientes que requerían elevación de seno. El estudio se desarrolló en dos fases quirúrgicas. En la primera de ellas, se llevó a cabo el procedimiento quirúrgico básico en todos los pacientes, un material se colocó en el seno derecho y el otro material en el seno izquierdo, según se determinó de forma aleatoria en un *split mouth design*. Se hizo un seguimiento clínico y radiológico de los pacientes, que fueron sometidos a CBCT (Cone Beam Computer Tomography) 6 meses después de la cirugía como un método de diagnóstico rutinario. Las imágenes obtenidas se procesaron con el software Image J y la gradación del color térmico se utilizó con la finalidad de observar cambios en la radiopacidad del área injertada.

Durante la segunda fase quirúrgica se colocaron los implantes funcionales, tres implantes 3i T3® Implante Certain® Tapered en cada lado, colocados 6 meses después de la elevación de seno. En el momento de la inserción de los implantes, se extrajo una muestra de hueso con una trefina del seno maxilar previamente aumentado, en total, se obtuvieron y enviaron 60 muestras para su análisis histomorfométrico.

Las muestras se procesaron para su observación en un microscopio electrónico de barrido con imágenes de electrones retrodispersados (SEM-BSE). El análisis histomorfométrico se llevó a cabo en las muestras de hueso para determinar el contenido de hueso vital, de tejido conectivo y material residual del injerto. Además, el

proceso de degradación química de los biomateriales del senoinjerto se analizó utilizando mapas elementales de rayos X en modo de escaneo. Los mapas elementales y los *Line Scans* permitieron obtener información adicional. El análisis se llevó a cabo en una selección de diferentes puntos de interés tanto del centro como de la periferia de las muestras con el propósito de detectar cambios en los ratios Ca/P. La información se recogió de forma deliberada en puntos de interés estratégicos dentro del biomaterial residual (RB), cercanos y distales al hueso neoformado (NB) y en la superficie de contacto hueso-implante, si la hubiese. Un total de 900 puntos de las 60 biopsias fueron analizados.

Tras la inserción de los implantes dentales, se realizó la evaluación de la frecuencia de la resonancia utilizando el Ostell™ Mentor para medir la estabilidad primaria del implante. El valor de la frecuencia de la resonancia se representa a través de un parámetro cuantitativo conocido como ISQ. La medición de los valores ISQ se llevó a cabo durante el procedimiento quirúrgico en el inicio (T1), tres meses después de la cirugía (T2) y 6 meses después de la cirugía (T3). Estos valores se registraron en dirección buco-lingual (B-L) y mesio-distal (M-D)

En los resultados de la caracterización de los materiales de hidroxiapatita natural desproteinizados, el análisis de difracción de rayos X reveló la estructura típica de la hidroxiapatita para ambos materiales. Ambos senoinjertos son porosos y muestran poros interconectados. Se observaron importantes diferencias en términos de porosidad, cristalinidad, densidad, área de superficie y composición de ratio calcio/fósforo. El PBM presenta el nivel de porosidad más alto (59,90%); sin embargo, alrededor del cuarenta por ciento (38,11%) de esta porosidad se corresponde con entradas de poro submicrométrico. Por su parte, la porosidad del BBM es de un 49,13% pero presenta una menor proporción de poros submicrométricos, solo el 3,66%. En términos de cristalinidad, los gránulos del PBM presentan baja cristalinidad y el tamaño de los cristales es de 325 nm, mientras que la estructura del material bovino muestra una alta cristalinidad, con un tamaño de los cristales de 732 nm. La mayor densidad se encontró en el BBM, con 2,98 g/cm³ respecto a los 2,85 g/cm³ del PBM. Se observó una mayor área de superficie en el PBM (97,84 m²/g) en comparación con los datos obtenidos del BBM (2,77 m²/g). Se encontraron diferencias estadísticamente significativas entre la composición del ratio calcio/fósforo del PBM (2.22± 0.08) y la del BBM (2.31±0.09).

Aunque la radiopacidad del volumen aumentado se incrementó con el tiempo en ambos materiales, las zonas de control mostraron una mayor densidad de radiopacidad comparadas con las del PBM.

La microscopía electrónica de barrido reveló que el hueso neoformado se había adherido a ambas hidroxiapatitas. Las mediciones histomorfométricas de las biopsias de hueso mostraron diferencias estadísticamente significativas. Para el PBM, el hueso neoformado representó el $(25,92 \pm 1,61\%)$, el material residual del injerto $(24,64 \pm 0,86\%)$ y el tejido conectivo $(49,42 \pm 1,62\%)$; por su parte, para el BBM el hueso neoformado representó el $(26,83 \pm 1,42\%)$, el material residual del injerto, el $(30,80 \pm 0,88\%)$ y el tejido conectivo no mineralizado, el $(42,79 \pm 2,88\%)$.

En todos los casos, el análisis EDX encontró un descenso significativo del porcentaje del ratio Ca/P en el biomaterial residual con respecto a la composición inicial, mientras que en la interfase se encontró un aumento gradual de los porcentajes de ratio Ca/P, lo que sugiere un aumento en la capacidad osteoconductiva de los materiales y el reemplazo por hueso neoformado en la periferia. El PBM presentó numerosas regiones de reabsorción y un ratio de Ca/P medio de $1,08 \pm 0,32$ respecto al ratio de Ca/P medio de $1,85 \pm 0,34$ del BBM. También se encontraron diferencias estadísticamente significativas en la interfase y en el hueso neoformado entre ambos grupos. Para el PBM, el ratio Ca/P en la interfase fue de $1,93 \pm 0,18$ y de $2,14 \pm 0,08$ para el BBM. En el caso de la hueso neoformado, el ratio Ca/P fue de $1,84 \pm 0,14$ para el PBM y de $2,00 \pm 0,08$ para el BBM.

El *Line Scan* mostró un aumento de la porosidad dentro del material y una degradación más rápida del PBM en comparación con la observada en el BBM, hecho que está relacionado con la cristalinidad del material. La imagen BSE mostró la reabsorción del injerto PBM en relación con el hueso circundante y material residual en forma de gránulos que consistían en áreas de muy pocas y pequeñas partículas. Todo ello muestra la casi completa reabsorción del PBM de forma similar en el centro y en la periferia de las muestras.

De acuerdo con los mapas elementales de rayos X y las imágenes SEM de la interfase entre los implantes de BBM y de PBM y el hueso natural, tanto la zona de reacción como las zonas próximas a esta, estaban compuestas de Ca y P. No se observaron

diferencias morfológicas claras entre el hueso neoformado y el hueso viejo en el que se insertaron los implantes.

Los valores ISQ medios, en el inicio fueron de 63.8 ± 2.97 para el material sinterizado (BBM) y de 62.6 ± 2.11 para el material no sinterizado (PBM). Los valores ISQ medios a los tres meses fueron de 73.5 ± 4.21 para el BBM y de 67 ± 4.99 para PBM. Los valores ISQ medios a los seis meses fueron de 74.65 ± 2.93 para el BBM y de 72.9 ± 2.63 para PBM. En todos los periodos estudiados se observaron diferencias estadísticamente significativas.

Como conclusión general del trabajo realizado en esta Tesis Doctoral, podemos decir que la información recogida en este estudio muestra el efecto de la temperatura de sintetizado en las propiedades fisicoquímicas de las dos hidroxiapatitas naturales estudiadas y su influencia en el comportamiento biológico de las mismas. Las diferencias encontradas en las características fisicoquímicas de ambos senoinjertos justifican esta distinción en su comportamiento in vivo. Las hidroxiapatitas evaluadas en este estudio demostraron ser biocompatibles y osteoconductoras cuando se utilizan en la elevación de seno maxilar. Se encontró una diferencia significativa en los tiempos de reabsorción y en la estabilidad de los implantes en ambos grupos. La hidroxiapatita no sintetizada de origen bovino con alta porosidad, baja cristalinidad, baja densidad, alta área de superficie y bajo ratio calcio/fósforo presenta un alto ratio de reabsorción pero podría no soportar la presión del seno lo que conllevaría la reneumatización del seno. Por su parte, la hidroxiapatita natural de origen bovino, con una baja porosidad, alta cristalinidad, alta densidad, baja área de superficie y alto ratio calcio/fósforo, presenta un ratio de reabsorción bajo que inhibe la reabsorción del hueso neoformado, tensa la membrana del seno, mantiene el espacio y el suelo del seno maxilar aumentado estable, incrementado la estabilidad primaria del implante y reduciendo el tiempo de carga del implante.

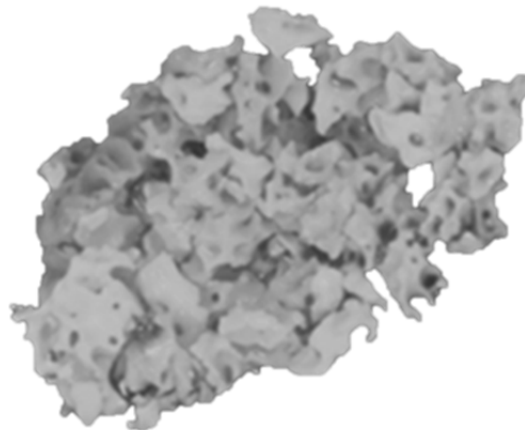
La información detallada sobre las características de los materiales de injertos es crucial a la hora de evaluar sus resultados clínicos. La influencia de las propiedades fisicoquímicas de los materiales de injerto óseo en osteointegración se han traducido en periodos de curación más cortos desde la colocación a la reparación. Un conocimiento profundo sobre los diferentes aspectos de las propiedades de los biomateriales y su relación e influencia hacia la regeneración ósea es de crucial importancia.



UNIVERSITAS
Miguel
Alonso

MATERIAL &

METHODS





4. MATERIAL AND METHODS

4. Materials and Methods

4.1. Grafts

Two different types of commercial bone grafts used in dentistry were characterized and evaluated in vivo regarding of the bone tissue response:

- (PBM, OsteoBiol® mp3 deproteinized porcine bone substitute material) was made up of granulated small bone particles of 600-1000µm in size, is a ceramic derived from cancellous-cortical porcine bone. The material is obtained at low processing temperature (130°C). According to the commercial specifications this material is claimed to preserve the structure and composition of the natural bone components.

- (BBM, Endobon® deproteinized bovine bone substitute material) was made up of granulated small bone particles of 500-1000µm in size, is a ceramic derived from cancellous bovine bone, fully deproteinated by a high temperature manufacturing process for safety from bacteria, viruses and prions. This process consists of two steps: firstly pyrolysis at a temperature of more than 900° that eliminates the organic element and secondly a ceramization process at temperatures greater than 1200° that creates a crystalline structure. (Fig. 1)



Figure 1: *A-* PBM, OsteoBiol® mp3 deproteinized porcine bone substitute material. *B-* BBM, Endobon® deproteinized bovine bone substitute material

4.2. Graft Characterization

These biomaterials were characterized in terms of morphology, composition, crystallinity, particle size distribution, porosity, and pore size.

4.2.1. SEM-EDX

For microstructural examination samples were studied using a scanning electron microscope (SEM, HITACHI S-3500N, Ibaraki, Japan). Quantitative analyses were made by an Energy Dispersive X-ray Spectroscopy (EDX) system coupled to the above-described electron microscope. The calibration was carried out with Bayer standards. A weight percentage was calculated from measured net intensities with a program that corrected for the influences of atomic number, absorption and fluorescence (ZAF corrections). The relative counting error ε_n has been calculated as $\varepsilon_n = (N^{1/2}/N) \cdot 100$ (N = accumulated counts) with a probability of 98.5%. The samples were pre-coated with palladium for SEM images and carbon coated for EDX analysis, under an argon atmosphere using a sputtering machine (Polaron K550X Sputter Coater, Germany).

4.2.2. XRD- X-Ray Diffractometry

This technique consisted of directing an X-ray beam of wavelength 1.5418 Angstroms onto the samples, in order to record the crystalline phases that were presented. Through these recordings, the intensities of the diffraction lines corresponding to the phases could be determined, and hence the phases present could be qualitatively determined.

The mineralogical characterization of the powder materials was performed by X-ray diffractometry (XRD). XRD patterns were obtained in Bruker-AXS D8 Advance, Karlsruhe, Germany automated diffractometer and compared with the database provided by the Joint Committee on Powder Diffraction Standards (JCPD). The following Scherrer formula was used to determine the crystal size of each material, based on the relevant XRD pattern. The instrument broadening corrections were taken into account, and it was assumed that the lattice strain was negligibly small.

$$D_{hkl} = \frac{k\lambda}{B_{1/2} \cos \theta_{hkl}}$$

In this equation K is the Scherrer constant (0.89) which depends on the crystal shape, the diffraction line indexes (Shull 1946) and the dispersion of crystallite sizes of the powder (Pielaszek, 2003), λ is the wavelength of the Cu $K_{\alpha 1}$ ($\lambda=1.54056\text{\AA}$); $B_{1/2}$ corresponds to full width at half maximum (rad) for (hkl) reflection, and θ_{hkl} is the diffraction angle ($^{\circ}$). The line broadening of the (300) reflection corresponding to the maximum intensity peak was used to evaluate the crystal size.

4.2.3 FTIR-Fourier transforms infrared spectroscopy

Fourier transform infrared spectroscopy (FTIR-ThermoNicolet IR200, Waltham, MA, USA) was used to provide information concerning the chemical composition and the major functional groups. The FTIR spectra were recorded between 400 and 4000 cm^{-1} at 2 cm^{-1} resolution. The pellets were prepared by mixing each sample powder with KBr matrix at a level of 1 wt%. The background data were collected for the KBr matrix and subtracted from each spectrum. All spectra were recorded at ambient temperature. Analytical-grade collagen samples (purchased from Sigma-Aldrich, Germany) were also used for comparative purposes.

4.2.3. Helium gas pycnometry

The particle's real density (sample mass/Volume of the solid (excluding empty spaces)) was determined by Helium gas pycnometry (Quantachrome Instruments, Boyton Beach, FL, USA).

Particle's real density was determined excluding sample interstices and most pores, since the small volume of the gas molecules (He) enables their penetration in almost all empty spaces. An exception is given by the sample's closed pores, that is, those pores that are not opened to the surface. The density, measured in this way, provides the closest value to the solid density of the sample, justifying the use of the term "real" or "true" density.

4.2.4. MIP-Mercury Intrusion Porosimetry

The particle's apparent density was determined by mercury porosimetry. Information concerning the sample porosity and the pore size distribution was obtained by mercury porosimetry using the Poremaster-60 GT (Quantachrome Instruments, Boyton Beach,

FL, USA) in a pressure range between 5.395 KPa to 410785.062 KPa, corresponding to a range of pore diameters between 300 μm to 0.0035 μm .

4.2.4. Statistical analysis

At least 7 runs were performed for each sample, and at least three different samples were analyzed for each material. Mean and standard deviations were obtained for all investigated groups. The Kolmogorov-Smirnov test was used to check normality. Comparisons between BBM and PBM groups were performed with Student's t (parametric data) or Mann-Whitney (non-parametric data). All statistical analyses were performed with the aid of appropriate software (MedCalc v15.8, Belgium). Significance was evaluated at a level of $p < 0.05$.

4.3. Sinus lifts procedure and Implant Insertion

4.3.1. Patient selection and protocol

Ten partially edentulous patients (five females and five males), of ages ranging from 37 to 60 years, attended the Department of Oral and Maxillofacial Surgery. Patients who demanded fixed restorative appliances in the posterior maxilla were selected for maxillary sinus augmentation due to a lack of sufficient bone tissue for the placement of endosseous dental implants. The protocol for harvesting bone samples was approved by the University Ethics Committee and informed consent was obtained from all patients. The study was designed following guidelines laid down by the Declaration of Helsinki for experimentation on human subjects. Possible complications arising from surgical therapy were treated following standard dental management protocols.

4.3.2. Inclusion and exclusion criteria

The inclusion criteria were as follows: maxillary partial bilateral edentulism involving the premolar-molar areas. In cases with a crestal bone height between 7 and 0 mm having a high postero-lateral atrophy (Cawood V–VI) (Cawood & Howell 1988) are most likely to have a two-stage lateral antrostomy. (Fig. 2)

Exclusion criteria were: patients suffering an uncontrolled systemic disease or condition known to alter bone metabolism (i.e., osteoporosis, diabetes mellitus, etc.); subjects who were taking/had taken medications known to modify bone metabolism such as

bisphosphonates, corticosteroids, etc.; women who were pregnant or trying to get pregnant at the time of the screening; patients who presented existing sinus conditions, sepsis, a history of cancer and/or radiation to the oral cavity; complications derived from any of these conditions and affecting the sinus area.



Figure 2: Maxillary partial bilateral edentulism involving the premolar-molar areas. *A*- Frontal view. *B* - Oclusal view.

4.3.3. Surgical procedure. First phase (Sinus Grafting)

The study was performed in two surgical phases. In the first phase all patients took 875/125 mg of amoxicillin/ clavulanic acid, every 8 h starting 1 day before surgery. A dosage of 300 mg of Clindamycin every 8 h was prescribed to penicillin allergic patients. This medication was maintained for 7 days. All surgical procedures were performed under local anesthesia (Ultracain, Aventis Inc., Frankfurt, Germany).

The basic surgical procedure was represented in all patients by maxillary sinus floor elevation via a lateral approach. A conventional lateral wall approach was used to perform the sinus grafting in all patients. Fullthickness flaps were elevated to expose the alveolar crest and the lateral wall of the maxillary sinus. A trap door was made in the lateral sinus wall. The sinus membrane was elevated with curettes of different shapes until it became completely detached from the lateral and inferior walls of the sinus. After membrane elevation, a bioabsorbable collagen barrier membrane was placed under the sinus membrane and adapted to make contact with the peripheral bony walls (Evolution Fine® OsteoBiol®, Tecnos Dental S.R.L., Torino, Italy). In one side sinus cavities were grafted with (PBM) (OsteoBiol® mp3, Tecnos Dental S.R.L., Torino, Italy). After grafting, an absorbable collagen membrane (Evolution Fine® OsteoBiol®, Tecnos Dental S.R.L., Torino, Italy) was placed over the window to minimize soft tissue invasion. In the other side the sinus cavities were grafted with (BBM) (Endobon®, RegenerOss™, BIOMET3i. Palm Beach Gardens, FL, USA). The

grafting materials were mixed with venous blood from de defect area and carefully packed in the created volume following elevation of the mucous membrane. After bone grafting, A short-term absorbable collagen membrane (Evolution Fine® OsteoBiol®, TecnoS Dental S.R.L., Torino, Italy) was placed over the window. Primary closure was achieved in both cases, suturing with 3–0 silk suture (Laboratory Arago´ n, Barcelona, Spain). (Figure 3-4)



Figure 3. *A- A short-term absorbable collagen membrane. B- Grafting materials mixed with venous blood.*

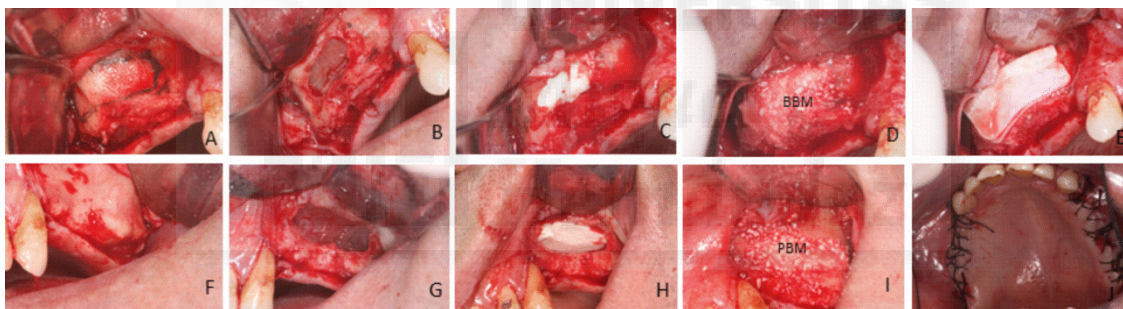


Figure 4: *Surgical procedure. A- A crestal incision was made slightly palatally supplemented by buccal releasing incisions mesially and distally. Fullthickness flaps were elevated to expose the alveolar crest and the lateral wall of the maxillary sinus. B- A trap door was made in the lateral sinus wall. The elevation of the Schneiderian membrane was accomplished by initially exposing and mobilizing the membrane followed by hand instrumentation to further elevate the membrane along the medial wall of the sinus. The sinus membrane was elevated with curettes of different shapes. C- A bioabsorbable collagen barrier membrane was applied underneath the Schneiderian membrane aiming to prevent a dislocation of grafting material in case of membrane perforation. Randomly, one of the two bone substitute materials was placed into the newly created space between the collagen membrane and the sinus floor. D- The bovine porous bone mineral was mixed with venous blood and packed carefully in the sinus cavity, especially in the posterior and anterior parts. E- After bone grafting, a second absorbable collagen membrane was placed was placed over the window. F- In the other side a crestal incision was performed slightly palatal, supplemented with two buccal releasing incisions, mesially and distally. Full-thickness flaps were elevated to expose the alveolar crest and the lateral wall of the maxillary sinus. G- A trap door was made in the lateral sinus wall using a round bur under sterile saline solution irrigation. The sinus membrane was elevated with curets of different shapes until it became completely detached from the lateral and inferior wall of the sinus. H- A bioabsorbable collagen barrier membrane*

was placed under the sinus membrane and adapted to make contact with the peripheral bony walls. **I-** The maxillary sinuses were filled with porcine bone material and A short-term absorbable collagen bovine membrane was placed over the window. **J-** Flaps were sutured.

Antibiotics and analgesics were given for 1 week. All patients took 875/125mg of amoxicillin/clavulanic acid, every eight hours starting one day before surgery. 300mg of Clindamycin every eight hours was prescribed to penicillin-allergic patients. This medication was maintained for seven days. Sutures were removed 2 weeks after surgery. During the postoperative period, the patients were followed up clinically and radiologically at monthly intervals.

4.3.4 Radiographic Thermal Imaging Analysis

During the postoperative period, the patients were followed up at monthly intervals, clinical and radiologically. All patients underwent CBCT after 6 month of surgery as a routine diagnostic approach using a I-CAT ®(Imaging Sciences International, Hatfield, USA) Cone Beam 3D and analyzed using a I-Cat vision software. The images obtained were processed by Image J software, developed by the National Institute of Health (NIH) of the United States of America, a 3D plug-in with a thermal LUT with a grid size of 128x128, smoothing of 6.0, perspective of 0.2 at a scale of 1:1; color thermal graduation was used to observe the changes in radiopacity in the grafted area (intrasinus bone graft). The scale was graduated with values from 0 to 240. Where 0-20 was the values assigned to the air, 20 to 100 was the values assigned to water and soft tissues, 100 to 140 was the values assigned to bone with lower density and 140 to 220 was the values assigned to bone with higher density. (Figure 5)

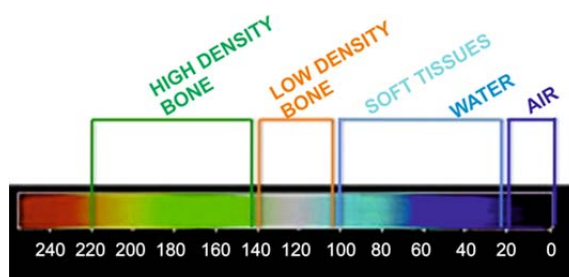


Figure 5. Color graduated density scale for thermal imaging interpretation.

4.3.5. Surgical procedure. Second phase (Implant Insertion)

After healing period, the second surgical phase was performed. The functional implants were placed on each side. Each side received three implants 3i T3® Implante Certain® Cónico (BIOMET 3i ® Palm Beach Gardens, Florida) placed 6 months after augmentation. All patients took 875/125 mg of amoxicillin/ clavulanic acid, every 8 h starting 1 day before surgery. A dosage of 300 mg of Clindamycin every 8 h was prescribed to penicillin allergic patients. This medication was maintained for 7 days.

All surgical procedures were performed under local anesthesia (Ultracain, Aventis Inc., Frankfurt, Germany) in an outpatient setting by the same surgeon who was familiar with the implant system. For the procedure, a full thickness mucoperiosteal flap was elevated at the sides.

A 3 x 10 mm diameter trephine under sterile saline solution irrigation was used to retrieve a central core of bone at the moment of implant insertion, 60 bone samples were retrieved for histomorphometric analysis. Three biopsies were taken for each individual in each slide. Nevertheless, the biopsy value used for analysis is unique for each individual and was computed as the mean of the three biopsies taken, thus avoiding possible dependency problems. After the retrieval, the functional implants were placed in the same sites as the trephined holes on each side.

The osteotomy using a conical drill, with copious irrigation using saline solution was realized on the crest of the bone. Then, osteotomies for the implants installation were produced using the initial drill to determine the depth and the direction of the site. After the implants were positioned in the local predetermined at the crestal bone level. A total of 60 conical implants with internal hexagon connection were applied, all 11.5 mm in length and 4.0 in diameter. The implants were selected based on the prior evaluation of each case. All implants were installed using surgical guides, and the wounds were sutured in a tension free state. Antibiotics and analgesics were given for one week. Patients were asked to rinse with chlorhexidine 0.12% three times daily for 2 weeks postoperative. Sutures were removed 2 weeks after surgery. All implants were prepared with a healing abutment until the initiation of rehabilitation. (Figure 6-7)

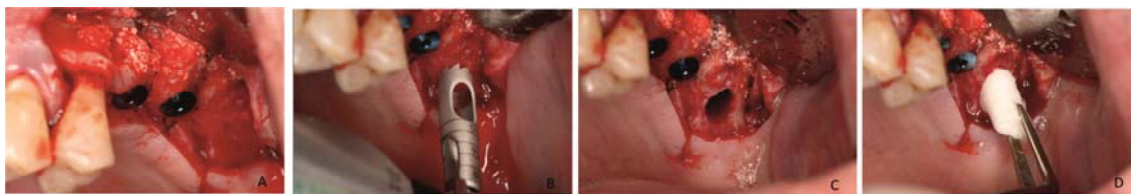


Figure 6: *A- The functional implants were placed on each side. B- 3 x 10 mm diameter trephine under sterile saline solution irrigation was used to retrieve a central core bone. C- Each side received three implants. D – The functional implants were placed in the same sites as the trephined holes on each side.*

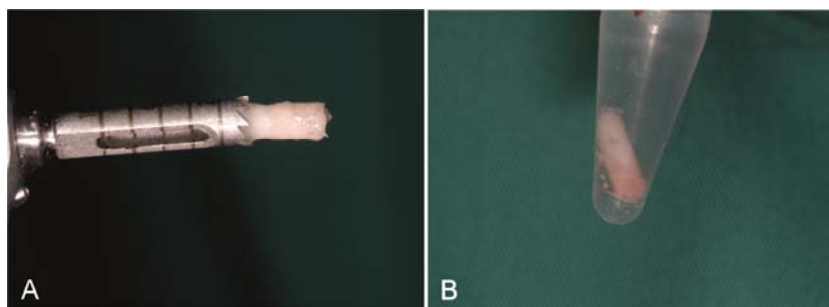


Figure 7: *A- A sample of bone core for histomorphometric analysis. B- 60 bone biopsies were obtained from sixty grafted sites.*

4.4. Sample processing and analysis

In order to investigate the relationship between xenograft biomaterial particles and bone, cross-sections of the non-decalcified tissue were examined for an ultrastructural study in SEM. Therefore, human specimens were fixed by immersion in 4% formalin solution, dehydrated in a graded ethanol series, and embedded in plastic resin (Technovit A 7210VCL; Kulzer & Co., Hanau, Germany). Then, the specimens were polished using a manual grinder with 800 grit silicon carbide paper, mounted on an aluminum stub, and carbon coated under an argon atmosphere using a sputtering machine (Polaron K550X Sputter Coater, Germany) for the SEM.

4.4. 1 SEM- (BSE) Back-scattered SEM imaging

BSE- Back-scattered electron imaging was used to highlight contrasts between resin, bone and biomaterial. With image J polygon selection tool, irregular shaped areas were outlined by the selection of three different regions of interest, bone, residual material and black spaces. The three were calculated in samples of 200 micrometers x 200 micrometers. Images in pseudocolors, obtained using backscattered electrons, were used to evaluate and measure the histomorphometric parameters. A different color was applied to anyone to increase difference. Histomorphometric analysis was

performed on the bone core samples to determine the vital bone content, connective tissue content, and residual graft material content. Quantitative data was recorded as the mean value \pm SD. Comparisons between BBM and PBM for each parameter (NB) new bone, (RG) residual graft material, (CT) connective tissue, were made with the aid of statistical software (MedCalc v15.8, Belgium). The Kolmogorov–Smirnov test, assessed the conformity of the parameters to normal distribution. Student T test was used for the intergroup comparisons of parameters with normal distribution. Mann Whitney U test was used for the intergroup comparisons of parameters without normal distribution. Significance was evaluated at a level of $p < 0.05$. (Fig. 8)

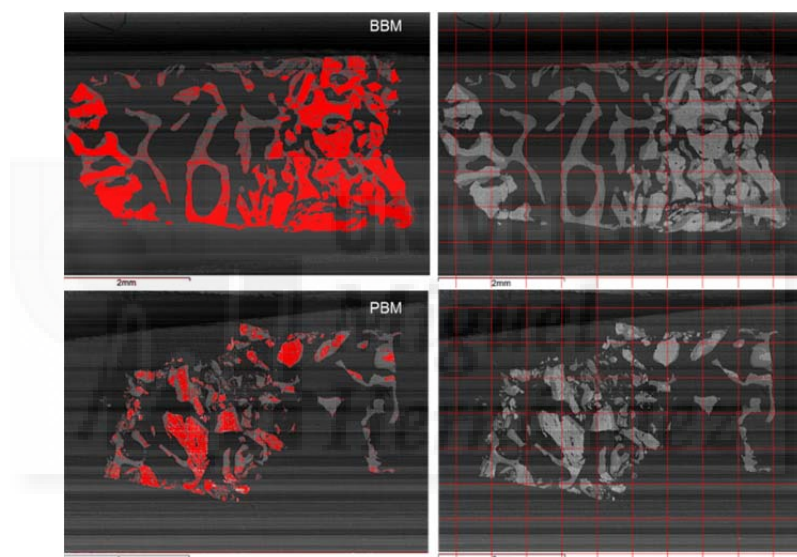


Figure 8: *Histomorphometric analysis was performed using BSE- Back-scattered electron imaging on the bone core samples to determine the vital bone content, connective tissue content, and residual graft material content*

4.4. 2 SEM- (EDX) X-ray elemental maps in scanning mode

In addition the chemistry of the interphases and the chemical degradation process of the xenograft biomaterials were analyzed using X-ray elemental maps in scanning mode. Analysis was carried out at a selection of different points, taking different points of interest from the middle and from the periphery of the samples to detect changes in Ca/P ratios. Data were then collected from deliberately targeted sites of interest within

the residual biomaterial, close to and distal from new bone and at the bone-implant interface if present (an average of approximately 15 points/section, depending on the biomaterial content). Additional information was obtained from line scans and elemental maps. A total of more than 900-point analyses were carried out on the sixty biopsies. Comparisons between BBM and PBM groups for each parameter (RB, INT, and NB) were performed with Student's t (parametric data) or Mann-Whitney (non-parametric data).

4.5. Measuring of implant stability

After dental implant insertion, the resonance frequency evaluation was performed using the Ostell™ Mentor (Integration Diagnostics AB, Göteborg, Sweden) for measure the primary stability of the implant. A Smartpeg™ (Integration Diagnostics AB, Göteborg, Sweden) was placed into each implant and tightened to approximately 4-5 Ncm. The transducer probe was aimed at the small magnet at the top of the Smartpeg at a distance of 2 or 3 mm and held stable during the pulsing until the instrument beeped and displayed the ISQ value. (Figure 9)

The RF value is represented by a quantitative parameter called ISQ. The range of ISQ is from 1 to 100. An increased ISQ indicates increased stability, whereas decreased values indicate a decrease in implant stability. The ISQ values were measured during the surgical procedure (T1- baseline), at 3 months (T2) after surgery and at 6 months (T3) after surgery. The measurements were taken twice in the bucco-lingual direction and twice in the mesio-distal direction. The mean of the two measurements in each direction was regarded as the representative ISQ for that direction. The highest values were recorded for the bucco-lingual (B-L) direction and mesio-distal (M-D) direction. ISQ values were evaluated separately. Additionally, each implant was evaluated at all visits for mobility, pain and signs of infection.

All data were recorded, reviewed, and entered into a computing system. Analyses were performed using specific software (MedCalc, Belgium). The influence of age, gender (Male, Female), group (BBM, PBM), ISQ measurement direction (BL, MD) and time period of evaluation (T1) baseline, (T2) 3 months, (T3) 6 months on ISQ values was evaluated by Analysis of Variance and Multiple Regression at 5% significance level

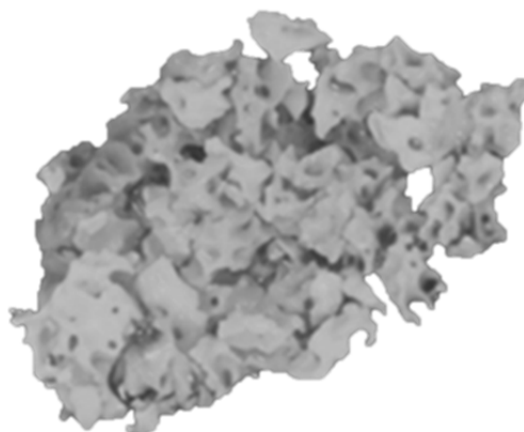
(Backward method) with the aid of appropriate software (MedCalc, v15.8. Belgium). Significance was evaluated at a level of $p < 0.05$.



Figure 9: **A-** The rigidity of implant-bone contact was measured by RFA (Osstell™ Mentor, Integration Diagnostic AB, Sweden). RFA measurements were obtained before the healing cap was screwed into the fixtures of the implants. **B-** A Smartpeg (Smartpeg™, Integration Diagnostic AB, type 4 regular neck) was attached manually to the fixture with the aid of a mount, and a torque of 4-5 Ncm was applied. **C-** All measurements were carried out by the same investigator. Measurements were taken at the time of implant placement and (baseline) at stage 2 and to stage 3. In all cases, ISQ was calculated as the average of 4 measurements per implant (twice in the bucco-lingual direction and twice in the mesio-distal direction).



RESULTS





5. RESULTS

5.1 Characterization of Deproteinized Hydroxyapatite Materials

5.1.1. SEM-EDX Analysis

SEM micrographs provided information about morphology of the obtained BBM scaffolds (Figure 10) and the PBM scaffolds (Figure 11). SEM micrographs show important differences depending on the heat treatment. BBM consists of 500-1000 μ m average particles. The BBM consisted of a highly porous network with the pore size of 0.5 mm in average (Figure 10A). Micropores from 1 μ m to 5 μ m were also visualized. On the other hand, when the granules were evaluated in larger magnification it was possible to observe the porous surface roughness of the granules with apatite crystals (white particles) (Figure 10B and 10C).

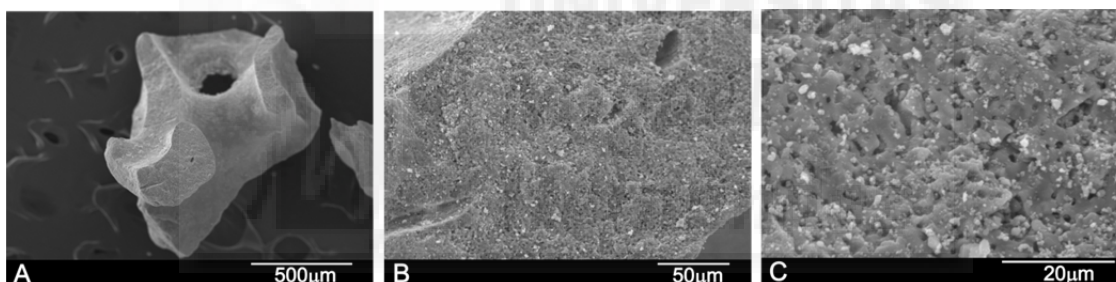


Figure 10: Scanning electron micrographs of Bovine HAs scaffolds deproteinized at high temperature prior to the insertion for maxillary sinus floor elevation (BBM). **A-** Low magnification. **B-** High magnification showing macro and micro porosity. **C-** Detail of the micro porosity on the scaffold surface together apatite crystals (white).

The PBM consisted of small grains of 600 μ m average (Figure 11A). At high magnification the PBM shows a surface roughness (Figure 11B). Due to the presence of collagen, the material does not show at high magnification a microporosity in its surface (Figure 11B) and also the surface is not as clear as in the BBM xenograft.

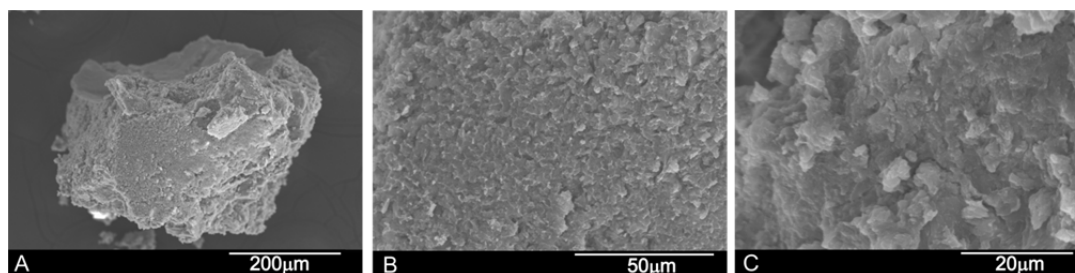


Figure 11: Scanning electron micrographs of Porcine HAs scaffolds deproteinized at low temperature (PBM). *A* - Low magnification image of the HA grafts, *B* - High magnification image. *C* - A detail of the surface roughness of the scaffold *B*.

EDX was used to determine the elemental composition in an area reaching from graft particles before implantation. The Ca/P ratios for both HAs xenografts were 2.31 ± 0.09 for the BBM material and 2.22 ± 0.08 for the PBM material. The Kolmogorov-Smirnov test rejected Normality for the PBM group. Statistically significant difference was found between BBM and PBM (Mann-Whitney test, $p < 0.0051$).

EDX also denoted the differences between both xenograft materials (Table 1). The Ca/P ratio shows a statistically significant difference in EDX analysis of the grafts before implantation.

Table 1. Ca/P ratios of the grafts before implantation. Values as Medians. Statistically significant difference was found between BBM and PBM (Mann-Whitney test, $p < 0.0051$).

Ca/P Ratios (wt%)	PBM	BBM
Mean	2.22	2.31
SD	0.08	0.09
Median	2.22	2.28

5.1.2. XRD Analysis

Figure 12 shows the X-ray diffraction patterns of the BBM and the PBM materials and synthetic HA and osseous matrix for comparative purposes. The XRD of the grafts can be associated with the chemical composition of the samples.

As expected, the XRD pattern from the mineral samples corresponds to hydroxyapatite, with coincident peak positions and relative intensities. However, these materials present diverse degrees of crystallinity, as indicated in the different peak widths. That is the

case of PBM; the diffractogram exhibits broad peaks with a low signal-to-noise ratio, corresponding to a low-crystallinity material. On the other hand, the sharp and well-resolved peaks found in the XRD spectrum of BBM indicate a highly crystalline hydroxyapatite. The HA corresponded to JCPDS card no. 09-0432 and presents hexagonal system with main diffraction plan [211]. No other secondary phases were detected.

Based on XRD patterns, the crystal size of BBM xenograft implants is 732 nm and PBM presents a crystal size of 325 nm-

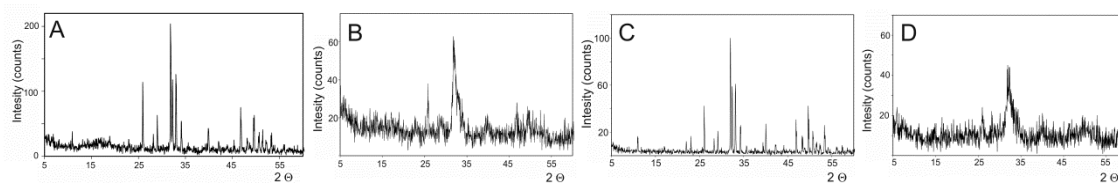


Figure 12. Laboratory XRD X-ray powder diffraction pattern. **A-** BBM. **B-** PBM obtained materials. **C-** Synthetic HA. **D -** Osseous matrix for comparative purpose.

5.1.3. FTIR Analysis

Figure 13 includes the FTIR spectra of BBM and PBM obtained materials as well as the spectrum of collagen for comparative purposes. As expected, both deproteinized hydroxyapatite materials shown the typical bands originated by the hydroxyapatite, the main constituent of the bovine and porcine bone: $1125\text{-}1040\text{ cm}^{-1}$ (ν_3); 963 cm^{-1} (ν_1) and between 550 and 610 cm^{-1} (ν_4). These are the more intense phosphate stretching bands observed at around 1043 cm^{-1} and 1092 cm^{-1} . In addition, a double band at $1410\text{-}1480\text{ cm}^{-1}$ (ν_3) and low-intensity band and at 885 cm^{-1} (ν_2) that corresponds to stretching vibrations of CO_3^{2-} , substituting for phosphate in the apatite lattice that correspond to a natural carbonate-hydroxyapatite. (Antonakos et al 2007)

The third group of vibrational spectra includes the spectra relating to the collagen only present in the PBM material. In the figure is included the Type I collagen for comparison purposes. Above 1300 cm^{-1} , almost all the bands are exclusively assigned to collagen vibrations, the exception being those originated by CO_3^{2-} at 1460 cm^{-1} . (Ren

et al 2014) and a broad band presented at 3500 attributed to the presence of structural OH- groups. (Ślósarczyk et al 1997)

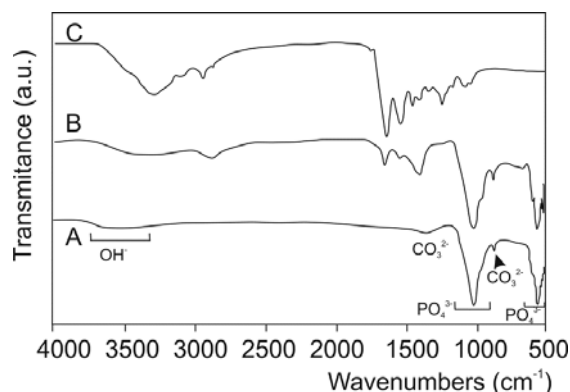


Figure 13. FTIR spectra. **A-** BBM. **B-** PBM obtained materials. **C -** Collagen for comparative purpose.

2.1.3. MIP Analysis

When analyzing a granular material by mercury porosimetry, two kinds of spaces can be detected: those that correspond to the empty spaces between the particles (commonly designated by “interstices” or “interparticle” spaces) and those that correspond to the spaces of the particles themselves (known as “pores” or “intraparticle” spaces). The results obtained for the granules of PBM (Figure 14) show that with increasing pressure, mercury penetrates to the increasingly smaller pores. The cumulative curve (Figure 14A) denotes a small intrusion in pores between 300 μm and 3.5 μm , followed by a plateau between 3.5 and 0.02 μm where no intrusion is detected, and then a significant mercury penetration into pores that are smaller than this value. The initial rise of the curve corresponds mostly to the filling of the spaces between the particles (and may also include some of the largest pores of cancellous bone), whereas the later stage of rise is related to the pores of the individual particles. The range of the intraparticle pores is more obvious in (Figure 14B) in which one intense peak whose mode is in the range 0.01-0.004 μm is clearly visible. The peak on the left (84 μm) corresponds to the intrusion of the mercury in the interparticle spaces. The size of these spaces, related to the way the particles are packed, depends on the particle size and shape as well as the particle size distribution. However, the distinction between inter- and intraparticle spaces is not always so apparent. This interpretation aims to elucidate the kind of information that can be extracted from the pore size distribution curves and highlight

the importance of always specifying the size range of the measured pores. It should be stressed that the mercury intrusion technique is especially suited to the analysis of intraparticle pores, being not so adequate to the measurement of large spaces (300 μm).

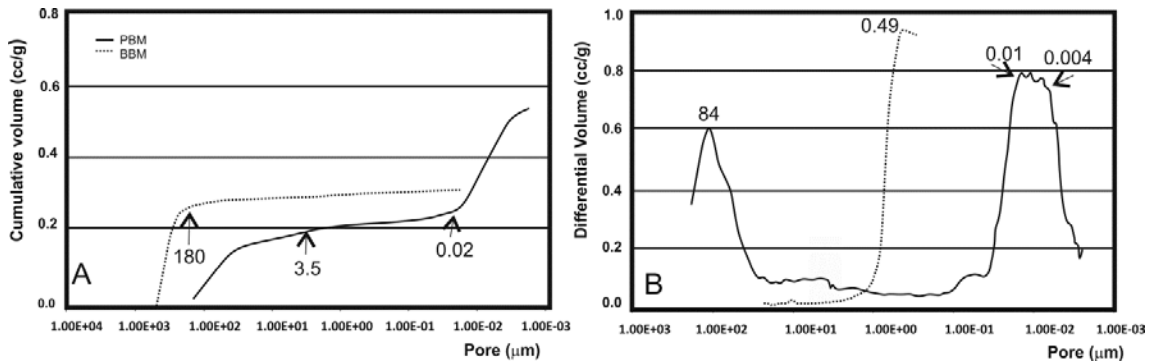


Figure 14. Mercury intrusion curves of the PBM and BBM ceramics measured by mercury porosimetry. *A-* cumulative intruded volume versus pore diameter. *B-* Differential-intruded volume versus pore diameter.

On the other hand the results obtained for the granules of BBM denote a mercury intrusion in pores between 300 μm and 180 μm , followed by a plateau between 180 and 0.02 μm where no intrusion is detected. The range of the intra and inter-particle pores is not obvious in (Figure 14B) in which only one intense peak whose mode is about 0.49 μm is clearly visible in the interparticle spaces but the proportion of interparticles in the BBM is clearly minor than in the PBM.

Table 2 summarizes these results in terms of the total intruded volume, mode of intraparticle pores, total porosity, and intraparticle porosity (taken as the percentage of the particles internal pores < 1 μm), relative to the total porosity).

Analysis of Table 2 suggests that PBM has the greatest porosity (59.90%). However, about forty per cent (38.11%) of this porosity corresponds to submicron pore entrances. Similar porosity value was determined for the BBM samples. This also exhibits a much smaller proportion of submicron pores, only (3.66%).

Table 2. Mercury-Intruded Volume, Mode (Most Frequent Diameter) of Intraparticle Pores, Total Porosity, and Intraparticle Porosity of the Commercial Samples.

	Intruded Volum (cc/g)	Mode of Intraparticle Pores (µm)	Total Porosity (%) ^a	Intraparticle Porosity (%) ^b
PBM	0.524	0.01-0.004	59.90	38.11
BBM	0.323	0.49	49.13	3.66

^a Corresponding to 1µm < pores < 300µm

^b Corresponding to pores < 1µm

Table 3 provides a comprehensive microstructural characterization of the xenograft materials and synthetic HA and osseous matrix for comparative purposes. The tendency was for density to increase with the increasing heating temperature and lower porosity.

Table 3.—Physical characteristic of the two xenograft materials studied and HA synthetic and osseous matrix for comparative purposes. [HA= hydroxyapatite; Coll= collagen]

	Real Density (g/cc)	Aparent Density (g/cc)	Surface Area (m ² /g)	Phase/s	Particle size (µm)	Cristal size (nm)
PBM	2.85	1.14	9.78	HA+Coll	600- 1000	325
BBM	2.98	1.51	2.77	HA	500- 1000	732
HA synthetic	3.16	1.62	3.10	HA	600- 1000	731
Osseous Matrix	1.46	1.24		HA+Coll	400-700	68.4

5.2. Radiological Results

After a six-month follow-up period of these ten partially edentulous patients treated with xenografts materials for sinus floor augmentation, there was a 100% success rate. No perforation of the sinus membrane or other clinical complications such as sinusitis or pain resulted from surgery. The increased volumes produced by the xenografts procedures were stable by the end of the healing period at can be seen in the Figure 15.



Figure 15: *A - Preoperative panoramic image before the sinus lift. B - Postoperative panoramic image 6 month after the sinus lift.*

After a six-month follow-up period of these ten partially edentulous patients treated with xenograft materials for sinus floor augmentation, there was a 100% success rate. No perforation of the sinus membrane or other clinical complications, such as sinusitis or pain, resulted from surgery. The increased volumes produced by the xenografts procedures were stable by the end of the healing period at can be seen in Figure 16. Deproteinized bone particles of two different temperatures induced osteoconduction 6 month after implantation.

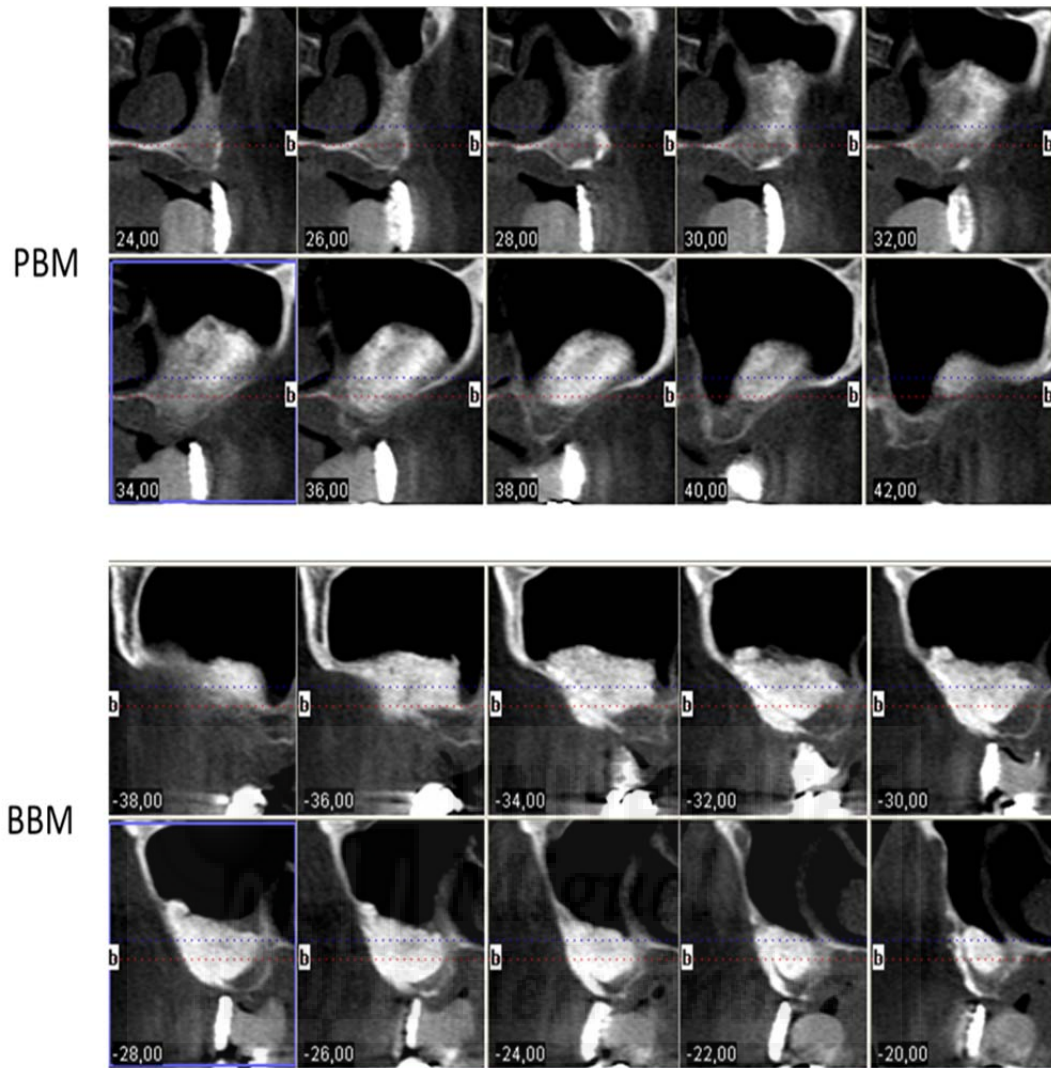


Figure 16. *i-CAT Vision postoperative image 6 month after the sinus lift.*

5.2.2 Termographic Results

Bone density at the implant site could be crucial, and it has been reported that it correlates with failure rates and primary stability. Bone density in the grafted area with both biomaterials was evaluated radiologically as a routine diagnostic approach. Color thermal graduation was used to observe the changes in radiopacity in intrasinus bone grafted area. At the moment of implant insertion, after a healing period of six months, the augmentation sites treated with the PBM show more dense new bone formation achieved along the inner surface of replaced bony widow than the area on the bone graft (Figure 17 A-B) whilst the BBM shows that more dense new bone formation was

achieved in the area on the bone graft respect the original augmentation density (Figure 17 C-D). Bone area was different in the groups after implantation and increased with time. Bone initially formed at the sinus wall and proliferated into the center of the augmented sinus cavity. The newly formed bone was consistently in close contact with the particles, and no gaps were present at the bone particle interface. The particles appeared to have acted as a scaffold, supporting the formation of new bone. Scaffolding is a critical component in tissue engineering because it provides the three-dimensional clues for cell seeding, migration, and growth as well as for new tissue formation.

Although radiopacity of the augmented volume increased with time for both xenograft materials, the control sites receiving showed a higher density of radiopacity compared with the PBM. The preservation of maxillary sinus membrane is important to avoid displacement of graft materials into the sinus cavity. Even, non-observed small perforations can cause a risk if left untreated.

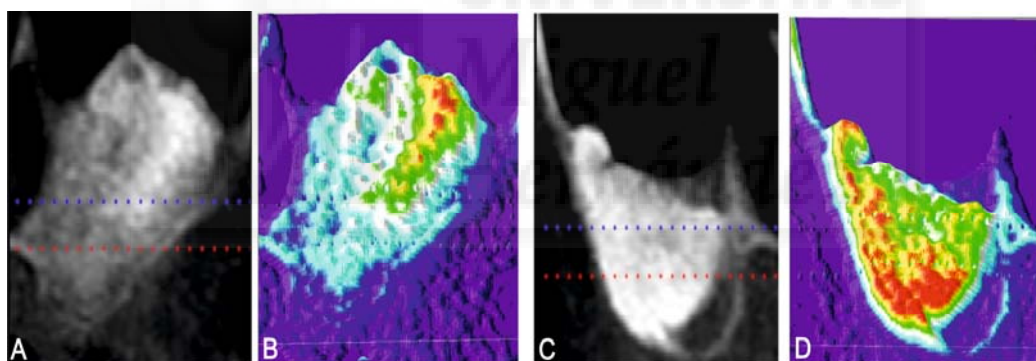


Figure 17. X- Ray of the implant site six months after xergraft materials implantation and the corresponding colour bone density **A, B-** PBM and **C, D-** BBM material.

5.3. Histomorphometric Results of retrieved bone biopsies

5.3.1. SEM-EDX Analysis

A section of the material-bone interfaces after 6 months sinus elevation is shown in Figure 18. SEM-BSE evaluation confirmed that the residual graft particles were surrounded by newly formed bone, which presented characteristics of mature bone with well-organized lamellae (Figure 18). BBM material shows a progressive structure

disolution and a result of these processed free graft particles were found in many areas. The asterisk (*) and (•) respectively denote the graft particles and ingrown bone region in Figure 18 A and B. On the other hand the PBM material degrades faster and at the same time the new bone is reabsorbed, so we can only see material particles (*) surrounded by non-mineralized connective tissue (Figure 18 C and B).

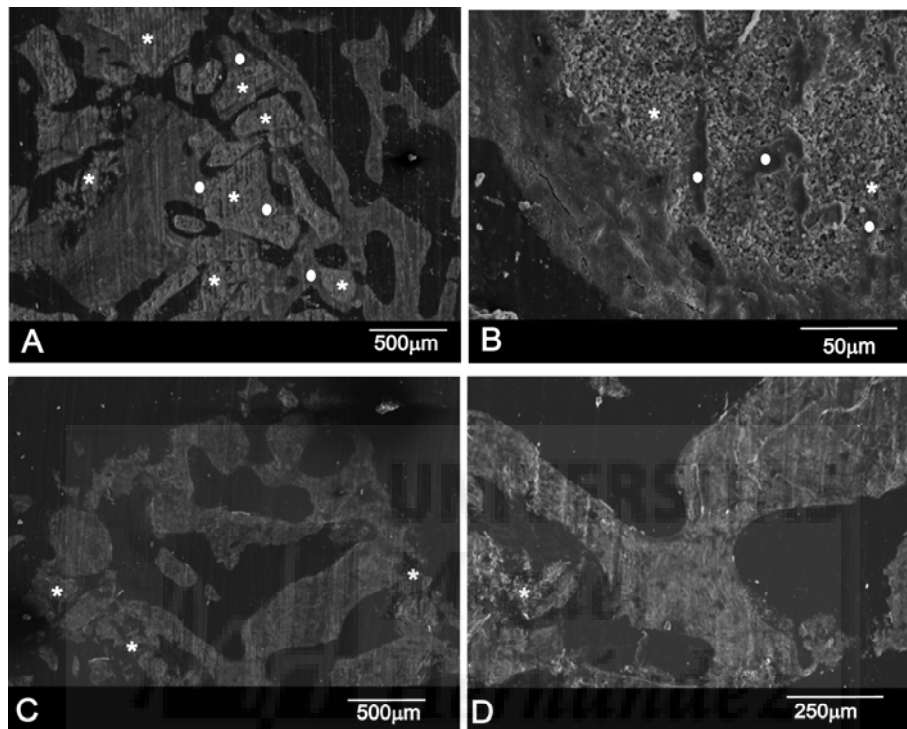
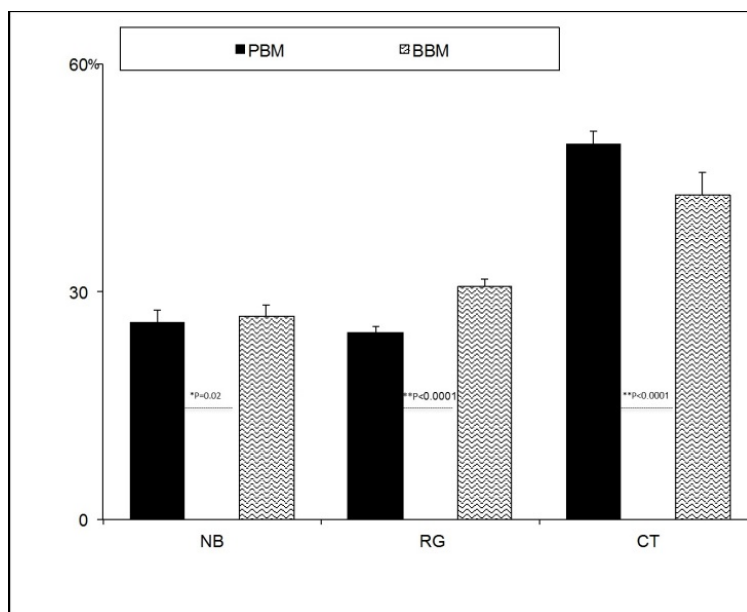


Figure 18. SEM-BSE of a resin-embedded bone section containing bone and residual biomaterials **A, B** - BBM and **C, D** - PBM material [*materials particles as results of the degradation process •new bone]. Section of bone retrieved from patient's maxillary sinus 6 months after sinus elevation.

Histomorphometrically the BBM group showed that newly formed bone had become closely attached to both HAs. Histomorphometric measurements on the bone biopsies showed that for the PBM, the newly formed bone represented ($25.92 \pm 1.61\%$), residual graft material ($24.64 \pm 0.86\%$) and for connective tissue ($49.42 \pm 1.62\%$), while for the BBM newly formed bone ($26.83 \pm 1.42\%$), residual graft material ($30.80 \pm 0.88\%$) and non-mineralized connective tissue ($42.79 \pm 2.88\%$). Statistically significant differences were seen when comparing BBM and PBM regarding NB (Mann-Whitney test, $p=0.02$), RG (Student's t test, $p<0.0001$), and CT (Mann-Whitney, $p<0.0001$). The mean and SD values for all parameters in each group are on (Graphic 1).



Graphic 1: *Histomorphometric measurements on the bone biopsies. Histomorphometry shows the percentage of newly formed bone, marrow spaces, and residual grafted material. The figure shows mean and SD values for all parameters in each group. Statistically significant differences were seen when comparing BBM and PBM regarding NB (Mann-Whitney test, $p=0.02$), RG (Student's t test, $p<0.0001$), and CT (Mann-Whitney, $p<0.0001$).*

SEM-BSE cross-sections micrographs after 6-months sinus augmentation of both materials are shown in figure 19. It is important to highlight the absence of either inflammatory cells or fibrous connective tissue formation in the vicinity of the xenograft materials and around the newly formed woven bone, which would, otherwise, implies bone tissue intolerance to the implants. The behavior of both implants is different. BBM is still present in the implantation area after 6-months, meanwhile the PBM material is almost degraded.

Figure 19A confirmed that the BBM residual graft particles (*) were surrounded by newly formed bone, which presented characteristics of mature bone, and EDX analysis supported these findings. Six month after implantation in the BBM group, most of the residual biomaterial had been resorbed. The patterns of resorption in the interface of BBM group showed resorption regions mainly on its surface, and also more uneven surface morphology in comparison with the PBM. The newly formed bone was found in most parts of the convex augmented space. Newly formed bone had become closely attached to HA particles from the implant. For PBM xenograft (Figure 19B) the behavior is different, in them almost a complete resorption zone is observed. The patterns of resorption in the interface of the PBM group showed numerous resorption

regions starting from inside of the graft toward its periphery. PBM group had the highest rate of resorption in comparison with the other BBM group.

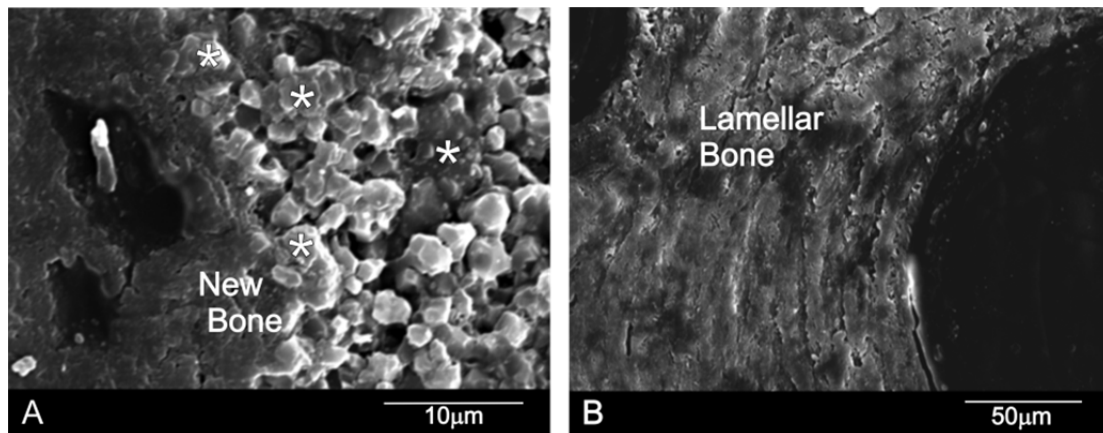
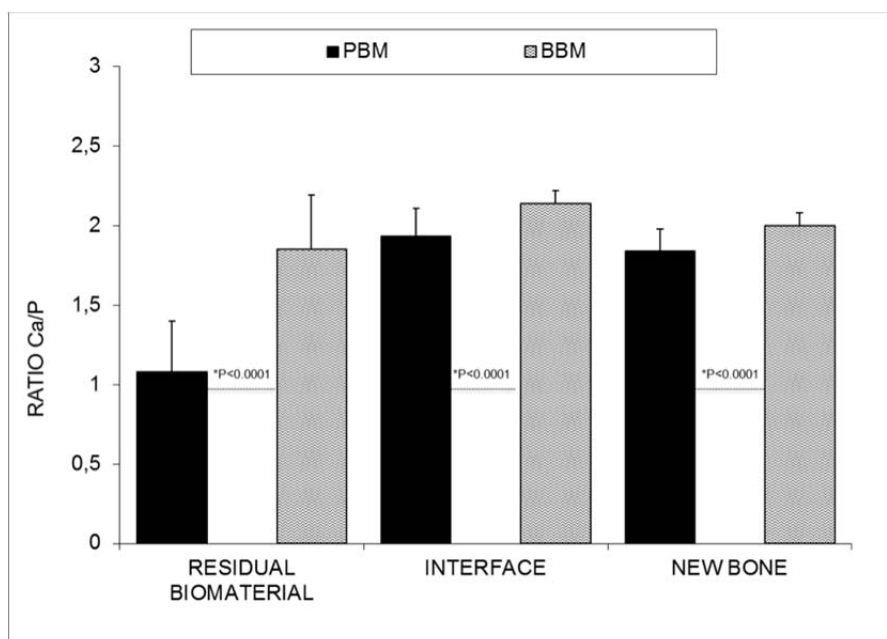


Figure 19. SEM-BSE cross-sections. *A- BBM. B- PBM xenograft materials after six months sinus augmentation [*= residual graft particles]*

5.3.2. EDX Analysis

Graphic 2 shows the results of the Ca/P ratio of the retrieved bone biopsies following maxillary sinus augmentation. EDX analysis found a significant decrease in the residual biomaterials (RB) with respect to the initial composition (Table 4). The PBM showed numerous regions of resorptions, and presented an average Ca/P rate of 1.08 ± 0.32 with respect to the average Ca/P rate 1.85 ± 0.34 of BBM. Statistically significant differences were found too in the interface and in the new bone between the groups. Ca/P ratio in the interface was 1.93 ± 0.18 for the PBM with respect the 2.14 ± 0.08 of the BBM, and the ratio in the new bone was 1.84 ± 0.14 for the PBM with respect the 2.00 ± 0.08 of the BBM. In all cases, a decrease in the percentage of Ca/P ratio was found in the residual biomaterial, with respect to the initial composition (Table 4), while a gradual increase in the percentages of Ca/P ratio was found at the interface, suggesting an increase in the osteoinductive capacity of the materials and replacement by new bone at its periphery.



Graphic 2. - Comparisons between BBM and PBM groups for each parameter (Residual Bone, Interface, and New Bone). The Kolmogorov-Smirnov test rejected normality for all groups. Statistically significant differences were found for each parameter between group comparisons (Mann-Whitney test, $p < 0.0001$).

5.3.3. Line scan

To investigate in detail the distribution of Ca/P in selected areas and individual biomaterial particles, line scans were carried out in a selection of different points from the implant through the middle to the periphery of the samples to detect changes to Ca/P ratios as shown in the figure 5 following the recommendation of Lindgren et al. 2010. EDX analysis of the residual graft material particles in the retrieved tissue revealed Ca/P in every variable relative proportion. Analysis indicated that this individual particle contained both Ca/P with more concentrated at the interface area, consistent with the replacement of Ca/P with precipitated as it gradually dissolves.

The data of interest are in the interface area where there will be a greater diffusion of ions. According to the EDX analysis and high magnification SEM examination of the interfaces developed between both studied grafts and the surrounded tissue, the reaction zone was characterized by the intermittent presence of calcium phosphate phase, which corresponded in structure and morphology to a new bone tissue. The intermediate-new bone contained calcium and phosphorous elements with average Ca/P ratio for PBM 1.93 ± 0.18 and BBM 2.14 ± 0.08 . These results indicated the bone chemical maturity, reaching the stoichiometric Ca/P ratio of natural bone. This compositional micro

characterization of the interface indicated that calcium and phosphorous along the periphery of the implant interfaces remained well textured, as degradation of the material continued inside the implant. This results in an increase in the porosity inside the material, which can be observed by comparing the SEM images of the figure 20. A faster degradation of PBM in relation with BBM can be observed, fact that it is related with the crystallinity of the material.

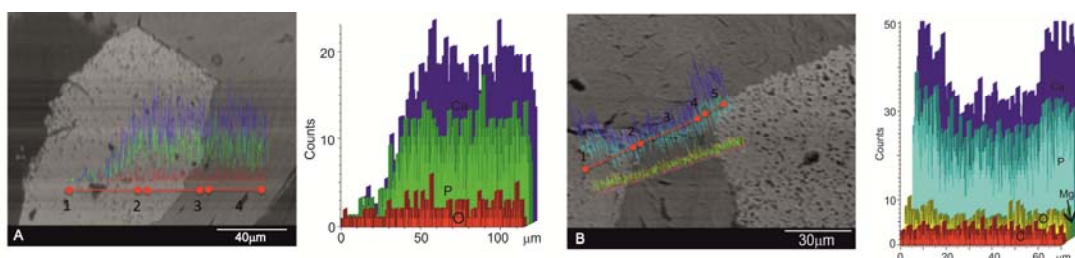


Figure 20. - SEM line-scan. **A**- BBM. **B**- PBM xenograft materials after 6-months implantation showing the relative concentration of the principals ions along a line passing through graft biomaterial particle (point 1) and interface (point 2) to the new bone (point 3) interface (point 4) and a graft biomaterial particle (point 5) To clarify, the scan results are also shown separately in the figure next to each SEM image.

5.3.4. Elemental X-ray maps

SEM image of the polished cross-sections of the implants after 6-months implantation is shown in figure 21. Equivalent elemental X-ray maps of calcium and phosphorous are also presented. At 6-months implantation, the outside surface of the BBM implant (arrows in Figure 21 A) presented active regions, where the degradation process of the material originated. These observations lead to the conclusion that the interfacial activities at 6 months were already well in progress, resulting in a remodeling of the interface in terms of its morphology and chemistry (calcium and phosphorous ions). The implant peripheral regions suffered intensive bone resorption, which produced significantly more irregular surface compared with the PBM implant (Fig. 21B).

Figure 21B shows a biopsy of PBM-BSE image showing the resorbed PBM graft in relation to surrounding bone, granular residual material consisting of areas of very few and smaller particles. These indicated the almost complete resorption of the PBM similarly in the middle, and at the periphery of the samples.

According to the elemental X-ray maps and SEM images of the interface between the BBM and PBM implants and the natural bone, the reaction zone was composed of Ca and P phase as well as a short distance away from the reaction zone. There were no obvious morphological differences between the newly formed bone and the old bone into which the implants were inserted.

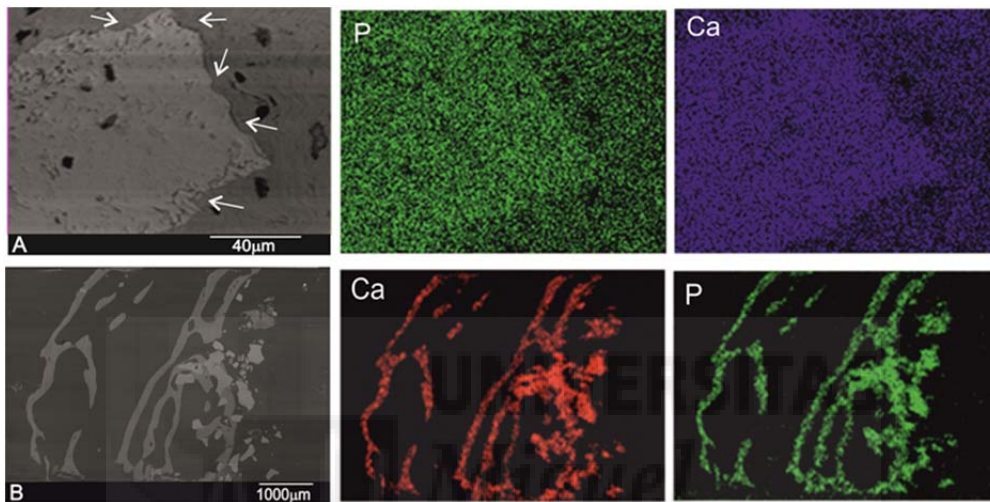


Figure 21. : SEM image of polished cross-section of a biopsy. **A-** BBM. **B-** PBM xenograft material after 6 month implantation and elemental X-ray maps of Calcium and Phosphorous. [Arrows refers to irregular boundary with partial degraded implant]

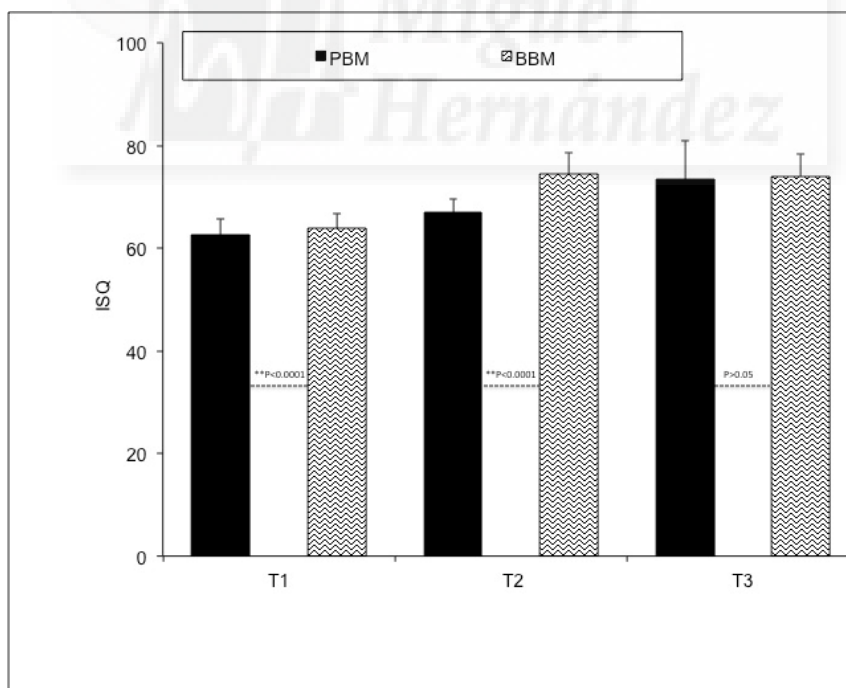
5.4. Resonance Frequency analysis Results

Primary implant stability in relation with bone density can also be evaluated by the implant stability quotient (ISQ). Detailed distributions for the implants and ISQ values over investigated time periods are depicted in (Table 5). Three implants were no osseointegrated at the end of the study, leaving 57 implants for control (95% rate of success). Dropouts were not observed during evaluation period.

Table 5. Demographic data.

Number of patients (total)	10					
Number of implants (total)	60					
<i>Osseointegrated (%)</i>	57 (95)					
<i>No osseointegrated</i>	3 (5)					
Vestibule-Lingual (ISQ values)	T1		T2		T3	
	PBM	BBM	PBM	BBM	PBM	BBM
<i>Mean</i>	62.4	63.4	66.9	73.9	72.6	73.8
<i>SD</i>	2.92	2.88	2.67	4.11	7.67	2.99
<i>Median</i>	62.5	63.2	66.6	70.6	73.7	74
Mesio-Distal (ISQ values)	T1		T2		T3	
	PBM	BBM	PBM	BBM	PBM	BBM
<i>Mean</i>	62.8	64.2	67.1	75.2	74.2	74.2
<i>SD</i>	3.23	3.18	2.33	4.29	7.59	3.01
<i>Median</i>	62.5	64.8	69.1	72.4	75.8	75.5

ISQ: Implant stability quotient; T1: baseline; T2: at 3 months; T3: at 6 months.



Graphic 3. Implant stability quotient for both xenograft materials

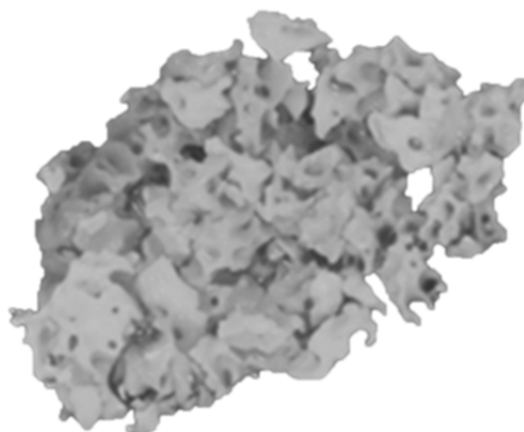
Overall, the mean and standard deviation of ISQ values. ISQ (Baseline) averaged values were 63.8 ± 2.97 for a sintered (BBM), and 62.6 ± 2.11 for a non-sintered PBM differences were statistically significant. ISQ (Stage 2) average values were 73.5 ± 4.21 for BBM and 67 ± 4.99 for PBM, differences were statistically significant. ISQ (Stage 3) average values were 74.65 ± 2.93 for BBM and 72.9 ± 2.63 for PBM; differences were statistically significant. The detailed distributions for the Groups are depicted in (Graphic 3). The analysis of variance demonstrated a statistically significant difference ($p < 0.0001$). The regression equation (R^2 adjusted = 0.58, Multiple correlation coefficient = 0.78) demonstrated significant influences regarding age ($p = 0.0120$; $r = -0.13$), gender ($p < 0.0001$; $r = -0.48$), group ($p = 0.0017$; $r = 0.16$), position ($p = 0.0002$; $r = 0.19$) and time ($p < 0.0001$; $r = 0.69$) on ISQ values.





UNIVERSITAS
Miguel
Fernández

DISCUSSION





5. DISCUSSION

In the present study, two different xenogenic bone substitute materials were characterized and *in vivo* evaluated in sinus floor elevation procedures. This study compared BBM processing at high temperature (1200 °C) and PBM processing at low temperature (130°C) with different physicochemical properties as bone substitutes for the healing of sinus lift procedures. In this paper, the effect of sintering temperature on the relative density, porosity, crystallinity, composition and phase purity of porous hydroxyapatite ceramics made of natural bone was studied and reported. The HAs' characterization ensured an overall understanding about the role played by both on the biological behavior of these bone substitutes. Moreover, this investigation gains further importance because of the scarce scientific documentation in the literature over the comparison between BBM and PBM in sinus lift procedure.

The graft materials were randomly grafted in all patients. The random use of graft can minimize the bias of operator. The lateral sinus grafting in the same patient, the “split mouth design,” is the ideal way to compare a treatment against its control because bias and variability are minimized.

In this study, a reabsorbable collagen membrane was positioned. The repositioned preservation of maxillary sinus membrane is important to avoid displacement of particular graft materials into the sinus cavity. Even none observed small perforations can cause risk if left untreated. Using an internal and external membrane in this study, the negative factors to regenerate the new bone could be minimized. Some studies have shown that the application of a barrier membrane over the lateral window has advantages, such as reducing the invagination of soft tissue, increasing vital bone formation, and higher survival rates of implants. (Wallace et al. 2012)

However, controversy remains regarding the effect of placement of a barrier membrane over the lateral window. A histomorphometric meta-analysis concluded that the effect of barrier membranes in lateral window sinus augmentation does not influence the amount of vital bone formation after sinus augmentation, additionally; the type of grafting material used and healing time did not influence the histomorphometric outcome. (Suárez-López et al. 2015)

This study demonstrated that sinus augmentation with both BBM and PBM produce an increase in the vertical bone dimension compared to baseline values, which accommodates dental implant placement.

Natural HAs grafts may be a suitable alternative for the use of autogenous graft. However, the use of these materials is sometimes avoided due to lack of information or to contradiction between manufacturers' specifications and clinical results. (Tadic & Epple 2004) The HA derived either from natural sources or sintetic sources can form a strong chemical bond with host bone tissue. This makes it recognized as a good bone substitute material. Xenografts have different properties depending on their origin, constitution and processing. Xenografts that usually come from cows and pig could be osteoinductive and osteoconductive and with low cost with high availability but have the disadvantages of immune response and risk of transmission of animal diseases. Significant differences in the use of biomaterials of animal or synthetic origin have yet to be reported some evidences suggest that synthetic materials have a lower risk of disease transmission. (Rodella et al. 2011) However, synthetic hidroxyapatites do not completely match the chemical composition of human bone. (Simunek et al. 2008) Deproteinization is an indispensable process for the elimination of antigenicity in xenograft bones. Valid strategies to eliminate the antigenicity of xenograft bones are of vital importance in the development of xenogenic bone graft substitutes. (Barakat et al. 2008) Eliminating the antigens that potentially cause an immune response is a prerequisite for xenogenic bone grafting. It has been shown that deproteinized bones not only lose their immune reactivity but also retain their osteoinduction and osteoconduction activities. (Castro-Cesena et al. 2013) Many investigations on HA have centered on a wide range of powder processing techniques, composition and experimental conditions with the aim of determining the most viable synthesis method and conditions to produce well-defined particle morphology. Some authors have reported the same observations in reaction to the microscopic structure, in commercial products subjected to thermal processes of deproteinization. The sintering temperature is seen as important factors that could alter the HA's characteristics. (Hong et al. 2003) However, effect of sintering temperature to physico-chemical properties of Natural HA (HA from natural source) especially HA from bovine bone has not been fully understood and researches in this area are still wide open. The most important parameters that can affect the properties of HA are the temperature and duration of heat treatment. (Herliansyaha et al. 2009)

Both used materials differ significantly in terms of processing temperature; our results showed that the hidroxyapatite examined had variable physicochemical properties

according with Muralithran & Ramesh's study. (Muralithran G & Ramesh S. 2000) This discrepancy may affect the materials' performance, so significant differences were found in terms of new bone formation, residual graft material and non-mineralized connective tissue after six months of healing.

The extensive characterization of the graft materials BBM and PBM performed in this work revealed that these two commercial bone grafts, although used in the clinical practice for the same purposes, possess markedly different properties either chemical (e.g., composition, crystallinity, Ca/P ratio) and physical (e.g., particle size and shape, surface area, density and pore size distribution). It is thus not surprising to find out that they induce different responses after sinus lift elevation. The differences found in the explored characteristics seem to justify this distinct in vivo performance. Some studies have demonstrated that osteointegration and degradation processes are influenced by physical and chemical properties of the material. (Ducheyne & Qiu 1999; Rosa et al. 2002; Karageorgiou & Kaplan 2005; Yang et al 2005; von Doernberg et al. 2006; Carvalho et al. 2007; Habibovic et al. 2008; Ghanaati et al 2012; Danoux et al. 2016) Despite different responses were somehow anticipated since these materials, as the results show, have quite distinct properties, the following discussion will try to interpret the in vivo response of these two biomaterials in terms of their physical and chemical characteristics.

Histologic and histomorphometric evaluation of the newly formed tissues in sinus augmentation procedures is useful in understanding the nature of newly formed tissue and the grafts. The histologic examination of 60 biopsies taken from the 10 patients in this study indicated statistically significant differences in histomorphometric parameters were found between the BBM and PBM graft materials. PBM is a porcine bone graft undergoes a low heat while BBM is a sintered bovine bone graft at high-temperature. The manufacturing process, based on high-temperature heating, removes all organic components and proteins, and eliminates potential immunologic reactions. Deproteinization occurs at a very high temperature that enhances material crystallinity. (Accorsi-Mendonça et al. 2008)

The histomorphometric results of the study for BBM are not in accordance with the literature. (Panagiotou et al. 2015) In the present study, histomorphometric analysis of the biopsies after 6 month showed a percentage of newly formed bone represented $25.92 \pm 1.61\%$, residual graft material $24.64 \pm 0.86\%$ and connective tissue $49.42 \pm 1.62\%$ for

the PBM, while for the BBM newly formed bone $26.83 \pm 1.42\%$, residual graft material $30.80 \pm 0.88\%$ and non-mineralized connective tissue $42.79 \pm 2.88\%$.

Contrary to a similar radiological and histomorphometric desing study at 8 month after sinus lift procedure of two xenograft of bovine origin deproteinized at diferent temperatures. DBB-1 deproteinization occurs at a low heat (300°C) and DBB-2 at a very high temperature ($1,200^{\circ}\text{C}$), significant differences were not found in terms of new bone formation, residual graft material. In histomorphometric analysis, new bone formation and residual graft materials were 29.13% and 24.63% , and 14.77% , and 13.01% in DBB-2 + CM and DBB-1 +CM groups, respectively. Aldo the healing period was two months longer in the study performed by Panagiotou et al. we agree with their study that the particles related to both graft materials were still observed in the specimens, demonstrating the slow resorption rate of the BBM materials. Because DBB-1 has a less crystalline structure compared to DBB-2 and might be more prone to degradation, residual DBB-1 particles might resorb faster.

A similar study that compared the sintered and the nonsintered bone substitute materials in the sinuses of eight patients showed significant differences were not found in terms of new bone formation, residual graft material. After the examined two xenogeneic bone substitute materials both are gained from the same bovine origin. They differ mainly in the way of deproteinization. The histological analysis revealed comparable results for the sintered (SBM) and the non-sintered xenogeneic bone substitute material (NSBM). In sites treated by the sintered materials $29.71 \pm 13.7\%$ of the augmented site consisted of new bone, whereas the percentage of new bone was $30.57 \pm 16.1\%$ in the non-sintered group, together with the percentage of bone substitute materials in the augmented area (40.68 ± 16.3 for the sintered, $43.43 \pm 19.1\%$ for the non-sintered group). (Fienitz et al. 2016) Even the histomorphometric results have a lower percentage of residual graft particles for the sintered group against with our results.

According to other studies, also compared two xenograft materials prepared by deproteinizing technique at low temperature (Bio-Oss) or high temperature (Cerabone) in the sinus cavity. They observed a significantly higher volumetric loss of the initial graft size for the non-sintered material according with our study. Bio-Oss has significantly higher surface area and smaller crystallite size compared Cerabone. This might have a crucial influence on the resorption rate. (Riachi et al. 2012) According to the data observed in the present study, PBM has higher surface area $97,78 \text{ m}^2/\text{g}$

compared to 2.77 m²/g of the BBM. Lower density 2,85 g/cm³ compared to 2,98g/cm³ of the BBM and smaller crystallite size 325 nm compared to 732 nm for BBM.

On the sintering characteristic of hydroxyapatite (HA), the resulting microstructure and properties are influenced by the thermal history during the fabrication process. In the present study, according to the results of research concerned with the effect of sintering temperature (Herliansyaha et al. 2009), our results show that the sintering temperature is a critical factor influencing the phase stability, densification behavior, crystallinity and porosity of bovine hydroxyapatite ceramics.

In the BBM process increasing sintering temperature caused an increase in the sample crystallite size and induced HA densification resulting in grains growth with the formation of dense grain boundary phases. These differences were associated with significantly higher resorption rate of the initial graft volume observed for PBM material. Depending on the degrees of crystallinity, albumin solution or cell suspension were suggested to selectively adsorb on the HA surfaces as such, this study demonstrated the importance of determining the effects of the physical and chemical characteristics of HA surfaces on cell activity. (Yang et al. 2005)

Dissolution of HA was dependent on its crystallinity, with dissolution increasing with decreasing degrees of crystallinity. Albumin adsorption and cell attachment were seen to selectively adsorb on the HA surface, and the degree of adsorption was dependent on HA crystallinity. (Conz et al. 2011)

In our study of characterization of both HA the XRD pattern from the mineral samples correspond to hydroxyapatite, with coincident peak positions and relative intensities. However, these materials present diverse degrees of crystallinity, as indicated in the different peak widths. In the case of PBM, the diffractogram exhibits broad peaks with a low signal-to-noise ratio, corresponding to a low-crystallinity material. On the other hand, the sharp and well-resolved peaks found in the XRD spectrum of BBM indicate a highly crystalline hydroxyapatite. Crystallinity is highly dependent on sintering temperature: the higher the sintering temperature, the more perfect the crystal and thus the lower the degradation rate. The resorption increases with the decrease in crystallinity. Resorbable calcium phosphate materials are usually unsintered Ca-P materials (Hamada et al. 2010). So PBM sinterized a low temperature has a less crystalline structure compared to BBM sinterized at high temperature and might be more prone to degradation too. Tissues respond differently to biomaterials of different

crystallinities. Related with physical properties, the tendency for the density was to increase with the increasing annealing temperature.

Major differences in the adhesive response of epithelial cells and osteoblast precursor cells to different crystallographic structures have been reported. (Danoux et al. 2016)

The determination of the crystal structure of a new material is frequently the prerequisite for the rational understanding of the solid-state properties of a material. Physicochemical and crystallographic characteristics of the biomaterials will determine the osteogenic cells behavior, contributing to the success and quality of the new bone tissue. (Rodrigues et al. 2003) However, to clarify this speculation, long-term histomorphometric analysis and biochemical evaluation of the materials is needed.

With respect to the porosity, other factor presumably governing the degradation mostly mentioned in the literature, in our characterization study it is likely that the porcine bone mineral particles' microstructure and delicate porous morphology enhance the degradation of this material according to other studies. (Annaz et al. 2004; Cyster et al. 2005)

Respect the new bone formation methods for bone deproteinization have to allow the heterologous deproteinized bone has good biological safety and meets all the demands of scaffold material for tissue engineering. Moreover, the quantity and quality of the newly formed bones must be improved. The trabecular porous architecture of deproteinized bones acts as a support structure for blood vessels and bone cell expansion, which is extremely important for ossification. (Liu et al. 2003)

PBM has the greatest porosity 59.90% however, about forty per cent 38.11% of this porosity corresponds to submicron pore entrances and BBM porosity was 49.13% but this exhibit a much smaller proportion of submicron pores, only 3.66%.

If the pore size is too small the vascular supply can be compromised and the osteoconduction decreased. This study confirms the findings of earlier studies that tabulated the relation between pore and the quantity of neoformed osseous tissue. They concluded that pore size and granulometry should not be overly reduced, as both pore diameter and interporotic connections have a significant effect on the type and quantity of newly formed bone tissue. (Annaz et al. 2005; Cyster et al. 2005; Cathup et al. 2012; Figueiredo et al. 2013)

Properties such as solubility and surface reactivity are highly dependent on the calcium phosphate composition and surface texture. Such characteristics will strongly affect the nature of the biologically equivalent (carbonated) apatite formed when calcium phosphates enter in contact with bone tissue. (Monteiro et al. 2003) In our study statistically significant difference was found between PBM 2.22 ± 0.08 and BBM 2.31 ± 0.09 in ratio calcium/phosphate composition. The slow dissolution capacity of BBM graft was attributed to the to the small quantity of tricalcium calcium phosphate produced during heat treatment. The annealing temperature will affect the type and amount of other calcium phosphate phase and/or other Ca compounds, which will be present with the HA phase. (Joschek et al. 2000)

Proteins, albumin and collagen are present in the human serum and the first contact between a host tissue and an implanted biomaterial will proceed through them. The presence of collagen on the surface of a biomaterial will produce the attraction of bone-progenitor's cells that will attach to the biomaterial and start bone regeneration. In that way, the presence of as much collagen as possible on the surface should be favored (Detsch & Boccaccini 2015) Deproteinized bones at low temperature showed lower protein content, and a higher collagen content were preserved. (Liu et al. 2003)

The Tecnos patented manufacturing process used to produce PBM achieves biocompatibility by avoiding temperatures higher than 120°C that would cause ceramization of the granules, preserving part of the collagen matrix of the original animal bone. The result is a unique biomaterial consisting of mineral components and an organic matrix with a level of porosity very similar to autogenous bone that resorbs quickly.

In our study the FTIR patterns of the PBM graft is compared with natural human bone. The FTIR of PBM and natural human bone represent the dual-phase composition of these samples. This is because each spectrum presents the more intense characteristic peaks of hydroxyapatite, superimposed on a broad band arising from collagen. It seems that low temperature processing of PBM graft higher collagen content were preserved. The role of the collagen composition of the PBM used in this study is useful for its intrinsic characteristic of agglutination that assist in the structuring of the composite, having influence on the morphology and size of hydroxyapatite crystals and at the same time contributing in the process of osteoclast adhesion onto the biomaterial surface. (Rodriguez et al. 2003)

While in some cases the resorption of a bone grafts may be desirable, in this study the degradation of PBM was associated with a poorer cellular response.

A scaffold that mimics an inorganic and organic matrix has a relevant role in the bone repair process, presenting a surface that allows cell adhesion and also a three-dimensional structure that allows a network connection between the pores and bone cell ingrowth. (Yang et al. 2005)

It was hypothesized that hydrolytic enzymes (collagenase) released from activated PMN cells were involved in the rapid degradation of the porcine collagen portion of the graft. However, there are no studies reporting on the outcome of this material after maxillary sinus floor elevation. (Alayan et al. 2016)

The aforementioned properties of the graft material lead the researchers to choose BBM as the gold standard of the xenografts has been demonstrated to be a biologically inert osteoconductive material for sinus augmentation procedures. (Corbella et al. 2016) Highly crystalline calciumphosphate apatite (BBM) exhibit osteoconductivity which allows the bone cells to grow on a surface by adhesion, spreading, migration, proliferation, and differentiation to form a bone matrix. This biocompatibility was reported related to enhanced cell adhesion to hydroxyapatite. In a previous study, the production of a thin film of poorly crystalline, exhibit a high cellular activity such as adhesion, proliferation, and differentiation with the formation of calcified matrix. (Hong et al. 2003)

For these reasons, PBM was chosen to evaluate whether the regeneration of new bone could be accelerated. A mayor capability of inducing new bone formation was observed in BBM groups, even though the higher quantity of collagen type I in PBM group may suggest a greater potential for bone formation over time as compared with BBM. (Swetha et al. 2010)

Biocompatibility, osteoconduction and low rate resorption in a short time after surgery are favorable properties of xenografts, but long-term studies must be carried out to understand the pattern of biodegradation of xenografts and its influence in bone gain. (Rodrigues et al. 2003)

Long-term maintenance of the early histologic results obtained with xenogeneic bone has been shown at 9 years by (Traini et al. 2007) and at 11 years by (Mordenfeld et al. 2010). Ideally, bone substitute biomaterial is eliminated slowly after implantation in the patient, but its biodegradation rate allows the mechanical strength of the graft to be

maintained during healing, balancing the resorption rate of the biomaterial with the patient's ability to form new bone. (Galindo-Moreno et al. 2013)

This demonstrates that variations in the physic-chemical properties of a bone substitute material clearly influence in the degradation process. Further studies are needed to determine whether resorption of deproteinized bone particles proceeds slowly enough to provide sufficient time for bone maturation. Considering that biomaterials with the same range of initial particle size (small size) were used in both groups, 600-1000 μm for the PBM group and 500-1000 μm for the BBM, the particles might be degraded biologically or chemically.

The histologic examination of 60 biopsies taken from the 10 patients in this study indicated statistically significant differences in EDX analysis parameters found between the BBM and PBM graft materials before and after sinus augmentation. EDX provides information on the chemical elements present in the graft material and surrounding tissues and can reveal changes in phase composition (Munar et al. 2006).

One of the purpose of this study was to investigate the resorption of these grafts by examining the appearance of the remaining particles using these techniques and to observe the interface between bone and biomaterial to determine whether any changes in the Ca/P ratio produced by the dissolution of the component during the healing process could be detected in bone biopsies retrieved from maxillary sinus augmentation. EDX analysis of the residual graft material particles in the retrieved bone biopsies after 6 month in augmented sinus lift revealed a Ca/P ratio in every variable relative proportion and is useful in understanding the nature either resorbable or non-resorbable, with this classification being related to the extent of dissolution of Ca/P materials. (Fulmer et al. 2002)

In the present study, Ca/P variations in the graft material were analyzed in both grafts, observing a decrease related to the dispersion of Ca and P through material degradation. Analysis was carried out at a selection of different points, to take different points of interest from the middle and from the periphery of the samples to detect changes to Ca/P ratios. EDX analysis monitored the resorption process of both xenografts. Elemental analysis showed that there was a gradual diffusion of Ca ions from the biomaterial to the newly forming bone at the interface. Few studies have made use of

EDX analysis as a tool for understanding the degradation process of a biomaterial. (Wierzchos et al. 2008)

According to the EDX analysis the Ca/P ratio was found significant decreased in the residual biomaterial (RB) with respect to the initial composition in the PBM group, showed numerous regions of resorptions with respect to the BBM group, although when we observe BBM group before and after, we can see a moderate decreased in the residual BBM with respect to the initial composition.

Changes in composition of calcium phosphate-based materials from one manufacturer to another or even from different batches of the same manufacturer and directly affect the clinical result, becoming a limiting factor for the use of this material. (Slater et al. 2008)

Natural bone is made up by mainly of fine carbonated hydroxyapatite crystals (65%) and collagen matrices (23%) with an organized three-dimensional geometrical structure and has many biological properties as well as excellent mechanical properties. (Hamada et al. 2010)

Since industries created a self-setting calcium phosphate ceramic with low crystallinity hydroxyapatite, several commercial calcium phosphate ceramic have become available for clinical therapeutics in dentistry, as biomimetic bone materials containing hydroxyapatite/ collagen, with high biocompatibility and characteristics similar to natural bone. This is the case of the PBM used in this study. According to the study of Kalkura (Kalkura et al. 2004) we observed in the previous characterization of the porcine bone mineral the low crystallinity structure of the graft and the presence of two phases HA+Col by XDR analysis.

Due to the low processing temperature, this material is claimed to preserve the structure and composition of the natural bone components. Major differences in the adhesive response of cells to different crystallographic structures have been reported (Danoux et al. 2016). Thus, it has been shown that the addition of collagen to the HA results in a higher bone remodeling activity compared to pure HA, it appears that the addition of collagen to HA graft can enhance phagocytotic processes according to another study. (Rammelt et al. 2004)

Nannmark & Sennerby observed relevant significant levels of resorption of collagenized porcine bone particles (Nannmark & Sennerby 2008). According to the authors, this might suggest that the presence of collagen induced osteoclast adhesion to the biomaterial's surface. Perhaps the presence of collagen plays a key role in initiating resorption. Moreover, the low levels of residual graft material observed in this study confirm substantial resorption of the grafted material after 6 months, which is an added advantage for some authors. Elemental mapping of the residual porcine biomaterial at different points showed some categories of particles with different mean Ca/P ratios according to size. When compared with the original material composition, it became significant differences before and after used the DPHs, these findings marked different stages of the resorption process. However, other research (Orsini et al. 2006) using transmission electron microscopy of human biopsies following maxillary sinus elevation with porcine bone showed few signs of resorption after 5 months. Their histological results indicated only initial resorption of the biomaterial. The absence of collagen in the porcine bone used in Orsini's study could be the explanation for its incomplete resorption and would therefore support our hypothesis. In any case, the rapid resorption of porcine bone containing collagen would appear to claim this material with an advantage over other biomaterials that do not contain collagen. Other authors have described this characteristic in studies of hydroxyapatite. When a bone porcine paste composed of 80% granulated mix and 20% pure collagen (Arcuri et al. 2005) was examined at 3 months, complete resorption and substitution with trabecular bone tissue were observed.

Because of the low resorption rate of inorganic bovine bone, it has been reported to undergo no, or limited, resorption. (Jensen et al. 2012; Mordenfeld et al. 2010; Orsini et al. 2005) The present study's findings were consistent with several reports in the literature (Cordaro et al. 2008; Traini et al. 2008; Briem et al. 2002) in which SEM analysis revealed a close relationship between the newly formed bone matrix and the bovine xenograft particle surface. Although histologic and histomorphometric findings have often corroborated the clinical success of bovine bone mineral, the published literature includes few descriptions of its ultrastructural features. The purpose of our evaluation was therefore to add to the clinician's knowledge of this biomaterial through an understanding of the interactions that occur in close proximity to bovine bone mineral. EDX bone tissue analysis showed the presence of calcium and phosphorus,

pointing to the presence of mineralized bone tissue on the particle surface. The results demonstrate a gradual diffusion of Ca ions from the biomaterial to the newly forming bone at the interface. This observation suggests that the graft surface could provide an optimal stratum for bone tissue ingrowth. (Briem et al. 2002) Moreover, the levels of residual graft material observed in this study confirmed substantial resorption of the BBM after 6 months. Elemental mapping of the residual BBM sinterized biomaterial at different points showed some categories of particles with different mean Ca/P ratios according to size. When compared with the original material composition, a significant resorption of the biomaterials was underway. It became evident that these findings marked different stages of the resorption process. In agree with our clinical findings a decrease in osteoclast count over time would explain the long-term (6 months, 3 years, and 7 years) persistence of bovine bone biomaterial. (Orsini et al. 2005) Conflicting results have been reported regarding the long-term behavior of bovine xenograft. Early studies reported that bovine xenografts are non-resorbable (Briem et al. 2002). Taylor's study describes signs of resorption (Taylor et al. 2002), whereas other reports a lack of it (Mordenfeld et al 2010). Traini's study discovered remnants of the bovine bone biomaterial remaining after as long as 9 years. According to a follow up study of sinus floor augmentation with bovine xenograft, the authors observed that there was a gradual diffusion of Ca ions from the bovine xenograft into the adjacent newly forming bone at the interface as part of the resorption process. (Traini et al. 2008)

However, other research (Cordaro et al. 2008) of human biopsies following maxillary sinus elevation with bovine bone found few signs of resorption after 6 months, with histological results indicating only initial resorption of the biomaterial. In the current study, we found an incomplete bone graft resorption phenomenon whereby the biomaterial was seen to decrease partially. In spite of this limited resorption capacity, we did observe a widening of intergrain boundaries as well as the partial dissociation of superficial hydroxyapatite crystallites on the implant surface. This was made visible by elemental analysis at different points in the periphery of the samples. In the present study, sites of interest for point analysis were selected at random at the graft site, and it was interesting to determine whether any differences in Ca/P ratio could be detected in peripheral or in the central regions that might indicate different rates of resorption. In the case of the BBM the resorption occurs mainly in the peripheral regions. But the

BBM studied is not completely resorbable over the time period covered by this study according with other study.

According to the Moon's study, also comparing two xenograft materials prepared by deproteinizing technique at low temperature (Bio-Oss) or high temperature (Cerabone) in the sinus cavity, it was observed a significantly higher volumetric loss of the initial graft size for the non-sintered material, as it was also observed in our study. Bio-Oss has significantly higher surface area compared with Cerabone. (Moon et al. 2015)

According to our study Lee et al in a randomized controlled clinical trial compare sinuses grafted with DPBM (Deproteinized porcine bone mineral) and DBBM (Deproteinized bovine bone mineral), smaller sizes of residual biomaterials were observed in the histological samples from the DPBM compared to DBBM sites, despite the use of the same sizes of both biomaterials. (Lee et al. 2016)

This might have a crucial influence on the resorption rate. (Riachi et al. 2012) So we came to the conclusion that the results of the resorption in the deproteinized biomaterials varied according to the manufactured process (sinterized or not sinterized).

After implantation, biodegradation is critical as this allows for the space to be formed into which the bone and vascular tissues can grow. Biodegradation can be envisioned as an in vivo process by which a material breaks down into simpler components, reducing the complexity of chemical compounds by the action of cells, by simple physical breakdown and/or chemical erosion. (Le Geros 2002)

A completely resorbable ceramic has been the goal of several studies; however, a high rate of resorption or solubilization can interfere with bone formation as the biomaterial may degrade faster than the rate of bone formation. These phenomena lead to a change in the bioceramic physical structure which will interfere with cell attachment. (Chou et al. 2005) Moreover, the release of high concentrations of calcium to the microenvironment results in a change of the pH, promotes a mild inflammatory response and favors fibrous tissue formation. (Berger et al. 2001) Furthermore, higher calcium ion levels have been shown to effect osteoclastic activity, varying from its inhibition to its stimulation or no effects. Instead the presence of moderate extracellular Ca^{2+} resulting from resorption activity might be involved in the stimulation of osteoblasts. Yamaguchi et al. showed that moderately high extracellular Ca^{2+} is a

chemotactic and proliferating signal for osteoblasts and stimulates pre-osteoblast differentiation. (Xu et al. 2004)

PBM material is the fastest undergoes remodeling so it can be considered as the most active in terms of resorption but not in the new bone formation. BBM seemed to be a gradually resorbed material, partially substituted by newly formed bone according to our results. It could be that this ion increase creates areas of biological apatite on the agglutinated Ca and P deposits and crystals, which in turn facilitates osteoconduction. (Briem et al. 2002)

Some materials, such as autogenous bone, cannot withstand sinus pressure during the first several weeks and lose density and height over time. (Sbordone et al. 2013) An ideal bone graft material should be biocompatible, increase bone volume in the grafted area to promote initial stability at implant sites, and be resorbed with time and replaced by native bone. However, the process of bone resorption and the distribution of osteoclasts after deproteinized bone implantation have not been examined in detail, which are relevant to enhance our understanding of the complex role of osteoclasts in bone tissue engineering. (Detsch & Boccaccini 2015)

In vitro study with osteoclastic precursor cells on bone substitute materials showed that there are specific parameters that inhibit or enhance resorption. Moreover, analyses of the bone-material interface reveal that biomaterials composition has a significant influence on their degradation in contact with osteoclasts. Crystallinity, grain size, surface bioactivity and density of the surface seem to have a less significant effect on osteoclastic activity. In addition, the topography of the scaffold surface can be tailored to affect the development and spreading of osteoclast cells. (Schilling et al. 2004)

This suggests that resorption of collagen deproteinized bone material occurred faster than bone formation. Collagen is mostly absorbed by enzymatic digestion. It is noteworthy that TRAP-positive osteoclastic cells were seen on the surface of collagen deproteinized. This implies that collagen fibrils were resorbed not only enzymatically but also phagocytically. This is the case of non-sinterized PBM. (Schaefer et al. 2011)

Further long-term studies are needed to determine whether resorption of deproteinized bone particles proceeds slowly enough to provide sufficient time for bone maturation. Our results demonstrate that slowly resorbed sinterized BBM particles promote the

stable augmentation of the maxillary sinus floor and inhibit the resorption of the newly formed bone, maintained the space, and stably augmented the maxillary sinus floor. The newly formed bone showed minimal osteoclastic resorption. These findings indicated that the particles inhibited pressure-induced osteoclastic bone resorption in the sinus spaces augmented by non-sinterized PBM. Our study showed that most of the newly formed bone in augmented sinus spaces grafted with PBM had disappeared 6 months after implantation. The grafting material is an important determinant of the success or failure of bone augmentation procedures. With various bone grafting options available to surgeons, one must carefully match the clinical problem with the capabilities of graft material. Sintering process provides strength to a finished material, but when applied to bone, decreases remodeling and resorption capability of the biomaterial but one of the most important factors is the possibility of them being resorbed and substituted by newly formed bone.

In this study it has been assumed the difference in the physical and chemical properties between both grafts influence in the biological response produced by a biomaterial so significant differences were found in terms of degradation process after six months of healing. According to others studies, among several factors, phase composition (Monteiro et al. 2003), chemical composition (von Doernberg et al. 2006), porosity (Costa-Rodrigues et al. 2012), dispersant concentration on the pore morphology (Cyster et al. 2005), particles size (Detsch et al. 2015) ultrastructural geometry of the particle (Raynaud et al. 2002), surface roughness (Costa-Rodrigues et al. 2012) and cristallinity (Chen et al. 2008) are likely to affect the ceramics solubility. Different applications require materials with different resorption rates (Conz et al. 2011) which may be adjusted for the desired purpose.

The last aim of this randomized split-mouth designed was to compare the stability of dental implants placed in the maxillary sinus after sinus floor grafting with BBM and PBM by means of RFA, immediately after implant placement (T1) and at 3(T2) and 6 months (T3) after implant installation. This clinical study describes a comparison of the resonance frequency analysis of implants placed delayed with the maxillary sinus grafting with two biomaterials deproteinized at different temperature at three different time periods. A total of 60 implants were installed in 10 patients. Three implants were lost throughout the study time period, and the survival rate of dental implants in the

present study was 95%. Furthermore, the results showed a positive correlation between the biomaterial used and ISQ values. The results of a systematic review of survival of implants in bone grafts, Aghaloo & Moy, found that survival of implants in the maxillary sinus grafting technique was 95.6%. (Aghaloo & Moy 2007) At present, there is no agreement regarding the advantages of the use of grafting material in maxillary sinus elevation techniques with dental implant insertion as the question whether these techniques and materials may determine implant survival in comparison with pristine bone is still unsolved. (Nasr et al. 2016; Rammelsberg et al. 2012) To find the answer to this question, it was retrospectively examined long term stability up to 20.2 years after the placement of implants both in augmented and non-augmented sites. The results of this retrospective study determined that implants inserted in augmented site were found to have similar implant survival compared to those inserted in non-augmented sites. (Knöfler et al. 2016) Supported by evidence, it can be stated that implants inserted in augmented bone have similar implant survival in comparison with those placed in native bone. (Jensen et al. 2009) In our study the grafting material implicated may not compromise the implant survival.

For clinicians, one of the most important parameters to measure the scope of mechanical loading capability is implant stability. The baseline information that it provides serves as a tool to evaluate clinical outcomes and time course. (Atsumi et al. 2007) Several attempts have been made in order to find innovative techniques that allow the measure of implant stability. (Cehreli et al. 2009) As the optimal technique should be one that is simple and noninvasive, Periotest could be considered as a candidate. (Andreotti et al. 2016) Nevertheless, Periotest readings cannot always be considered as a biomechanical parameter because of its strong relation to the excitation direction and position. (Oh & Kim 2012) For that reason and as an alternative, resonance frequency analysis (RFA), a noninvasive technique that presents high reproducibility results, was proposed. (Gupta & Padmanabhan 2013; Herrero-Climent et al. 2012; 2013) This technique has developed into one of the most widely used techniques to measure implant stability immediately, this makes possible determining the probable loading protocol and to assess the long-term survival of implants. ISQ values between 60 and 80 are broadly accepted as a standard for achieving primary stability. In clinical practice, it can be considered ISQ values over 55 at the moment of implant placement as representing clinically relevant stability and as a sign of successful osseointegration. (Sennerby &

Meredith 2008) The comparison of the type of bone graft and initial implant stability was performed in this study. The results of this study showed that implants placed delayed (2-stage) with the maxillary sinus lift with different biomaterials presented different ISQ. The difference was statistically significant. To compare the efficacy of 1-stage versus 2-stage lateral maxillary sinus lift procedures in Felice's study, no statistically significant differences were observed between implants placed according to 1- or 2-stage sinus lift procedures. However, this study may suggest that the risk of implant failures is slightly higher in patients with a residual bone between 1 and 3 mm below the maxillary sinus in a 1-stage lateral sinus lift procedure. (Felice et al. 2013)

From a clinical point of view, it seems to be relevant to know the significance of RFA measurements and the relationship between its values and the success or failure of implant osseointegration. In a previous study, it has been observed that implants retrieved after 6 months showed a strict correlation between RFA values and the percentage of bone implant contact (BIC). (Degidi et al. 2010) The aim of the present study was to determine whether the same correlation existed at earlier time points, specifically in implants inserted after 3 or 6 months. A statistically significant correlation was detected between RFA values and healing time. During the bone-healing period, the implants' ISQ value varied with time. At the surgical phase (baseline), the average ISQ for all implants were 63.8 ± 2.97 for a sintered (BBM), and 62.6 ± 2.11 for a non-sintered (PBM); differences were statistically significant. ISQ (Stage 2) average values were 73.5 ± 4.21 for (BBM) and 67 ± 4.99 for (PBM), differences were statistically significant. ISQ (Stage 3) average values were 74.65 ± 2.93 for (BBM) and, 72.9 ± 2.63 for (PBM); differences were statistically significant.

Kohal et al. investigate the amount of mineralization of a bovine bone substitute material in sinus floor augmentation after healing times of 3 and 6 months. The biopsies of both groups showed remnants of the well-integrated bone substitute material but bone maturation in the augmented sinus using the bovine bone material was similar after 3 and 6 months. Results demonstrate that bone maturation in the augmented sinus with a bovine substitute material is similar after 3 and 6 months, and that placing the implant after 3 months of this procedure in which bovine bone material is used, can be considered clinically acceptable. (Kohal et al. 2015)

According to this, the present study examined the same implants 3 and 6 months after their installation, for the implants inserted with a two-step procedure. RFA values after 3 months showed that the grafted sites provide good stability to implants and that on the average, the BBM are better than PBM group sites. This difference is still present after 6 months and it is also statistically significant. The importance of bony quality in relation to implant stability has previously been highlighted. Given the relative lack of bone there is some concern about the initial stability of implants placed in grafted bone. Resonance frequency analysis enables the qualitative measurement of stability under load, and has been advocated as a mean of assessing the stability of implants at the time of placement and at later phases in the provision of restorations. (Al-Khaldi et al. 2011)

This is the first study to compare ISQ with density values after sinus lift procedures after 6 month of healing and primary stability. The primary, initial stability (IS) is a crucial factor for the establishment of osseointegration (Friberg et al. 2002; Esposito et al. 2013; Javed & Romanos 2015) and might be subject to the influence of the following factors: bone quality, surgery technique and implant macro-design. (Schiuma et al. 2013)

Their study demonstrates the existence of a strong correlation between implant displacement and bone properties, and states as a conclusion that a better bone quality can lead to better implant stability. Anil & Aldosari also proved that implants placed in bone with a high degree of density have higher initial stability values than those placed in soft bone, according to the results of insertion torque (IT), implant stability quotients (ISQ) and removal torque values (RTV). (Anil & Aldosari 2015) However, the ISQ can be improved through changes of the implant macro-design (Romanos et al 2016) as well Sennerby et al. confirmed that comparing tapered implants with parallel implants, when using a different drilling protocol in soft bone, the former showed a higher primary stability than the latter. (Sennerby et al. 2015)

A previous study on the same pool of implants used in our study (tapered implants) demonstrated that grafted bone can offer a good primary stability to the implants and that, during the surgical procedure, only a few mechanical characteristics of the implants (length and diameter) were able to influence the ISQ values. (Gehrke et al. 2015) Degidi et al have suggested that, the length and width of the implant can

influence primary stability because of the increased bone-implant contact surface area. (Degidi et al. 2007)

In the present study, the macro-design, the length and the diameter of the implant were not used as evaluation factors as all implants used were 4 mm in diameter and 11.5 mm in length with tapered internal hexagon implants. Consistent with those studies that have reported no statistically significant differences in ISQ due to length or diameter ISQ. (Balleri et al. 2002; Ostman et al. 2006) From the clinical point of view, implants that have been placed in soft or grafted bone show better mechanical stability values when they present a narrow diameter and tapered macro-design. (O'Sullivan et al. 2000; Romanos et al. 2014) In fact, nearly every implant company offer tapered-design implants in the case of alveolar ridges with deficient bone quality and quantity.

This should be taken into account for alveolar ridges with deficiencies in bone quality and quantity and that is the reason why almost every company in the sector has introduced tapered-design implants.

In our study we used a small particle size of two different deproteinized bone grafts. Jensen et al evaluated the influence of the particle size of DBBM on bone formation and implant stability when used for sinus floor elevation in a mini-pig model. In the initial healing phase small particle size DBBM showed marginally higher osteoconductive capacity than large particle size DBBM. However, no differences were observed in amount and speed of bone formation, BIC, or implant stability between the two test groups. However, at baseline and at 6 and 12 weeks the BIC values were comparable or even higher than in our study in human. Primary implant stability is dependent not only on the thickness of the bone into which the implant is placed but also on the bone density, the thread configuration and shape of the implant, and the presence of an implant neck. Therefore, all these factors should be taken into consideration when making the clinical decision to perform a one-stage or a two-stage procedure. (Jensen et al. 2015)

As was evidenced in a review of Browaeys et al. on the use of biomaterials in sinus augmentation, within the limitation of the animal studies examined and only based on histological examination, the biomaterial used in grafting procedure does not influence initial osseointegration of dental implants. In general, autogenous bone is the most

predictable material of choice for augmentation procedures, despite a 40% resorption, because it is highly osteoconductive and less dependent on sinus floor endosteal bone migration. Autogenous bone together with bovine bone mineral can be favorable for graft success insofar it acts as a space maintainer due to the slowly reabsorption. When combined with autogenous bone, porous hydroxyapatite seems to be appropriate as it improve bone formation and bone-to-implant contact in augmented sinuses. (Browaeys et al. 2007)

The grafting material is an important determinant of the success or failure of bone augmentation procedures. Increased air pressure can cause bone resorption and antrum repneumatization after sinus augmentation. Various graft materials, including autografts, allografts, alloplasts, and xenografts, have been used for sinus augmentation to increase bone volume and height. However, among these materials, there are some of them, such as freeze-dried demineralized bone and autogenous bone, that cannot withstand sinus pressure in the first weeks and tend to lose density and height as time goes by Xu et al. (Xu et al. 2004) In our study sinus spaces augmented by deproteinized bovine bone grafts, the BBM particles provided an ideal scaffold for osteogenesis. As we showed in a previous study the newly formed bone showed minimal osteoclastic resorption. These findings indicated that the particles inhibited pressure-induced osteoclastic bone resorption in the sinus spaces augmented by deproteinized bone grafts. Further long-term studies are needed to determine whether resorption of deproteinized bone particles proceeds slowly enough to provide sufficient time for bone maturation. Our results demonstrate that slowly resorbed deproteinized bone particles promote the stable augmentation of the maxillary sinus floor and inhibit the resorption of the newly formed bone. The grafting material is an important determinant of the success or failure of bone augmentation procedures.

The correlation between RFA values and good bone quality reported by the present study seems to confirm the different importance of factors determining RFA values at implant insertion and if it is able to maintain this stability after 3 or 6 months. In fact, good quality bone probably reacts better to implant insertion, and after the bone remodeling, the stability of the implant could be higher.

Long-term stability is also reported by Degidi et al., in this study 108 dental implants were placed after 6months of a sinus floor augmentation with a mixture of autogenous

and deproteinized bovine bone; after 3 years of loading, the implant stability was recorded using an Osstell instrument. The mean RFA values reported were 67.4 ± 14.5 for residual bone and 65.6 ± 13.8 for the augmented sites. Unfortunately, no more data are available at the moment about the importance of bone quality in the determination of long-term RFA values; so more studies have to be carried out. (Degidi et al. 2009)

Healing times of 6–9 months before implant placement are usually recommended for sinus elevation in combination with grafting material. (Jensen & Sennerby 1998) and an additional 3–6 months of implant healing time will be needed. However, the extended integration periods and multiple surgeries do pose a challenge to patient acceptance. (Lai et al. 2008)

Our results also indicate that implants inserted in a grafted sinus, regardless of the substitute material, can be predictably loaded as the implants inserted in a grafted area. Previous studies concluded that the prognosis of implants inserted in augmented sinuses and fixed restoration supported by these implants seemed not to be influenced by factors such as graft material, type of restoration, residual bone height and time of implant placement. Within the limits of this review, the prognosis of implants and fixed restorations seemed not to be influenced by the type of restorations, graft material, residual bone height and time of implant placement. However, conclusions of this review are based on studies with low level of evidence; therefore, careful interpretation is required. Multicentre randomised controlled clinical trials with sufficient statistical power concentrating on few factors are needed to reach sound conclusions. (Tuna et al. 2012)

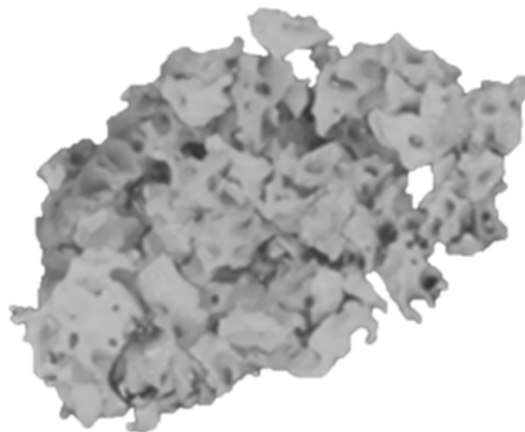
The differences between the two HAs, found in terms of porosity, crystallinity, density, surface area and composition, may determine different behavior of this material and affect the early implant stability in this clinical situation. The HA of bovine origin sinterized with high crystallinity, low porosity, great density and higher granule size presents higher stability, this demonstrates that variations in the physic-chemical properties of a bone substitute material clearly influence the implant stability. A deep knowledge of graft material characteristics when evaluating their clinical outcomes is of utmost importance. Physical and chemical properties of bone substitute materials can influence osseointegration and shorten healing times from implant placement to

restoration. Understanding not only biomaterial properties, but also their relation and influence towards bone healing seems to be crucial.



CONCLUSIONS

CONCLUSIONES





7. CONCLUSIONS

As a conclusion of the work done in this Doctoral Thesis we can say that the data from this study show:

-Both HAs assessed in the study were shown to be biocompatible and osteoconductive when used for maxillary sinus elevation.

-Both HAs assessed in the study used like grafting material for maxillary sinus elevation may not compromise the implant survival.

- The effect of sintering temperature on the physico-chemical properties of Natural HAs influence the biological behavior.

- The resorption in the deproteinized biomaterials varied according to the manufactured process (sinterized or not sinterized).

-The differences found in the physico-chemical characteristics of both xenografts justify this distinct in vivo performance.

-The PBM non-sintered hydroxiapatite with high porosity, low cristallinity, low density, high surface area and low calcium/phosphate ratio presents high resorption rate but might not withstand the sinus pressure leading to a repneumatization of the sinus.

-The BBM sintered hydroxiapaite with low porosity, high cristallinity, high density, low surface area and high calcium/phosphate ratio presents a slow resorption rate that inhibit the resorption of the newly formed bone, tents the sinus lining, maintains the space, and stablies augmented the maxillary sinus floor increased the early implant stability.

Detailed information about graft material characteristics is crucial to evaluate their clinical outcomes. The influence of physico-chemical properties of the bone graft materials on osseointegration has translated to shorter healing times from implant placement to restoration. A sound understanding of various aspects of biomaterial properties and their relation and influence towards bone healing is of utmost importance.



7. CONCLUSIONES

Como conclusión del trabajo realizado en esta Tesis Doctoral, podemos decir que la información recogida en este estudio muestra:

-Ambas hidroxiapatitas naturales utilizadas en este estudio mostraron ser biocompatibles y osteoconductoras al ser utilizadas en el procedimiento de elevación del seno maxilar.

-Ambas hidroxiapatitas naturales utilizadas como material de relleno en el procedimiento de elevación del seno maxilar no comprometieron la supervivencia de los implantes.

- El efecto de la temperatura de sintetizado en las propiedades fisicoquímicas de ambas hidroxiapatitas naturales utilizadas en este estudio influye en el comportamiento biológico de las mismas.

- La reabsorción de los biomateriales desproteinizados varía de acuerdo al proceso de fabricación (sinterizados o no sinterizados)

- Las diferencias encontradas en las características fisicoquímicas de ambos senoinjertos justifican esta distinción en su comportamiento in vivo.

-La hidroxiapatita no sintetizada de origen porcino con alta porosidad, baja cristalinidad, baja densidad, alta área de superficie y bajo ratio calcio/fósforo presenta un alto ratio de reabsorción pero podría no soportar la presión del seno lo que conllevaría la reneumatización del seno.

-La hidroxiapatita natural de origen bovino, con una baja porosidad, alta cristalinidad, alta densidad, baja área de superficie y alto ratio calcio/fósforo, presenta un ratio de reabsorción bajo que inhibe la reabsorción del hueso neoformado, tensa la membrana del seno, mantiene el espacio y el suelo del seno maxilar aumentado estable, incrementado la estabilidad primaria del implante y reduciendo el tiempo de carga del implante.

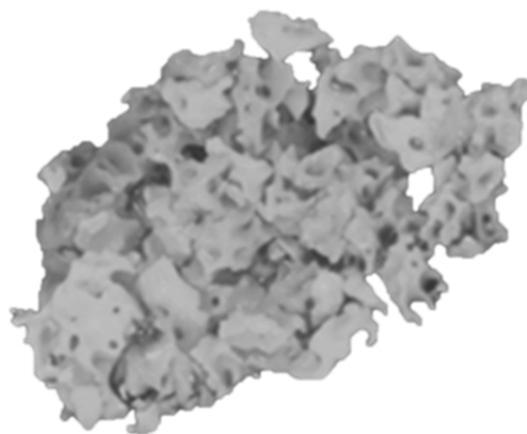
La información detallada sobre las características de los materiales de injertos es crucial a la hora de evaluar sus resultados clínicos. La influencia de las propiedades fisicoquímicas de los materiales de injerto óseo en osteointegración se han traducido en

periodos de curación más cortos desde la colocación a la reparación. Un conocimiento profundo sobre los diferentes aspectos de las propiedades de los biomateriales y su relación e influencia hacia la regeneración ósea es de crucial importancia.





REFERENCES





8. REFERENCES

- Accorsi-Mendonça. T.; Conz, M.B.; Barros, T.C., de Sena, L.A., Soares, G.de A.; Granjeiro, J.M. Physicochemical characterization of two deproteinized bovine xenografts. *Braz.Oral Res.* 2008; 22: 5-10.
- Aghaloo, T.L.; Moy, P.K. Which hard tissue augmentation techniques are the most successful in furnishing bony support for implant placement? *Int J Oral Maxillofac Implants.* 2007; 22: 49-70.
- Alayan, J.; Vaquette, C.; Farah, C.; Ivanovski, S. A histomorphometric assessment of collagen-stabilized anorganic bovine bone mineral in maxillary sinus augmentation - a prospective clinical trial. *Clin. Oral Implants Res.* 2016; 27: 850-858.
- Al-Khaldi, N.; Sleeman, D.; Allen, F. Stability of dental implants in grafted bone in the anterior maxilla: longitudinal study. *Br J Oral Maxillofac Surg.* 2011; 49 319-323.
- Andreotti, A.M.; Goiato, M.C.; Nobrega, A.S.; Freitas da Silva, E.V.; Filho, H.G.; Pellizzer, E.P.; Micheline Dos Santos, D. Relationship between implant stability measurements obtained by two different devices: A Systematic Review. *J Oral Implantol.* 2016; 21: 1-13.
- Anil, S.; Aldosari, A. Impact of bone quality and implant type on the primary stability: an experimental study using bovine bone. *J Oral Implantol.* 2015; 41: 144–148.
- Annaz, B.; Hing, K.A.; Kayser, M.; Buckland, T.; Di Silvio, L. An ultrastructural study of cellular response to variation in porosity in phase-pure hydroxyapatite. *J. Microsc.* 2004; 216: 97–109.
- Antonakos, A.; Liarokapis, E.; Leventouri T. Micro-Raman and FTIR studies of synthetic and natural apatites. *Biomaterials* 2007; 28: 3043–3054.

-Arasawa, M.; Oda, Y.; Kobayashi, T.; Uoshima, K.; Nishiyama, H.; Hoshina, H.; Saito, C. Evaluation of bone volume changes after sinus floor augmentation with autogenous bone grafts. *Int. J. Oral Maxillofac. Surg.* 2012; 41: 853-857.

-Arcuri, C.; Cecchetti, F.; Germano, F.; Motta, A.; Santacroce, C. Clinical and histological study of a xenogenic bone substitute used as a filler in postextractive alveolus. *Minerva Stomatol.* 2005; 54: 351-362.

-Ashok, M.; Sundaram, N.M.; Kalkura, S.N. Crystallization of hydroxyapatite at physiological temperature. *Mater Lett.* 2003; 57: 2066-2070.

-Atsumi, M.; Park, S.H.; Wang, H.L. Methods used to assess implant stability: current status. *Int J Oral Maxillofac Implants.* 2007; 22: 743-754.

-Azran, Y.M.; Idris, B.; Rusnah, M.; Rohaida, C.H. HAp physical investigation the effect of sintering temperature. *Med J Malaysia.* 2004; 59: 79-80.

-Balleri, P.; Cozzolino, A.; Ghelli, L.; Momicchioli, G.; Varriale, A. Stability measurements of osseointegrated implants using Osstell in partially edentulous jaws after 1 year of loading: a pilot study. *Clin Implant Dent Relat Res.* 2002; 4: 128-132.

-Barakat, N.A.; Khalil, K.A.; Faheem, A. Sheikh; A.M.Omranc; Babita Gaihrec, Soeb M. Khild; Hak Yong Kim Physiochemical characterizations of hydroxyapatite extracted from bovine bones by three different methods: Extraction of biologically desirable Hap. *Mater. Sci. Eng. C Mater. Biol. Appl.* 2008; 28: 1381–1387.

-Barone, A.; Ricci, M.; Covani, U.; Nannmark, U.; Azarmehr, I.; Calvo-Guirado, J.L. Maxillary sinus augmentation using prehydrated corticocancellous porcine bone: hystomorphometric evaluation after 6 months. *Clin Implant Dent Relat Res* 2012; 14: 373-379.

-Barone, A; Ricci, M.; Mangano, F.; Covani, U. Morbidity associated with iliac crest harvesting in the treatment of maxillary and mandibular atrophies: a 10-year analysis. *J. Oral Maxillofac. Surg.* 2011; 69: 2298-2304.

- Baqain, Z.H.; Moqbel, W.Y.; Sawair, F.A. Early dental implant failure: risk factors. *Br J Oral Maxillofac Surg.* 2012; 50: 239-243.
- Beretta, M.; Poli, P.P.; Grossi, G.B.; Pieroni, S.; Maiorana, C. Long-term survival rate of implants placed in conjunction with 246 sinus floor elevation procedures: results of a 15-year retrospective study. *J. Dent.* 2015; 43: 78-86.
- Berger, C.E.; Rathod, H.; Gillespie, J.I.; Horrocks, B.R.; Datta, H.K. Scanning electrochemical microscopy at the surface of bone-resorbing osteoclasts: evidence for steady-state disposal and intracellular functional compartmentalization of calcium. *J Bone Miner Res.* 2001; 16: 2092-2102.
- Bertazzo, S.; Zambuzzi, W.F.; Campos, D.D.; Ogeda, T.L.; Ferreira, C.V.; Bertran, C.A. Hydroxyapatite surface solubility and effect on cell adhesion. *Colloids Surf B Biointerfaces* 2010; 78: 177-184.
- Blokhuis, T.J.; Termaat, M.F.; den Boer F.C.; Patka, P.; Bakker, F.C.; Haarman, H.J. Properties of calcium phosphate ceramics in relation to their in vivo behavior. *J. Trauma* 2000; 48: 179-86.
- Boyne, P.J.; James, R.A. Grafting of the maxillary sinus floor with autogenous marrow and bone. *J. Oral Surg.* 1980; 38: 613-616.
- Briem, D., Linhart, W., Lehmann, W., Meenen, N. M. & Rueger, J.M. Long-term outcomes after using porous hydroxyapatite ceramics (Endobon®) for surgical management of fractures of the head of the tibia. *Unfallchirurg.* 2002; 105: 128-133.
- Browaeys, H.; Bouvry, P.; De Bruyn, H. A literature review on biomaterials in sinus augmentation procedures. *Clin. Implant Dent. Relat. Res.* 2007; 9: 166-177.
- Burg, K.J.; Porter, S.; Kellam, J.F. Biomaterials development for bone tissue engineering. *Biomaterials.* 2000; 21: 2347- 2359.
- Busenlechner D, Huber CD, Vasak C, Dobsak A, Gruber R, Watzek G. Sinus augmentation analysis revised: the gradient of graft consolidation. *Clin Oral Implants Res.* 2009; 20: 1078-1083.

-Carreño Carreño, J.; Aguilar-Salvatierra, A.; Gómez-Moreno, G.; García Carreño, E.M.; Menéndez López-Mateos, M.L.; Perrotti, V.; Piattelli, A.; Calvo-Guirado J.L.; Menéndez-Núñez, M. (2016) Update of Surgical Techniques for Maxillary Sinus Augmentation: A Systematic Literature Review. *Implant Dent* 2016; 25: 839-844.

-Carvalho, A.L.; Faria, P.E.; Grisi, M.F.; Souza, S.L.; Taba, M.J.; Palioto, D.B.; Novaes, A.B.; Fraga, A.F.; Ozyegin, L.S.; Oktar, F.N; Salata, L.A. Effects of granule size on the osteoconductivity of bovine and synthetic hydroxyapatite: a histologic and histometric study in dogs. *J. Oral Implantol.* 2007; 33: 267-276.

-Castro-Ceseña, A.B; Sánchez-Saavedra, M.P; Novitskaya, E.E.; Chen, P.Y.; Hirata, G.A. ; McKittrick, J. Kinetic characterization of the deproteinization of trabecular and cortical bovine femur bones. *Mater. Sci. Eng. C Mater. Biol. Appl.* 2013; 33: 4958-4964.

-Cawood, J.I.; Howell R.A. A classification of the edentulous jaws. *Int J Oral Maxillofac Surg* 1988; 17: 232-236.

-Cehreli, M.C.; Karasoy, D.; Akca, K.; Eckert, S.E. Meta-analysis of methods used to assess implant stability. *Int J Oral Maxillofac Implants* 2009; 24: 1015-1032.

-Costa-Rodrigues, J.; Fernandes, A.; Lopes, M.A.; Fernandes, M.H. Hydroxyapatite surface roughness: complex modulation of the osteoclastogenesis of human precursor cells. *Acta Biomater.* 2012; 8: 1137-1145.

-Chen, F.P.; Wang, K.; Liu, C. S. Crystalline structure and its effects on the degradation of linear calcium polyphosphate bone substitute. *Appl. Surf. Sci.* 2008; 255: 270–272.

-Chou, Y.F.; Huang, W.; Dunn, L.C.; Miller, T.A.; Wu, B.M. The effect of biomimetic apatite structure on osteoblast viability, proliferation and gene expression. *Biomaterials* 2005; 26: 285-295.

-Cyster, L.A.; Grant, D.M.; Howdle, S.M.; Rose, F.R.; Irvine, D.J.; Freeman, D.; Scotchford, C.A.; Shakesheff, K.M. The influence of dispersant concentration on the

pore morphology of hydroxyapatite ceramics for bone tissue engineering. *Biomaterials* 2005; 26: 697-702.

-Coathup, M.J.; Hing, K.A.; Samizadeh, S.; Chan, O.; Fang, Y.S.; Campion, C.; Buckland, T.; Blunn, G.W. Effect of increased strut porosity of calcium phosphate bone graft substitute biomaterials on osteoinduction. *J. Biomed Mater. Res. A* 2012; 100: 1550–1555.

-Conz, M.B.; Granjeiro, J.M.; Soares, G.A. Physicochemical characterization of six commercial hydroxyapatites for medical-dental applications as bone graft. *J Appl Oral Sci* 2005; 13: 136-140.

-Conz, M.B.; Granjeiro, J.M.; Soares G. de A. Hydroxyapatite crystallinity does not affect the repair of critical size bone defects. *J Appl Oral Sci*. 2011; 19: 337-342.

-Corbella, S.; Taschieri, S.; Weinstein, R.; Del Fabbro, M. Histomorphometric outcomes after lateral sinus floor elevation procedure: a systematic review of the literature and meta-analysis. *Clin. Oral Implants Res*. 2016; 27:1106-1122.

-Corbella, S.; Taschieri, S.; Del Fabbro, M. Long-term outcomes for the treatment of atrophic posterior maxilla: a systematic review of literature. *Clin Implant Dent Relat Res*. 2015; 17: 120-132.

-Cordaro, L.; Bosshardt, D.D.; Palatella, P.; Rao, W.; Serino, G.; Chiapasco, M. Maxillary sinus grafting with Bio-Oss® or Straumann® Bone Ceramic: histomorphometric result from a randomized controlled multicenter clinical trial. *Clin. Oral Implants Res*. 2008; 19: 796-803.

-Danesh-Sani, A.S.; Loomer, P.M.; Wallace, S.S. A comprehensive clinical review of maxillary sinus floor elevation: anatomy, techniques, biomaterials and complications. *Br J Oral Maxillofac Surg*. 2016 a; 54: 724-730.

-Danesh-Sani, S.A; Engebretson, S.P.; Janal, M.N. Histomorphometric results of different grafting materials and effect of healing time on bone maturation after sinus floor augmentation: a systematic review and meta-analysis. *J. Periodontal Res.* 2016b. doi: 10.1111/jre.12402. [Epub ahead of print]

-Danoux, C.; Pereira, D.; Döbelin, N.; Stähli, C.; Barralet, J.; van Blitterswijk, C.; Habibovic, P. The Effects of Crystal Phase and Particle Morphology of Calcium Phosphates on Proliferation and Differentiation of Human Mesenchymal Stromal Cells. *Adv Healthc Mater.* 2016; 5: 1775-1785.

-Degidi, M.; Perrotti, V.; Piattelli, A.; Iezzi, G. Mineralized bone-implant contact and implant stability quotient in 16 human implants retrieved after early healing periods: a histologic and histomorphometric evaluation. *Int J Oral Maxillofac Implants.* 2010; 25: 45-48.

-Degidi, M.; Daprile, G.; Piattelli, A. RFA values of implants placed in sinus grafted and nongrafted sites after 6 and 12 months. *Clin Implant Dent Relat Res.* 2009;11: 178-182.

-Degidi, M.; Piattelli, A.; Iezzi, G.; Carinci, F. Do longer implants improve clinical outcome in immediate loading? *Int J Oral Maxillofac Surg.* 2007 ; 36: 1172-1176.

-Detsch, R.; Boccaccini, A.R. The role of osteoclasts in bone tissue engineering. *J Tissue Eng Regen Med.* 2015; 9: 1133- 49.

-Ducheyne, P.E.; Qiu, Q. Bioactive ceramics: the effect of surface reactivity on bone formation and bone cell function. *Biomaterials* 1999; 20: 2287-2303.

-Esposito, M.; Barausse, C.; Pistilli, R.; Sammartino ,G.; Grandi, G; Felice, P. Short implants versus bone augmentation for placing longer implants in atrophic maxillae: One-year post-loading results of a pilot randomised controlled trial. *Eur J Oral Implantol.* 2015; 8: 257- 268.

-Esposito, M.; Grusovin, M.G.; Rees, J.; Karasoulos, D.; Felice, P.; Alissa, R.; Worthington, H.; Coulthard, P. Effectiveness of sinus lift procedures for dental implant rehabilitation: a Cochrane systematic review. *Eur J Oral Implantol.* 2010; 23: 7-26.

-Esposito, M.; Grusovin, M.G.; Maghaireh, H.; Worthington HV. Interventions for replacing missing teeth: different times for loading dental implants. *Cochrane Database Syst Rev.* 2013; 28, 3, CD003878.

-Fan, T.; Li, Y.; Deng, W.W.; Wu, T.; Zhang, W. Short Implants (5 to 8 mm) Versus Longer Implants (>8 mm) with Sinus Lifting in Atrophic Posterior Maxilla: A Meta-Analysis of RCTs. *Clin Implant Dent Relat Res.* 2017; 19: 207-215.

-Felice, P.; Pistilli, R.; Piattelli, M.; Soardi, E.; Pellegrino, G.; Corvino, V.; Esposito, M. 1-stage versus 2-stage lateral maxillary sinus lift procedures: 4-month post-loading results of a multicenter randomised controlled trial. *Eur J Oral Implantol.* 2013; 6: 153-165.

-Felice, P.; Soardi, E.; Pellegrino, G.; Pistilli, R.; Marchetti, C., Gessaroli, M., Esposito, M. Treatment of the atrophic edentulous maxilla: short implants versus bone augmentation for placing longer implants. Five-month post-loading results of a pilot randomised controlled trial. *Eur J Oral Implantol.* 2011; 4:191-202.

-Ferreira, C.E.; Novaes, A.B.; Haraszthy, V.I.; Bittencourt, M.; Martinelli, C.B.; Luczyszyn, S.M. A clinical study of 406 sinus augmentations with 100% anorganic bovine bone. *J Periodontol.* 2009; 80: 1920-1927.

-Fienitz, T.; Moses, O.; Klemm, C.; Happe, A.; Ferrari, D.; Kreppel, M.; Ormianer, Z.; Gal, M., Rothamel, D. Histological and radiological evaluation of sintered and non-sintered deproteinized bovine bone substitute materials in sinus augmentation procedures. A prospective, randomized-controlled, clinical multicenter study. *Clin Oral Investig.* 2016 [Epub ahead of print]

-Figueiredo, A.; Coimbra, P.; Cabrita, A.; Guerra, F.; Figueiredo, M. Comparison of a xenogeneic and an alloplastic material used in dental implants in terms of physico-

chemical characteristics and in vivo inflammatory response. *Mater Sci Eng C Mater Biol Appl.* 2013; 3: 3506-3513.

-Frenken, J.W.; Bouwman, W.F.; Bravenboer, N.; Zijdeveld, S.A.; Schulten, E.A.; ten Bruggenkate, C.M. The use of Straumanns Bone Ceramic in a maxillary sinus floor elevation procedure: a clinical, radiological, histological and histomorphometric evaluation with a 6-month healing period. *Clin Oral Implants Res.* 2010; 21: 201-208.

-Friberg, B.; Ekestubbe, A.; Sennerby, L. Clinical outcome of Brånemark System implants of various diameters: a retrospective study. *Int J Oral Maxillofac Implants.* 2002; 17: 671-677.

-Froum, S.J.; Tarnow, DP; Wallace SS; Rohrer MD; Cho SC. Sinus floor elevation using anorganic bovine bone matrix (OsteoGraf/N) with and without autogenous bone: a clinical, histologic, radiographic, and histomorphometric analysis—Part 2 of an ongoing prospective study. *Int. J Periodontics Restorative Dent.* 1998; 18: 528- 43.

-Fulmer, M.T.; Ison, I.C.; Hankermayer, C.R.; Constantz, B.R.; Ross, J. Measurements of the solubilities and dissolution rates of several hydroxyapatite. *Biomaterials* 2002; 23: 751-755.

-Galindo-Moreno, P.; Hernández-Cortés, P.; Mesa, F.; Carranza, N.; Juodzbalys, G.; Aguilar, M.; O'Valle, F. Slow resorption of anorganic bovine bone by osteoclasts in maxillary sinus augmentation. *Clin Implant Dent Relat Res.* 2013; 15: 858-66.

-Gehrke, S.A.; da Silva, U.T.; Del Fabbro, M. Does Implant Design Affect Implant Primary Stability? A Resonance Frequency Analysis-Based Randomized Split-Mouth Clinical Trial. *J Oral Implantol.* 2015; 41:281-286.

-Ghanaati, S.; Barbeck, M; Detsch, R.; Deisinger, U.; Hilbig, U.; Rausch, V.; Sader, R.; Unger, R.E.; Ziegler, G.; Kirkpatrick, C.J. The chemical composition of synthetic bone substitutes influences tissue reactions in vivo: histological and histomorphometrical analysis of the cellular inflammatory response to hydroxyapatite, beta-tricalcium phosphate and biphasic calcium phosphate ceramics. *Biomed Mater.* 2012; 7: 015005.

-Gupta, R.K.; Padmanabhan, T.V. An evaluation of the resonance frequency analysis device: examiner reliability and repeatability of readings. *J Oral Implantol.* 2013; 39: 704-707.

-Habibovic, P.; Kruyt, M.C.; Juhl, M.V.; Clyens, S.; Martinetti, R.; Dolcini, L.; Theilgaard, N.; van Blitterswijk, C.A. Comparative in vivo study of six hydroxyapatite-based bone graft substitutes. *J Orthop Res.* 2008; 26: 1363-1370.

-Hamada, H.; Ohshima, H.; Ito, A.; Higuchi, W.I.; Otsuka, M. Effect of geometrical structure on the biodegradation of a three-dimensionally perforated porous apatite/collagen composite bone cell scaffold. *Biol Pharm Bull.* 2010; 33: 1228–1232.

-Herliansyah, M.K.; Hamdia, M.; de-Ektessabic, A.I.; Wildanb, M.W., J.A. Toque, J.Á. The influence of sintering temperature on the properties of compacted bovine. *Mater Sci Eng C Mater Biol Appl.* 2009; 29: 1674–1680.

-Herrero-Climent, M.; Albertini, M.; Rios-Santos, J.V.; Lázaro-Calvo, P.; Fernández-Palacín, A.; Bullon, P. Resonance frequency analysis-reliability in third generation instruments: Osstell mentor®. *Med Oral Patol Oral Cir Bucal.* 2012; 17: 801-806.

-Herrero-Climent, M.; Santos-García, R.; Jaramillo-Santos, R.; Romero-Ruiz, M.M.; Fernández-Palacin, A.; Lázaro-Calvo, P.; Bullón, P.; Ríos-Santos, J.V. Assessment of Osstell ISQ's reliability for implant stability measurement: a cross-sectional clinical study. *Med Oral Patol Oral Cir Bucal.* 2013; 18: 877-882.

-Hong, J.Y.; Kim, Y.J., Lee, H.W., Lee, W.K.; Ko, J.S.; Kim, H.M. Osteoblastic cell response to thin film of poorly crystalline calcium phosphate apatite formed at low temperatures. *Biomaterials* 2003; 24: 2977-2984.

-Hutmacher, D.W.; Schantz, J.T.; Lam, C.X.; Tan, K.C.; Lim, T.C. State of the art and future directions of scaffold-based bone engineering from a biomaterials perspective. *J Tissue Eng Regen Med.* 2007; 1: 245-260.

-Iezzi, G.; Scarano, A.; Di Stefano, D.; Arosio, P.; Doi, K.; Ricci, L.; Piattelli, A.; Perrotti, V. Correlation between the bone density recorded by a computerized implant motor and by a histomorphometric analysis: a preliminary in vitro study on bovine ribs. *Clin Implant Dent Relat Res.* 2015; 17: 35- 44.

-Javed, F.; Romanos, G.E. Role of implant diameter on long-term survival of dental implants placed in posterior maxilla: a systematic review. *Clin Oral Investig.* 2015; 19: 1-10.

-Jensen, S.S.; Aaboe, M.; Janner, S.F.; Saulacic, N.; Bornstein, M.M.; Bosshardt, D.D.; Buser, D. Influence of particle size of deproteinized bovine bone mineral on new bone formation and implant stability after simultaneous sinus floor elevation: a histomorphometric study in minipigs. *Clin Implant Dent Relat Res.* 2015; 17: 274-85.

-Jensen, S.S.; Terheyden, H. Bone augmentation procedures in localized defects in the alveolar ridge: clinical results with different bone grafts and bone-substitute materials. *Int J Oral Maxillofac Implants.* 2009; 24: 218-236.

-Jensen, O.T.; Sennerby, L. Histologic analysis of clinically retrieved titanium microimplants placed in conjunction with maxillary sinus floor augmentation. *Int J Oral Maxillofac Implants* 1998; 13: 513-521.

-Jensen, T.; Schou, S.; Stavropoulos, A.; Terheyden, H.; Holmstrup, P. Maxillary sinus floor augmentation with Bio- Oss or Bio-Oss mixed with autogenous bone as graft: a systematic review. *Clin Oral Implant Res.* 2012; 23: 263-273.

-Joschek, S.; Nies, B.; Krotz, R.; Göferich, A. Chemical and physicochemical characterization of porous hydroxyapatite ceramics made of natural bone. *Biomaterials* 2000; 21: 1645-1658.

-Kalkura, S.N.; Anee, T.K.; Ashok, M.; Betzel, C. Investigations on the synthesis and crystallization of hydroxyapatite at low temperature. *Bio-medical materials and engineering* 2004; 1: 581-592.

- Karageorgiou, V.; Kaplan, D. Porosity of 3D biomaterial scaffolds and osteogenesis. *Biomaterials* 2005; 26: 5474–5491.
- Khouly, I.; Veitz-Keenan, A. Insufficient evidence for sinus lifts over short implants for dental implant rehabilitation. *Evid Based Dent.* 2015; 16: 21-22.
- Knöfler, W.; Barth, T.; Graul, R.; Krampe, D. Retrospective analysis of 10,000 implants from insertion up to 20 years-analysis of implantations using augmentative procedures. *Int J Implant Dent.* 2016; 2: 25.
- Kohal, R.J.; Gubik, S.; Strohl, C.; Stampf, S.; Bächle, M.; Hürtle, A.A.; Patzelt, S.B. Effect of two different healing times on the mineralization of newly formed bone using a bovine bone substitute in sinus floor augmentation: a randomized, controlled, clinical and histological investigation. *J Clin Periodontol.* 2015; 42: 1052-1059.
- Kolerman, R.; Samorodnitzky, G.R.; Barnea, E.; Tal, H. Histomorphometric analysis of newly formed bone after bilateral maxillary sinus augmentation using two different osteoconductive materials and internal collagen membrane. *Int J Periodontics Restorative Dent.* 2012; 32: 21-28.
- Kutty, M.; Ramesh, S. The Effects of Sintering Temperature on the Properties of Hydroxyapatite. *Ceram. Int.* 2000; 26: 221-230.
- Lai, H.C.; Zhang, Z.Y.; Wang, F.; Zhuang, L.F.; Liu, X. Resonance frequency analysis of stability on ITI implants with osteotome sinus floor elevation technique without grafting: a 5-month prospective study. *Clin Oral Implants Res.* 2008; 19: 469- 475.
- Lee JS; Shin HK; Yun JH; Cho KS. Randomized Clinical Trial of Maxillary Sinus Grafting using Deproteinized Porcine and Bovine Bone Mineral. *Clin Implant Dent Relat Res.* 2016 doi: 10.1111/cid.12430. [Epub ahead of print]
- Le Geros, R.Z Biodegradation and bioresorption of calcium phosphate ceramics. *Clin Mater* 1993; 14: 65-88.

-Le Geros RZ Properties of Osteoconductive Biomaterials: Calcium Phosphates. Clin Orthop Relat Res. 2002; 395: 81-98.

-Lindgren, C.; Hallman, M.; Sennerby, L.; Sammons, R. Back-scattered electron imaging and elemental analysis of retrieved bone tissue following sinus augmentation with deproteinized bovine bone or biphasic calcium phosphate. Clinical Oral Implants Research 2010; 21: 924-930.

-Lioubavina-Hack, N.; Lang, N.P.; Karring, T. Significance of primary stability for osseointegration of dental implants. Clin Oral Implants Res. 2006; 17: 244-250.

-Liu J, Ye X, Wang H, Zhu M, Wang B, Yan H The influence of pH and temperature on the morphology of hydroxyapatite synthesized by hydrothermal method. Ceram Int. 2003; 29: 629-633.

-Lundgren, S.; Cricchio, G.; Hallman, M.; Jungner, M.; Rasmusson, L.; Sennerby L. Sinus floor elevation procedures to enable implant placement and integration: techniques, biological aspects and clinical outcomes. Periodontol 2000. 2017; 73: 103-120.

-Mardas, N.; Chadha, V.; Donos, N. Alveolar ridge preservation with guided bone regeneration and a synthetic bone substitute or a bovine-derived xenograft: a randomized, controlled clinical trial. Clin Oral Implants Res 2010; 21: 688-698.

-Marquezan, M.; Osório, A.; Sant'Anna, E.; Souza, M.M.; Maia, L. Does bone mineral density influence the primary stability of dental implants? A systematic review. Clin Oral Implants Res. 2012; 23: 767-774.

-Mate-Sanchez de Val, J.E.; Calvo-Guirado, J.L.; Gomez Moreno, G.; Perez Albacete-Martinez, C.; Mazón, P.; de Aza, P.N. Influence of hydroxyapatite granule size, porosity and crystallinity on tissue reaction in vivo. Part A: Synthesis, characterization of the materials and SEM analysis. Clin. Oral Implant. Res. 2016; 27: 1331-1338.

-Monteiro, M.M.; Campos da Rocha, N.C.; Rossi, A.M.; de Almeida Soares, G. Dissolution properties of calcium phosphate granules with different compositions in simulated body fluid. *J Biomed Mater Res A*. 2003; 65: 299-305.

-Moon, J.W.; Sohn, D.S.; Heo, J.U. Histomorphometric analysis of maxillary sinus augmentation with calcium phosphate nanocrystal-coated xenograft. *Implant Dentistry* 2015; 24: 333-337.

-Mordenfeld A; Hallman M; Albrektsson T. Histological & histomorphometrical analyses of biopsies harvested 11 years after maxillary sinus augmentation with 80% Bio-Oss and 20 % autogenous bone. *Clin Oral Implants Res*. 2010; 21: 961-970.

-Munar, M.L.; Udoh, K; Ishikawa, K.; Matsuya, S.; Nakagawa, M. Effects of sintering temperature over 1,300 degrees C on the physical and compositional properties of porous hydroxyapatite foam. *Dent Mater J*. 2006; 25: 51-58.

-Muralithran, G.; Ramesh, S. The effects of sintering temperature on the properties of hydroxyapatite. *Ceram Int* 2000; 26: 221-230.

-Nannmark, U.; Sennerby, L. The bone tissue responses to prehydrated and collagenated cortico-cancellous porcine bone grafts: a study in rabbit maxillary defects. *Clin Implant Dent Relat Res*. 2008; 10: 264-270.

-Nasr, S.; Slot, D.E.; Bahaa, S.; Dörfer, C.E.; Fawzy El-Sayed, K.M. Dental implants combined with sinus augmentation: What is the merit of bone grafting? A systematic review. *J Craniomaxillofac Surg*. 2016; 44: 1607-1617.

-Nedir, R.; Nurdin, N.; Abi- Najm, S.; El Hage, M.; Bischof, M. Short implants placed with or without grafting into atrophic sinuses: the 5-year results of a prospective randomized controlled study. *Clin Oral Implants Res*. 2016 Jun 13. doi: 10.1111/clr.12893. [Epub ahead of print]

-Nevins, M.; Camelo, M.; De Angelis, N.; Hanratty, J.J.; Khang, W.G.; Kwon, J.J.; Rasperini, G.; Rocchietta, I.; Schupbach, P.; Kim, D.M. The clinical and histologic efficacy of xenograft granules for maxillary sinus floor augmentation. *Int J Periodontics Restorative Dent.* 2011; 31: 227–235.

-Nkenke, E.; Stelzle, F. Clinical outcomes of sinus floor augmentation for implant placement using autogenous bone or bone substitutes: a systematic review. *Clinical Oral Implants Research* 2009; 20: 124-133. □

-Nkenke E, Weisbach V, Winckler E, Kessler P, Schultze-Mosgau S, Wiltfang J, Neukam FW. Morbidity of harvesting of bone grafts from the iliac crest for prosthetic augmentation procedures: a prospective study. *Int J Oral Maxillofac Surg.* 2004; 33: 157–163.

-Oh, J.S.; Kim, S.G. Clinical study of the relationship between implant stability measurements using Periotest and Osstell mentor and bone quality assessment. *Oral Surg Oral Med Oral Pathol Oral Radiol.* 2012; 113: 35-40.

-Orsini, G.; Scarano, A.; Piattelli, M.; Piccirilli, M.; Caputi, S.; Piattelli, A. Histologic and ultrastructural analysis of regenerated bone in maxillary sinus augmentation using a porcine bone-derived biomaterial. *J Periodontol.* 2006; 77: 1984-1990.

-Orsini, G.; Traini, T.; Scarano, A.; Degidi, M.; Perrotti, V.; Piccirilli, M.; Piattelli, A. Maxillary sinus augmentation with Bio-Oss particles: a light, scanning, and transmission electron microscopy study in man. *J Biomed Mater Res B Appl Biomater.* 2005; 74: 448–457.

-Ostman, P.O; Hellman, M.; Wendelhag, I.; Sennerby, L. Resonance frequency analysis measurements of implants at placement surgery. *Int J Prosthodont.* 2006; 19: 77-83.

-O'Sullivan, D.; Sennerby, L.; Meredith, N. Measurements comparing the initial stability of five designs of dental implants: a human cadaver study. *Clin Implant Dent Relat Res.* 2000; 2: 85-92.

-Panagiotou, D.; Ozkan Karaca, E; Dirikan Ipci, S; Cakar G; Olgac V.; Yilmaz, S. Comparison of two different xenografts in bilateral sinus augmentation: Radiographic and histologic findings. *Quintessence Int.* 2015; 46: 611–619.

-Pielaszek, R., Diffraction studies of microstructure of nanocrystals exposed to high pressure, Ph.D. Thesis, Warsaw University, Dept. Phys, Warsaw, Poland, 2003.

-Pinchasov, G.; Juodzbaly, G. Graft-free sinus augmentation procedure: a literature review. *J Oral Maxillofac Res.* 2014, 5. doi: 10.5037/jomr.2014.5101.

-Pjetursson, B.E.; Tan, W.C.; Zwahlen, M.; Lang, N.P. A systematic review of the success of sinus floor elevation and survival of implants inserted in combination with sinus floor elevation. *J Clin Periodontol.* 2008; 35: 216-240.

-Poinern, G.J.; Brundavanam, R.; Le, X.T.; Djordjevic, S.; Prokic, M.; Fawcett, D. Thermal and ultrasonic influence in the formation of nanometer scale hydroxyapatite bio-ceramic. *Int J Nanomedicine* 2011; 6: 2083-2095.

-Rammelsberg, P.; Schmitter, M.; Gabbert, O.; Lorenzo-Bermejo, J.; Eiffler, C.; Schwarz, S. Influence of bone augmentation procedures on the short-term prognosis of simultaneously placed implants. *Clin Oral Implants Res.* 2012; 23: 1232-1237.

-Rammelt, S; Schulze, E.; Witt, M.; Petsch, E.; Biewener, A.; Pompe, W.; Zwipp, H. Collagen type I increases bone remodelling around hydroxyapatite implants in the rat tibia. *Cells Tissues Organs.* 2004; 178: 146-157.

-Raynaud, S.; Champion, E.; Bernache-Assollant, D. Calcium phosphate apatites with variable Ca/P atomic ratio II. Calcination and sintering. *Biomaterials.* 2002; 23: 1073-1080.

-Ren F, Y. Ding, Y, Leng, Y. Infrared spectroscopic characterization of carbonated apatite: a combined experimental and computational study, *Journal of biomedical materials research. Part A*, 2014, 102: 496-505.

-Riachi, F.; Naaman, N.; Tabarani, C.; AboeIsaad, N.; Berberi, A.; Salameh, Z. Influence of material properties on rate of resorption of two bone graft materials. *Int J Dent*. 2012:737262. doi: 10.1155/2012/737262.

-Rodella, L.F.; Favero, G.; Labanca, M. Biomaterials in maxillofacial surgery: membranes and grafts. *Int J Biomed Sci*. 2011; 7: 81-88.

-Rodrigues, C.V.M.; Serricella, P.; Linhares, A.B.; Guerdes, R.M.; Borojevic, R.; Rossi, A.M. Characterization of a bovine collagen-hydroxyapatite composite scaffold for bone tissue engineering. *Biomaterials*. 2003; 24: 4987-4997.

-Romanos, G.E.; Ciornei, G.; Jucan, A.; Malmstrom, H.; Gupta, B. In vitro assessment of primary stability of Straumann® implant designs. *Clin Implant Dent Relat Res*. 2014; 16: 89-95.

-Romanos, G.E.; Delgado-Ruiz, R.A., Sacks, D.; Calvo-Guirado, J.L. Influence of the implant diameter and bone quality on the primary stability of porous tantalum trabecular metal dental implants: an in vitro biomechanical study. *Clin Oral Implants Res*. 2016; 1–7 doi: 10.1111/clr.12792

-Rosa, A.L., Beloti, M.M.; Oliveira, P.T.; Van Noort, R. Osseointegration and osseointegration of hydroxyapatite of different microporosities. *J Mater Sci Mater Med*. 2002; 13: 1071–1075.

-Sennerby, L.; Meredith, N. Implant stability measurements using resonance frequency analysis: biological and biomechanical aspects and clinical implications. *Periodontol* 2000. 2008; 47: 51-66.

-Sennerby, L.; Pagliani, L.; Petersson, A.; Verrocchi, D.; Volpe, S.; Andersson, P. Two different implant designs and impact of related drilling protocols on primary stability in different bone densities: an in vitro comparison study. *Int J Oral Maxillofac Implants*. 2015; 30: 564-568.

-Sbordone, C.; Toti, P.; Guidetti, F.; Califano, L.; Bufo, P.; Sbordone, L. Volume changes of autogenous bone after sinus lifting and grafting procedures: a 6-year computerized tomographic follow-up. *J Craniomaxillofac Surg.* 2013; 41: 235–241.

-Scarano, A.; Piatelli, A.; Perrotti, V.; Manzon, L.; Lezzi, G. Maxillary sinus augmentation in human using cortical porcine bone: a histological and histomorphometrical evaluation after 4 and 6 months. *Clin Implant Dent Relat Res.* 2011; 13: 13-18.

-Schaefer, S.; Detsch, R.; Uhl, F.; Deisinger, U.; Ziegler, G. How degradation of calcium phosphate bone substitute materials is influenced by phase composition and porosity. *Adv Mater.* 2011; 13: 342- 350.

-Schilling, A.F.; Linhart, W.; Filke, S.; Gebauer, M.; Schinke, T.; Rueger, J.M.; Amling, M. Resorbability of bone substitute biomaterials by human osteoclasts. *Biomaterials.* 2004; 25: 3963- 3972.

-Schiuma, D.; Plecko, M.; Kloub, M.; Rothstock, S.; Windolf, M.; Gueorguiev, B. Influence of peri-implant bone quality on implant stability. *Med Eng Phys.* 2013; 35: 82-87.

-Sharan, A.; Madjar, D. Maxillary sinus pneumatization following extractions: a radiographic study. *Int J Oral Maxillofac Implants.* 2008; 23: 48-56.

-Shull, C.G. The determination of X-ray diffraction line widths, *Phys Rev.* 1946; 70: 679-684.

-Simunek, A.; Kopecka, D.; Somanathan, R.V.; Pilathadka, S.; Brazda, T. Deproteinized bovine bone versus beta-tricalcium phosphate in sinus augmentation surgery: a comparative histologic and histomorphometric study. *Int J Oral Maxillofac Implants* 2008; 23: 935-942.

-Slater, N.; Dasmah, A.; Sennerby, L.; Hallman, M.; Piattelli, A.; Sammons, R. Back-scattered electron imaging and elemental microanalysis of retrieved bone tissue following maxillary sinus floor augmentation with calcium sulphate. *Clin Oral Implants Res.* 2008; 19: 814-822.

-Ślósarczyk, A.; Paluszkiwicz, C.; Gawlicki, M.; Paszkiewicz Z. The FTIR spectroscopy and QXRD studies of calcium phosphate based materials produced from the powder precursors with different CaP ratios, *Ceramics International* 1997; 23: 297-304.

-Smiler, D.G. The sinus lift graft: basic technique and variations. *Pract Periodontics Esthet Dent* 1997; 9: 885-893.

-Sohn, D.S.; Lee, J.S.; Ahn, M.R.; Shin, H.I. New bone formation in the maxillary sinus without bone grafts. *Implant Dent* 2008; 17: 321-331.

-Sohn, D.S.; Moon, J.W.; Lee, W.H.; Kim, S.S.; Kim, C.W.; Kim, K.T.; Moon, Y.S. Comparison of new bone formation in the maxillary sinus with and without bone grafts: immunochemical rabbit study. *Int J Oral Maxillofac Implants.* 2011; 26: 1033-1042.

-Suárez-López Del Amo, F.; Ortega-Oller, I.; Catena, A.; Monje, A.; Khoshkam, V.; Torrecillas-Martínez, L.; Wang, H.L.; Galindo-Moreno, P. Effect of Barrier Membranes on the Outcomes of Maxillary Sinus Floor Augmentation: A Meta-Analysis of Histomorphometric Outcomes. *Int J Oral Maxillofac Implants* 2015; 30: 607-618.

-Swami, V.; Vijayaraghavan, V.; Swami, V. Current trends to measure implant stability. *J Indian Prosthodont Soc.* 2016, 16, 124-130.

-Swetha, M.; Sahithi, K.; Moorthi, A.; Srinivasan, N.; Ramasamy, K.; Selvamurugan, N. Biocomposites containing natural polymers and hydroxyapatite for bone tissue engineering. *Int. J. Biol. Macromol.* 2010; 1: 1-4.

-Tadic, D.; Epple, M. A thorough physicochemical characterization of 14 calcium phosphate-based bone substitution materials in comparison to natural bone. *Biomaterials* 2004; 25: 987-994.

-Tatum H Jr. Maxillary and sinus implant reconstruction. *Dent Clin North Am* 1986; 30: 207-229.

-Taylor, J.C.; Cuff, S.E.; Leger, J.P.; Morra, A.; Anderson, G.I. In vitro osteoclast resorption of bone substitute biomaterials used for implant site augmentation: a pilot study. *Int J Oral Maxillofac Implants.* 2002; 17: 321-330.

-Traini, T.; Degidi, M.; Sammons, R.; Stanley, P.; Piattelli, A. Histologic and elemental microanalytical study of anorganic bovine bone substitution following sinus floor augmentation in humans. *J Periodontol.* 2008; 79: 1232-1240.

Traini, T., Valentini, P., Lezzi, G. & Piattelli, A. A histologic and histomorphometric evaluation of anorganic bovine bone retrieved 9 years after a sinus augmentation procedure. *J Periodontol.* 2007; 78: 955-961.

Traini, T.; Piattelli, A.; Caputi, S.; Degidi, M.; Mangano, C.; Scarano, A.; Perrotti, V.; Lezzi G. Regeneration of Human Bone Using Different Bone Substitute Biomaterials. *Clin Implant Dent Relat Res.* 2015; 17: 150-162.

-Tuna, T.; Yorgidis, M.; Strub, J.R. Prognosis of implants and fixed restorations after lateral sinus elevation: a literature review. *J Oral Rehabil.* 2012; 39: 226-238.

-von Doernberg, M.C.; von Rechenberg, B.; Bohner, M.; Grünenfelder, S.; van Lenthe, G.H.; Müller, R.; Gasser, B.; Mathys, R.; Baroud, G.; Auer, J. In vivo behavior of calcium phosphate scaffolds with four different pore sizes. *Biomaterials* 2006; 27: 5186-5198.

-Wallace, S.S.; Froum, S.J. Effect of maxillary sinus augmentation on the survival of endosseous dental implants. A systematic review. *Ann. Periodontol.* 2003; 8: 328-343.

-Wallace, S.S.; Tarnow, D.P.; Froum, S.J.; Cho, S.C.; Zadeh, H.H.; Stoupe, J.; Del Fabbro, M.; Testori, T. Maxillary sinus elevation by lateral window approach: evolution of technology and technique. *J Evid Based Dent Pract* 2012; 12: 161-171.

-Wenz, B.; Oesch, B.; Horst, M. Analysis of the risk of transmitting bovine spongiform encephalopathy through bone grafts derived from bovine bone. *Biomaterials* 2001; 22: 1599-1606.

-Wierzchos, J.; Falcioni, T.; Kiciak, A.; Woliński, J.; Koczorowski, R.; Chomicki, P.; Porembka, M.; Ascaso, C. Advances in the ultrastructural study of the implant-bone interface by backscattered electron imaging. *Micron.* 2008 ; 39:1363-1370.

-Wood, R.M.; Moore, D.L. Grafting of the maxillary sinus with intraorally harvested autogenous bone prior to implant placement. *Int J Oral Maxillofac Implants* 1988; 3: 209-214.

-Xu, H.; Shimizu, Y.; Asai, S.; Ooya, K. Experimental sinus grafting with the use of deproteinized bone particles of different sizes. *Clin Oral Implant Res* 2003; 14: 548-555.

-Xu, H.; Shimizu, Y.; Asai, S.; Ooya, K. Grafting of deproteinized bone particles inhibits bone resorption after maxillary sinus floor elevation. *Clin Oral Implant Res.* 2004; 15: 126-133.

-Yang, Y.; Dennison, D.; Ong, J.L. Protein Adsorption and Osteoblast Precursor Cell Attachment to Hydroxyapatite of Different Crystallinities. *Int J Oral Maxillofac Implants* 2005; 20: 187-192.

-Zinser, M.J.; Randelzhofer, P.; Kuiper, L.; Zöller, J.E.; De Lange, G.L. The predictors of implant failure after maxillary sinus floor augmentation and reconstruction: a

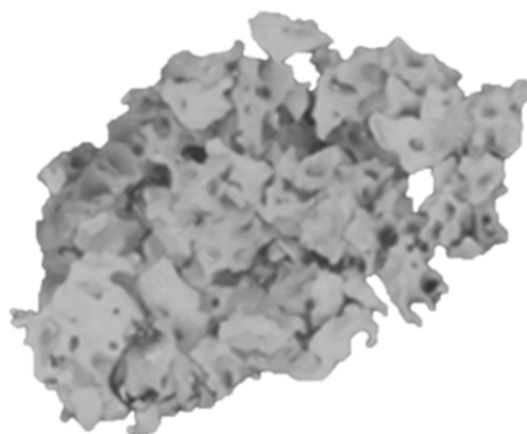
retrospective study of 1045 consecutive implants. *Oral Surg Oral Med Oral Pathol Oral Radiol.* 2013; 115: 571-582.





APPENDIX I

Published Papers





Article

Comparison of Two Xenograft Materials Used in Sinus Lift Procedures: Material Characterization and In Vivo Behavior

María Piedad Ramírez Fernández ^{1,*}, Patricia Mazón ², Sergio A. Gehrke ³,
Jose Luis Calvo-Guirado ¹ and Piedad N. De Aza ⁴

¹ Cátedra Internacional de Investigación en Odontología, Universidad Católica San Antonio de Murcia, Avda. Jerónimos, 135, 30107 Guadalupe, Murcia, Spain; jlcalvo@ucam.edu

² Departamento de Materiales, Óptica y Tecnología Electrónica, Universidad Miguel Hernández, Avda. Universidad s/n, 03202-Elche, Alicante, Spain; pmazon@umh.es

³ Biotecnos Research Center, Rua Dr. Bonazo n° 57, 97015-001-Santa Maria (RS), Brazil; sergio.gehrke@hotmail.com

⁴ Instituto de Bioingeniería, Universidad Miguel Hernandez, Avda. Ferrocarril s/n. 03202-Elche, Alicante, Spain; piedad@umh.es

* Correspondence: mpramirez@ucam.edu; Tel.: +34-968-278-775 (ext. 774)

Academic Editor: Franz E. Weber

Received: 13 February 2017; Accepted: 30 May 2017; Published: 7 June 2017

Abstract: Detailed information about graft material characteristic is crucial to evaluate their clinical outcomes. The present study evaluates the physico-chemical characteristics of two xenografts manufactured on an industrial scale deproteinized at different temperatures (non-sintered and sintered) in accordance with a protocol previously used in sinus lift procedures. It compares how the physico-chemical properties influence the material's performance in vivo by a histomorphometric study in retrieved bone biopsies following maxillary sinus augmentation in 10 clinical cases. An X-ray diffraction analysis revealed the typical structure of hydroxyapatite (HA) for both materials. Both xenografts were porous and exhibited intraparticle pores. Strong differences were observed in terms of porosity, crystallinity, and calcium/phosphate. Histomorphometric measurements on the bone biopsies showed statistically significant differences. The physico-chemical assessment of both xenografts, made in accordance with the protocol developed on an industrial scale, confirmed that these products present excellent biocompatibility, with similar characteristics to natural bone. The sintered HA xenografts exhibited greater osteoconductivity, but were not completely resorbable ($30.80 \pm 0.88\%$ residual material). The non-sintered HA xenografts induced about $25.92 \pm 1.61\%$ of new bone and a high level of degradation after six months of implantation. Differences in the physico-chemical characteristics found between the two HA xenografts determined a different behavior for this material.

Keywords: hydroxyapatite; xenografts; physico-chemical-characterization; tissue reaction

1. Introduction

The use of dental implants for the rehabilitation of missing teeth has increased treatment options for patients. Loss of teeth in the posterior maxillary area can lead to adverse consequences. It is not uncommon to observe severe maxillary sinus pneumatization, which reduces the implant prosthetic alternatives to replace missing teeth. In this anatomical situation, it can be very difficult to obtain effective primary stability. Maxillary sinus augmentation has been shown to be a predictable method to increase posterior maxillary bone height, and allows placing dental implants when the residual alveolar ridge is deficient in bone volume [1].

Nowadays, there are several types of graft materials used in sinus lift procedures, each with its advantages and disadvantages [2]. The ideal bone grafting material should have both osteoinductive and osteoconductive properties. Osteoinduction is defined as primitive, undifferentiated, and pluripotent cells stimulated by inductive means to induce bone-forming cells and osteogenesis processes. Osteoconduction is defined as bone growth on a surface, which is called the osteoconductive surface, and allows the osteogenesis process itself down into pores [3].

Natural bone is a complex inorganic-organic nanocomposite material in which hydroxyapatite [$\text{Ca}_{10}(\text{PO}_4)_6(\text{OH})_2$] nanocrystallites and collagen fibrils are well organized in hierarchical architecture overall length scales, including nanoscales. Hydroxyapatite (HA) is the major inorganic component of natural bone and has been applied widely in the medical field as a bone repair material given its excellent bioactive and biocompatibility properties. HAs are known for being biocompatible and bioactive (ability to form a direct chemical bond with surrounding tissues; osteoconductive; and non-toxic, non-inflammatory, and non-immunogenic properties) [4].

Technological evolution, along with a better understanding of bone-healing biology, has led to the development of several bone grafts [5]. Biomaterials that mimic the structure and composition of bone tissue on the nanoscale are important for the development of bone tissue engineering applications. Synthetic hydroxyapatites are the most widely used [6], but do not completely match the chemical composition of human bone [7]. After the increasing application of synthetic HAs in the last decade, a shift back to natural HAs has taken place [8].

Fortunately, bones from other species possess a similar tissue structure to that of human bones. These bones also exhibit osteoinduction and osteoconduction activities, which potentially satisfy the requirements of ideal bone graft substitutes [9]. Information from all reviews does, however, substantiate the finding that implant survival with bone replacement grafts, especially the most rigorously evaluated group (xenografts), equals or betters those achieved with autogenous bone [10]. These data, coupled with lower patient morbidity achieved by eliminating the need for a secondary surgical (donor) site, appears to position bone replacement grafts as the graft material of choice today. The histologic results with xenografts present a pattern that has been called “bone bridging”. Residual xenograft particles are surrounded partly by new vital bone, and are joined to nearby particles through this mechanism [11].

The availability of bovine bone is practically unlimited, and possesses a great physico-chemical and structural similarity to human bone [12]. For many years now, bovine cortico-spongy bone has been the first choice for buccal and maxillofacial surgery. There are numerous reports in the literature which have observed successful regenerative procedures in patients treated with maxillary sinus augmentation using bovine bone [13–17].

Other xenograft materials of other origins have been introduced into the clinical and research fields of dentistry under the banner of preventing the bovine-specific disease transmission [18]. Deproteinized porcine bone mineral is a substitute for deproteinized bovine bone mineral, and several researchers have already introduced it into clinical dental procedures based on the structural/physiological similarities of bone tissue between human and swine [19]. These xenografts have led to a great deal of research thanks to their potential as an adequate bone substitute for maxillary sinus augmentation [20–22].

Eliminating antigens that potentially cause an immune response is a prerequisite for xenogenic bone grafting. It has been shown that deproteinized bones not only lose their immune reactivity, but also retain their osteoinduction and osteoconduction activities [23].

The physico-chemical properties and mechanical strength of deproteinized tissue-engineered bone meet the demands of ideal scaffold materials. In the bioceramics field the need to correlate the chemical and physical composition of HA with cellular interactions still remains [24].

It has been assumed that the difference between filling materials used in sinus elevation procedures may modulate the quality and quantity of newly formed bone. The selection of biomaterials

constitutes a key point for successful tissue regeneration practice. The mechanisms behind tissue response to HAs have not yet been comprehensively established [25].

All substitute material aspects must be studied. Some studies have demonstrated that osteointegration and degradation processes are influenced by the material's physico-chemical properties [26], including granule size [12], morphology [27], crystallinity [28], porosity [29–31], surface roughness [32] and the calcium/phosphate ratio in the composition [33,34]. Part of a biological response produced by a biomaterial is conditioned by its physico-chemical properties. The work reported herein indicates the vast importance of fully characterizing the materials used. The many alternatives available, compared to the few comparative studies conducted, leave the choice of grafting material to the surgeon's preference, and are not always scientifically-based [34].

Based on these data, the present study developed a protocol for the characterization of xenografts. The objective of this study was to characterize the physico-chemical properties of two xenografts deproteinized at different temperatures, and to know how the physico-chemical properties influence the material's performance *in vivo*.

2. Results

2.1. Graft Implants Characterization

2.1.1. Scanning Electron Microscopy-Energy Dispersive X-ray Spectroscopy (SEM-EDX) Analysis

The SEM micrographs provided information about the morphology of the obtained bovine HAs scaffold (Figure 1) and the porcine HAs scaffolds (Figure 2). The bovine HAs scaffold (called BBM from this point onward) consisted of a highly porous network with an average pore size of 0.5 mm (Figure 1A). Micropores from 1 μm to 5 μm were also visualized. When granules were evaluated at larger magnifications, it was possible to observe their porous surface roughness with apatite crystals (white particles) (Figure 1B,C).

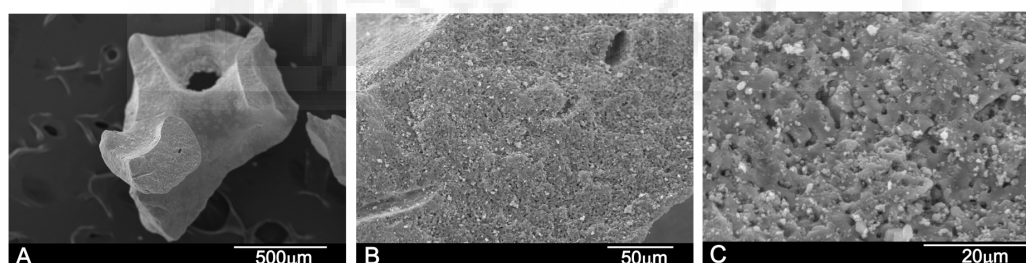


Figure 1. Scanning electron micrographs of the Bovine HAs scaffolds deproteinized at high temperature prior to the insertion for maxillary sinus floor elevation (BBM): (A) low magnification; and (B) high magnification showing macro- and microporosity; and (C) details of the microporosity on the scaffold surface together with apatite crystals (white).

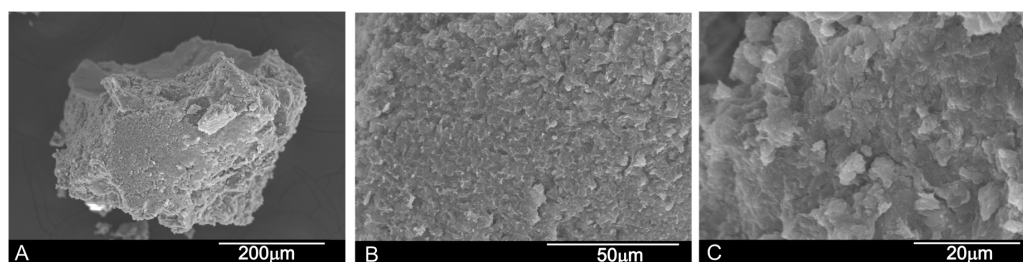


Figure 2. Scanning electron micrographs of Porcine HAs scaffolds deproteinized at low temperature (PBM): (A) low magnification image of the HA grafts; (B) high magnification image; and (C) details of the scaffold's surface roughness.

The porcine HAs scaffold (called PBM from this point onward) consisted of small grains of 500 μm on average (Figure 2A). At high magnification, the PBM shows surface roughness (Figure 2B). Due to the presence of collagen, the material shows no microporosity on its surface (Figure 2B) at high magnification, and the surface is not as clear as in the BBM xenograft.

EDX was used to determine the elemental composition in an area reached from graft particles before implantation. The Ca/P ratios for both the HA xenografts were 2.31 ± 0.09 for the BBM material and 2.22 ± 0.08 for the PBM material. The Kolmogorov–Smirnov test rejected Normality for the PBM group. A statistically significant difference was found between BBM and PBM (Mann–Whitney test, $p < 0.0051$).

2.1.2. X-ray Diffraction Analysis (XRD)

Figure 3 shows the X-ray diffraction patterns of the BBM and the PBM materials. The XRD of the grafts can be associated with the chemical composition of samples.

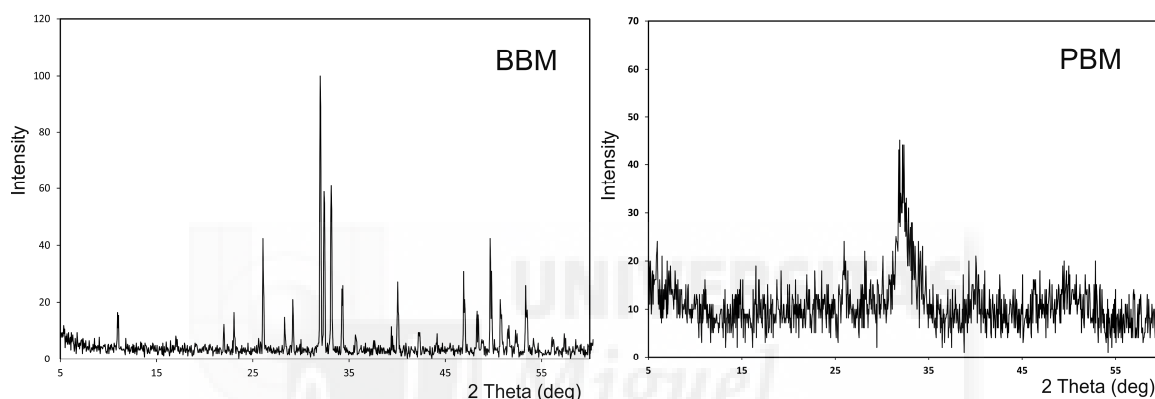


Figure 3. X-ray diffraction pattern of the BBM and PBM materials.

As expected, the XRD pattern from the mineral samples corresponded to HA, with coincident peak positions and relative intensities. However, these materials presented diverse degrees of crystallinity, as indicated in the different peak widths. That occurred with PBM, as the diffractogram exhibited broad peaks with a low signal-to-noise ratio, which corresponded to a low-crystallinity material. The sharp and well-resolved peaks found in the XRD spectrum of BBM indicated a highly crystalline HA. The HA corresponded to JCPDS card no. 09-0432 and presented a hexagonal system with a main diffraction plan [211]. No other secondary phases were detected.

2.1.3. Mercury Intrusion Porosimetry (MIP) Analysis

When analyzing a granular material by mercury porosimetry, two kinds of spaces can be detected: those that correspond to the empty spaces between particles (commonly designated by “interstices” or “interparticle” spaces) and those that correspond to the spaces of the particles themselves (known as “pores” or “intraparticle” spaces). The results obtained for the granules of PBM (Figure 4) showed that with increasing pressure, mercury penetrated to the increasingly smaller pores. The cumulative curve (Figure 4A) denotes a small intrusion in the pores between 300 μm and 3.5 μm , followed by a plateau between 3.5 μm and 0.02 μm where no intrusion is detected, and then significant mercury penetration into the pores below this value. The initial rise of the curve corresponds mostly to the filling of the spaces between particles (and may also include some of the largest pores of cancellous bone), whereas the later stage of rise is related to the pores of individual particles. The range of the intraparticle pores is more obvious in (Figure 4B) in which one intense peak, whose mode falls within the 0.01–0.004 μm range, is clearly visible. The peak on the left (84 μm) corresponds to the intrusion of mercury in the interparticle spaces. The size of these spaces, related to the way that

particles are packed, depends on both particle size and shape, as well as one particle size distribution. However, the distinction made between inter- and intraparticle spaces is not always so apparent. This interpretation aimed to elucidate the kind of information that can be extracted from pore size distribution curves and to highlight the importance of always specifying the size range of measured pores. It should be stressed that the mercury intrusion technique is especially suited for analyzing intraparticle pores, but is not adequate for measuring large spaces (300 μm).

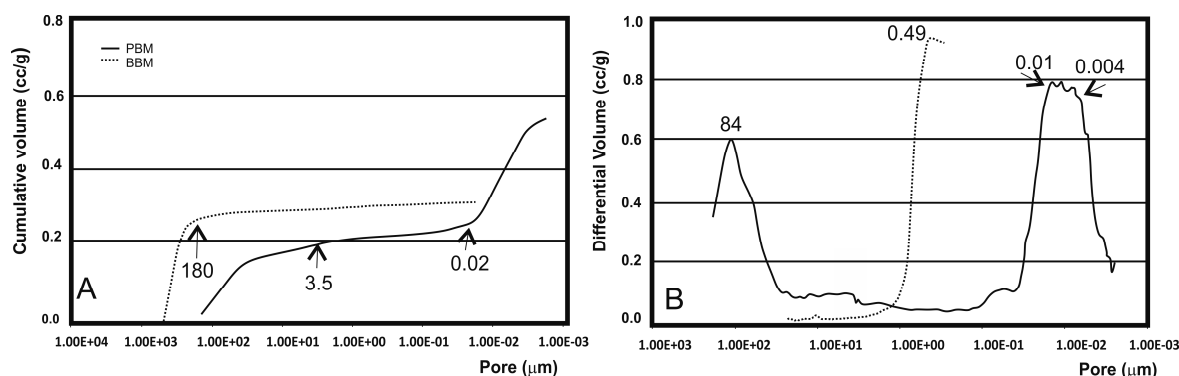


Figure 4. Mercury intrusion curves of the PBM and BBM ceramics measured by mercury porosimetry: (A) cumulative intruded volume versus pore diameter; and (B) differential-intruded volume versus pore diameter.

The results obtained for the granules of BBM denoted mercury intrusion in the pores between 300 μm and 180 μm, followed by a plateau between 180 μm and 0.02 μm where no intrusion was detected. The range of the intra- and inter-particle pores is not obvious in (Figure 4B), in which only one intense peak, whose mode is about 0.49 μm, is clearly visible in the interparticle spaces, but the proportion of interparticles in BBM is clearly lower than in PBM.

Table 1 summarizes these results in terms of the total intruded volume, mode of intraparticle pores, total porosity and intraparticle porosity (taken as the percentage of the particles’ internal pores <1 μm in relation to total porosity). An analysis of Table 1 suggested that PBM had the greatest porosity (59.90%). However, about 40% (38.11%) of this porosity corresponded to submicron pore entrances. A similar porosity value was determined for the BBM samples. This also exhibited a much smaller proportion of submicron pores, with only 3.66%.

Table 1. Mercury-intruded volume, mode (most frequent diameter) of intraparticle pores, total porosity, and intraparticle porosity of commercial samples.

Materials	Intruded Volume (cc/g)	Mode of Intraparticle Pores (μm)	Total Porosity (%) ^a	Intraparticle Porosity (%) ^b
PBM	0.524	0.01–0.004	59.90	38.11
BBM	0.323	0.49	49.13	3.66

^a Corresponding to 1 μm < pores < 300 μm; ^b Corresponding to pores < 1 μm.

2.2. Clinical and Radiographic Results

Dropouts were not observed during evaluation period and all returned for implant placement. Both groups presented similar baseline characteristics in terms of alveolar bone height values. All patients were operated on successfully.

After a six-month follow-up period of these 10 partially edentulous patients treated with xenograft materials for sinus floor augmentation, the success rate was 100%. No sinus membrane perforation or other clinical complications, such as sinusitis or pain, resulted from surgery. The increased volumes produced by the xenograft procedures were stable by the end of the healing period. The radiographic

findings showed that both treatment modalities resulted in bone gain at six months in both groups. The increase in alveolar bone height scores was evident between pre-augmentation and 6 months after in both groups. All 10 augmented sinuses provided 12 mm or more available bone for implant placement, as seen in (Figure 5).



Figure 5. (A) Preoperative panoramic image before the sinus lift; and (B) postoperative panoramic image 6 months after the sinus lift.

Bone density in the grafted area with both biomaterials was evaluated radiologically as a routine diagnostic approach (Figure 6). At the moment of implant insertion, after a healing period of six months, the augmentation sites treated with the PBM show less dense new bone formation achieved along the inner surface of replaced bony widow than the area on the bone graft whilst the BBM shows that more dense new bone formation was achieved in the area on the bone graft respect the original augmentation density. Bone area was different in the groups after implantation and increased with time. Bone initially formed at the sinus wall and proliferated into the center of the augmented sinus cavity. Three implants were not osseointegrated at the end of the study, leaving 57 implants for control (95% rate of success).



Figure 6. i-CAT (Imagen-computerized axial tomography) Vision postoperative image. It shows increased volumes produced by the xenograft procedures after six months of maxillary sinus elevation with a porcine hydroxyapatite (cuts 24–42).

2.3. Histomorphometric Results

SEM-BSE Analysis

A section of the material–bone interfaces six months after sinus elevation is shown in Figure 7. The Scanning Electron Microscopy with Back-Scattered (SEM-BSE) evaluation confirmed that the residual graft particles were surrounded by newly formed bone, which presented mature bone characteristics with well-organized lamellae (Figure 7). The BBM material shows progressive structure

dissolution, and the result of these processed free graft particles were found in many areas. Asterisks (*) and bullets (●), respectively, denote the graft particles and ingrown bone region in Figure 7A,B.

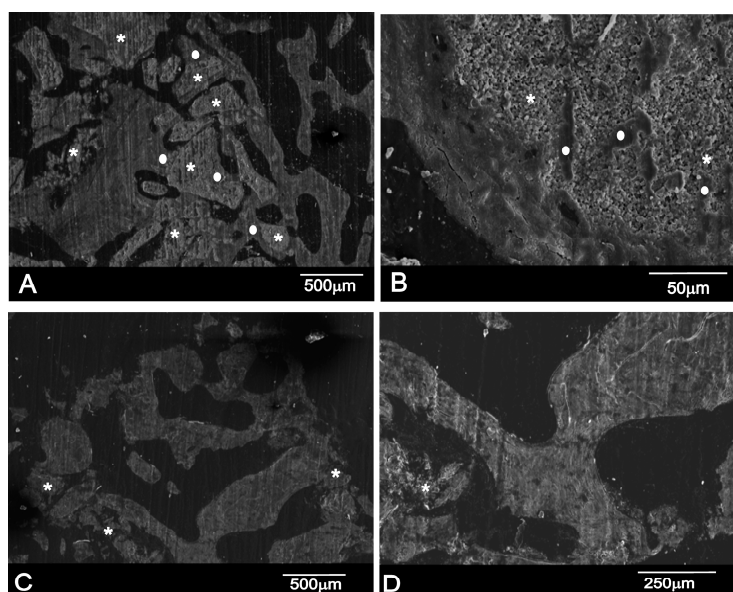


Figure 7. SEM-BSE of a resin-embedded bone section that contains bone and residual biomaterials: (A,B) the BBM material; and (C,D) the PBM material (* material particles as a result of the degradation process, and ● new bone). Section of the bone retrieved from a patient's maxillary sinus six months after sinus elevation.

In many fields, it was observed that the majority of the residual graft particles were connected by bridges to new bone. The bone-to-biomaterial interface was characterized by numbers of projections of newly formed bone into the graft particles. In most cases, the particle perimeter appeared to be lined by bone that adhered tightly to the biomaterial surface; although some bone was detached from the particle surface, this was only in a few very small areas. In backscattered electron images, particles of hydroxyapatite crystals were seen to be a white-gray color due to low organic content and a relatively high Ca/P ratio, whereas newly formed bone had a darker gray color because of the presence of collagen, marrow, and fat.

The PBM material degrades faster and, at the same time, new bone is reabsorbed, so we can see only material particles (*) surrounded by non-mineralized connective tissue (Figure 7B,C).

In histomorphometric terms, the BBM group showed that newly formed bone had become closely attached to both HAs. The histomorphometric measurements on the bone biopsies showed that, for PBM, the newly formed bone represented $25.92 \pm 1.61\%$, and $24.64 \pm 0.86\%$ for the residual graft material and $49.42 \pm 1.62\%$ for connective tissue, while $26.83 \pm 1.42\%$ represented the BBM newly formed bone, $30.80 \pm 0.88\%$ for the residual graft material, and $42.79 \pm 2.88\%$ for the non-mineralized connective tissue. Statistically significant differences were seen when comparing BBM and PBM in relation to NB (Mann–Whitney test, $p = 0.02$), RG (Mann–Whitney test, $p < 0.0001$), and CT (Mann–Whitney test, $p < 0.0001$). The mean and standard deviation (SD) values for all the parameters in each group are found in (Figure 8).

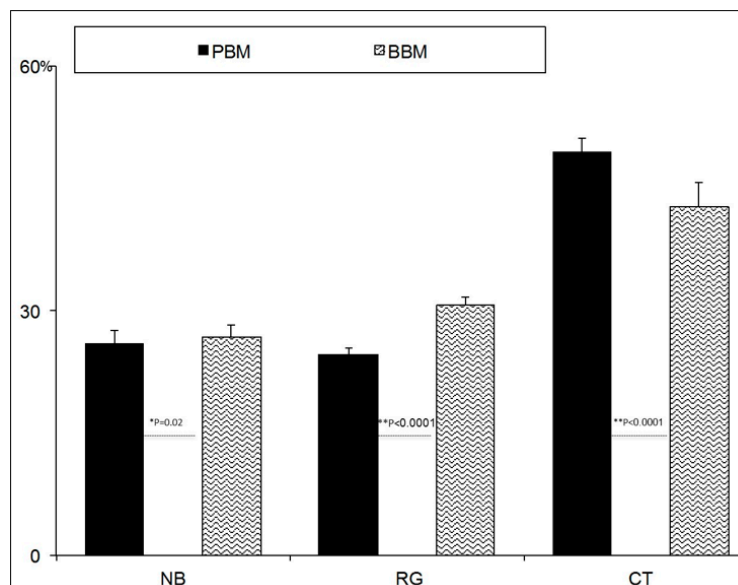


Figure 8. Histomorphometric measurements on bone biopsies. Histomorphometry shows the percentage of newly formed bone, marrow spaces and the residual grafted material. The figure provides the mean and SD values for all the parameters in each group. Statistically significant differences were seen when comparing BBM and PBM in relation to NB (new bone) (Mann–Whitney test, * $p = 0.02$), RG (residual graft material) (Mann–Whitney test, ** $p < 0.0001$), and CT (connective tissue) (Mann–Whitney test, ** $p < 0.0001$).

3. Discussion

In the present study, two different xenogenic bone substitute materials were characterized and evaluated in vivo in sinus floor elevation procedures. This study compared BBM processing at high temperature (1200 °C) and PBM processing at low temperature (130 °C) with different physico-chemical properties as bone substitutes for healing in sinus lift procedures. In this paper, the effect of sintering temperature on the porosity, crystallinity, composition and phase purity of porous HA ceramics made of natural bone was studied and reported. The characterization of HAs ensured an overall understanding about the role played by the biological behavior of these bone substitutes. Moreover, further importance is attached to this research because of the scarce scientific documentation in the literature comparing BBM and PBM in sinus lift procedures.

This study demonstrated that sinus augmentation with both BBM and PBM produces an increased vertical bone dimension compared to the baseline values, which accommodates dental implant placement.

Natural HA grafts may be a suitable alternative for using autogenous grafts. However, using these materials is sometimes avoided through lack of information, or due to contradictions between manufacturers' specifications and clinical results [9]. The HA derived from either natural sources or synthetic sources can form a strong chemical bond with the host bone tissue. This allows it to be recognized as a good bone substitute material. Xenografts have different properties depending on their origin, constitution and processing. Those that usually come from cows and pigs could be osteoinductive and osteoconductive, low-cost and offer good availability, but have the disadvantages of immune response and the risk of transmitting animal diseases. Significant differences in the use of biomaterials of animal or synthetic origin have yet to be reported. Some evidence suggests that synthetic materials have a lower risk of disease transmission [35]. Deproteinization is an indispensable process to eliminate antigenicity in xenograft bones. Valid strategies to eliminate the antigenicity of xenograft bones are of vital importance in the development of xenogenic bone graft substitutes [36]. It has been shown that deproteinized bones not only lose their immune reactivity, but also retain their osteoinduction and osteoconduction activities [23]. Sintering temperature is seen as an important

factor that can alter the characteristics of HA [37]. However, the effect of sintering temperature on the physico-chemical properties of natural HA, especially HA from bovine bone, is still not fully understood and research into this area is still underway. The most important parameters that can affect the properties of HA are temperature and heat treatment duration [38]. Both used materials differ significantly in processing temperature terms. Our results showed that the examined HA had variable physico-chemical properties according to the study of Muralithran and Ramesh's [39]. This discrepancy may affect the materials' performance, and indeed significant differences were found in terms of new bone formation, residual graft material and non-mineralized connective tissue after six months of healing.

The extensive characterization of the graft materials BBM and PBM made herein revealed that these two commercial bone grafts, despite being used in the clinical practice for the same purposes, possess markedly different properties, which are both chemical (e.g., composition, crystallinity, Ca/P ratio) and physical (e.g., particle size and shape, and pore size distribution). It is thus not surprising to find that they induce different responses after sinus lift elevation. The differences found in the explored characteristics seem to justify this distinct *in vivo* performance. Some studies have demonstrated that osteointegration and degradation processes are influenced by the material's physical and chemical properties [12,27–34]. Despite different responses being somehow anticipated since these materials, as the results show, have quite distinct properties, the following discussion attempts to interpret the *in vivo* response of these two biomaterials in terms of their physico-chemical characteristics.

The histologic examination of 60 biopsies taken from the 10 patients in this study indicated statistically significant differences in the histomorphometric parameters between the BBM and PBM graft materials. In the present study, a histomorphometric analysis of the biopsies done after six months showed a percentage of newly formed bone, which represented $25.92 \pm 1.61\%$ and $24.64 \pm 0.86\%$ for the residual graft material and $49.42 \pm 1.62\%$ for the connective tissue for PBM, while, for BBM, newly formed bone represented $26.83 \pm 1.42\%$, with $30.80 \pm 0.88\%$ for residual graft material and $42.79 \pm 2.88\%$ for non-mineralized connective tissue. New bone formation methods for bone deproteinization have to allow the heterologous deproteinized bone to have good biological safety and to meet all the scaffold material demands of tissue engineering. Moreover, the quantity and quality of newly formed bones must improve. The trabecular porous architecture of deproteinized bones acts as a support structure for blood vessels and bone cell expansion, which are extremely important for ossification [24]. PBM obtained the greater porosity 59.90%, but 38.11% of this porosity corresponded to submicron pore entrances. BBM porosity was 49.13%, but exhibited a much smaller proportion of submicron pores, only 3.66%. If pore size was too small, vascular supply could be compromised and osteoconduction decreased. This study confirmed the findings of earlier studies, which have reported the relation between pore and the quantity of neoformed osseous tissue. They concluded that pore size and granulometry should not be over-reduced as both pore diameter and interporotic connections have a significant effect on the type and quantity of newly formed bone tissue [40–43].

Contrarily to a similar radiological and histomorphometric design study at 8 months after a sinus lift procedure of two xenografts of bovine bone origin deproteinized at different temperatures, Deproteinized bovine bone (DBB-1) deproteinization occurred at low heat (300 °C) and (DBB-2) at a very high temperature (1200 °C), and no significant differences were found in new bone formation and residual graft material. In the histomorphometric analysis, new bone formation and residual graft materials were 29.13% and 24.63%, and 14.77%, and 13.01% in the DBB-2 + Collagen membrane (CM) and DBB-1 + CM groups, respectively. Although the healing period was two months longer in the study by Panagiotou et al. [44], we agree with their study in that the particles related to both graft materials were still observed in specimens, which demonstrates the slow resorption rate of the BBM materials. Since DBB-1 has a less crystalline structure compared to DBB-2, and might be more prone to degradation, residual DBB-1 particles might resorb more quickly. In our study into the characterization of both Has, the XRD patterns from the mineral samples corresponded to HA, with coincident peak

positions and relative intensities. However, these materials presented diverse degrees of crystallinity, as indicated by the different peak widths. For PBM, the diffractogram exhibits broad peaks with a low signal-to-noise ratio, which corresponds to a low-crystallinity material. The sharp well-resolved peaks found in the XRD spectrum of BBM indicate a highly crystalline HA. Thus, PBM sinterized at low temperature acquires a less crystalline structure compared to the BBM sinterized at high temperature, and might also be more prone to degradation. Tissues respond differently to biomaterials of different crystallinities. Major differences in the adhesive response of epithelial cells and osteoblast precursor cells to different crystallographic structures have been reported [27].

Regarding the sintering characteristics of HA, the resulting microstructure and properties were influenced by thermal history during the fabrication process. In the present study, the results showed that sintering temperature was a critical factor which influenced the phase stability, densification behavior, crystallinity and porosity of bovine HA ceramics. According to the results of research on the effect of sintering temperature, the density and hardness of HA increases with a rising sintering temperature, according to the results obtained [38].

A similar study that compared the sintered and non-sintered bone substitute materials in the sinuses of eight patients has indicated no significant differences in new bone formation and residual graft material terms. The examined xenogenic bone substitute materials were both gained with the same bovine origin. They differed mainly in the deproteinization way. The histological analysis revealed comparable results for the sintered (SBM) and non-sintered xenogeneic bone substitute material (NSBM). At the sites treated by sintered materials $29.71 \pm 13.7\%$ of the augmented site consisted of new bone, whereas the percentage of new bone was $30.57 \pm 16.1\%$ in the non-sintered group, together with the percentage of bone substitute materials in the augmented area ($40.68 \pm 16.3\%$ for the sintered group, and $43 \pm 19.1\%$ for the non-sintered group) [45]. Even the histomorphometric results revealed a lower percentage of residual graft particles for the sintered group compared with our results.

According to other studies, which have also compared two xenograft materials prepared by a deproteinizing technique at low temperature (Bio-Oss) or high temperature (Cerabone) in the sinus cavity, compared to our study they observed a significantly greater volumetric loss of the initial graft size for the non-sintered material. Bio-Oss has a significantly larger surface area and a smaller crystallite size compared to Cerabone. This might have a crucial influence on the resorption rate [46]. In the BBM process, an increasing sintering temperature caused increased sample crystallinity and induced HA densification, which resulted in grain growth with the formation of dense grain boundary phases. These differences were associated with significantly higher resorption rates for the initial graft volume observed for the PBM material. Depending on the degrees of crystallinity, albumin solution or cell suspension has been suggested to selectively adsorb on HA surfaces as such, and this study demonstrated the importance of determining the effects of the physico-chemical characteristics of HA surfaces on cell activity [28]. Dissolution of HA is dependent on its crystallinity, with dissolution increasing with lowering degrees of crystallinity. Albumin adsorption and cell attachment are seen to selectively adsorb on the HA surface, and the degree of adsorption is dependent on HA crystallinity [47].

Properties like solubility and surface reactivity are highly dependent on calcium phosphate composition and surface texture. Such characteristics strongly affect the nature of the biologically equivalent (carbonated) apatite formed when calcium phosphates come into contact with bone tissue [48]. In our study, a statistically significant difference was found between PBM 2.22 ± 0.08 and BBM 2.31 ± 0.09 in the calcium/phosphate composition ratio. The slow dissolution capacity of the BBM graft was attributed to the small quantity of tricalcium phosphate produced during heat treatment. The annealing temperature affects the type and amount of other calcium phosphate phases and/or other Ca compounds, which are present with the HA phase [49].

Deproteinized bones at low temperature have shown lower protein content, and a higher collagen content has been preserved [24]. The Tecross patented manufacturing process, used to produce PBM, achieves biocompatibility by avoiding temperatures above $120\text{ }^{\circ}\text{C}$, which would cause the ceramization

of granules by preserving part of the collagen matrix of the original animal bone. The result was a unique biomaterial that consisted of mineral components and an organic matrix with a very similar level of porosity to autogenous bone that quickly resorbs. The role of the collagen composition of the PBM used herein is useful for its intrinsic agglutination characteristic, which helps in structuring the composite, influence the morphology and size of HA crystals and, at the same time, contribute in the process of osteoclast adhesion to the biomaterial surface [4,50].

It has been hypothesized that the hydrolytic enzymes (collagenase) released from activated PMN cells are involved in the rapid degradation of the graft's porcine collagen portion. However, no studies have reported the outcome of this material after maxillary sinus floor elevation [51].

The aforementioned properties of the graft material have led researchers to choose bovine bone material as the gold standard of xenografts because it has been demonstrated to be a biologically inert osteoconductive material for sinus augmentation procedures [52].

Biocompatibility, osteoconduction and low rate resorption after surgery are favorable properties of xenografts, but long-term studies must be carried out to understand xenografts' pattern of biodegradation and its influence on bone gain [50].

4. Materials and Methods

4.1. Grafts

Two different types of commercial bone grafts used in dentistry were characterized and evaluated *in vivo* in relation to the bone tissue response:

1. (PBM, OsteoBio[®] mp3 deproteinized porcine bone substitute material) was made up of granulated small bone particles, 600–1000 μm in size, and is a ceramic that derives from cancellous-cortical porcine bone. The material is obtained at a low processing temperature (130 $^{\circ}\text{C}$). According to its commercial specifications, this material is claimed to preserve the structure and composition of natural bone components.
2. (BBM, Endobon[®] deproteinized bovine bone substitute material) was made up of granulated small bone particles, 500–1000 μm in size, and is a ceramic that derives from cancellous bovine bone, which is fully deproteinated by a high temperature manufacturing process for safety from bacteria, viruses and prions. This process consists of two steps: firstly, pyrolysis at a temperature above 900 $^{\circ}\text{C}$ to eliminate the organic element; secondly, a ceramization process at temperatures above 1200 $^{\circ}\text{C}$ to create a crystalline structure.

4.2. Graft Characterization

These biomaterials were characterized in morphology, composition, crystallinity, particle size distribution, porosity and pore size terms.

4.2.1. SEM-EDX

An analysis using SEM-EDX made it possible to determine the (qualitative and semi-quantitative) chemical composition on the sample's surface. The quantities indicated in the EDX microanalysis tables are only semi-quantitative, and serve as an indicator of the quantities of each element present. The microstructure and composition of the porous ceramic were studied under a scanning electron microscope (SEM, HITACHI S-3500N, Ibaraki, Japan). Quantitative analyses were done by an Energy Dispersive X-ray Spectroscopy (EDX) system (Inca-Oxford Instruments, High Wycombe, UK) coupled to the above-described electron microscope using the ZAF (atomic number, absorption and fluorescence) correction software and Bayer standards. Microanalysis data were obtained from the mean of 10 independent determinations. Samples were pre-coated with palladium for the SEM images and were carbon-coated for the EDX analysis in an argon atmosphere using a sputtering machine (Polaron K550X Sputter Coater, Laughton, UK).

4.2.2. X-ray Diffraction (XRD)

This technique consisted of directing an X-ray beam of wavelength 1.5418 Angstroms onto samples to record the presented crystalline phases. With these recordings, the intensities of the diffraction lines that corresponded to the phases were determined and, hence, the present phases could be qualitatively determined. The mineralogical characterization of the powder material was performed by XRD (Bruker-AXS D8Advance, Karlsruhe, Germany) by Cu-K α radiation at 40 kV and 30 mA. Scans were taken with 2θ values, which varied from 5° to 60° at a rate of $0.05^\circ/\text{min}$.

4.2.3. Mercury Intrusion Porosimetry (MIP)

Information on sample porosity and pore size distribution was obtained by mercury porosimetry using the Poremaster-60 GT (Quantachrome Instruments, Boyton Beach, FL, USA) within a pressure range between 5.395 KPa and 410,785.062 KPa, which corresponds to a range of pore diameters between 300 μm and 0.0035 μm .

4.2.4. Statistical Analysis

At least seven runs were performed per sample, and at least three different samples were analyzed per material. The mean and standard deviations were obtained for all the investigated groups. The Kolmogorov–Smirnov test was used to check normality. Comparisons between groups BBM and PBM were made with Student's *t* (parametric data) or Mann–Whitney (non-parametric data). All the statistical analyses were performed with the appropriate software (MedCalc v15.8, MedCalc, Ostend, Belgium). Significance was evaluated at a level of $p < 0.05$.

4.3. Implant Procedure

4.3.1. Patient Selection and Protocol

Ten partially edentulous patients (five females and five males), with ages ranging from 37 to 60 years and who came to the Department of Oral and Maxillofacial Surgery, were recruited. Patients who demanded fixed restorative appliances in the posterior maxilla were selected for maxillary sinus augmentation due to lack of sufficient bone tissue to place endosseous dental implants. The protocol for harvesting bone samples was approved by the University Ethics Committee (UCAM Ethics Committee; approval ID: 6635) and informed consent was obtained from all the patients. The study was designed following the guidelines set out in the Declaration of Helsinki for experimentation on human subjects. Any possible complications to arise from the surgical therapy were treated following standard dental management protocols.

4.3.2. Inclusion and Exclusion Criteria

The inclusion criteria were as follows: maxillary partial bilateral edentulism involving the premolar-molar areas. The cases with a crestal bone height between 0 and 7 mm and a high postero-lateral atrophy (Cawood V–VI) are most likely to have a two-stage lateral antrostomy.

The exclusion criteria were: patients suffering an uncontrolled systemic disease or condition known to alter bone metabolism (i.e., osteoporosis, diabetes mellitus, etc.); subjects who were taking/had taken medications known to modify bone metabolism, e.g., bisphosphonates, corticosteroids, etc.; women who were pregnant or trying for pregnancy at the time of screening; patients who presented existing sinus conditions, sepsis, a history of cancer and/or radiation in the oral cavity; complications derived from any of these conditions that affect the sinus area.

4.3.3. Surgical Procedure: First Phase

The study was performed in two surgical phases. In the first phase all the patients took 875/125 mg of amoxicillin/clavulanic acid, every 8 h, starting 1 day before surgery. A dose of

300 mg of Clindamycin every 8 h was prescribed to penicillin-allergic patients. This medication was maintained for 7 days. All the surgical procedures were performed under local anesthesia (Ultracain, Aventis Inc., Frankfurt, Germany). The basic surgical procedure was represented in all the patients by maxillary sinus floor elevation via a lateral approach.

A conventional lateral wall approach was used to perform sinus grafting in all the patients. Fullthickness flaps were elevated to expose the alveolar crest and the lateral wall of the maxillary sinus. A trap door was made in the lateral sinus wall. The sinus membrane was elevated with different shaped curettes until it was completely detached from the lateral and inferior walls of the sinus.

After membrane elevation, a bioabsorbable collagen barrier membrane was placed under the sinus membrane and adapted to come into contact with the peripheral bony walls (Evolution Fine[®] OsteoBioI[®], Tecness Dental S.R.L., Torino, Italy). On one side, sinus cavities were grafted with (PBM) (OsteoBioI[®] mp3, Tecness Dental S.R.L., Torino, Italy). After grafting, an absorbable collagen membrane (Evolution Fine[®] OsteoBioI[®], Tecness Dental S.R.L., Torino, Italy) was placed over the window to minimize soft tissue invasion. On the other side, sinus cavities were grafted with (BBM) (Endobon[®], RegenerOssTM, BIOMET3i, Palm Beach Gardens, FL, USA). Grafting materials were mixed with venous blood from the defect area and were carefully packed in the created volume following mucous membrane elevation. After bone grafting, a short-term absorbable collagen membrane (Evolution Fine[®] OsteoBioI[®], Tecness Dental S.R.L., Torino, Italy) was placed over the window. Primary closure was achieved in both cases by suturing with 3–0 silk suture (Laboratory Arago' n, Barcelona, Spain) (Figure 9).

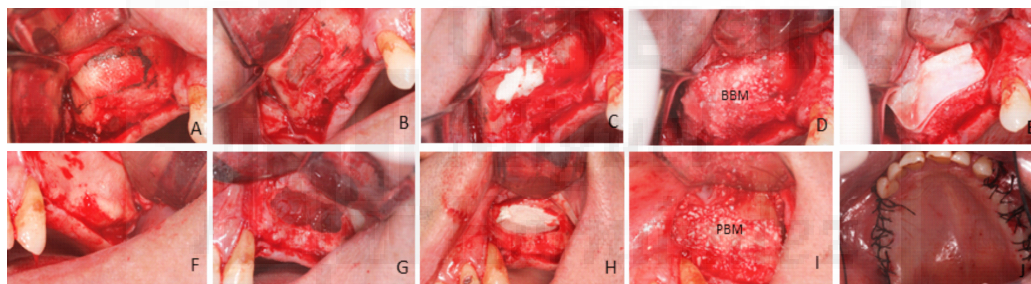


Figure 9. Surgical procedure: (A) A crestal incision was made slightly palatally, supplemented by buccal releasing incisions mesially and distally. Fullthickness flaps were elevated to expose the alveolar crest and the lateral wall of the maxillary sinus. (B) A trap door was made in the lateral sinus wall. Schneiderian membrane elevation was accomplished by initially exposing and mobilizing the membrane, followed by hand instrumentation to further elevate the membrane along the medial wall of the sinus. The sinus membrane was elevated with different shaped curettes. (C) A bioabsorbable collagen barrier membrane was applied underneath the Schneiderian membrane to prevent the dislocation of grafting material if membrane perforation occurred. Randomly, one of the two bone substitute materials was placed into the newly created space between the collagen membrane and the sinus floor (D). The bovine porous bone mineral was mixed with venous blood and was packed carefully in the sinus cavity, especially in the posterior and anterior parts (E). After bone grafting, a second absorbable collagen membrane was placed over the window (F). On the other side, a crestal incision was made slightly palatally, supplemented mesially and distally with two buccal releasing incisions. Full-thickness flaps were elevated to expose the alveolar crest and the lateral wall of the maxillary sinus. (G) A trap door was made in the lateral sinus wall using a round bur under sterile saline solution irrigation conditions. The sinus membrane was elevated with different shapes curettes until it was completely detached from the lateral and inferior wall of the sinus. (H) A bioabsorbable collagen barrier membrane was placed under the sinus membrane and was adapted to come into contact with the peripheral bony walls. (I) The maxillary sinuses were filled with porcine bone material and a short-term absorbable collagen bovine membrane was placed over the window. (J) Flaps were sutured.

Antibiotics and analgesics were prescribed for 1 week. All the patients took 875/125 mg of amoxicillin/clavulanic acid every 8 h, starting 1 day before surgery. Moreover, 300 mg of Clindamycin every 8 h was prescribed to penicillin-allergic patients. This medication was maintained for 7 days. Sutures were removed 2 weeks after surgery. During the postoperative period, patients were followed up clinically and radiologically at monthly intervals.

4.3.4. Surgical Procedure: Second Phase (Bone Biopsy Harvesting)

After a 6-month healing period, the second surgical phase was performed. A 3×10 mm diameter trephine, under sterile saline solution irrigation conditions, was used to retrieve a central core of bone upon implant insertion, and 60 bone samples were retrieved for the analysis. Three biopsies were taken from each individual on each side. Nevertheless, the biopsy value used for the analysis is unique to each individual, and was computed as the mean of the three taken biopsies, thus avoiding possible dependency problems. After retrieval, functional implants were placed at the same sites as the trephined holes on each side (Figure 10).

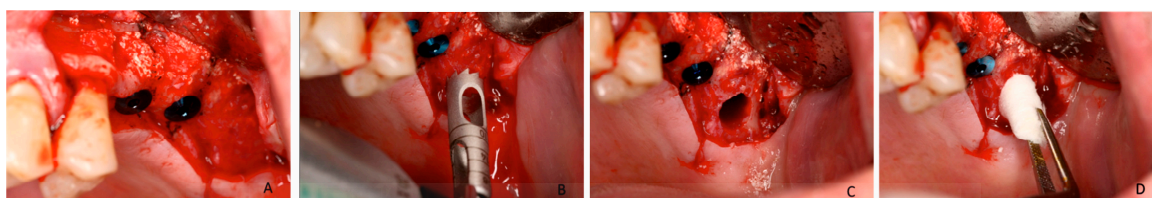


Figure 10. A 3×10 mm diameter trephine under sterile saline solution irrigation conditions was used to retrieve a central core of bone upon implant insertion. Sixty bone biopsies were obtained from 60 grafted sites. (A) The functional implants were placed on each side; (B) 3×10 mm diameter trephine under sterile saline solution irrigation was used to retrieve a central core bone; (C) each side received three implants; and (D) the functional implants were placed in the same sites as the trephined holes on each side.

4.4. Sample Processing and Analysis

Samples were fixed by immersion in 4% formalin solution, dehydrated in a graded ethanol series, and embedded in plastic resin (Technovit A 7210VCL; Kulzer & Co., Hanau, Germany). They were then polished by a manual grinder with 800 grit silicon carbide paper, mounted on an aluminum stub and carbon-coated (Polaron sputter coater). Each block was processed for scanning electron microscopy (SEM). The blocks that contained the entire graft area were obtained using a precision saw. BSE- Back-scattered electron imaging was used to highlight the contrasts among resin, bone and biomaterial. With the image J polygon selection tool irregular shaped areas were outlined by selecting three different regions of interest: bone, residual material and black spaces. All three were calculated in samples of 200 micrometers \times 200 micrometers. The images in pseudocolors, obtained, using backscattered electrons, were used to evaluate and measure the histomorphometric parameters. The selections were outlined in colors, once created this sections were measured by pixels number and was expressed as percentage. A different color was applied to anyone to enhance a difference. The histomorphometric analysis was performed on the bone core samples to determine vital bone content, connective tissue content and residual graft material content (Figure 11).

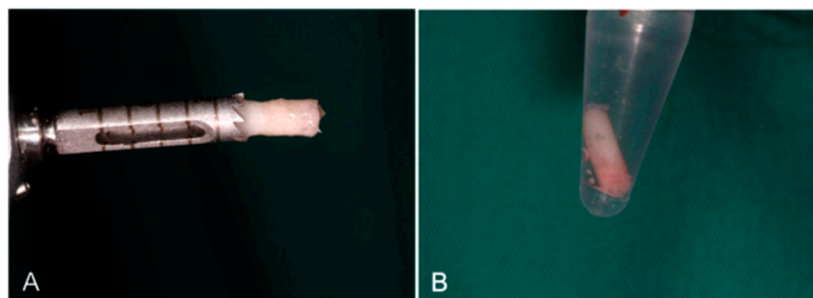


Figure 11. (A) A sample of bone core for histomorphometric analysis; (B) Sixty bone biopsies were obtained from sixty grafted sites.

4.5. Statistical Analysis

Quantitative data were recorded as the mean value \pm SD. Comparisons between BBM and PBM for each parameter (NB) new bone, (RG) residual graft material and (CT) connective tissue were made with the help of statistical software (MedCalc v15.8, MedCalc, Ostend, Belgium). The conformity of the parameters to normal distribution was assessed by the Kolmogorov–Smirnov test. A Mann–Whitney U test was used for the intergroup comparisons of the parameters without normal distribution. Significance was evaluated at a level of $p < 0.05$.

5. Conclusions

The differences found in the physico-chemical characteristics of both xenografts in accordance with the protocol developed on industrial scale justify this distinct *in vivo* performance. The differences found in porosity, crystallinity and composition terms determine the different behavior of these materials.

The HAs assessed herein are shown to be biocompatible and osteoconductive when used for maxillary sinus elevation purposes. PBM displayed a high level of degradation over the study period. Detailed information about graft material characteristics is crucial to evaluate its clinical outcomes. More histological and histomorphometrical studies are needed to better understand the resorption times of these biomaterials. A more detailed process of resorption of the biomaterials analyzed will be developed in future work.

Acknowledgments: Part of this work has been supported by a Spanish Ministry of Economy and Competitiveness (MINECO) (contract grant number: MAT2013-48426-C2-2-R).

Author Contributions: María Piedad Ramírez Fernández performed the implantation and the post implantation characterization; Patricia Mazón collaborated in the materials characterization; Sergio Alexander Gehrke performed the statistical analysis; Jose Luis Calvo Guirado conceived the *in vivo* experiments and helped in the implantation procedure, and Piedad de Aza performed the materials characterization. All authors contributed to the analyses and discussion of the results as well as prepared the manuscript.

Conflicts of Interest: The authors declare no conflict of interest.

References

1. Beretta, M.; Poli, P.P.; Grossi, G.B.; Pieroni, S.; Maiorana, C. Long-term survival rate of implants placed in conjunction with 246 sinus floor elevation procedures: Results of a 15-year retrospective study. *J. Dent.* **2015**, *43*, 78–86. [[CrossRef](#)] [[PubMed](#)]
2. Danesh-Sani, A.S.; Loomer, P.M.; Wallace, S.S. A comprehensive clinical review of maxillary sinus floor elevation: Anatomy, techniques, biomaterials and complications. *Br. J. Oral Maxillofac. Surg.* **2016**, *54*, 724–730. [[CrossRef](#)] [[PubMed](#)]
3. Urist, M.R. Bone: Formation by autoinduction. 1965. *Clin. Orthop. Relat. Res.* **2002**, *395*, 4–10. [[CrossRef](#)]
4. Swetha, M.; Sahithi, K.; Moorthi, A.; Srinivasan, N.; Ramasamy, K.; Selvamurugan, N. Biocomposites containing natural polymers and hydroxyapatite for bone tissue engineering. *Int. J. Biol. Macromol.* **2010**, *1*, 1–4. [[CrossRef](#)] [[PubMed](#)]

5. Danesh-Sani, S.A.; Engebretson, S.P.; Janal, M.N. Histomorphometric results of different grafting materials and effect of healing time on bone maturation after sinus floor augmentation: A systematic review and meta-analysis. *J. Periodontal Res.* **2016**. [[CrossRef](#)] [[PubMed](#)]
6. Frenken, J.W.; Bouwman, W.F.; Bravenboer, N.; Zijdeveld, S.A.; Schulten, E.A.; ten Bruggenkate, C.M. The use of Straumanns Bone Ceramic in a maxillary sinus floor elevation procedure: A clinical, radiological, histological and histomorphometric evaluation with a 6-month healing period. *Clin. Oral Implant Res.* **2010**, *21*, 201–208. [[CrossRef](#)] [[PubMed](#)]
7. Simunek, A.; Kopecka, D.; Somanathan, R.V.; Pilathadka, S.; Brazda, T. Deproteinized bovine bone versus beta-tricalcium phosphate in sinus augmentation surgery: A comparative histologic and histomorphometric study. *Int. J. Oral Maxillofac. Implant* **2008**, *23*, 935–942.
8. Esposito, M.; Grusovin, M.G.; Rees, J.; Karasoulos, D.; Felice, P.; Alissa, R.; Worthington, H.; Coulthard, P. Effectiveness of sinus lift procedures for dental implant rehabilitation: A Cochrane systematic review. *Eur. J. Oral Implantol.* **2010**, *23*, 7–26.
9. Tadic, D.; Epple, M. A thorough physicochemical characterization of 14 calcium phosphate-based bone substitution materials in comparison to natural bone. *Biomaterials* **2004**, *25*, 987–994. [[CrossRef](#)]
10. Jensen, T.; Schou, S.; Stavropoulos, A.; Terheyden, H.; Holmstrup, P. Maxillary sinus floor augmentation with Bio-Oss or Bio-Oss mixed with autogenous bone as graft: A systematic review. *Clin. Oral Implant Res.* **2012**, *23*, 263–273. [[CrossRef](#)] [[PubMed](#)]
11. Froum, S.J.; Tarnow, D.P.; Wallace, S.S.; Rohrer, M.D.; Cho, S.C. Sinus floor elevation using anorganic bovine bone matrix (OsteoGraf/N) with and without autogenous bone: A clinical, histologic, radiographic, and histomorphometric analysis—Part 2 of an ongoing prospective study. *Int. J. Periodontics Restor. Dent.* **1998**, *18*, 528–543.
12. Carvalho, A.L.; Faria, P.E.; Grisi, M.F.; Souza, S.L.; Taba, M.J.; Palioto, D.B.; Novaes, A.B.; Fraga, A.F.; Ozyegin, L.S.; Oktar, F.N.; et al. Effects of granule size on the osteoconductivity of bovine and synthetic hydroxyapatite: A histologic and histometric study in dogs. *J. Oral Implantol.* **2007**, *33*, 267–276. [[CrossRef](#)]
13. Orsini, G.; Traini, T.; Scarano, A.; Degidi, M.; Perrotti, V.; Piccirilli, M.; Piattelli, A. Maxillary sinus augmentation with Bio-Oss particles: A light, scanning, and transmission electron microscopy study in man. *J. Biomed. Mater. Res. B Appl. Biomater.* **2005**, *74*, 448–457. [[CrossRef](#)] [[PubMed](#)]
14. Cordaro, L.; Bosshardt, D.D.; Palatella, P.; Rao, W.; Serino, G.; Chiapasco, M. Maxillary sinus grafting with Bio-Oss® or Straumann® Bone Ceramic: Histomorphometric result from a randomized controlled multicenter clinical trial. *Clin. Oral Implant Res.* **2008**, *19*, 796–803. [[CrossRef](#)] [[PubMed](#)]
15. Traini, T.; Valentini, P.; Lezzi, G.; Piattelli, A. A histologic and histomorphometric evaluation of anorganic bovine bone retrieved 9 years after a sinus augmentation procedure. *J. Periodontol.* **2007**, *78*, 955–961. [[CrossRef](#)] [[PubMed](#)]
16. Traini, T.; Degidi, M.; Sammons, R.; Stanley, P.; Piattelli, A. Histologic and elemental microanalytical study of anorganic bovine bone substitution following sinus floor augmentation in humans. *J. Periodontol.* **2008**, *79*, 1232–1240. [[CrossRef](#)] [[PubMed](#)]
17. Nevins, M.; Camelo, M.; de Angelis, N.; Hanratty, J.J.; Khang, W.G.; Kwon, J.J.; Rasperini, G.; Rocchietta, I.; Schupbach, P.; Kim, D.M. The clinical and histologic efficacy of xenograft granules for maxillary sinus floor augmentation. *Int. J. Periodontics Restor. Dent.* **2011**, *31*, 227–235. [[CrossRef](#)]
18. Wenz, B.; Oesch, B.; Horst, M. Analysis of the risk of transmitting bovine spongiform encephalopathy through bone grafts derived from bovine bone. *Biomaterials* **2001**, *22*, 1599–1606. [[CrossRef](#)]
19. Lee, J.S.; Shin, H.K.; Yun, J.H.; Cho, K.S. Randomized Clinical Trial of Maxillary Sinus Grafting using Deproteinized Porcine and Bovine Bone Mineral. *Clin. Implant Dent. Relat. Res.* **2016**. [[CrossRef](#)] [[PubMed](#)]
20. Orsini, G.; Scarano, A.; Piattelli, M.; Piccirilli, M.; Caputi, S.; Piattelli, A. Histologic and ultrastructural analysis of regenerated bone in maxillary sinus augmentation using a porcine bone-derived biomaterial. *J. Periodontol.* **2006**, *77*, 1984–1990. [[CrossRef](#)] [[PubMed](#)]
21. Scarano, A.; Piattelli, A.; Perrotti, V.; Manzon, L.; Lezzi, G. Maxillary sinus augmentation in human using cortical porcine bone: A histological and histomorphometrical evaluation after 4 and 6 months. *Clin. Implant Dent. Relat. Res.* **2011**, *13*, 13–18. [[CrossRef](#)] [[PubMed](#)]
22. Barone, A.; Ricci, M.; Covani, U.; Nannmark, U.; Azarmehr, I.; Calvo-Guirado, J.L. Maxillary sinus augmentation using prehydrated corticocancellous porcine bone: Hystomorphometric evaluation after 6 months. *Clin. Implant Dent. Relat. Res.* **2012**, *14*, 373–379. [[CrossRef](#)] [[PubMed](#)]

23. Castro-Ceseña, A.B.; Sánchez-Saavedra, M.P.; Novitskaya, E.E.; Chen, P.Y.; Hirata, G.A.; McKittrick, J. Kinetic characterization of the deproteinization of trabecular and cortical bovine femur bones. *Mater. Sci. Eng. C Mater. Biol. Appl.* **2013**, *33*, 4958–4964. [[CrossRef](#)] [[PubMed](#)]
24. Liu, J.; Ye, X.; Wang, H.; Zhu, M.; Wang, B.; Yan, H. The influence of pH and temperature on the morphology of hydroxyapatite synthesized by hydrothermal method. *Ceram. Int.* **2003**, *29*, 629–633. [[CrossRef](#)]
25. Le Geros, R.Z. Properties of Osteoconductive Biomaterials: Calcium Phosphates. *Clin. Orthop. Relat. Res.* **2002**, *395*, 81–98. [[CrossRef](#)]
26. Blokhuis, T.J.; Termaat, M.F.; den Boer, F.C.; Patka, P.; Bakker, F.C.; Haarman, H.J. Properties of calcium phosphate ceramics in relation to their in vivo behavior. *J. Trauma* **2000**, *48*, 179–186. [[CrossRef](#)] [[PubMed](#)]
27. Danoux, C.; Pereira, D.; Döbelin, N.; Stähli, C.; Barralet, J.; van Blitterswijk, C.; Habibovic, P. The Effects of Crystal Phase and Particle Morphology of Calcium Phosphates on Proliferation and Differentiation of Human Mesenchymal Stromal Cells. *Adv. Healthc. Mater.* **2016**, *5*, 1775–1785. [[CrossRef](#)] [[PubMed](#)]
28. Yang, Y.; Dennison, D.; Ong, J.L. Protein Adsorption and Osteoblast Precursor Cell Attachment to Hydroxyapatite of Different Crystallinities. *Int. J. Oral Maxillofac. Implant* **2005**, *20*, 187–192.
29. Rosa, A.L.; Beloti, M.M.; Oliveira, P.T.; van Noort, R. Osseointegration and osseointegration of hydroxyapatite of different microporosities. *J. Mater. Sci. Mater. Med.* **2002**, *13*, 1071–1075. [[CrossRef](#)] [[PubMed](#)]
30. Karageorgiou, V.; Kaplan, D. Porosity of 3D biomaterial scaffolds and osteogenesis. *Biomaterials* **2005**, *26*, 5474–5491. [[CrossRef](#)] [[PubMed](#)]
31. Von Doernberg, M.C.; von Rechenberg, B.; Bohner, M.; Grünenfelder, S.; van Lenthe, G.H.; Müller, R.; Gasser, B.; Mathys, R.; Baroud, G.; Auer, J. In vivo behavior of calcium phosphate scaffolds with four different pore sizes. *Biomaterials* **2006**, *27*, 5186–5198. [[CrossRef](#)] [[PubMed](#)]
32. Ducheyne, P.E.; Qiu, Q. Bioactive ceramics: The effect of surface reactivity on bone formation and bone cell function. *Biomaterials* **1999**, *20*, 2287–2303. [[CrossRef](#)]
33. Ghanaati, S.; Barbeck, M.; Detsch, R.; Deisinger, U.; Hilbig, U.; Rausch, V.; Sader, R.; Unger, R.E.; Ziegler, G.; Kirkpatrick, C.J. The chemical composition of synthetic bone substitutes influences tissue reactions in vivo: Histological and histomorphometrical analysis of the cellular inflammatory response to hydroxyapatite, beta-tricalcium phosphate and biphasic calcium phosphate ceramics. *Biomed. Mater.* **2012**, *7*, 015005. [[CrossRef](#)] [[PubMed](#)]
34. Habibovic, P.; Kruyt, M.C.; Juhl, M.V.; Clyens, S.; Martinetti, R.; Dolcini, L.; Theilgaard, N.; van Blitterswijk, C.A. Comparative in vivo study of six hydroxyapatite-based bone graft substitutes. *J. Orthop. Res.* **2008**, *26*, 1363–1370. [[CrossRef](#)] [[PubMed](#)]
35. Rodella, L.F.; Favero, G.; Labanca, M. Biomaterials in maxillofacial surgery: Membranes and grafts. *Int. J. Biomed. Sci.* **2011**, *7*, 81–88. [[PubMed](#)]
36. Barakata, N.A.M.; Khalil, K.A.; Sheikh, F.A.; Omran, A.M.; Gaihre, B.; Khild, S.M.; Kim, H.Y. Physicochemical characterizations of hydroxyapatite extracted from bovine bones by three different methods: Extraction of biologically desirable Hap. *Mater. Sci. Eng. C Mater. Biol. Appl.* **2008**, *28*, 1381–1387. [[CrossRef](#)]
37. Hong, J.Y.; Kim, Y.J.; Lee, H.W.; Lee, W.K.; Ko, J.S.; Kim, H.M. Osteoblastic cell response to thin film of poorly crystalline calcium phosphate apatite formed at low temperatures. *Biomaterials* **2003**, *24*, 2977–2984. [[CrossRef](#)]
38. Herliansyah, M.K.; Hamdia, M.; de-Ektessabic, A.I.; Wildanb, M.W.; Toque, J.A. The influence of sintering temperature on the properties of compacted bovine. *Mater. Sci. Eng. C Mater. Biol. Appl.* **2009**, *29*, 1674–1680. [[CrossRef](#)]
39. Muralithran, G.; Ramesh, S. The effects of sintering temperature on the properties of hydroxyapatite. *Ceram. Int.* **2000**, *26*, 221–230. [[CrossRef](#)]
40. Annaz, B.; Hing, K.A.; Kayser, M.; Buckland, T.; di Silvio, L. An ultrastructural study of cellular response to variation in porosity in phase-pure hydroxyapatite. *J. Microsc.* **2004**, *216*, 97–109. [[CrossRef](#)] [[PubMed](#)]
41. Cyster, L.A.; Grant, D.M.; Howdle, S.M.; Rose, F.R.; Irvine, D.J.; Freeman, D.; Scotchford, C.A.; Shakesheff, K.M. The influence of dispersant concentration on the pore morphology of hydroxyapatite ceramics for bone tissue engineering. *Biomaterials* **2005**, *26*, 697–702. [[CrossRef](#)] [[PubMed](#)]
42. Coathup, M.J.; Hing, K.A.; Samizadeh, S.; Chan, O.; Fang, Y.S.; Champion, C.; Buckland, T.; Blunn, G.W. Effect of increased strut porosity of calcium phosphate bone graft substitute biomaterials on osteoinduction. *J. Biomed. Mater. Res. A* **2012**, *100*, 1550–1555. [[CrossRef](#)] [[PubMed](#)]

43. Figueiredo, A.; Coimbra, P.; Cabrita, A.; Guerra, F.; Figueiredo, M. Comparison of a xenogeneic and an alloplastic material used in dental implants in terms of physico-chemical characteristics and in vivo inflammatory response. *Mater. Sci. Eng. C Mater. Biol. Appl.* **2013**, *3*, 3506–3513. [[CrossRef](#)] [[PubMed](#)]
44. Panagiotou, D.; Ozkan Karaca, E.; Dirikan Ipci, S.; Cakar, G.; Olgac, V.; Yilmaz, S. Comparison of two different xenografts in bilateral sinus augmentation: Radiographic and histologic findings. *Quintessence Int.* **2015**, *46*, 611–619. [[CrossRef](#)] [[PubMed](#)]
45. Riachi, F.; Naaman, N.; Tabarani, C.; Aboelsaad, N.; Berberi, A.; Salameh, Z. Influence of material properties on rate of resorption of two bone graft materials. *Int. J. Dent.* **2012**, *2012*. [[CrossRef](#)] [[PubMed](#)]
46. Fienitz, T.; Moses, O.; Klemm, C.; Happe, A.; Ferrari, D.; Kreppel, M.; Ormianer, Z.; Gal, M.; Rothamel, D. Histological and radiological evaluation of sintered and non-sintered deproteinized bovine bone substitute materials in sinus augmentation procedures. A prospective, randomized-controlled, clinical multicenter study. *Clin. Oral Investig.* **2016**. [[CrossRef](#)] [[PubMed](#)]
47. Conz, M.B.; Granjeiro, J.M.; Soares, G.A. Physicochemical characterization of six commercial hydroxyapatites for medical-dental applications as bone graft. *J. Appl. Oral Sci.* **2005**, *13*, 136–140. [[CrossRef](#)] [[PubMed](#)]
48. Monteiro, M.M.; da Rocha, N.C.C.; Rossi, A.M.; de Almeida Soares, G. Dissolution properties of calcium phosphate granules with different compositions in simulated body fluid. *J. Biomed. Mater. Res. A* **2003**, *65*, 299–305. [[CrossRef](#)] [[PubMed](#)]
49. Joschek, S.; Nies, B.; Krotz, R.; Göferich, A. Chemical and physicochemical characterization of porous hydroxyapatite ceramics made of natural bone. *Biomaterials* **2000**, *21*, 1645–1658. [[CrossRef](#)]
50. Rodrigues, C.V.M.; Serricella, P.; Linhares, A.B.; Guerdes, R.M.; Borojevic, R.; Rossi, A.M. Characterization of a bovine collagen-hydroxyapatite composite scaffold for bone tissue engineering. *Biomaterials* **2003**, *24*, 4987–4997. [[CrossRef](#)]
51. Alayan, J.; Vaquette, C.; Farah, C.; Ivanovski, S. A histomorphometric assessment of collagen-stabilized anorganic bovine bone mineral in maxillary sinus augmentation—A prospective clinical trial. *Clin. Oral Implants Res.* **2016**, *27*, 850–858. [[CrossRef](#)] [[PubMed](#)]
52. Corbella, S.; Taschieri, S.; Weinstein, R.; Del Fabbro, M. Histomorphometric outcomes after lateral sinus floor elevation procedure: A systematic review of the literature and meta-analysis. *Clin. Oral Implants Res.* **2016**, *27*, 1106–1122. [[CrossRef](#)] [[PubMed](#)]



© 2017 by the authors. Licensee MDPI, Basel, Switzerland. This article is an open access article distributed under the terms and conditions of the Creative Commons Attribution (CC BY) license (<http://creativecommons.org/licenses/by/4.0/>).

Article

SEM-EDX Study of the Degradation Process of Two Xenograft Materials Used in Sinus Lift Procedures

María Piedad Ramírez Fernández ¹, Sergio A. Gehrke ², Carlos Pérez Albacete Martínez ¹, Jose L. Calvo Guirado ¹ and Piedad N. de Aza ^{3,*}

¹ Catedra Internacional de Investigación en Odontología, University Católica San Antonio de Murcia, Avda. Jerónimos, 135, 30107 Guadalupe, Murcia, Spain; mpramirez@ucam.ed (M.P.R.F.); cperezalbacete@ucam.edu (C.P.A.M.); jlcalvo@ucam.edu (J.L.C.G.)

² Biotecnos Research Center, Rua Dr. Bonazo n° 57, 97015-001 Santa Maria (RS), Brazil; Sergio.gehrke@hotmail.com

³ Instituto de Bioingeniería, Universidad Miguel Hernandez, Avda, Ferrocarril s/n, 03202-Elche Alicante, Spain

* Correspondence: piedad@umh.es; Tel.: +34-966-658-485; Fax: +34-965-222-033

Academic Editor: Mohan Jacob

Received: 20 February 2017; Accepted: 11 May 2017; Published: 17 May 2017

Abstract: Some studies have demonstrated that in vivo degradation processes are influenced by the material's physico-chemical properties. The present study compares two hydroxyapatites manufactured on an industrial scale, deproteinized at low and high temperatures, and how physico-chemical properties can influence the mineral degradation process of material performance in bone biopsies retrieved six months after maxillary sinus augmentation. Residual biomaterial particles were examined by field scanning electron microscopy (SEM) and energy dispersive X-ray spectroscopy (EDX) to determine the composition and degree of degradation of the bone graft substitute material. According to the EDX analysis, the Ca/P ratio significantly lowered in the residual biomaterial (1.08 ± 0.32) compared to the initial composition (2.22 ± 0.08) for the low-temperature sintered group, which also presented high porosity, low crystallinity, low density, a large surface area, poor stability, and a high resorption rate compared to the high-temperature sintered material. This demonstrates that variations in the physico-chemical properties of bone substitute material clearly influence the degradation process. Further studies are needed to determine whether the resorption of deproteinized bone particles proceeds slowly enough to allow sufficient time for bone maturation to occur.

Keywords: hydroxyapatite; xenografts; tissue reaction; resorption; biocompatibility; biomedical applications

1. Introduction

Alveolar bone resorption and pneumatization of the maxillary sinus after tooth extraction limit the quantity and quality of the bone needed for successful implant placement, especially in the edentulous posterior maxilla. Many authors have studied posterior maxillary atrophy rehabilitation, and have reported various maxillary sinus floor augmentation techniques that increase bone volume and height [1–3]. The maxillary sinus elevation procedure is currently considered the most predictable of pre-prosthetic surgical techniques. Maxillary sinus grafting, combined with Schneiderian membrane elevation, has been proposed to re-establish the ideal quantity and quality of bone prior to implant [4].

Grafting material is an important determinant of bone augmentation procedures being a success or a failure [5]. Ideal bone graft material should be biocompatible [6], increase bone volume in the grafted area to promote initial stability at implant sites [7], and be resorbed with time and be replaced

with native bone [8]. The success of scaffold-based bone regeneration approaches strongly depends on the performance of the biomaterial used. Among the efforts made by regenerative medicine toward restitution ad integrum, scaffolds should be completely degraded within an adequate period of time. Degradation of bone graft substitute materials involves both chemical dissolution (physico-chemical degradation) and resorption (cellular degradation by osteoclasts) [9]. Based on its physico-chemical properties, bone-graft material may be either resorbable or non-resorbable in relation to the extent of dissolution of Ca–P materials [10]. The factors that affect dissolution properties are similar to those that affect biodegradation or bioresorption [11].

Materials should also be fully degradable and this degradation should ideally match the osteogenic rate. However, no clear insight has yet been provided as to the exact relationship between the material properties of these calcium phosphate ceramics and their degradation behavior [12]. Therefore, long-term studies must be carried out to understand the pattern of biodegradation of xenografts and their influence on bone gain.

An ideal bone graft substitute has long since been sought for problems associated with gold-standard autologous bone grafts. Although autogenous bone is regarded as the gold standard, autogenous bone grafts can also exhibit unpredictable bone resorption, which may not be a desirable characteristic in sinus grafting. Indeed the practice of augmented sinuses using autogenous bone as the sole grafting material has been shown to undergo significant re-pneumatization and augmented volume loss according to several clinical reports found in the literature [13–16], which has led to searches for alternative graft materials. Therefore, the goal is to seek an ideal scaffold that provides good mechanical support temporarily while maintaining bioactivity, and which can biodegrade later at a tailorable rate [17]. Several grafting materials have been used for this treatment, but very few materials are presently considered useful [18]. Synthetic and natural calcium phosphate-based materials may be a suitable alternative for using autogenous graft [19]. Natural hydroxyapatite ceramics have drawn attention because it might be possible to use them as an alternative to autogenous free bone grafting due to their chemical composition and their biological and crystallographic similarity to the mineral portion of hard tissues [14]. Deproteinized xenografts, primarily constituted of natural apatites that are sintered or not, have good physico-chemical properties. However, information of manufacturers' specifications sometimes contradicts clinical results. Some results have shown that the examined HA had variable physico-chemical properties, which disagrees with the manufacturers' specifications. This discrepancy may affect the material's performance [20]. Many reviews have discussed a number of biomaterials and their manufacturing processes for biodegradable scaffold fabrication, but very little work has been done to obtain biomaterials with patient-specific degradation rates [21–24].

One of the future challenges in bone tissue engineering is to design and manufacture biodegradable scaffolds with a homogeneous growth rate over their entire volume using pore size gradients or specific distributions. This requires manufacturing processes with higher resolution and biofabrication capabilities [25].

Bovine bone has practically unlimited availability and a striking physico-chemical and structural similarity to human bone [26]. However, some studies have pointed out that this material is not completely reabsorbable because it will completely disappear within one year. Moreover, the rate and mechanism of its reabsorption are still unclear [14]. Deproteinized porcine bone mineral has been recently developed and has become commercially available in maxillary sinus grafting, in which demineralized bovine bone mineral is widely used [27].

Xenografts are usually of bovine or porcine origin, and are constituted by HA similarly to human bone ($\text{Ca}_{10}(\text{PO}_4)_6(\text{OH})_2$). This type of graft can be deproteinized and/or demineralized under different physicochemical conditions, which selectively modulate the tissue response of the host organism [22].

Deproteinization is an indispensable process to eliminate antigenicity in xenograft bones. Valid strategies to eliminate the antigenicity of xenograft bones are of vital importance for the development of xenogenic bone graft substitutes [23]. Bone deproteinization methods have to allow the heterologous

deproteinized bone to offer good biological safety and to meet all the demands of scaffold material for tissue engineering purposes [28]. Many research works on HA have centered on a wide range of powder processing techniques, and also on composition and experimental conditions, to determine the most viable synthesis method [29–32]. Some authors have reported the same observations in reactions to the microscopic structure in commercial products subjected to thermal deproteinization processes. Sintering temperature is considered an important factor that could alter the characteristics of HA [21,33–36]. However, the effect of sintering temperature on the physico-chemical properties of natural HA (HA of a natural source), especially HA from bovine bone, is not yet fully understood, and research in this area is still wide open [37]. The most important parameters that can affect the properties of HA are temperature and heat treatment duration [31].

Regarding the sintering characteristics of HA, the resulting microstructure and properties are not only influenced by the characteristics and impurities of materials, but are also found to depend on thermal history during the fabrication process [3].

Some studies have demonstrated that degradation processes are influenced by the material's physico-chemical properties [26,38–42]. Different applications require materials with distinct resorption rates, which can be regulated by a mixture of several calcium phosphate phases [43]. Based on these data, the objective of this study was to compare the physico-chemical properties of two deproteinized HA materials, and to assess the influence of these properties on the degradation process of the material's performance in retrieved bone biopsies following use in maxillary sinus augmentation.

2. Results

2.1. Characterization of Deproteinized Hydroxyapatite Materials

Figure 1 shows the XRD pattern of the studied deproteinized hydroxyapatite materials, and the synthetic HA and osseous matrix for comparison purposes. As seen, the deproteinized bovine hydroxyapatite (DBHa) material presents a high crystalline HA with no other phase, which corresponds to high-temperature processing. Based on the XRD patterns, the crystal size of the DBHa xenograft implants is 732 nm. The deproteinized porcine hydroxyapatite (DPHa) material presents a low crystallinity HA phase (with a crystal size of 325 nm) with broad peaks related to low-temperature sintering

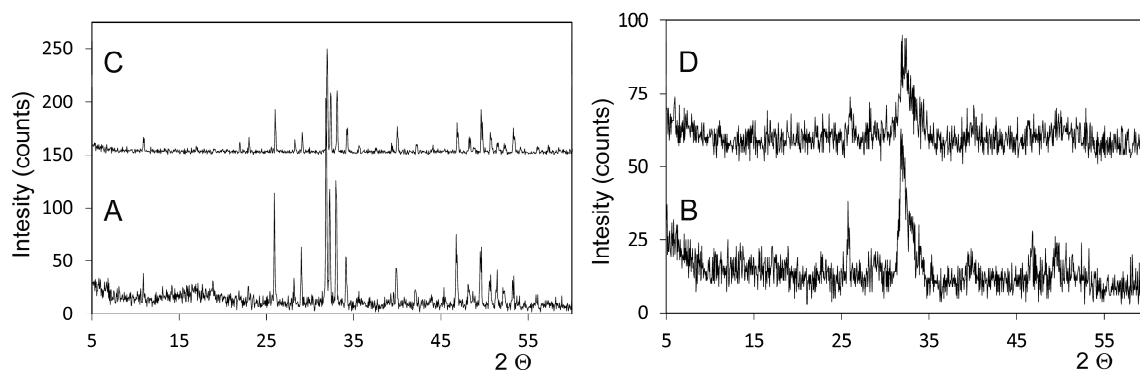


Figure 1. Laboratory XRD X-ray powder diffraction pattern of the obtained (A) DBHa and (B) DPHa materials, and also (C) the synthetic HA and (D) osseous matrix for comparison purposes.

Figure 2 includes the FTIR spectra of the obtained DBHa and DPHa materials, as well as the spectrum of collagen for comparison purposes. As expected, both the deproteinized HA materials show the typical bands brought about by HA, the main constituent of bovine and porcine bone: $1125\text{--}1040\text{ cm}^{-1}$ (ν_3); 963 cm^{-1} (ν_1), and between 550 and 610 cm^{-1} (ν_4). These are the most intense phosphate stretching bands observed at around 1043 cm^{-1} and 1092 cm^{-1} . In addition, a double band appears at $1410\text{--}1480\text{ cm}^{-1}$ (ν_3) and a low-intensity band at 885 cm^{-1} (ν_2), which correspond to the

stretching vibrations of CO_3^{2-} , by substituting for phosphate in the apatite lattice that corresponds to natural carbonate-hydroxyapatite [44].

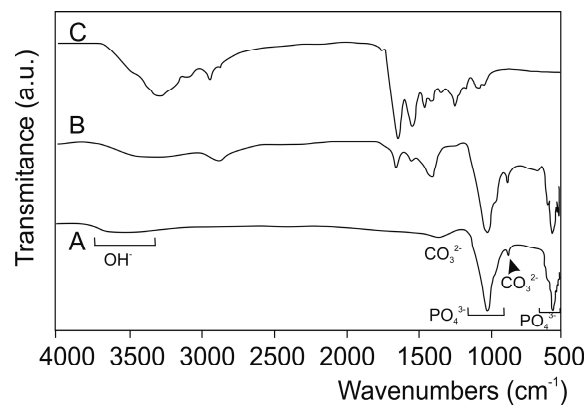


Figure 2. FTIR spectra of the obtained (A) DBHa and (B) DPHa materials and (C) collagen for comparison purposes.

The third group of vibrational spectra includes the spectra related to the collagen present only in the DPHA material. The figure includes Type I collagen for comparison purposes. Above 1300 cm^{-1} , almost all the bands are exclusively assigned to collagen vibrations, the exception being those brought about by CO_3^{2-} at 1460 cm^{-1} , and a broad band present at 3500 , which is attributed to the presence of the structural OH- groups [12,45,46].

Figure 3 shows the xenograft materials before insertions for maxillary sinus floor elevation. The SEM micrographs illustrate major differences depending on heat treatment. DBHa consists of $500\text{--}1000\text{ }\mu\text{m}$ average particles with rounded edges and $100\text{ }\mu\text{m}$ pores. At high magnification, the DBHa material shows a porous surface with white HA crystals (Figure 3A,B). DPHA has HA particles of about $600\text{--}1000\text{ }\mu\text{m}$ on average, with sharper edges and collagen (arrows in Figure 3B,C). Collagen is attached to the particle's surfaces or by linking different particles. Figure 3D depicts details of a sample similar to the previous one, but shows a bundle of collagen over a smooth particle area.

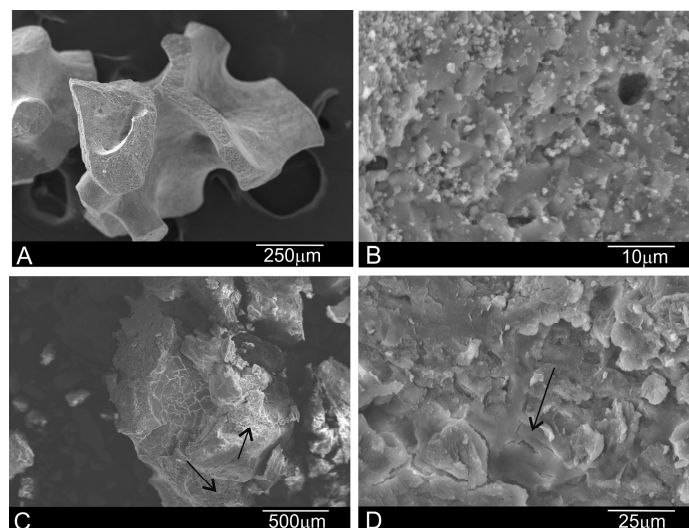


Figure 3. Scanning electron micrographs of the (A,B) DBHa and (C,D) DPHA xenograft materials before implantation [arrows = collagen].

EDX also denoted the differences between both xenograft materials (Table 1). The Ca/P ratio revealed a statistically significant difference in the EDX analysis of grafts before implantation.

Table 1. Ca/P ratios of grafts before implantation. Values as medians. A statistically significant difference was found between DBHa and DPHa (Mann–Whitney test, $p < 0.0051$).

Ca/P Ratios (wt %)	DPHa	DBHa
Mean	2.22	2.31
SD	0.08	0.09
Median	2.22	2.28

Table 2 provides a comprehensive microstructural characterization of the xenograft materials and the synthetic HA and osseous matrix for comparison purposes. The tendency was for density to become higher with increasing heating temperature and lower porosity.

Table 2. The physical characteristics of the two studied xenograft materials and the HA synthetic and osseous matrix for comparison purposes [HA = hydroxyapatite; Coll = collagen].

Materials Characterized	Real Density (g/cc)	Apparent Density (g/cc)	Surface Area (m ² /g)	Total Porosity (%) ^a	Phase/s	Particle Size (μm)	Crystal Size (nm)
DPHa	2.85	1.14	9.78	59.90	HA + Coll	600–1000	325
DBHa	2.98	1.51	2.77	49.13	HA	500–1000	732
HA Synthetic	3.16	1.62	3.10	46.4	HA	600–1000	731
Osseous Matri	1.46	1.24	–	69.3	HA + Coll	400–700	68.4

^a Corresponding to 1 μm < pores < 300 μm.

2.2. Results of Retrieved Bone Biopsies

The SEM-BSE cross-sections micrographs six months after the sinus augmentation of both materials are shown in Figure 3. It is important to highlight the absence of either inflammatory cells or fibrous connective tissue formation in the vicinity of the xenograft materials and around the newly formed woven bone, which would otherwise imply bone tissue intolerance to implants. The behavior of both implants differs. DBHa material is still present in the implantation area after six months, while the DPHa material is almost degraded.

Figure 4A confirms that the DBHa residual graft particles (*) were surrounded by newly formed bone, which presented mature bone characteristics, and the EDX analysis supported these findings (Figure 4). Six months after implantation in the DBHa group, most of the residual biomaterial had been resorbed. The patterns of resorption at the interface of the DBHa group show resorption regions mainly on its surface, and a more uneven surface morphology compared with DPHa. The newly formed bone is found in most of the convex augmented space. Newly formed bone is closely attached to the HA particles from the implant. For the DPHa xenograft (Figure 4B), behavior differs as an almost complete resorption zone is observed in them. The patterns of resorption at the interface of the DPHa group show numerous resorption regions, starting from inside the graft and moving toward its periphery. The DPHa group has the highest resorption rate compared with the other DBHa group.

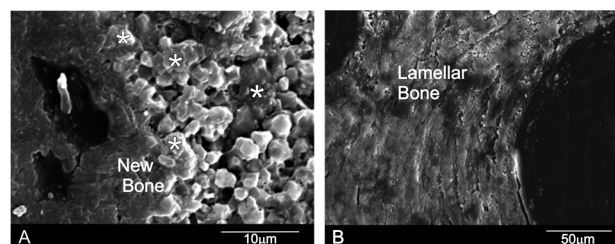


Figure 4. The SEM-BSE cross-sections of the (A) DBHa and (B) DPHa xenograft materials six months after sinus augmentation (* = residual graft particles).

Figure 5 shows the results of the Ca/P ratio of the retrieved bone biopsies following maxillary sinus augmentation. The EDX analysis indicated a significant decrease in the residual biomaterials (RB) compared with the initial composition (Table 1). The DPHa shows numerous regions of resorptions, with an average Ca/P rate of 1.08 ± 0.32 compared with the average Ca/P rate 1.85 ± 0.34 of DBHa. Statistically significant differences appear between groups at the interface and in new bone. The Ca/P ratio at the interface is 1.93 ± 0.18 for DPHa compared with 2.14 ± 0.08 of DBHa, and the ratio in new bone is 1.84 ± 0.14 for DPHa compared with 2.00 ± 0.08 of DBHa. In all cases, a drop in the Ca/P ratio percentage takes place in the residual biomaterial compared with the initial composition (Table 1), while the Ca/P ratio percentages gradually increase at the interface, which suggests an increase in the osteoinductive capacity of the materials and replacement with new bone on their periphery.

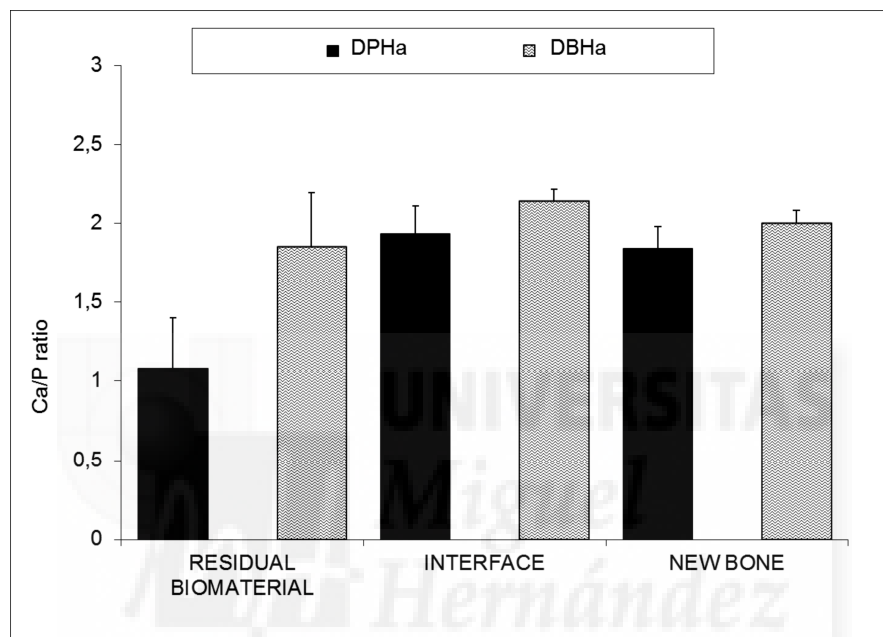


Figure 5. Comparisons between the DBHa and DPHa groups for each parameter (residual bone, interface, and new bone). The Kolmogorov–Smirnov test rejected normality for all the groups. Statistically significant differences were found for each parameter between the group comparisons (Mann–Whitney test, $p < 0.0001$).

To investigate in detail the distribution of Ca/P in selected areas and individual biomaterial particles, line scans were carried out with a selection of different points from the implant through the middle to the periphery of samples to detect changes in the Ca/P ratios (see Figure 5), following the recommendation of Lindgren [47]. The EDX analysis of the residual graft material particles in the retrieved tissue revealed Ca/P to be in every variable relative proportion. The analysis indicated that this individual particle contained Ca/P, which was more concentrated in the interface area. This is consistent with the replacement of Ca/P with the precipitate as it gradually dissolves.

The data of interest were found in the interface area, where the diffusion of ions was greater. According to the EDX analysis and the high magnification SEM examination of the interfaces made between both studied grafts and the surrounding tissue, the reaction zone was characterized by the intermittent presence of the calcium phosphate phase, which corresponded in structure and morphology to new bone tissue. The intermediate new bone contained calcium and phosphorous elements with average Ca/P ratios for DPHa 1.93 ± 0.18 and DBHa 2.14 ± 0.08 . These results indicated bone chemical maturity, and reached the stoichiometric Ca/P ratio of natural bone. This compositional microcharacterization of the interface indicated that the calcium and phosphorous along the periphery of the implant interfaces remained well textured as the material's degradation continued inside the

implant. This led to increased porosity inside the material, which can be observed by comparing the SEM images of Figure 6. Faster degradation of DPHa compared to DBHa is observed, which is related with the material's crystallinity (Figure 1).

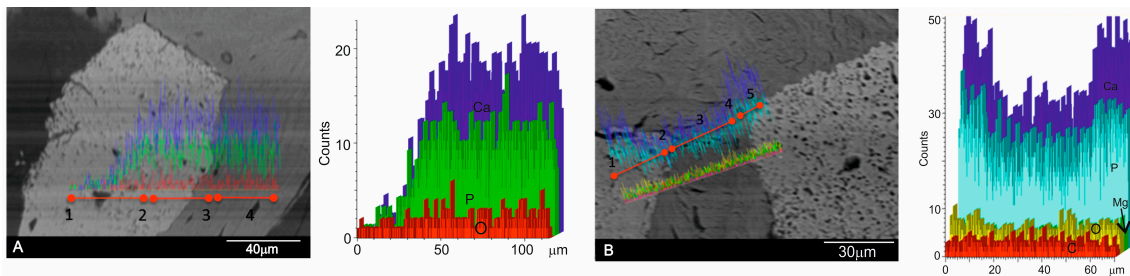


Figure 6. The SEM line-scan of the (A) DBHa and (B) DPHa xenograft materials six months after implantation showing the relative concentration of the principal ions along a line that passes through a graft biomaterial particle (point 1) and the interface (point 2) to the new bone (point 3) interface (point 4), and a graft biomaterial particle (point 5). In order to clarify, the scan results are also shown separately in the figure next to each SEM image.

The SEM image of the polished cross-sections of implants six months after implantation is shown in Figure 7. The equivalent elemental X-ray maps of calcium and phosphorous are also presented. At six months after implantation, the outside DBHa implant surface (arrows in Figure 7A) presented active regions, where the degradation process of the material came about. These observations led to the conclusion that the interfacial activities at six months were already making full progress, which resulted in the remodeling of the interface in terms of its morphology and chemistry (calcium and phosphorous ions). The implant peripheral regions underwent intensive bone resorption, which produced significantly more irregular surfaces compared with the DPHa implant (Figure 7B). Figure 7B provides a biopsy of the DPHa-BSE image showing the resorbed DPHa graft in relation to the surrounding bone, a granular residual material consisting of areas with very few and smaller particles. These findings indicate the almost complete resorption of DPHa, and similar results in the middle and on the periphery of samples.

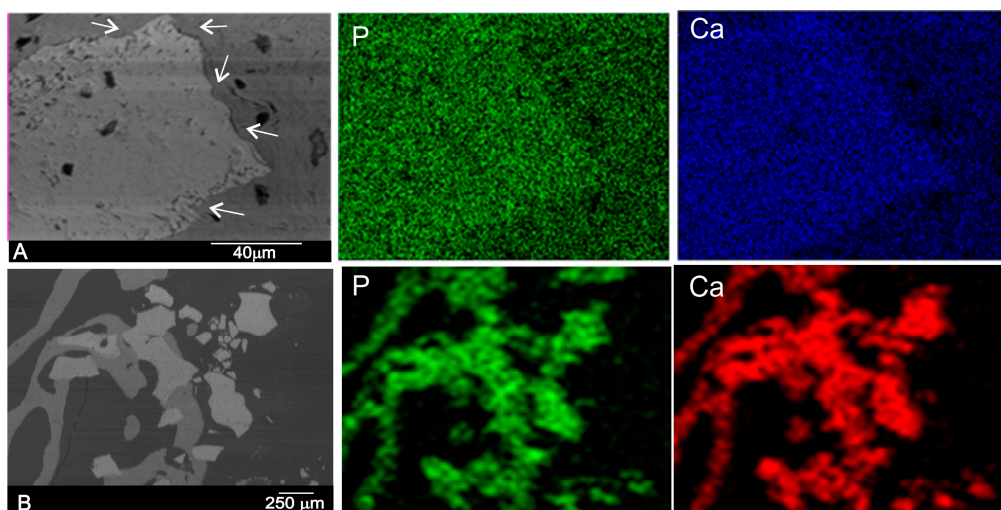


Figure 7. SEM image of the polished cross-section of a biopsy of the (A) DBHa and (B) DPHa xenograft material six months after implantation and the elemental X-ray maps of calcium and phosphorous (arrows refer to the irregular boundary with a partial degraded implant).

According to the elemental X-ray maps and the SEM images of the interface between the DBHa and DPHa implants and natural bone, the reaction zone was composed of Ca and P phases, and was a short distance away from the reaction zone. No obvious morphological differences were observed between the newly formed bone and the old bone into which the implants were inserted.

3. Discussion

In the present study, the degradation process of two different xenogeneic bone substitute materials was evaluated in sinus floor elevation in a split mouth design. Both natural HAs differed significantly in processing temperature terms as DPHa was a porcine bone graft that was subjected to a low-heat (130 °C) chemical process to extract organic components, while DBHa was a sintered bovine bone graft that was subjected to high temperature (1200 °C). Conflicting results have been reported on the long-term fate of deproteinized bone. In the literature, the resorption of deproteinized bone has been a subject of controversy [9,22,37]. The mostly widely mentioned factors in the literature that presumably govern degradation are crystallography, stoichiometry, and porosity [48].

The manufacturing process, based on high-temperature heating, removes all organic components and proteins, and eliminates potential immunologic reactions. When deproteinization occurs at very high temperatures (1200 °C), it enhances material crystallinity, which is the case of DBHa [49].

In the present study, and according to the results of research on the effect of sintering temperature [31], our results reveal that sintering temperature is a critical factor that influences the phase stability, densification behavior, crystallinity, and porosity of hydroxyapatite ceramics. In line with other studies, we observed that changes in the composition and crystallinity of calcium phosphate-based materials from the manufacturer directly affect the clinical result [23] as biomaterials sintered at high temperature lead to non-absorbable products [9].

If we allowed biomaterials with the same initial particle size range (small size) to be used in both groups, 600–1000 µm for the DPHa group and 500–1000 µm for the DBHa, then particles might be degraded biologically or chemically.

The histological examination of 60 biopsies, taken from the 10 patients in this study, indicated statistically significant differences in the EDX analysis parameters between the DBHa and DPHa graft materials, and both before and after sinus augmentation. EDX provided information on the chemical elements present in the graft material and the surrounding tissues which can reveal changes in phase composition [50]. The purpose of this study was two-fold: to investigate the resorption of these grafts by examining the appearance of remaining particles by means of these techniques; to observe the interface between bone and biomaterial to determine whether any changes in the Ca/P ratio caused by component dissolution during the healing process could be detected in bone biopsies retrieved from maxillary sinus augmentation. The EDX analysis of the residual graft material particles in the retrieved bone biopsies six months after an augmented sinus lift revealed a Ca/P ratio in every variable relative proportion, which is useful for understanding the either resorbable or non-resorbable nature, and this classification is related to the dissolution extent of the Ca–P materials [10].

In the present study, the Ca/P variations in the graft material were analyzed in both grafts, and a decrease related to the dispersion of Ca and P through material degradation took place. An analysis was carried out with a selection of various points in order to take different points of interest from both the middle and periphery of samples to detect changes in the Ca/P ratios. The EDX analysis monitored the resorption process of both xenografts. An elemental analysis showed that a gradual diffusion of the Ca ions from the biomaterial occurred to the newly forming bone at the interface. Very few studies have used EDX analysis as a tool to understand the degradation process of a biomaterial [51].

According to the EDX analysis, the Ca/P ratio significantly lowered in the residual biomaterial (RB) compared with the initial composition in the DPHa group, and showed numerous regions of resorptions in relation to the DBHa group. However when we observed the DBHa group before and after, we observed a moderate decrease in the residual DBHa compared with the initial composition.

Changes in the composition and crystallinity of the calcium phosphate-based materials from one manufacturer to another, or even from different batches of the same manufacturer, directly affect the clinical result, and are a limiting factor for this material's use [52].

Natural bone is made up of mainly fine carbonated HA crystals (65%) and collagen matrices (23%) with an organized three-dimensional geometrical structure, and has many excellent biological and mechanical properties [53].

Since industries created a self-setting calcium phosphate ceramic with low crystallinity HA, several commercial calcium phosphate ceramics have become available for clinical therapeutics in dentistry, such as biomimetic bone materials that contain HA/collagen, with high biocompatibility and similar characteristics to natural bone. This is the case of DPHa used herein. It is a xenograft that derives from cancellous-cortical porcine bone. The TecnoSS patented manufacturing process used to produce these materials achieves biocompatibility by avoiding temperatures above 130 °C, which would cause ceramization of granules by preserving part of the collagen matrix of the original animal bone. The result is a unique biomaterial that consists in mineral components and a very similar organic matrix to autogenous bone. According to the study of Kalkura [31], we observed the low crystallinity structure of the graft and the presence of two phases HA + Col by XRD and FTIR analyses in the previous characterization of the porcine bone mineral.

Crystallite size is an indication of the material's crystallinity, which can be defined as the average size of a domain within a material that has a coherently diffracting monocrystalline structure. By increasing sintering temperature, the XRD patterns of the deproteinized graft materials exhibited an increased peak height and reduced peak width, which thus indicates increased crystallinity and a bigger crystallite size. Crystal size is inversely proportional to peak width. Broadening of peaks became evident at lower sintering temperatures, which indicates the initial crystal formation state. At higher sintering temperatures, crystal growth was evidenced by a sharpening to the peaks. For DPHa, the diffractogram exhibits broad peaks with a low signal-to-noise ratio, which correspond to a low-crystallinity material. The sharp, well-resolved peaks found in the XRD spectrum of DBHa indicate highly crystalline HA. So the DPHa sintered at low temperature had a less crystalline structure compared to the DBHa sintered at high temperature, and could also be more prone to degradation. Regarding physical properties, density tended to increase with an increasing annealing temperature.

Crystallinity is highly dependent on sintering temperature: the higher the sintering temperature, the more perfect the crystal and, thus, the lower the degradation rate. Resorption increases with decreasing crystallinity. Resorbable calcium phosphate materials are usually unsintered Ca-P materials [54].

Due to the low processing temperature, this material is claimed to preserve the structure and composition of natural bone components and enhances low crystallinity. Tissues respond differently to biomaterials with different crystallinities. The major differences in the adhesive response of cells to different crystallographic structures have been reported [55]. It has been shown that addition of collagen to HA results in higher bone remodeling activity compared to pure HA. According to another study, it would appear that addition of collagen to an HA graft could enhance phagocytotic processes [56].

Nannmark and Sennerby observed relevant significant levels of resorption of collagenized porcine bone particles [57]. According to these authors, this suggests that presence of collagen induces osteoclast adhesion to the biomaterial's surface. Perhaps presence of collagen plays a key role in initiating resorption. Moreover, the low levels of residual graft material observed in our study confirmed a substantial resorption of the grafted material after six months, which is an added advantage for some authors. The elemental mapping of the residual porcine biomaterial at different points showed some categories of particles with different mean Ca/P ratios according to size. Compared with the original material composition, significant differences appeared before and after using DPHs. These findings marked the different resorption process stages. However, other research works [58] have used transmission electron microscopy of human biopsies following maxillary sinus

elevation with porcine bone to show a few signs of resorption after five months. Their histological results indicated only the initial resorption of the biomaterial. Absence of collagen in the porcine bone used in Orsini's study could explain its incomplete resorption and would, therefore, support our hypothesis. In any case, the rapid resorption of porcine bone that contains collagen would appear to claim an advantage for this material over other biomaterials that do not contain collagen. Other authors have described this characteristic in studies into HA. When a bone porcine paste, composed of 80% granulated mix and 20% pure collagen [59], was examined at three months, complete resorption and substitution with trabecular bone tissue were observed. However in our study, this rapid resorption was not an advantage as DPHa did not maintain the space and stability in the augmented area of the maxillary sinus floor.

Regarding porosity, another factor that presumably governs degradation, and is mentioned frequently in the literature, and also in our characterization study, it is likely that the porcine bone mineral particles' microstructure and delicate porous morphology enhance the degradation of this material [60,61].

Given the low resorption rate of inorganic bovine bone, it has been reported to undergo no, or limited, resorption [14,62–64]. The present study's findings are consistent with several reports found in the literature [65–67] in which an SEM analysis revealed a close relationship between the newly formed bone matrix and the bovine xenograft particle surface. Although histological and histomorphometric findings have often corroborated the clinical success of bovine bone mineral, the published literature includes a few descriptions of its ultrastructural features. The purpose of our evaluation was to, therefore, add to clinicians' knowledge of this biomaterial by gaining an understanding of the interactions that occur in close proximity to bovine bone mineral. The EDX bone tissue analysis showed presence of calcium and phosphorus, and indicated presence of mineralized bone tissue on the particle surface. The results demonstrated that Ca ions gradually diffused from the biomaterial to the newly forming bone at the interface. This observation suggests that the graft surface might provide an optimal stratum for bone tissue ingrowth [64]. Moreover, the residual graft material levels observed herein confirmed a substantial resorption of the DBHa biomaterial after six months. The elemental mapping of the residual DBHa sintered biomaterial at different points showed some categories of particles with different mean Ca/P ratios according to size. Compared with the original material composition, a significant resorption of biomaterials was seen to be underway. It became evident that these findings marked different resorption process stages. In agreement with our clinical findings, a low osteoclast count over time would explain the long-term (six months, three years, and seven years) persistence of bovine bone biomaterial [64]. Conflicting results have been reported on the long-term behavior of bovine xenografts. Early studies reported that bovine xenografts are non-resorbable [68]. Taylor's study describes signs of resorption [69], whereas others report that they are lacking [62,65]. Traini's study discovered bovine bone biomaterial remnants remaining for as long as nine years. A follow-up study of sinus floor augmentation with bovine xenografts observed the gradual diffusion of Ca ions from the bovine xenograft to the adjacent newly forming bone at the interface as part of the resorption process [67].

However, other [65] studies done with human biopsies following maxillary sinus elevation with bovine bone have reported few signs of resorption after six months, with histological results indicating only initial biomaterial resorption. In the current study, we found an incomplete bone graft resorption phenomenon, whereby the biomaterial was seen to partially decrease. In spite of this limited resorption capacity, we observed how intergrain boundaries widened, and how the superficial hydroxyapatite crystallites on the implant surface were partially dissociated. These findings became visible by an elemental analysis done at different points on the periphery of samples. In the present study, the sites of interest for a point analysis were randomly selected at the graft site, and it was interesting to determine whether any differences in the Ca/P ratio could be detected in peripheral or central regions, as this could indicate different resorption rates. For DBHa, resorption occurred mainly in peripheral

regions, but the studied DBHa was not completely resorbable during the study period, according to another study.

According to Moon's study, which also compared two xenograft materials prepared by a low-temperature deproteinizing technique (Bio-Oss) or a high-temperature (Cerabone) one in the sinus cavity, a significantly greater volumetric loss of the initial graft size for the non-sintered material was observed, which also occurred in our study. Bio-Oss has a significantly larger surface area and a smaller crystallite size compared with Cerabone [70]. In contrast with Fienitz's study, a sintered material was compared to a non-sintered bovine bone substitute material by a sinus augmentation procedure. Despite their histological analysis revealing a lower resorption of the non-sintered bone substitute material, the differences found were not statistically significant [71].

In line with our study, in a randomized controlled clinical trial, Lee et al. compared sinuses grafted with DPBM (deproteinized porcine bone mineral) and DBBM (deproteinized bovine bone mineral). These authors observed smaller sized residual biomaterials in the histological samples from the DPBM sites compared to DBBM sites, and despite using the same sizes for both biomaterials [27].

This might have a crucial impact on the resorption rate [43]. Hence, we conclude that the results of resorption in deproteinized biomaterials varied according to the manufactured process (sintered or not sintered).

After implantation, biodegradation is critical as this allows for a space to be formed into which bone and vascular tissues can grow. Biodegradation can be envisioned as an *in vivo* process by which a material breaks down into simpler components, which reduces the complexity of chemical compounds by the action of cells, by simple physical breakdown and/or by chemical erosion [8].

A completely resorbable ceramic has been the goal of several studies. However, a high rate of resorption or solubilization can interfere with bone formation as the biomaterial may degrade faster than the rate of bone formation. These phenomena lead to a change in the bioceramic physical structure, which interferes with cell attachment [72]. Moreover, the release of high concentrations of calcium to the microenvironment changes pH, promotes a mild inflammatory response, and favors fibrous tissue formation [73]. Higher calcium ion levels have been shown to effect osteoclastic activity by varying from its inhibition to its stimulation, or there simply being no effects [74]. Instead presence of moderate extracellular Ca^{2+} that results from resorption activity might be involved in the stimulation of osteoblasts. Yamaguchi et al. showed that moderately high extracellular Ca^{2+} is a chemotactic and proliferating signal for osteoblasts, and its stimulates pre-osteoblast differentiation [41].

As DPHa material is the fastest to undergo remodeling, it can be considered the most active in resorption terms, but not in new bone formation. DBHa seemed to be a gradually resorbed material, and was partially substituted for newly formed bone according to our results. This increase in ions could possibly create areas of biological apatite on agglutinated Ca and P deposits and crystals which, in turn, would facilitate osteoconduction [63].

Some materials, such as autogenous bone, cannot withstand sinus pressure during the first several weeks and loses density and height over time [16]. An ideal bone graft material should be biocompatible, increase bone volume in the grafted area to promote initial stability at the implant sites, and be resorbed with time and replaced with native bone. In this study, DPHa was reabsorbed so quickly that it was unable to withstand sinus pressure. A repneumatization of sinus, or reduced augmentation—a phenomenon known as 'slumping'—was noted [75].

However, the bone resorption process and the distribution of osteoclasts after deproteinized bone implantation have not been examined in detail, which are relevant for enhancing our understanding of the complex role of osteoclasts in bone tissue engineering [74].

An *in vitro* study with osteoclastic precursor cells in bone substitute materials has shown that there are specific parameters that inhibit or enhance resorption. Moreover, analyses of the bone–material interface have revealed that biomaterials composition significantly influences their degradation when they come into contact with osteoclasts. The crystallinity, grain size, surface bioactivity, and density of

the surface seem to have a less significant effect on osteoclastic activity. In addition, the topography of the scaffold surface can be tailored to affect the development and spread of osteoclast cells [75].

This suggests that resorption of collagen deproteinized bone material occurs more quickly than bone formation. Collagen is absorbed mostly by enzymatic digestion. It is noteworthy that TRAP-positive osteoclastic cells have been seen on the surface of deproteinized collagen. This implies that collagen fibrils are resorbed not only enzymatically, but also phagocytically. This was the case of the non-sintered DPHa [76]. Our study showed that most of the newly formed bone in the augmented sinus spaces grafted with DPHa had disappeared six months after implantation, which caused the repneumatization of the sinus.

The study of Galindo et al. (2012) found that the osteoclast count significantly lowered, and a true reduction in biodegradation [77]. Further long-term studies are needed to determine whether resorption of deproteinized bone particles proceeds slowly enough to provide sufficient time for bone maturation to take place. Our results demonstrate that slowly resorbed sintered DBHa particles promoted stable maxillary sinus floor augmentation and inhibited the resorption of newly formed bone, maintained the space, and stably augmented the maxillary sinus floor. The newly formed bone showed minimal osteoclastic resorption. The slow biodegradation of DBHa bone particles tented the sinus lining, maintained the space, and stably augmented the maxillary sinus floor. Therefore, we conclude that DBHa bone particles can be successfully used as a bone graft material for sinus lift procedures.

The grafting material is an important determinant of bone augmentation procedures being a success or a failure. With the various bone grafting options available to surgeons, one must carefully match the clinical problem and the graft material's capabilities. The sintering process provides strength to a finished material. However, when applied to bone, one of the most important factors is the possibility of materials being resorbed and substituted for newly formed bone.

This study assumed the difference in the physico-chemical properties between the influence of both grafts on the biological response produced by a biomaterial, and significant differences were found in relation to the degradation process after six months of healing. According to others studies, phase composition [78], chemical composition [79], porosity [80], the dispersant concentration on the pore morphology [58], particle size [81], the ultrastructural geometry of particles [82], surface roughness [83], and crystallinity [17], among others, are likely to affect ceramic solubility. Different applications require materials with distinct resorption rates [9], which may be adjusted for the desired purpose [84].

4. Materials and Methods

4.1. Deproteinized Hydroxyapatite Materials

The raw materials employed in this study were two different types of commercial deproteinized HA materials used in dentistry: deproteinized porcine hydroxyapatite (DPHa) processed at 130 °C called OsteoBiol[®], deproteinized bovine hydroxyapatite (DBHa) processed in two steps: pyrolysis at 900 °C following ceramization at 1200 °C called Endobon[®].

The mineralogical characterization of the powder materials was performed by X-ray diffractometry (XRD). XRD patterns were obtained in a Bruker-AXS D8Advance (Karkruhe, Germany) automated diffractometer and were compared with the database provided by the Joint Committee on Powder Diffraction Standards (JCPD). The following Scherrer formula was used to determine the crystal size of each material based on the relevant XRD pattern. Instrument broadening corrections were taken into account, and it was assumed that the lattice strain was negligibly small.

$$D_{hkl} = \frac{k\lambda}{B_{\frac{1}{2}} \cos\theta_{hkl}}$$

In this equation k is the Scherrer constant (0.89), which depends on crystal shape, the diffraction line indexes [85] and the dispersion of the crystallite sizes of the powder [86]; λ is the wavelength of Cu $K_{\alpha 1}$ ($\lambda = 1.54056 \text{ \AA}$); $B_{1/2}$ corresponds to full width at half maximum (rad) for (hkl) reflection; and θ_{hkl} is the diffraction angle ($^{\circ}$). The line broadening of the (300) reflection that corresponds to the maximum intensity peak was used to evaluate crystal size.

The particles' real density (sample mass/volume of the solid (excluding empty spaces) was determined by helium-gas pycnometry (Quantachrome Instruments, Boyton Beach, FL, USA) and the particles' apparent density was determined by mercury porosimetry. Particles' real density was determined after excluding sample interstices and most pores since the small volume of the gas molecules (He) enables their penetration in almost all the empty spaces. One exception was samples' closed pores, i.e., those pores that do not open out to the surface. Density, measured in this way, provides the closest value to the sample's solid density, which justifies the use of the term 'real' or 'true' density.

Microstructural examinations were done under a scanning electron microscope (SEM, HITACHI S-3500N, Ibaraki, Japan). Quantitative analyses were run by an Energy Dispersive X-ray Spectroscopy (EDX) system, coupled to the above-described electron microscope. Calibration was carried out with Bayer standards. A weight percentage was calculated from the measured net intensities with a program that corrects for the influences of atomic number, absorption, and fluorescence (ZAF corrections). Relative counting error ϵ_n was calculated as $\epsilon_n = (N^{1/2}/N) \cdot 100$ (N = accumulated counts) with a probability of 98.5%.

Fourier transform infrared spectroscopy (FTIR-ThermoNicolet IR200, Waltham, MA, USA) was used to provide information on the chemical composition and major functional groups. FTIR spectra were recorded between 400 and 4000 cm^{-1} at 2 cm^{-1} resolution. Pellets were prepared by mixing each sample powder with the KBr matrix at a level of 1 wt %. Background data were collected for the KBr matrix and subtracted from each spectrum. All the spectra were recorded at ambient temperature. Analytical-grade collagen samples (purchased from Sigma-Aldrich, Darmstadt, Germany) were also used for comparison purposes.

4.2. Surgery and Bone Retrieval

Ten partially edentulous patients (six women and four men), whose ages ranged from 41 to 71 years, came to the Department of Oral and Maxillofacial Surgery, who had <5 mm subantral alveolar bone in the vertical direction, determined by conventional tomographic radiography. They were treated by a maxillary sinus floor augmentation procedure and delayed implant placement. Patients who received treatment with bisphosphonates or steroids, those currently undergoing chemotherapy and/or radiation to the oral cavity, and those with uncontrolled systemic disease or endocrine disorders were excluded from the study.

The protocol for harvesting bone samples was approved by the University Ethics Committee and informed consent was obtained from all patients. This study is consistent with the ethical principles set out in the Declaration of Helsinki for experimentation on human subjects. All the patients received antibiotics prior to surgery. Each subject was required to take 2 g of amoxicillin 1 h prior to surgery. For any patient allergic to amoxicillin, 600 mg of clindamycin were administered 1 h before surgery. All the surgical procedures were performed under local anesthesia (lidocaine hydrochloride 2% with 1:100,000 epinephrine or mepivacaine/carbocaine 3%, without epinephrine). Maxillary sinus augmentation was performed as previously described Tatum [79]. The grafts material was carefully packed in the space created by mucous membrane elevation. DBHa was placed in a subantral compartment and DPHa was placed in the contralateral subantral compartment. Upon implant surgery, and six months after the healing period, a biopsy was taken for histology purposes at the time of implant placement. Bone cores were harvested using a 3 × 10 mm diameter trephine bur under sterile saline solution irrigation conditions. Sixty bone samples were retrieved for the analysis.

Two biopsies per individual were obtained. Nevertheless, the biopsy value we used in our analysis was unique for each individual and was computed as the average value of its biopsies.

4.3. Specimen Preparation and Analysis

In order to investigate the relationship between xenograft biomaterial particles and bone, cross-sections of the non-decalcified tissue were examined for an ultrastructural study in SEM-EDX. Human specimens were fixed by immersion in 4% formalin solution, dehydrated in a graded ethanol series, and embedded in plastic resin (Technovit A 7210VCL; Kulzer & Co., Hanau, Germany). Then specimens were polished by a manual grinder with 800 grit silicon carbide paper, mounted on an aluminum stub, and carbon-coated in an argon atmosphere with a sputtering machine (Polaron K550X Sputter Coater, Laughton, UK) for the SEM-EDX analyses. Back-scattered SEM imaging (BSE) was also employed to highlight the contrast among the resin, bone, and biomaterials; generally, resin appeared black, bone was gray, and the biomaterial had a brighter contrast than bone. In addition, the chemistry of the interphases and the chemical degradation process of the xenograft biomaterials were analyzed using X-ray elemental maps in the scanning mode. An analysis was carried out by selecting different points, and by taking distinct points of interest from both the middle and the periphery of samples to detect changes in the Ca/P ratios. Data were then collected from deliberately targeted sites of interest from within the residual biomaterial, which were close to and distal from new bone, and also at the bone-implant interface if present (on average, approximately 15 points/section, depending on biomaterial content). Additional information was obtained from line scans and elemental maps. More than 900-point analyses were carried out on the 60 biopsies.

4.4. Statistical Analysis

The statistical analysis was performed by the computerized statistical package software (MedCalc v15.8, Ostend, Belgium). Comparisons between the DBHa and DPHa groups for each parameter (RB, INT, and NB) were made by the Student's *t* (parametric data) or Mann-Whitney (non-parametric data) tests.

5. Conclusions

The fastest resorption rate of the material was in DPHa group and was related to physico-chemical characteristic of this xenograft material. A significant difference in resorption time and in the stability of the material was found in DBHa, which showed greater stability and less resorption than the DBHa groups. The HA of porcine origin non-sintered with high porosity, low crystallinity, low density, high surface area, and low calcium/phosphate ratio presents low stability and high resorption rate.

This study demonstrates that variations in the physical properties of a bone substitute material clearly influence in the degradation process, as a consequence, biomaterials can be designed to demand depending on the needs of resorption, dimensional stability, and handling needed for each case. Further studies are required to establish to what extent the acceleration or slow-down of resorption phenomena affects the capacity of the bone augmentation area to receive and integrate dental implants. Our results demonstrate that slowly resorbed deproteinized bovine bone particles promote the stable augmentation of the maxillary sinus floor and inhibit the resorption of the newly formed bone.

This study demonstrates the effect of sintering temperature on the physico-chemical properties of natural HA and the influence on the degradation process. A significant difference in the resorption time and the stability of the material was found in both groups. The DPHa non-sintered HA with high porosity, low crystallinity, low density, large surface area, and a low calcium/phosphate ratio presented a high resorption rate, but could not withstand sinus pressure. This led to the repneumatization of the sinus. The DBHa sintered HA showed low porosity, high crystallinity, high density, small surface area, and a high calcium/phosphate ratio, and presented a slow resorption rate that inhibited the resorption of the newly formed bone, tented the sinus lining, maintained the space, and stabilized an augmented maxillary sinus floor.

Acknowledgments: Part of this work has been supported by a Spanish Ministry of Economy and Competitiveness (MINECO); contract grant number: MAT2013-48426-C2-2-R.

Author Contributions: María Piedad Ramírez Fernández performed the implantation and the post implantation characterization; Sergio Alexander Gehrke performed the statistical analysis; Carlos Perez Albacete Martinez co-wrote some sections; Jose Luis Calvo Guirado conceived the in vivo experiments and helps in the implantation procedure; Piedad N. de Aza performed the materials characterization. All the authors contributed to the analyses and discussion of the results as well as prepared the manuscript.

Conflicts of Interest: The authors declare no conflict of interest.

References

1. Jang, H.Y.; Kim, H.C.; Lee, S.C.; Lee, J.Y. Choice of Graft Material in Relation to Maxillary Sinus Width in Internal Sinus Floor Augmentation. *J. Oral Maxillofac. Surg.* **2010**, *68*, 1859–1868. [[CrossRef](#)] [[PubMed](#)]
2. Szpalski, C.; Wetterau, M.; Barr, J.; Warren, S.M. Bone tissue engineering: Current strategies and techniques—part I: Scaffolds. *Tissue Eng. Part B Rev.* **2012**, *18*, 246–257. [[CrossRef](#)] [[PubMed](#)]
3. Jensen, S.S.; Aaboe, M.; Janner, S.F.; Saulacic, N.; Bornstein, M.M.; Bosshardt, D.D.; Buser, D. Influence of particle size of deproteinized bovine bone mineral on new bone formation and implant stability after simultaneous sinus floor elevation: A histomorphometric study in minipigs. *Clin. Implant Dent. Relat. Res.* **2015**, *17*, 274–285. [[CrossRef](#)] [[PubMed](#)]
4. Danesh-Sani, S.A.; Engebretson, S.P.; Janal, M.N. Histomorphometric results of different grafting materials and effect of healing time on bone maturation after sinus floor augmentation: A systematic review and meta-analysis. *J. Periodontal. Res.* **2016**. [[CrossRef](#)] [[PubMed](#)]
5. Xu, H.; Shimizu, Y.; Asai, S.; Ooya, K. Experimental sinus grafting with the use of deproteinized bone particles of different sizes. *Clin. Oral Implants Res.* **2003**, *14*, 548–555. [[CrossRef](#)] [[PubMed](#)]
6. Burg, K.J.; Porter, S.; Kellam, J.F. Biomaterials development for bone tissue engineering. *Biomaterials* **2000**, *21*, 2347–2359. [[CrossRef](#)]
7. De Aza, P.N.; De Aza, A.H.; De Aza, S. Crystalline bioceramic materials. *Bol. Soc. Esp. Ceram. Vidr.* **2005**, *44*, 135–145. [[CrossRef](#)]
8. LeGeros, R.Z. Strategies to affect bone remodeling: Osteointegration. *J. Bone Mineral Res.* **1993**, *8*, 583–596. [[CrossRef](#)] [[PubMed](#)]
9. Conz, M.B.; Granjeiro, J.M.; de Almeida Soares, G. Hydroxyapatite crystallinity does not affect the repair of critical size bone defects. *J. Appl. Oral Sci.* **2011**, *19*, 337–342. [[CrossRef](#)] [[PubMed](#)]
10. Calvo-Guirado, J.L.; Ramirez-Fernandez, M.P.; Delgado-Ruiz, R.A.; Mate-Sanchez de Val, J.E.; Velasquez, P.; de Aza, P.N. Influence of biphasic α -TCP with and without the use of collagen membranes on bone healing of surgically critical size defects. A radiological, histological and histomorphometric study. *Clin. Oral Implants Res.* **2014**, *25*, 1228–1238. [[CrossRef](#)] [[PubMed](#)]
11. Fulmer, M.T.; Ison, I.C.; Hankermayer, C.R.; Constantz, B.R.; Ross, J. Measurements of the solubilities and dissolution rates of several hydroxyapatite. *Biomaterials* **2002**, *23*, 751–755. [[CrossRef](#)]
12. Mate-Sanchez de Val, J.E.; Calvo-Guirado, J.L.; Gomez Moreno, G.; Perez Albacete-Martinez, C.; Mazón, P.; de Aza, P.N. Influence of hydroxyapatite granule size, porosity and crystallinity on tissue reaction in vivo. Part A: Synthesis, characterization of the materials and SEM analysis. *Clin. Oral Implants Res.* **2016**, *27*, 1331–1338. [[CrossRef](#)] [[PubMed](#)]
13. Nkenke, E.; Stelzle, F. Clinical outcomes of sinus or augmentation for implant placement using autogenous bone or bone substitutes: A systematic review. *Clin. Oral Implants Res.* **2009**, *20*, 124–133. [[CrossRef](#)] [[PubMed](#)]
14. Jensen, T.; Schou, S.; Stavropoulos, A.; Terheyden, H.; Holmstrup, P. Maxillary sinus floor augmentation with Bio-Oss or Bio-Oss mixed with autogenous bone as graft in animals: A systematic review. *Int. J. Oral Maxillofac. Surg.* **2012**, *41*, 114–120. [[CrossRef](#)] [[PubMed](#)]
15. Arasawa, M.; Oda, Y.; Kobayashi, T.; Uoshima, K.; Nishiyama, H.; Hoshina, H.; Saito, C. Evaluation of bone volume changes after sinus floor augmentation with autogenous bone grafts. *Int. J. Oral Maxillofac. Surg.* **2012**, *41*, 853–857. [[CrossRef](#)] [[PubMed](#)]
16. Sbordone, C.; Toti, P.; Guidetti, F.; Califano, L.; Bufo, P.; Sbordone, L. Volume changes of autogenous bone after sinus lifting and grafting procedures: A 6-year computerized tomographic follow-up. *J. Craniomaxillofac. Surg.* **2013**, *41*, 235–241. [[CrossRef](#)] [[PubMed](#)]

17. Chen, F.P.; Wang, K.; Liu, C.S. Crystalline structure and its effects on the degradation of linear calcium polyphosphate bone substitute. *Appl. Surf. Sci.* **2008**, *255*, 270–272. [[CrossRef](#)]
18. Traini, T.; Piattelli, A.; Caputi, S.; Degidi, M.; Mangano, C.; Scarano, A.; Perrotti, V.; Iezzi, G. Regeneration of human bone using different bone substitute biomaterials. *Clin. Implant Dent. Relat. Res.* **2015**, *17*, 150–162. [[CrossRef](#)] [[PubMed](#)]
19. Frenken, J.W.; Bouwman, W.F.; Bravenboer, N.; Zijdeveld, S.A.; Schulten, E.A.; ten Bruggenkate, C.M. The use of Straumanns Bone Ceramic in a maxillary sinus floor elevation procedure: A clinical, radiological, histological and histomorphometric evaluation with a 6-month healing period. *Clin. Oral Implants Res.* **2010**, *21*, 201–208. [[CrossRef](#)] [[PubMed](#)]
20. Rodrigues, C.V.; Serricella, P.; Linhares, A.B.; Guerdes, R.M.; Borojevic, R.; Rossi, M.A.; Duarte, M.E.; Farina, M. Characterization of a bovine collagen–hydroxyapatite composite scaffold for bone tissue engineering. *Biomaterials* **2003**, *24*, 4987–4997. [[CrossRef](#)]
21. Calvo-Guirado, J.L.; Ramirez-Fernandez, M.P.; Mate-Sanchez de Val, J.E.; Negri, B.; Velasquez, P.; de Aza, P.N. Enhanced bone regeneration with a novel synthetic bone substitute in combination with a new natural cross-linked collagen membrane: Radiographic and histomorphometric study. *Clin. Oral Implants Res.* **2015**, *26*, 154–164. [[CrossRef](#)] [[PubMed](#)]
22. Conz, M.B.; Granjeiro, J.M.; de Almeida Soares, G. Physicochemical characterization of six commercial hydroxyapatites for medical dental applications as bone graft. *J. Appl. Oral Sci.* **2005**, *13*, 136–140. [[CrossRef](#)] [[PubMed](#)]
23. Barakat, N.A.M.; Khalil, K.A.; Faheem, A.S.; Omran, A.M.; Gaihre, B.; Khil, S.M.; Kim, H.Y. Physicochemical characterizations of hydroxyapatite extracted from bovine bones by three different methods: Extraction of biologically desirable Hap. *Mater. Sci. Eng. Part C* **2008**, *28*, 1381–1387. [[CrossRef](#)]
24. Calvo-Guirado, J.L.; Mate-Sanchez de Val, J.E.; Delgado Ruiz, R.A.; Romanos, G.; De Aza, P.N.; Velasquez, P. Bone neo-formation and mineral degradation of 4Bone® ParII: Histological and histomorphometric analysis in critical size defects in rabbits. *Clin. Oral Implants Res.* **2015**, *26*, 1402–1406. [[CrossRef](#)] [[PubMed](#)]
25. Manfro, R.; Fonseca, F.S.; Bortoluzzi, M.C.; Sendyk, W.R. Comparative, Histological and Histomorphometric Analysis of Three Anorganic Bovine Xenogenous Bone Substitutes: Bio-Oss, Bone-Fill and Gen-Ox Anorganic. *J. Oral Maxillofac. Surg.* **2014**, *13*, 464–470. [[CrossRef](#)] [[PubMed](#)]
26. Hutmacher, D.W.; Schantz, J.T.; Lam, C.X.; Tan, K.C.; Lim, T.C. State of the art and future directions of scaffold-based bone engineering from a biomaterials perspective. *J. Tissue Eng. Regen. Med.* **2007**, *1*, 245–260. [[CrossRef](#)] [[PubMed](#)]
27. Carvalho, A.L.; Faria, P.E.; Grisi, M.F.; Souza, S.L.; Taba, M.J.; Palioto, D.B.; Novaes, A.B.; Fraga, A.F.; Ozyegin, L.S.; Oktar, F.N.; et al. Effects of granule size on the osteoconductivity of bovine and synthetic hydroxyapatite: A histologic and histometric study in dogs. *J. Oral Implantol.* **2007**, *33*, 267–276. [[CrossRef](#)]
28. Lee, J.S.; Shin, H.K.; Yun, J.H.; Cho, K.S. Randomized clinical trial of maxillary sinus grafting using deproteinized porcine and bovine bone mineral. *Clin. Implant Dent. Relat. Res.* **2016**. [[CrossRef](#)] [[PubMed](#)]
29. Schwartz, Z.; Weesner, T.; van Dijk, S.; Cochran, D.L.; Mellonig, J.T.; Lohmann, C.H.; Carnes, D.L.; Goldstein, M.; Dean, D.D.; Boyan, B.D. Ability of deproteinized cancellous bovine bone to induce new bone formation. *J. Periodontol.* **2000**, *71*, 1258–1269. [[CrossRef](#)] [[PubMed](#)]
30. Azran, Y.M.; Idris, B.; Rusnah, M.; Rohaida, C.H. Hap physical investigation the effect of sintering temperature. *Med. J. Malays.* **2004**, *59*, 79–80. [[PubMed](#)]
31. Kalkura, S.N.; Anee, T.K.; Ashok, M.; Betzel, C. Investigations on the synthesis and crystallization of hydroxyapatite at low temperature. *Bio.-Med. Mater. Eng.* **2004**, *1*, 581–592. [[PubMed](#)]
32. Herliansyah, M.K.; Hamdia, M.; de-Ektessabic, A.I.; Wildanb, M.W.; Toque, J.A. The influence of sintering temperature on the properties of compacted bovine. *Mater. Sci. Eng. C* **2009**, *29*, 1674–1680. [[CrossRef](#)]
33. Poinern, G.J.; Brundavanam, R.; Le, X.T.; Djordjevic, S.; Prokic, M.; Fawcett, D. Thermal and ultrasonic influence in the formation of nanometer scale hydroxyapatite bio-ceramic. *Int. J. Nanomed.* **2011**, *6*, 2083–2095. [[CrossRef](#)] [[PubMed](#)]
34. Maté Sánchez de Val, J.E.; Calvo-Guirado, J.L.; Gomez Moreno, G.; Gherke, S.; Mazón, P.; De Aza, P.N. Influence of hydroxyapatite granule size, porosity and crystallinity on tissue reaction in vivo. Part B: A comparative study with biphasic synthetic biomaterials. *Clin. Oral Implants Res.* **2017**. [[CrossRef](#)]
35. Muralithran, G.; Ramesh, S. The effects of sintering temperature on the properties of hydroxyapatite. *Ceram. Int.* **2000**, *26*, 221–230. [[CrossRef](#)]

36. Ashok, M.; Sundaram, N.M.; Kalkura, S.N. Crystallization of hydroxyapatite at physiological temperature. *Mater. Lett.* **2003**, *57*, 2066–2070. [[CrossRef](#)]
37. Hong, J.Y.; Kim, Y.J.; Lee, H.W.; Lee, W.K.; Ko, J.S.; Kim, H.M. Osteoblastic cell response to thin film of poorly crystalline calcium phosphate apatite formed at low temperatures. *Biomaterials* **2003**, *24*, 2977–2984. [[CrossRef](#)]
38. Accorsi-Mendonça, T.; Conz, M.B.; Barros, T.C.; de Sena, L.A.; de Almeida Soares, G.; Granjeiro, J.M. Physicochemical characterization of two deproteinized bovine xenografts. *Braz. Oral Res.* **2008**, *22*, 5–10. [[CrossRef](#)] [[PubMed](#)]
39. Rabadan-Ros, R.; Velasquez, P.; Meseguer-Olmo, L.; de Aza, P.N. Morphological and structural study of a novel porous Nurse's A ceramic with osteoconductive properties for tissue engineering. *Materials* **2016**, *9*, 474. [[CrossRef](#)]
40. Rosa, A.L.; Beloti, M.M.; Oliveira, P.T.; Van Noort, R. Osseointegration and osseointegrativity of hydroxyapatite of different microporosities. *J. Mater. Sci. Mater. Med.* **2002**, *13*, 1071–1075. [[CrossRef](#)] [[PubMed](#)]
41. Ros-Tarraga, P.; Mazón, P.; Rodriguez, M.A.; Meseguer-Olmo, L.; de Aza, P.N. Novel resorbable and osteoconductive calcium silicophosphate scaffold induced bone formation. *Materials* **2016**, *9*, 785. [[CrossRef](#)]
42. De Aza, P.N.; Peña, J.I.; Luklinska, Z.B.; Meseguer-Olmo, L. Bioeutectic[®] Ceramics for biomedical applications obtained by laser floating method. *In vivo evaluation. Materials* **2014**, *7*, 2395–2410. [[CrossRef](#)]
43. Mate-Sanchez de Val, J.E.; Mazon, P.; Calvo-Guirado, J.L.; Delgado-Ruiz, R.A.; Ramirez-Fernandez, M.P.; Negri, B.; Abboud, M.; de Aza, P.N. Comparison of three novel β -tricalcium phosphate/collagen ceramic scaffolds: An in vivo study. *J. Biomed. Mater. Res. A* **2014**, *102*, 1037–1046. [[CrossRef](#)] [[PubMed](#)]
44. Antonakos, A.; Liarakapis, E.; Leventouri, T. Micro-Raman and FTIR studies of synthetic and natural apatites. *Biomaterials* **2007**, *28*, 3043–3054. [[CrossRef](#)] [[PubMed](#)]
45. Ren, F.; Ding, Y.; Leng, Y. Infrared spectroscopic characterization of carbonated apatite: A combined experimental and computational study. *J. Biomed. Mater. Res. Part A* **2014**, *102*, 496–505. [[CrossRef](#)] [[PubMed](#)]
46. Ślósarczyk, A.; Paluszkiwicz, C.; Gawlicki, M.; Paszkiewicz, Z. The FTIR spectroscopy and QXRD studies of calcium phosphate based materials produced from the powder precursors with different Ca/P ratios. *Ceram. Int.* **1997**, *23*, 297–304. [[CrossRef](#)]
47. Lindgren, C.; Hallman, M.; Sennerby, L.; Sammons, R. Back-scattered electron imaging and elemental analysis of retrieved bone tissue following sinus augmentation with deproteinized bovine bone or biphasic calcium phosphate. *Clin. Oral Implants Res.* **2010**, *21*, 924–930. [[CrossRef](#)] [[PubMed](#)]
48. Klein, M.O.; Kämmerer, P.W.; Götz, H.; Duschner, H.; Wagner, W. Long-term bony integration and resorption kinetics of a xenogeneic bone substitute after sinus floor augmentation: Histomorphometric analyses of human biopsy specimens. *Int. J. Periodontics Restorative Dent.* **2013**, *33*, 101–110. [[CrossRef](#)] [[PubMed](#)]
49. Munar, M.L.; Udoh, K.; Ishikawa, K.; Matsuya, S.; Nakagawa, M. Effects of sintering temperature over 1,300 degrees C on the physical and compositional properties of porous hydroxyapatite foam. *Dent. Mater. J.* **2006**, *25*, 51–58. [[CrossRef](#)] [[PubMed](#)]
50. Wierzchos, J.; Falcioni, T.; Kiciak, A.; Woliński, J.; Koczorowski, R.; Chomicki, P.; Porembaska, M.; Ascaso, C. Advances in the ultrastructural study of the implant-bone interface by backscattered electron imaging. *Micron* **2008**, *39*, 1363–1370. [[CrossRef](#)] [[PubMed](#)]
51. Slater, N.; Dasmah, A.; Sennerby, L.; Hallman, M.; Piattelli, A.; Sammons, R. Back-scattered electron imaging and elemental microanalysis of retrieved bone tissue following maxillary sinus floor augmentation with calcium sulphate. *Clin. Oral Implants Res.* **2008**, *19*, 814–822. [[CrossRef](#)] [[PubMed](#)]
52. Blokhuis, T.J.; Termaat, M.F.; den Boer, F.C.; Patka, P.; Bakker, F.C.; Haarman, H.J. Properties of calcium phosphate ceramics in relation to their in vivo behavior. *J. Trauma Acute Care Surg.* **2000**, *48*, 179–186. [[CrossRef](#)] [[PubMed](#)]
53. Hamada, H.; Ohshima, H.; Ito, A.; Higuchi, W.I.; Otsuka, M. Effect of geometrical structure on the biodegradation of a three-dimensionally perforated porous apatite/collagen composite bone cell scaffold. *Biol. Pharm. Bull.* **2010**, *33*, 1228–1232. [[CrossRef](#)] [[PubMed](#)]
54. Raynaud, S.; Champion, E.; Bernache-Assollant, D. Calcium phosphate apatites with variable Ca/P atomic ratio II. Calcination and sintering. *Biomaterials.* **2002**, *23*, 1073–1080. [[CrossRef](#)]

55. Danoux, C.; Pereira, D.; Döbelin, N.; Stähli, C.; Barralet, J.; van Blitterswijk, C.; Habibovic, P. The effects of crystal phase and particle morphology of calcium phosphates on proliferation and differentiation of human mesenchymal stromal cells. *Adv. Healthc. Mater.* **2016**, *5*, 1775–1785. [[CrossRef](#)] [[PubMed](#)]
56. Rammelt, S.; Schulze, E.; Witt, M.; Petsch, E.; Biewener, A.; Pompe, W.; Zwipp, H. Collagen type I increases bone remodelling around hydroxyapatite implants in the rat tibia. *Cells Tissues Org.* **2004**, *178*, 146–157. [[CrossRef](#)] [[PubMed](#)]
57. Nannmark, U.; Sennerby, L. The bone tissue responses to prehydrated and collagenated cortico-cancellous porcine bone grafts: A study in rabbit maxillary defects. *Clin. Implant Dent. Relat. Res.* **2008**, *10*, 264–270. [[CrossRef](#)] [[PubMed](#)]
58. Orsini, G.; Scarano, A.; Piattelli, M.; Piccirilli, M.; Caputi, S.; Piattelli, A. Histologic and ultrastructural analysis of regenerated bone in maxillary sinus augmentation using a porcine bone-derived biomaterial. *J. Periodontol.* **2006**, *77*, 1984–1990. [[CrossRef](#)] [[PubMed](#)]
59. Arcuri, C.; Cecchetti, F.; Germano, F.; Motta, A.; Santacroce, C. Clinical and histological study of a xenogenic bone substitute used as a filler in postextractive alveolus. *Miner. Stomatol.* **2005**, *54*, 351–362. [[PubMed](#)]
60. Annaz, B.; Hing, K.A.; Kayser, M.; Buckland, T.; Di Silvio, L. Porosity variation in hydroxyapatite and osteoblast morphology: A scanning electron microscopy study. *J. Microsc.* **2004**, *215*, 100–110. [[CrossRef](#)] [[PubMed](#)]
61. Cyster, L.A.; Grant, D.M.; Howdle, S.M.; Rose, F.R.; Irvine, D.J.; Freeman, D.; Scotchford, C.A.; Shakesheff, K.M. The influence of dispersant concentration on the pore morphology of hydroxyapatite ceramics for bone tissue engineering. *Biomaterials* **2005**, *26*, 697–702. [[CrossRef](#)] [[PubMed](#)]
62. Traini, T.; Valentini, P.; Lezzi, G.; Piattelli, A. A histologic and histomorphometric evaluation of anorganic bovine bone retrieved 9 years after a sinus augmentation procedure. *J. Periodontol.* **2007**, *78*, 955–961. [[CrossRef](#)] [[PubMed](#)]
63. Mordenfeld, A.; Hallman, M.; Albrektsson, T. Histological & histomorpho-metrical analyses of biopsies harvested 11 years after maxillary sinus augmentation with 80% Bio-Oss and 20% autogenous bone. *Clin. Oral Implants Res.* **2010**, *21*, 961–970. [[CrossRef](#)] [[PubMed](#)]
64. Galindo-Moreno, P.; Hernández-Cortés, P.; Mesa, F.; Carranza, N.; Juodzbaly, G.; Aguilar, M.; O'Valle, F. Slow resorption of anorganic bovine bone by osteoclasts in maxillary sinus augmentation. *Clin. Implant Dent. Relat. Res.* **2013**, *15*, 858–866. [[CrossRef](#)] [[PubMed](#)]
65. Orsini, G.; Traini, T.; Scarano, A.; Degidi, M.; Perrotti, V.; Piccirilli, M.; Piattelli, A. Maxillary sinus augmentation with Bio-Oss particles: A light, scanning, and transmission electron microscopy study in man. *J. Biomed. Mater. Res. Part B Appl. Biomater.* **2005**, *74*, 448–457. [[CrossRef](#)] [[PubMed](#)]
66. Cordaro, L.; Bosshardt, D.D.; Palatella, P.; Rao, W.; Serino, G.; Chiapasco, M. Maxillary sinus grafting with Bio-Oss® or Straumann® Bone Ceramic: Histomorphometric result from a randomized controlled multicenter clinical trial. *Clin. Oral Implants Res.* **2008**, *19*, 796–803. [[CrossRef](#)] [[PubMed](#)]
67. Traini, T.; Degidi, M.; Sammons, R.; Stanley, P.; Piattelli, A. Histologic and elemental microanalytical study of anorganic bovine bone substitution following sinus floor augmentation in humans. *J. Periodontol.* **2008**, *79*, 1232–1240. [[CrossRef](#)] [[PubMed](#)]
68. Briem, D.; Linhart, W.; Lehmann, W.; Meenen, N.M.; Rueger, J.M. Long-term outcomes after using porous hydroxyapatite ceramics (Endobon®) for surgical management of fractures of the head of the tibia. *Unfallchirurg* **2002**, *105*, 128–133. [[CrossRef](#)] [[PubMed](#)]
69. Taylor, J.C.; Cuff, S.E.; Leger, J.P.; Morra, A.; Anderson, G.I. In vitro osteoclast resorption of bone substitute biomaterials used for implant site augmentation: A pilot study. *Int. J. Oral Maxillofac. Implant.* **2002**, *17*, 321–330. [[PubMed](#)]
70. Moon, J.W.; Sohn, D.S.; Heo, J.U. Histomorphometric analysis of maxillary sinus augmentation with calcium phosphate nanocrystal-coated xenograft. *Implant. Dent.* **2015**, *24*, 333–337. [[CrossRef](#)] [[PubMed](#)]
71. Fienitz, T.; Moses, O.; Klemm, C.; Happe, A.; Ferrari, D.; Kreppel, M.; Ormianer, Z.; Gal, M.; Rothamel, D. Histological and radiological evaluation of sintered and non-sintered deproteinized bovine bone substitute materials in sinus augmentation procedures. A prospective, randomized-controlled, clinical multicenter study. *Clin. Oral Investig.* **2017**, *21*, 787–794. [[CrossRef](#)] [[PubMed](#)]
72. Bertazzo, S.; Zambuzzi, W.F.; Campos, D.D.; Ogeda, T.L.; Ferreira, C.V.; Bertran, C.A. Hydroxyapatite surface solubility and effect on cell adhesion. *Colloids Surf. B Biointerf.* **2010**, *78*, 177–184. [[CrossRef](#)] [[PubMed](#)]

73. Chou, Y.F.; Huang, W.; Dunn, L.C.; Miller, T.A.; Wu, B.M. The effect of biomimetic apatite structure on osteoblast viability, proliferation and gene expression. *Biomaterials* **2005**, *26*, 285–295. [[CrossRef](#)] [[PubMed](#)]
74. Berger, C.E.; Rathod, H.; Gillespie, J.I.; Horrocks, B.R.; Datta, H.K. Scanning electrochemical microscopy at the surface of bone-resorbing osteoclasts: Evidence for steady-state disposal and intracellular functional compartmentalization of calcium. *J. Bone Miner. Res.* **2001**, *16*, 2092–2102. [[CrossRef](#)] [[PubMed](#)]
75. Xu, H.; Shimizu, Y.; Asai, S.; Ooya, K. Grafting of deproteinized bone particles inhibits bone resorption after maxillary sinus floor elevation. *Clin. Oral Implants Res.* **2004**, *15*, 126–133. [[CrossRef](#)] [[PubMed](#)]
76. Detsch, R.; Boccaccini, A.R. The role of osteoclasts in bone tissue engineering. *J. Tissue Eng. Regen. Med.* **2015**, *9*, 1133–1149. [[CrossRef](#)] [[PubMed](#)]
77. Ramesh, S.L.; Jeffrey, C.K.L.; Tan, C.Y.; Wong, Y.H.; Ganesan, P.; Ramesh, S.; Kutty, M.G.; Chandran, H.; Devaraj, P. Sintering behaviour and properties of magnesium orthosilicate-hydroxyapatite ceramic. *Ceram. Int.* **2016**, *42*, 15756–15761. [[CrossRef](#)]
78. Schilling, A.F.; Linhart, W.; Filke, S.; Gebauer, M.; Schinke, T.; Rueger, J.M.; Amling, M. Resorbability of bone substitute biomaterials by human osteoclasts. *Biomaterials* **2004**, *25*, 3963–3972. [[CrossRef](#)] [[PubMed](#)]
79. Schaefer, S.; Detsch, R.; Uhl, F.; Deisinger, U.; Ziegler, G. How degradation of calcium phosphate bone substitute materials is influenced by phase composition and porosity. *Adv. Eng. Mater.* **2011**, *13*, 342–350. [[CrossRef](#)]
80. Monteiro, M.M.; Campos da Rocha, N.C.; Rossi, A.M.; de Almeida Soares, G. Dissolution properties of calcium phosphate granules with different compositions in simulated body fluid. *J. Biomed. Mater. Res. A* **2003**, *65*, 299–305. [[CrossRef](#)] [[PubMed](#)]
81. von Doernberg, M.C.; von Rechenberg, B.; Bohner, M.; Grünenfelder, S.; van Lenthe, G.H.; Müller, R.; Gasser, B.; Mathys, R.; Baroud, G.; Auer, J. In vivo behavior of calcium phosphate scaffolds with four different pore sizes. *Biomaterials*. **2006**, *27*, 5186–5198. [[CrossRef](#)] [[PubMed](#)]
82. Costa-Rodrigues, J.; Fernandes, A.; Lopes, M.A.; Fernandes, M.H. Hydroxyapatite surface roughness: Complex modulation of the osteoclastogenesis of human precursor cells. *Acta Biomater.* **2012**, *8*, 1137–1145. [[CrossRef](#)] [[PubMed](#)]
83. Rezwani, K.; Chen, Q.Z.; Blaker, J.J.; Boccaccini, A.R. Biodegradable and bioactive porous polymer/inorganic composite scaffolds for bone tissue engineering. *Biomaterials* **2006**, *27*, 3413–3431. [[CrossRef](#)] [[PubMed](#)]
84. Tatum, H., Jr. Maxillary and sinus implant reconstructions. *Dent. Clin. N. Am.* **1986**, *30*, 207–229. [[PubMed](#)]
85. Shull, C.G. The determination of X-ray diffraction line widths. *Phys. Rev.* **1946**, *70*, 679–684. [[CrossRef](#)]
86. Wejrzanowski, T.; Pielaszek, R.; Opalińska, A.; Matysiak, H.; Łojkowski, W.; Kurzydłowski, K.J. Quantitative methods for nanopowders characterization. *Appl. Surf. Sci.* **2016**, *253*, 204–208. [[CrossRef](#)]





1 Article

2 **Implant stability of biological hydroxyapatites used** 3 **in dentistry.**

4 **Maria Piedad Ramírez Fernández**^{1,*}, **Sergio A.Gehrke**², **Patricia Mazón**³, **Jose L.Calvo-Guirado**¹,
5 **Piedad N. De Aza**⁴

6 ¹ Cátedra Internacional de Investigación en Odontología. Universidad Católica San Antonio de Murcia,
7 Avda. Jerónimos, 135, 30107 Guadalupe, Murcia Spain; jlcalvo@ucam.edu.

8 ² Biotecnos Research Center, Rua Dr. Bonazo nº 57 Santa Maria (RS), 97015-001, Brasil;
9 sergio.gehrke@hotmail.com

10 ³ Departamento de Materiales, Óptica y Tecnología Electrónica, Universidad Miguel Hernández, Avda.
11 Universidad s/n, Elche (Alicante) 03202, Spain; pmazon@umh.es

12 ⁴ Instituto de Bioingeniería. Universidad Miguel Hernandez, Avda. Ferrocarril s/n. 03202- Elche,
13 Alicante, Spain; piedad@umh.es

14 * Correspondence: mpramirez@ucam.edu; Tel.: +34 968278775/774

15 Academic Editor: name

16 Received: 9 May 2017; Accepted: 9 June 2017; Published: date

17 **Abstract:** The aim of the present study was to monitor implant stability after sinus floor elevation
18 with two biomaterials during the first 6 months of healing by a resonance frequency analysis
19 (RFA), and how physico-chemical properties affect the implant stability quotient (ISQ) at the
20 placement and healing sites. Bilateral maxillary sinus augmentation was performed in 10 patients
21 in a split-mouth design using a bobine HA (BBM) as a control and porcine HA (PBM). Six months
22 after sinus lifting, 60 implants were placed in the posterior maxilla. The ISQ was recorded on the
23 day of surgery from RFA at T1 (baseline), T2 (3 months), and T3 (6 months). Statistically significant
24 differences were found in the ISQ values during the evaluation period. The ISQ (baseline) was
25 63.8 ± 2.97 for BBM and 62.6 ± 2.11 for PBM. The ISQ (T2) was $\sim 73.5 \pm 4.21$ and 67 ± 4.99 , respectively.
26 The ISQ (T3) was $\sim 74.65 \pm 2.93$ and 72.9 ± 2.63 , respectively. All the used HAs provide
27 osseointegration and statistical increases in the ISQ at baseline, T2 and T3 (follow-up), respectively.
28 The BBM, sintered at high temperature with high crystallinity and low porosity, presented higher
29 stability, which demonstrates that variations in the physico-chemical properties of a bone
30 substitute material clearly influence implant stability.

31 **Keywords:** Hydroxyapatite, Xenografts; Implant design; Implant surface

32

33 **1. Introduction**

34 The edentulous ridge in the posterior maxilla often presents a limited bone volume due to both
35 lack of alveolar bone after ridge remodeling and maxillary sinus pneumatization [1]. Adequate
36 alveolar ridges play a crucial role when it comes to rehabilitation with implants, and some
37 augmentation technique is necessary for patients who suffer from alveolar atrophy [2]. The most
38 predictable and commonly used means of facilitating implant therapy in the atrophic posterior
39 maxilla has been sinus augmentation [3]. Although alternatives, e.g., using shorter implants, are
40 beginning to be investigated [4–6], any available scientific evidence is modest and insufficient to
41 conclude that the success of sinus lift procedures in bone with a residual height between 4 mm and 9
42 mm will be better, or not, than when short implants are used [7,8]. Maxillary sinus floor grafting has
43 become the commonest surgical intervention when increasing alveolar bone height before placing
44 endosseous dental implants in the posterior maxilla [9].

45 Several factors influence maxillary sinus floor grafting results : specific surgical techniques, a
46 simultaneous *versus* a delayed procedure, using barrier membranes over the lateral window,
47 implant surface characteristics, the length and width of implants, and selecting the graft material
48 [10].

49 As regards the last factor/variable, researchers have not reached an agreement about the most
50 suitable material for sinus augmentation [11]. In the clinical practice, the main purpose of bone
51 augmentation procedures is bone formation, where implants are positioned to best support
52 prosthetic rehabilitation. The bone tissue around dental implants must be mechanically competent
53 after augmentation procedures [12].

54 Today not many controlled research works evaluate the use of different bone grafting materials
55 for sinus augmentation. Sinus elevation, performed with a wide variety of different graft materials,
56 has been used. However, it still remains unclear which is the most suitable bone grafting material for
57 enhancing bone regeneration in the augmented sinus [13, 14]. Deproteinized xenografts, constituted
58 primarily of natural apatites, which are either sintered or not, have good physical and
59 physico-chemical properties. Deproteinization is an indispensable process followed to eliminate
60 antigenicity in xenograft bones. Different physicochemical conditions selectively modulate the host
61 organism's tissue response [15]. Some authors have reported the same observations in reaction to the
62 microscopic structure in commercial products subjected to thermal deproteinization processes [16,
63 17]. Sintering temperature is considered an important factor that might alter the HA's characteristics
64 [18]. However, the sintering temperature effect on the physico-chemical properties of natural HA
65 (HA of a natural source), especially HA from bovine bone, is still not fully understood and research
66 in this area is still wide open.

67 The ultra-structural interface of the graft bone tissue interface, as well as the ideal time point of
68 placing implants, have not yet been described [19].

69 Typical surgical protocols are simultaneous one-stage lateral or crestal antrostomy when the
70 residual crestal bone is greater than 3-6 mm, or a two-stage delayed procedure, which is
71 recommended when the residual bone is less than 3-6 mm. Furthermore, the risk of implant failure is
72 halved when the two-stage technique is used [20].

73 The graft consolidation gradient reflects the features of each bone substitute at sinus
74 augmentation sites [21]. According to some studies, the physico-chemical properties of each bone
75 material graft may influence the osseointegration process, and this influence may result in shorter
76 healing times between implant placement and restoration. Therefore, a profound understanding of
77 not only the different aspects of biomaterial properties, but also of their relation to and influence on
78 bone healing has proved to be of utmost importance [22].

79 An undisturbed healing period of at least 3 to 6 months at surgical sites is the generally
80 accepted protocol after implant placement. This can ensure uneventful healing and improve
81 osseointegration between the implant and bone. The reason for this approach is based on the fact
82 that the functional force around the bone-implant interface causes implant micromotion during
83 wound healing, while implant micromotion may induce fibrous tissue rather than bone contact,
84 which results in clinical failure. All these concerns about waiting periods **have** long since been a
85 challenge for both patients and clinicians. Changing trends and demands have rendered the
86 introduction of early loading techniques necessary as a result of searching for faster dental function
87 restoration using implants [23]. Successful osseointegration is a prerequisite for functional dental
88 implants; absence of osseointegration has been reported for implants with no primary stability [24].

89 Implant stability can be defined as the combination of both mechanical and biological stability.
90 While mechanical stability appears as the result of bone tissue compression during implantation,
91 biological stability is obtained as a result of the formation of new bone cells on the implant surface
92 during the osseointegration process. Hence implant stability is associated with the quality and
93 quantity of local bone [25]. Nowadays, the technique most frequently used to detect implant stability
94 during healing times and in subsequent follow-ups is the non invasive diagnostic tool known as
95 resonance frequency analysis (RFA) [26-27]. Continuous monitoring at various time points is
96 important to determine the implant stability status and to estimate a long-term prognosis for

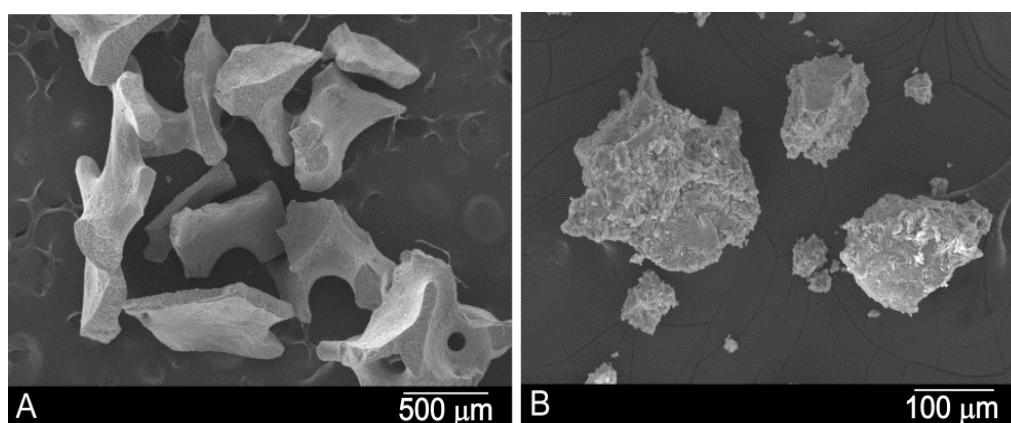
97 successful therapy [28]. Evaluating bone density has long since been one of the most important
98 parameters to quantify bone quality as it is thought to be a major determinant of primary stability. In
99 other words, primary implant stability is dependent on not only the thickness of the bone into which
100 the implant is placed, but also on bone density. Therefore, all these factors should be taken into
101 account when making the clinical decision to perform a one-stage or a two-stage procedure [29]. The
102 level of bone density at the implant site could be of utmost importance as it is related with failure
103 rates and primary stability. When it comes to evaluating primary implant stability in relation with
104 bone density, the implant stability quotient (ISQ) and the resonance frequency analysis can be used
105 [30]. The primary stability of a dental implant, absence of mobility at the osseous site after implant
106 insertion, and the quality of the receptor bone site are highly correlated. Likewise, primary stability
107 is also strictly correlated to the mechanical relationship between the implant surface and the
108 recipient bone. This relationship can determine implant placement outcomes by avoiding
109 micromovements on the interface [31].

110 Optimal outcomes in implant survival terms have been demonstrated for implants placed in the
111 maxillary sinus filled with deproteinized bovine bone mineral, and this material can be considered a
112 safe predictable graft material for sinus floor augmentation [32]. However, very little is known about
113 the physico-chemical properties of used grafts and the impact on both bone density and early
114 implant stability after they have been employed. The aim of this randomized split-mouth design was
115 to compare the stability of dental implants placed after sinus floor elevation with two HAs during
116 the first 6 months of healing by means of RFA, and to monitor how the physico-chemical properties
117 affect the implant stability quotient (ISQ) at the placement and healing sites.

118 2. Results

119 2.1. Graft Implants Characterization

120 Figure 1 shows the xenograft materials before inserting for maxillary sinus floor elevation.
121 The BBM (Bovine Bone Mineral) consists of HA particles of 500-1000 μm on average, with rounded
122 edges and pores of 100 μm on average. The PBM (Porcine Bone Mineral) consists of HA and
123 collagen particles of 600-1000 μm on average. A summary of the microstructural parameter studied
124 in a previous paper is shown in Table 1 to provide a better understanding of the materials'
125 microstructure [33].
126



127

128 **Figure 1.** Scanning electron micrographs of (A) the BBM and (B) PBM xenograft materials before
129 implantation.

130

131

132

133

Table 1. Physical properties of the two xenograft materials [33].

Phase/s	Ca/P ratio	Particle size (μm)	Crystal size (nm)	Real Density (g/cc)	Porosity (%)	Surface Area (m^2/g)
PBM	HA+Coll	2.22 \pm 0.08	600-1000	325	2.85	59.90
BBM	HA	2.31 \pm 0.09	500-1000	732	2.98	49.13

134

2.2 Radiological and Thermographic Results

135

136

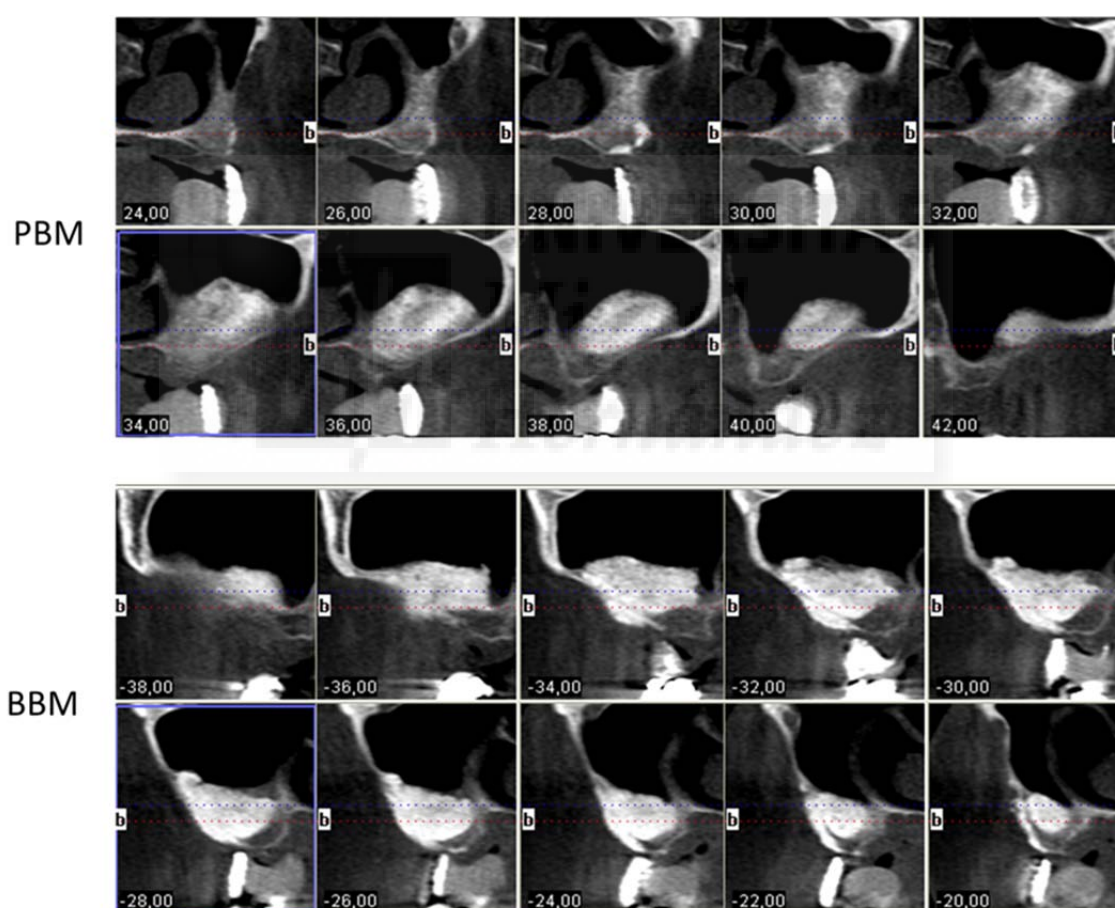
137

138

139

140

After a 6-month follow-up period of our ten partially edentulous patients treated with xenograft materials for sinus floor augmentation, the success rate was 100%. No sinus membrane perforation or other clinical complications, such as sinusitis or pain, resulted from surgery. The increased volumes produced by the xenograft procedures were stable by the end of the healing period, as seen in Figure 2. Deproteinized bone particles of two different temperatures induced osteoconduction 6 months after implantation.



141

142

143

144

Figure 2. The i-CAT Vision postoperative image shows the increased volumes produced by the xenograft procedures 6 months after maxillary sinus elevation with a porcine hydroxyapatite (axial cuts 24-42) and a bovine hydroxyapatite (axial cuts -38-20).

145

146

147

148

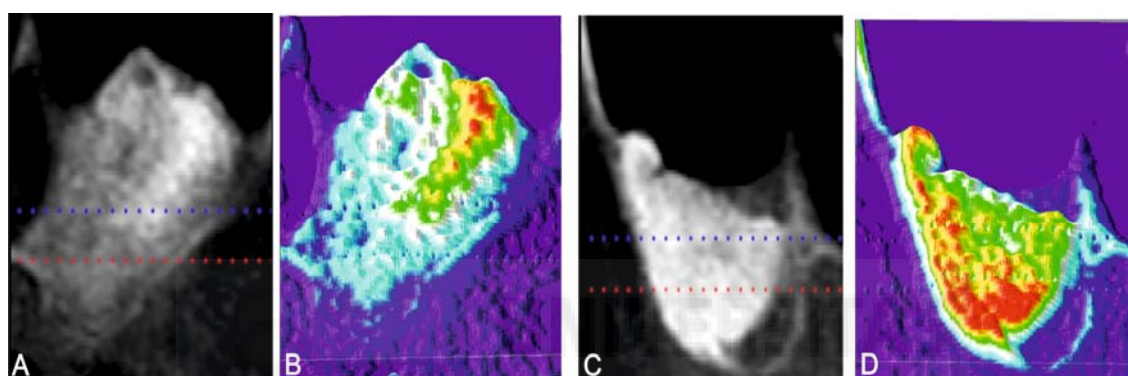
149

150

Bone density at the implant site could be crucial as it has been reported to correlates with failure rates and primary stability. The bone density in the grafted area with both biomaterials was evaluated radiologically as a routine diagnostic approach. Color thermal graduation was used to observe changes in radiopacity in the intrasinus bone grafted area. At the time of implant insertion, and after a 6-month healing period, the augmentation sites treated with the PBM showed denser new bone formation, which was achieved along the inner surface of the replaced bony window

151 than the area on the bone graft (Fig. 3 A-B). The BBM shows that denser new bone formation was
 152 achieved in the area on the bone graft compared to the original augmentation density (Fig. 3 C-D).
 153 The bone area differed in the groups after implantation and increased with time. Bone initially
 154 formed on the sinus wall and proliferated into the center of the augmented sinus cavity. Newly
 155 formed bone came consistently into close contact with particles, and no gaps were present on the
 156 bone particle interface. Particles appeared to act as a scaffold by supporting new bone formation.
 157 Scaffolding is a critical component in tissue engineering because it provides the three-dimensional
 158 clues for cell seeding, migration and growth, and also for new tissue formation.

159 Although the radiopacity of the augmented volume increased with time for both xenograft
 160 materials, the receiving control sites showed a higher density of radiopacity compared with the
 161 PBM. Maxillary sinus membrane preservation is important to avoid the displacement of graft
 162 materials into the sinus cavity. However, nonobserved small perforations can imply a risk if left
 163 untreated.



164

165 **Figure 3.** X-Ray of the implant site 6 months after xenograft materials implantation and the
 166 corresponding color bone density (A, B) the PBM material and (C, D) the BPM material.

167 2.3. ISQ Results

168 Primary implant stability in relation with bone density can also be evaluated by the implant
 169 stability quotient (ISQ). Detailed distributions for the implants and ISQ values over the investigated
 170 time periods are depicted in Table 2. Three implants were not osseointegrated at the end of the
 171 study, which left 57 implants for controls (a 95% success rate). Dropouts were not observed during
 172 the evaluation period.

173

Table 2. Demographic data.

Number of patients (total)	10					
Number of implants (total)	60					
<i>Osseointegrated (%)</i>	57 (95)					
<i>Non osseointegrated</i>	3 (5)					
Vestibule-Lingual (ISQ values)	T1		T2		T3	
	PBM	BBM	PBM	BBM	PBM	BBM
<i>Mean</i>	62.4	63.4	66.9	73.9	72.6	73.8
<i>SD</i>	2.92	2.88	2.67	4.11	7.67	2.99
<i>Median</i>	62.5	63.2	66.6	70.6	73.7	74
Mesio-Distal (ISQ values)	T1		T2		T3	
	PBM	BBM	PBM	BBM	PBM	BBM

Mean	62.8	64.2	67.1	75.2	74.2	74.2
SD	3.23	3.18	2.33	4.29	7.59	3.01
Median	62.5	64.8	69.1	72.4	75.8	75.5

174 ISQ: Implant stability quotient; T1: baseline; T2: at 3 months; T3: at 6 months.

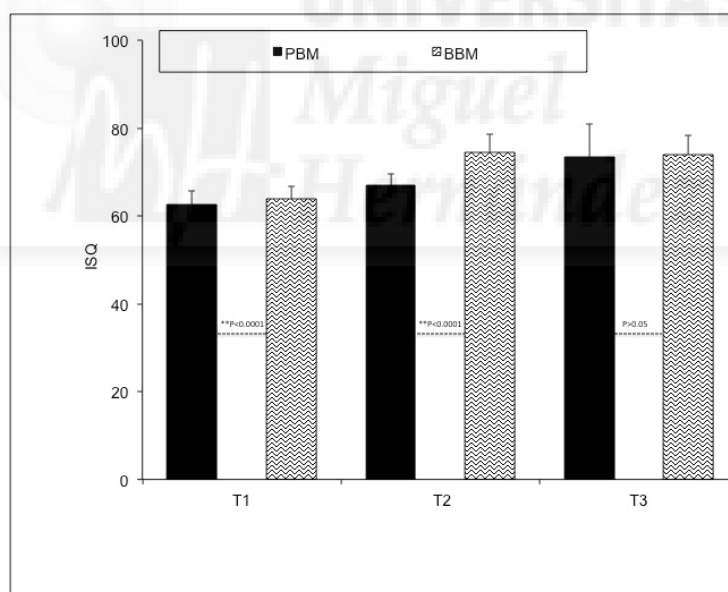
175 The means and standards deviation of the ISQ values.

176 The ISQ (Baseline) averaged values were 63.8 ± 2.97 for a sintered BBM and 62.6 ± 2.11 for a non
 177 sintered PBM, and differences were statistically significant. The ISQ (Stage 2) average values were
 178 73.5 ± 4.21 for the BBM and 67 ± 4.99 for the PBM, and differences were statistically significant. The
 179 ISQ (Stage 3) average values were 74.65 ± 2.93 for the BBM and 72.9 ± 2.63 for the PBM, and
 180 differences were statistically significant. The detailed distributions for the groups are depicted in
 181 Figure 4. The analysis of variance demonstrated a statistically significant difference ($p < 0.0001$).

182
 183 In the Vestibule-Lingual direction, the mean and standard deviation ISQ values measured at
 184 Baseline, Stage 2, and Stage 3 were 63.4 ± 2.88 , 73.9 ± 4.11 and 73.8 ± 2.99 , respectively for the BBM, and
 185 were respectively 62.4 ± 2.92 , 66.9 ± 2.67 and 72.6 ± 7.67 for the measured PBM ISQ values.

186 In the Mesio-Distal direction, the mean and standard deviation ISQ values measured at
 187 Baseline, Stage 2, and Stage 3 were 64.2 ± 3.18 , 75.2 ± 4.29 and 74.2 ± 3.01 , respectively for the BBM, and
 188 were respectively 62.8 ± 3.23 , 67.1 ± 2.33 and 74.2 ± 7.59 for the measured PBM ISQ values.

189 The multivariate regression analysis (R^2 adjusted = 0.58, multiple correlation coefficient = 0.78)
 190 demonstrated significant influences on the ISQ values in relation to age ($p = 0.0120$; $r = -0.13$), gender
 191 ($p < 0.0001$; $r = -0.48$), group ($p = 0.0017$; $r = 0.16$), position ($p = 0.0002$; $r = 0.19$) and time ($p < 0.0001$; $r = 0.69$).



192

193 **Figure 4.** Implant stability quotient for both xenograft materials

194 3. Discussion

195 This clinical study describes a comparison of the RFA of implants placed and delayed with
 196 maxillary sinus grafting with two biomaterials deproteinized at different temperatures during three
 197 distinct time periods. Sixty implants were fitted in 10 patients. Three implants were lost throughout
 198 the study time period, and the survival rate of dental implants in the present study was 95%. The
 199 results also showed a positive correlation between the used biomaterial and the ISQ values. The
 200 results of a systematic review of the survival of implants in bone grafts, Aghaloo and Moy, found
 201 that the survival of implants by the maxillary sinus grafting technique was 95.6% [2]. Presently, no
 202 agreement about the advantages of using grafting material in maxillary sinus elevation techniques
 203 with dental implant insertions has been reached because the question whether these techniques and

204 materials may determine implant survival, compared to pristine bone, remains unsolved [34, 35].
205 To find the answer to this question, long-term stability up to 20.2 years was retrospectively
206 examined after the placement of implants at both augmented and non augmented sites. The results
207 of this retrospective study determined that the implants inserted into an augmented site had a
208 similar implant survival to those inserted into non augmented sites [36]. Based on evidence, it can
209 be stated that the implants inserted into augmented bone offer a similar implant survival to those
210 placed in native bone [37]. In our study the implicated grafting material might not compromise
211 implant survival.

212 For clinicians, one of the most important parameters to measure the scope of mechanical
213 loading capability is implant stability. The baseline information that it provides serves as a tool to
214 evaluate clinical outcomes and time courses [28]. Several attempts have been made to find
215 innovative techniques that allow implant stability to be measured [27]. An RFA, which is a non
216 invasive technique that presents high reproducibility results, has been proposed [23, 38, 39]. This
217 technique has become one of the most widely used techniques to measure implant stability
218 immediately, which makes determining the probable loading protocol and assessing the long-term
219 survival of implants possible-[25]. The comparison of the type of bone graft and initial implant
220 stability was performed herein. The results of this study showed that the implants placed and
221 delayed (2-stage) with the maxillary sinus lift with different biomaterials presented distinct ISQs,
222 with statistically significant differences.

223 From a clinical point of view, it would appear relevant to know the significance of RFA
224 measurements and the relationship between their values and implant osseointegration success or
225 failure. A previous study has observed that implants retrieved after 6 months show a strict
226 correlation between the RFA values and the percentage of bone implant contact (BIC) [40]. The aim
227 of the present study was to determine whether the same correlation existed at earlier time points,
228 specifically in implants inserted after 3 or 6 months. A statistically significant correlation was
229 detected between the RFA values and healing time. During the bone-healing period, the implants'
230 ISQ value varied with time. In the surgical phase (baseline), the average ISQs for all the implants
231 were 63.8 ± 2.97 for a sintered BBM, and 62.6 ± 2.11 for a non sintered (PBM), with statistically
232 significant differences. The ISQ (Stage 2) average values were 73.5 ± 4.21 for the BBM and 67 ± 4.99 for
233 the PBM, where differences were statistically significant. The ISQ (Stage 3) average values were
234 74.65 ± 2.93 for the BBM and 72.9 ± 2.63 for the PBM, with statistically significant differences.

235 The present study examined the same implants 3 and 6 months after their installation for the
236 implants inserted by a two-step procedure. The RFA values after 3 months showed that the grafted
237 sites provided good implant stability and, on average, the BBM were better than the PBM group
238 sites. This difference was still present after 6 months and was also statistically significant. The
239 importance of bony quality in relation to implant stability has been previously highlighted. Given
240 the relative lack of bone, there is some concern about the initial stability of the implants placed in
241 grafted bone. An RFA enables the stability under load to be qualitatively measured, and has been
242 advocated as a means of assessing implant stability at the time of placement and in later phases
243 when providing restorations [41].

244 This is the first study to compare ISQs with density values after sinus lift procedures 6 months
245 after healing and primary stability. The primary initial stability (IS) is a crucial factor to establish
246 osseointegration [42-44], and might be subject to the influence of the following factors: bone quality,
247 surgery technique and implant macrodesign [44].

248 The above studies have demonstrated a strong correlation between implant displacement and
249 bone properties, and have concluded that better bone quality leads to better implant stability.
250 Al-Khalidi has also proven that implants with a high degree of density placed in bone have higher
251 initial stability values than those placed in soft bone [45], according to the results of insertion torque
252 (IT), ISQs and removal torque values (RTV) [46]. However, ISQs can improve through changes in
253 the implant macrodesign [47]. Moreover when using a different drilling protocol in soft bone,
254 Sennerby et al. confirmed that when comparing tapered implants with parallel implants, the former
255 showed a higher primary stability than the latter [48].

256 A previous study on the same pool of implants used in our study (tapered implants)
257 demonstrated that grafted bone can offer good primary stability to implants and that, during the
258 surgical procedure, only a few mechanical characteristics of implants (length and diameter) were
259 able to influence ISQ values [49]. Degidi et al have suggested that the length and width of implants
260 can influence primary stability because of the increased bone-implant contact surface area [50]. In
261 the present study, the macrodesign, and the length and diameter of the implant were not used as
262 evaluation factors as all the used implants were 4 mm in diameter and 11.5 mm in length, with
263 tapered internal hexagon implants, and are consistent with these studies, which report no
264 statistically significant differences in ISQ due to ISQ length or diameter [51, 52]. From the clinical
265 point of view, implants that have been placed in soft or grafted bone show better mechanical
266 stability values when they have a narrow diameter and a tapered macrodesign [53, 54]. In fact
267 nearly every implant company offers tapered-design implants for alveolar ridges with deficient
268 bone quality and quantity.

269 This should be taken into account for alveolar ridges with deficiencies in bone quality and
270 quantity, which is the reason why almost every company in the sector has introduced
271 tapered-design implants.

272 In our study we used a small particle size of two different deproteinized bone grafts. Jensen et
273 al evaluated the influence of the particle size of DBBM on bone formation and implant stability
274 when used for sinus floor elevation in a mini-pig model. In the initial healing phase, small particle
275 size DBBM showed marginally higher osteoconductive capacity than large particle size DBBM.
276 However, no differences were observed in the amount and speed of bone formation, BIC or implant
277 stability between the two test groups. However at the baseline and at 6 and 12 weeks, the BIC
278 values were comparable, or even higher, than in our study in humans. Primary implant stability is
279 dependent on not only the thickness of the bone into which the implant is placed, but also on bone
280 density, thread configuration and implant shape, and the presence of an implant neck. Therefore,
281 all these factors should be taken into account when making the clinical decision to perform a
282 one-stage or a two-stage procedure [55].

283 As evidenced in the review of Browaeys et al. on using biomaterials in sinus augmentation,
284 within the limitation of the animal studies examined, and based only on histological examinations,
285 the biomaterial used in grafting procedure does not influence the initial osseointegration of dental
286 implants [56].

287 The correlation between the RFA values and good bone quality reported herein seemed to
288 confirm the different importances of the factors that determine RFA values upon implant insertion
289 and if it is able to maintain this stability after 3 or 6 months. In fact good quality bone probably
290 reacts better to implant insertion, and implant stability after bone remodeling could be greater.

291 Long-term stability has also been reported by Hallman et al.. In their study 108 dental implants
292 were placed 6 months after sinus floor augmentation with a mixture of autogenous and
293 deproteinized bovine bone. After 3 years of loading, implant stability was recorded using an Osstell
294 instrument. The mean reported RFA values were 67.4 ± 14.5 for residual bone and 65.6 ± 13.8 for the
295 augmented sites. Unfortunately, no more data are currently available about the importance of bone
296 quality in determining long-term RFA values, so more studies have to be conducted [57].

297 Healing times of 6–9 months before implant placement are usually recommended for sinus
298 elevation in combination with grafting material [58], and an additional 3–6-month period of
299 implant healing time is needed. However, extended integration periods and multiple surgeries pose
300 a challenge for patient acceptance [59].

301 Our results also indicate that regardless of the substitute material, the implants inserted into a
302 grafted sinus can be predictably loaded as the implants inserted into a grafted area. Previous
303 studies have concluded that the prognosis of implants inserted into augmented sinuses and the
304 fixed restoration supported by these implants do not appear to be influenced by factors such as
305 graft material, restoration type, residual bone height and time of implant placement. Within the
306 limits of this review, the prognosis of implants and fixed restorations did not seem to be influenced
307 by the restoration type, graft material, residual bone height and time of implant placement.
308 However, the conclusions of this review are based on studies that provide a low level of evidence.
309 Therefore, careful interpretations are required. Multicenter randomized controlled clinical trials
310 with sufficient statistical power that concentrate on a few factors are needed to draw sound
311 conclusions [11].

312 The differences between the two HAs, in porosity, crystallinity, density, surface area and
313 composition terms, may determine different behaviors of this material, and might affect early
314 implant stability in this clinical situation. The HA of a bovine origin sintered with high crystallinity,
315 low porosity, high density and larger granule size presents better stability, which demonstrates that
316 variations in the physico-chemical properties of a bone substitute material clearly influence implant
317 stability. A profound knowledge of the graft material characteristics is of utmost importance when
318 assessing their clinical outcomes. The physico-chemical properties of bone substitute materials can
319 influence osseointegration and shorten healing times from implant placement to restoration.
320 Understanding not only biomaterial properties, but also their relation and influence on bone
321 healing, seems crucial.

322 4. Materials and Methods

323 4.1. Commercial xenograft materials

324 The commercial graft materials used in this study were two different types of bone
325 deprotenized hydroxyapatite materials of different origins employed in dentistry: deproteinized
326 porcine bone mineral hydroxyapatite (PBM), called OsteoBiol® (OsteoBiol, Tecness Dental SRL,
327 Torino, Italia); deproteinized bovine hydroxyapatite (BBM), called Endobon® (RegenerOss™,
328 BIOMET3i, Palm Beach, FL, USA). The physico-chemical and morphological characterizations of
329 both xenograft materials are found in a previous study [33].

330 4.2. Implant procedure

331 4.2.1. Patient selection and protocol

332 Ten partially edentulous patients (five females and five males), whose ages ranged from 37 to
333 60 years, attended the Department of Oral and Maxillofacial Surgery. Patients who demanded fixed
334 restorative appliances in the posterior maxilla were selected for maxillary sinus augmentation
335 because sufficient bone tissue was lacking to place endosseous dental implants. The protocol for
336 harvesting bone samples was approved by the University Ethics Committee and informed consent
337 was obtained from all the patients (UCAM-Ethics Committee, approval ID: 6637). The study was
338 designed following the Declaration of Helsinki guidelines for experimentation on human subjects.
339 Any possible complications that could arise from surgical therapy were treated following standard
340 dental management protocols.

341 4.2.2. Inclusion and exclusion criteria

342 Atrophy of the lateral-posterior maxilla and residual crestal bone height was classified
343 according to Cawood et al.'s subsumming classes I-VI. All the patients underwent CBCT before
344 surgery as a routine diagnostic approach to carefully evaluate the available bone at the intended
345 surgical site and for planning the grafting procedure.

346 The inclusion criteria were as follows: maxillary partial bilateral edentulism that involves
347 premolar-molar areas. The cases with a crestal bone height between 7 mm and 0 mm, and with high
348 postero-lateral atrophy (Cawood V-VI), are most likely to undergo a two-stage lateral antrostomy.

349 The exclusion criteria were: patients who suffer from an uncontrolled systemic disease or a
350 condition known to alter bone metabolism (i.e., osteoporosis, diabetes mellitus, etc.); subjects who
351 were taking/had taken medications known to modify bone metabolism; e.g., bisphosphonates,
352 corticosteroids, etc.; women who were pregnant or trying to get pregnant at the time of screening;
353 patients who presented existing sinus conditions, sepsis, a history of cancer and/or radiation to the
354 oral cavity; complications derived from any of these conditions that affect the sinus area.

355 4.2.3. Surgical procedure. First phase

356 The study was performed in two surgical phases. In the first phase all the patients took 875/125
357 mg of amoxicillin/ clavulanic acid every 8 h starting 1 day before surgery. A 300-mg dose of
358 Clindamycin every 8 h was prescribed to penicillin-allergic patients. This medication was
359 maintained for 7 days. All the surgical procedures were performed under local anesthesia
360 (Ultracain, Aventis Inc., Frankfurt, Germany). The basic surgical procedure was represented in all
361 the patients by maxillary sinus floor elevation via a lateral approach, as described by Boyne and
362 James (Fig. 5).



363

364 **Figure 5.** A lateral window is prepared and the schneiderian membrane is elevated.

365 After membrane elevation, a bioabsorbable collagen barrier membrane was placed under the
366 sinus membrane and adapted to come into contact with peripheral bony walls (Evolution Fine®
367 OsteoBiol®, TecnoSS Dental S.R.L., Torino, Italy). Sinuses were allocated to the non sintered HAS

368 (PBM) or to the sintered HAs (BBM) group via a standard randomization protocol
 369 (<http://www.randomization.com>). On one side, sinus cavities were grafted with the PBM
 370 (OsteoBiol® mp3, TecnoSS Dental S.R.L., Torino, Italy). After grafting, an absorbable collagen
 371 membrane (Evolution Fine® OsteoBiol®, TecnoSS Dental S.R.L., Torino, Italy) was placed over the
 372 window to minimize soft tissue invasion. On the other side, sinus cavities were grafted with the
 373 BBM (Endobon®, RegenerOss™, BIOMET3i, Palm Beach Gardens, FL, USA). The grafting
 374 materials were mixed with venous blood from the defect area and were carefully packed in the
 375 created volume following mucous membrane elevation. After bone grafting, a short-term
 376 absorbable collagen membrane (Evolution Fine® OsteoBiol®, TecnoSS Dental S.R.L., Torino, Italy)
 377 was placed over the window. Primary closure was achieved in both cases by suturing with 3-0 silk
 378 suture (Laboratory Aragón, Barcelona, Spain). Sutures were removed 2 weeks after surgery. During
 379 the postoperative period, patients were clinically and radiologically followed up at monthly
 380 intervals (Fig. 6).

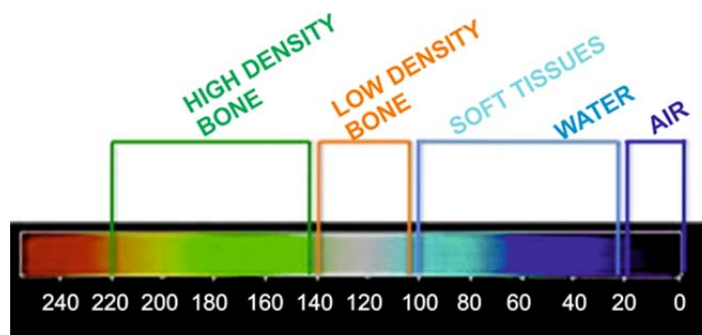


381

382 **Figure 6.** (A) A short-term absorbable collagen membrane. (B) Grafting materials mixed with
 383 venous blood.

384 4.2.4 Radiographic Thermal Imaging Analysis

385 During the post-operative period, patients were clinically and radiologically followed up at
 386 monthly intervals. All the patients underwent CBCT 6 months after surgery as a routine diagnostic
 387 approach using an I-CAT® (Imaging Sciences International, Hatfield, USA) Cone Beam 3D and were
 388 analyzed using the I-Cat vision software. The obtained images were processed by the Image J
 389 software, developed by the National Institute of Health (NIH) of the USA; a 3D plug-in with a
 390 thermal LUT and a grid size of 128x128, smoothing of 6.0, and a perspective of 0.2 on a 1:1 scale.
 391 Color thermal graduation was used to observe the changes in radiopacity in the grafted area
 392 (intrasinus bone graft). The scale was graduated with values from 0 to 240, where 0-20 were the
 393 values assigned to air, 20 to 100 were the values assigned to water and soft tissues, 100 to 140 were
 394 the values assigned to lower density bone, and 140 to 220 were the values assigned to higher
 395 density bone (Fig. 7).



396 **Figure 7.** Color-graduated density scale for thermal imaging interpretations.

397 4.2.5. Surgical procedure. Second phase. Implant Insertion

398 The second surgical phase was performed after the healing period. Functional implants were
 399 placed on each side. Each side received three implants (3i T3® Implante Certain® Cónico (BIOMET

3i ® Palm Beach Gardens, Florida) placed 6 months after augmentation. All the patients took 875 mg/125 mg units of amoxicillin/ clavulanic acid every 8 h starting 1 day before surgery. A dose of 300 mg of Clindamycin every 8 h was prescribed to penicillin-allergic patients. This medication was maintained for 7 days. All the surgical procedures were performed under local anesthesia (Ultracain, Aventis Inc., Frankfurt, Germany) in an outpatient setting by the same surgeon, who was familiar with the implant system. For the procedure, a full thickness mucoperiosteal flap was elevated on the sides. The osteotomy using a conical drill, with copious irrigation using saline solution, was done on the crest of the bone. Then osteotomies for fitting implants were produced using the initial drill to determine the depth and direction of the site. Afterward implants were positioned in the local, predetermined at the crestal bone level. Sixty conical implants with an internal hexagon connection were applied, which were all 11.5 mm long with a 4.0 mm diameter. Implants were selected according to the prior evaluation of each case. All the implants were fitted using surgical guides, and wounds were sutured in a tension-free state. Antibiotics and analgesics were given for 1 week. All the patients took 875/125 mg of amoxicillin/clavulanic acid every 8 h starting 1 day before surgery, and 300 mg of Clindamycin every 8 h were prescribed to penicillin-allergic patients. This medication was maintained for 7 days. Patients were asked to rinse with 0.12% chlorhexidine 3 times daily for 2 postoperative weeks. Sutures were removed 2 weeks after surgery. All the implants were prepared with a healing abutment until rehabilitation commenced.

4.3. Measuring implant stability

After dental implant insertion, the resonance frequency evaluation was made using the Ostell™ Mentor (Integration Diagnostics AB, Göteborg, Sweden) to measure the implant's primary stability. A Smartpeg™ (Integration Diagnostics AB, Göteborg, Sweden) was placed in each implant and was tightened to approximately 4-5 Ncm. The transducer probe was aimed at the small magnet at the top of the Smartpeg and at a distance of 2-3 mm, and was held stable during pulsing until the instrument beeped and displayed the ISQ value (Fig. 8). The RF value is represented by a quantitative parameter called ISQ. The ISQ range went from 1 to 100. An increased ISQ indicates increased stability, whereas low values indicate reduced implant stability. The ISQ values were measured during the surgical procedure (T1-baseline), at 3 months (T2) after surgery and at 6 months (T3) after surgery. Measurements were taken twice in the bucco-lingual direction and twice in the mesio-distal direction. The mean of the two measurements in each direction was regarded as the representative ISQ for that direction. The higher values were recorded for the bucco-lingual (B-L) direction and the mesio-distal (M-D) direction. The ISQ values were separately evaluated. Each implant was also evaluated during all visits for mobility, pain and signs of infection.



436

Figure 8: (A) Implant-bone contact rigidity was measured by RFA (Ostell™ Mentor, Integration Diagnostic AB, Sweden). RFA measurements were obtained before the healing cap was screwed into implant fixtures. (B) A Smartpeg (Smartpeg™, Integration Diagnostic AB, type 4 regular neck) was attached manually to the fixture with the help of a mount, and a torque of 4-5 Ncm was applied. (C) All the measurements were taken out by the same researcher. Measurements were taken at the time of implant placement and (baseline) at Stage 2 and at Stage 3. In all cases, an ISQ

442

443 was calculated as the average of four measurements per implant (twice in the bucco-lingual
444 direction and twice in the mesio-distal direction).

445 4.4 Statistical evaluation

446 All the data were recorded, reviewed and inputted into a computing system. Analyses were
447 performed using specific software (MedCalc, Belgium). The influence of age, gender (Male,
448 Female), group (BBM, PBM), ISQ measurement direction (BL, MD) and the evaluation time period,
449 (T1) baseline, (T2) 3 months, (T3) 6 months, on the ISQ values was evaluated by an analysis of
450 variance (ANOVA) and multiple regression at the 5% significance level (backward method) with
451 the help of appropriate software (MedCalc, v15.8. Belgium).

452 5. Conclusions

453 The differences between the two HAs found in porosity, crystallinity, density, surface area and
454 composition terms may determine the different behaviors of this material and might affect early
455 implant stability in this clinical situation. The HA of a bovine origin (BBM) sintered with high
456 crystallinity and low porosity presents better stability, which demonstrates that variations in the
457 physico-chemical properties of a bone substitute material clearly influence implant stability.
458 Detailed information about the graft material's characteristics is crucial to evaluate its clinical
459 outcomes. The influence of the physico-chemical properties of bone graft materials on
460 osseointegration has led to shorter healing times from implant placement to restoration. A sound
461 understanding of various aspects of biomaterial properties, and their relation to and influence on
462 bone healing, is of utmost importance.

463 **Acknowledgments:** Part of this work has been supported by the Spanish Ministry of Economy and
464 Competitiveness (MINECO); contract grant number: MAT2013-48426-C2-2-R.

465 **Author Contributions:** María Piedad Ramírez Fernández performed the implantation and the
466 post-implantation characterization; Sergio Alexander Gehrke performed the statistical analysis; Patricia
467 Mazón collaborated in the materials characterization; José Luis Calvo Guirado conceived the *in vivo*
468 experiments and helped in the implantation procedure; Piedad de Aza performed the materials
469 characterization. All the authors contributed to the analyses and the discussion of the results, and also
470 prepared the manuscript.

471 **Conflicts of Interest:** The authors declare no conflict of interest.

472 References

- 473 1. Sharan, A.; Madjar, D. Maxillary sinus pneumatization following extractions: a radiographic
474 study. *Int J Oral Maxillofac Implants*. **2008**, *23*, 48–56.
- 475 2. Aghaloo, T.L.; Moy, P.K. (2007) Which hard tissue augmentation techniques are the most
476 successful in furnishing bony support for implant placement? *Int J Oral Maxillofac Implants*.
477 **2007**, *22*, 49-70.
- 478 3. Corbella, S.; Taschieri, S.; Del Fabbro, M. Long-term outcomes for the treatment of atrophic
479 posterior maxilla: a systematic review of literature. *Clin Implant Dent Relat Res*. **2015**, *17*,
480 120-132. doi: 10.1111/cid.12077
- 481 4. Felice, P.; Soardi, E.; Pellegrino, G.; Pistilli, R.; Marchetti, C., Gessaroli, M., Esposito, M.
482 Treatment of the atrophic edentulous maxilla: short implants versus bone augmentation for
483 placing longer implants. Five-month post-loading results of a pilot randomised controlled trial.
484 *Eur J Oral Implantol*. **2011**, *4*, 191-202. doi: 10.1111/j.1600-0501.2010.01966.x.

- 485 5. Esposito, M.; Barausse, C.; Pistilli, R.; Sammartino, G.; Grandi, G.; Felice, P. Short implants
486 versus bone augmentation for placing longer implants in atrophic maxillae: One-year
487 post-loading results of a pilot randomised controlled trial. *Eur J Oral Implantol.* **2015**, *8*,
488 257-268.
- 489 6. Nedir, R.; Nurdin, N.; Abi-Najm, S.; El Hage, M.; Bischof, M. Short implants placed with or
490 without grafting into atrophic sinuses: the 5-year results of a prospective randomized
491 controlled study. *Clin Oral Implants Res.* **2016** Jun 13. doi: 10.1111/clr.12893. [Epub ahead of
492 print] DOI: 10.1111/clr.12893
- 493 7. Khouly, I.; Veitz-Keenan, A. Insufficient evidence for sinus lifts over short implants for
494 dental implant rehabilitation. *Evid Based Dent.* **2015**, *16*, 21-22. doi: 10.1038/sj.ebd.6401081.
- 495 8. Fan, T.; Li, Y.; Deng, W.W.; Wu, T.; Zhang, W. Short Implants (5 to 8 mm) Versus Longer
496 Implants (>8 mm) with Sinus Lifting in Atrophic Posterior Maxilla: A Meta-Analysis of RCTs.
497 *Clin Implant Dent Relat Res.* **2017**, *19*, 207-215. doi: 10.1111/cid.12432
- 498 9. Kolerman, R.; Samorodnitsky, G.R.; Barnea, E.; Tal, H. Histomorphometric analysis of newly
499 formed bone after bilateral maxillary sinus augmentation using two different osteoconductive
500 materials and internal collagen membrane. *Int J Periodontics Restorative Dent.* **2012**, *32*, 21-28.
- 501 10. Wallace, S.S.; Froum, S.J. Effect of maxillary sinus augmentation on the survival of endosseous
502 dental implants. A systematic review. *Ann. Periodontol.* **2003**, *8*, 328-43. doi:
503 10.1902/annals.2003.8.1.328
- 504 11. Tuna, T.; Yorgidis, M.; Strub, J.R. (2012) Prognosis of implants and fixed restorations after
505 lateral sinus elevation: a literature review. *J Oral Rehabil.* **2012**, *39*, 226-38. doi:
506 10.1111/j.1365-2842.2011.02259.x
- 507 12. Traini, T.; Piattelli, A.; Caputi, S.; Degidi, M.; Mangano, C.; Scarano, A.; Perrotti, V.; Iezzi, G.
508 Regeneration of Human Bone Using Different Bone Substitute Biomaterials. *Clin Implant Dent*
509 *Relat Res.* **2015**, *17*, 150-62. doi: 10.1111/cid.12089
- 510 13. Baqain, Z.H.; Moqbel, W.Y.; Sawair, F.A. Early dental implant failure: risk factors. *Br J Oral*
511 *Maxillofac Surg.* **2012**, *50*, 239-243. doi: 10.1016/j.bjoms.2011.04.074
- 512 14. Zinser, M.J.; Randelzhofer, P.; Kuiper, L.; Zöller, J.E.; De Lange, G.L. The predictors of implant
513 failure after maxillary sinus floor augmentation and reconstruction: a retrospective study of
514 1045 consecutive implants. *Oral Surg Oral Med Oral Pathol Oral Radiol.* **2013**, *115*, 571-582. doi:
515 10.1016/j.oooo.2012.06.015
- 516 15. Herliansyah, M.K.; Hamdia, M.; de-Ektessabic, A.I.; Wildanb, M.W., J.A. Toque, J.Á. The
517 influence of sintering temperature on the properties of compacted bovine. *Mater Sci Eng C Mater*
518 *Biol Appl.* **2009**, *29*, 1674-1680. <https://doi.org/10.1016/j.msec.2009.01.007>
- 519 16. Conz, M.B.; Granjeiro, J.M.; Soares, G.A. Physicochemical characterization of six commercial
520 hydroxyapatites for medical-dental applications as bone graft. *J Appl Oral Sci* **2005**, *13*, 136-140.
521 <http://dx.doi.org/10.1590/S1678-77572005000200008>.
- 522 17. Barakat, N.A.; Khalil, K.A.; Faheem, A. Sheikh; A.M. Omran; Babita Gaiher; Soeb M. Khild;
523 Hak Yong Kim Physicochemical characterizations of hydroxyapatite extracted from bovine
524 bones by three different methods: *Extraction of biologically desirable Hap. Mater. Sci. Eng. C*
525 *Mater. Biol. Appl.* **2008**, *28*, 1381-1387. DOI: 10.1016/j.msec.2008.03.003
- 526 18. Azran, Y.M.; Idris, B.; Rusnah, M.; Rohaida, C.H. HAP physical investigation the effect of
527 sintering temperature. *Med J Malaysia.* **2004**, *59*, 79-80.

- 528 19. Danesh-Sani, S.A.; Engebretson, S.P.; Janal, M.N. Histomorphometric results of different
529 grafting materials and effect of healing time on bone maturation after sinus floor
530 augmentation: a systematic review and meta-analysis. *J Periodontol Res.* **2016**. doi:
531 10.1111/jre.12402. [Epub ahead of print] doi: 10.1111/jre.12402
- 532 20. Felice, P.; Pistilli, R.; Piattelli, M.; Soardi, E.; Pellegrino, G.; Corvino, V.; Esposito, M. 1-stage
533 versus 2-stage lateral maxillary sinus lift procedures: 4-month post-loading results of a
534 multicenter randomised controlled trial. *Eur J Oral Implantol.* **2013**, *6*, 153-165. DOI:
535 10.1016/j.dental.2013.08.019
- 536 21. Busenlechner D, Huber CD, Vasak C, Dobsak A, Gruber R, Watzek G. Sinus augmentation
537 analysis revised: the gradient of graft consolidation. *Clin Oral Implants Res.* **2009**, *20*,
538 1078-1083. doi: 10.1111/j.1600-0501.2009.01733.x
- 539 22. Xu, H.; Shimizu, Y.; Asai, S.; Ooya, K. Experimental sinus grafting with the use of
540 deproteinized bone particles of different sizes. *Clin Oral Implant Res* **2003**, *14*, 548–555. DOI:
541 10.1034/j.1600-0501.2003.00933.x
- 542 23. Gupta, R.K.; Padmanabhan, T.V. An evaluation of the resonance frequency analysis device:
543 examiner reliability and repeatability of readings. *J Oral Implantol.* **2013**, *39*,704-707.
544 DOI:10.1563/AAID-JOI-D-11-00099
- 545 24. Lioubavina-Hack, N.; Lang, N.P.; Karring, T. Significance of primary stability for
546 osseointegration of dental implants. *Clin Oral Implants Res.* **2006**, *17*, 244-250. DOI:
547 10.1111/j.1600-0501.2005.01201.x
- 548 25. Sennerby, L.; Meredith, N. Implant stability measurements using resonance frequency
549 analysis: biological and biomechanical aspects and clinical implications. *Periodontol 2000.* **2008**,
550 *47*, 51-66. DOI:10.1111/j.1600-0757.2008.00267.x
- 551 26. Swami, V.; Vijayaraghavan, V.; Swami, V. Current trends to measure implant stability. *J Indian*
552 *Prosthodont Soc.* **2016**, *16*, 124-130. DOI: 10.4103/0972-4052.176539
- 553 27. Cehreli, M.C.; Karasoy, D.; Akca, K.; Eckert, S.E. Meta-analysis of methods used to assess
554 implant stability. *Int J Oral Maxillofac Implants* **2009**, *24*, 1015-1032.
- 555 28. Atsumi, M.; Park, S.H.; Wang, H.L. Methods used to assess implant stability: current status. *Int*
556 *J Oral Maxillofac Implants.* **2007**, *22*, 743-754. DOI: 10.4103/0972-4052.176539.
- 557 29. Lundgren, S.; Cricchio, G.; Hallman, M.; Jungner, M.; Rasmusson, L.; Sennerby L. Sinus floor
558 elevation procedures to enable implant placement and integration: techniques, biological
559 aspects and clinical outcomes. *Periodontol 2000.* **2017**, *73*, 103-120. doi: 10.1111/prd.12165
- 560 30. Iezzi, G.; Scarano, A.; Di Stefano, D.; Arosio, P.; Doi, K.; Ricci, L.; Piattelli, A.; Perrotti, V.
561 Correlation between the bone density recorded by a computerized implant motor and by a
562 histomorphometric analysis: a preliminary in vitro study on bovine ribs. *Clin Implant Dent*
563 *Relat Res.* **2015**, *17*, 35-44. doi: 10.1111/cid.12121
- 564 31. Marquezan, M.; Osório, A.; Sant'Anna, E.; Souza, M.M.; Maia, L. Does bone mineral density
565 influence the primary stability of dental implants? A systematic review. *Clin Oral Implants Res.*
566 **2012**, *23*, 767-774. doi: 10.1111/j.1600-0501.2011.02228.x
- 567 32. Ferreira, C.E.; Novaes, A.B.; Haraszthy, V.I.; Bittencourt, M.; Martinelli, C.B.; Luczyszyn, S.M.
568 A clinical study of 406 sinus augmentations with 100% anorganic bovine bone. *J Periodontol.*
569 **2009**, *80*, 1920-1927. doi: 10.1902/jop.2009.090263

- 570 33. Ramírez Fernández, M.P.; Gehrke, S.A.; Perrez Albacete Martinez, C.; Calvo Guirado, J.L., De
571 Aza, P.N. SEM-EDX Study of the degradation process of two xenograft materials used in sinus
572 lift procedures. *Materials* 2017; 10; 542 DOI: 10.3390/ma100050542.
- 573 34. Nasr, S.; Slot, D.E.; Bahaa, S.; Dörfer, C.E.; Fawzy El-Sayed, K.M. Dental implants combined
574 with sinus augmentation: What is the merit of bone grafting? A systematic review. *J*
575 *Craniofacial Surg.* **2016**, *44*, 1607-1617. doi: 10.1016/j.jcms.2016.06.022
- 576 35. Rammelsberg, P.; Schmitter, M.; Gabbert, O.; Lorenzo-Bermejo, J.; Eiffler, C.; Schwarz, S.
577 Influence of bone augmentation procedures on the short-term prognosis of simultaneously
578 placed implants. *Clin Oral Implants Res.* **2012**, *23*, 1232-1237. doi:
579 10.1111/j.1600-0501.2011.02295.x
- 580 36. Knöfler, W.; Barth, T.; Graul, R.; Krampe, D. Retrospective analysis of 10,000 implants from
581 insertion up to 20 years-analysis of implantations using augmentative procedures. *Int J Implant*
582 *Dent.* **2016**, *2*, 25. DOI: 10.1186/s40729-016-0061-3
- 583 37. Jensen, S.S.; Terheyden, H. Bone augmentation procedures in localized defects in the alveolar
584 ridge: clinical results with different bone grafts and bone-substitute materials. *Int J Oral*
585 *Maxillofac Implants.* **2009**, *24*, 218-236.
- 586 38. Herrero-Climent, M.; Albertini, M.; Rios-Santos, J.V.; Lázaro-Calvo, P.; Fernández-Palacín, A.;
587 Bullón, P. Resonance frequency analysis-reliability in third generation instruments: Osstell
588 mentor®. *Med Oral Patol Oral Cir Bucal.* **2012**, *17*, 801-806. doi:10.4317/medoral.17861
- 589 39. Herrero-Climent, M.; Santos-García, R.; Jaramillo-Santos, R.; Romero-Ruiz, M.M.;
590 Fernández-Palacín, A.; Lázaro-Calvo, P.; Bullón, P.; Ríos-Santos, J.V. Assessment of Osstell
591 ISQ's reliability for implant stability measurement: a cross-sectional clinical study. *Med Oral*
592 *Patol Oral Cir Bucal.* **2013**, *18*, 877-882. doi:10.4317/medoral.19120
- 593 40. Degidi, M.; Perrotti, V.; Piattelli, A.; Iezzi, G. Mineralized bone-implant contact and implant
594 stability quotient in 16 human implants retrieved after early healing periods: a histologic and
595 histomorphometric evaluation. *Int J Oral Maxillofac Implants.* **2010**, *25*, 45-48.
- 596 41. Al-Khalidi, N.; Sleeman, D.; Allen, F. Stability of dental implants in grafted bone in the anterior
597 maxilla: longitudinal study. *Br J Oral Maxillofac Surg.* **2011**, *49*, 319-323. doi:
598 10.1016/j.bjoms.2010.05.009
- 599 42. Friberg, B.; Ekstube, A.; Sennerby, L. Clinical outcome of Brånemark System implants of
600 various diameters: a retrospective study. *Int J Oral Maxillofac Implants.* **2002**, *17*, 671-677.
- 601 43. Esposito, M.; Grusovin, M.G.; Maghaireh, H.; Worthington HV. Interventions for replacing
602 missing teeth: different times for loading dental implants. *Cochrane Database Syst Rev.* **2013**, *28*,
603 3, CD003878. doi: 10.1002/14651858.CD003878.pub5.
- 604 44. Javed, F.; Romanos, G.E. Role of implant diameter on long-term survival of dental implants
605 placed in posterior maxilla: a systematic review. *Clin Oral Investig.* **2015**, *19*, 1-10. doi:
606 10.1007/s00784-014-1333-z
- 607 45. Schiuma, D.; Plecko, M.; Kloub, M.; Rothstock, S.; Windolf, M.; Gueorguiev, B. Influence of
608 peri-implant bone quality on implant stability. *Med Eng Phys.* **2013**, *35*, 82-87. doi:
609 10.1016/j.medengphy.2012.04.001
- 610 46. Anil, S.; Aldosari, A. Impact of bone quality and implant type on the primary stability: an
611 experimental study using bovine bone. *J Oral Implantol.* **2015**, *41*, 144-148. doi:
612 10.1563/AAID-JOI-D-11-00156

- 613 47. Romanos, G.E.; Delgado-Ruiz, R.A.; Sacks, D.; Calvo-Guirado, J.L. Influence of the implant
614 diameter and bone quality on the primary stability of porous tantalum trabecular metal dental
615 implants: an in vitro biomechanical study. *Clin Oral Implants Res.* **2016**, 1–7 doi:
616 10.1111/clr.12792
- 617 48. Sennerby, L.; Pagliani, L.; Petersson, A.; Verrocchi, D.; Volpe, S.; Andersson, P. Two different
618 implant designs and impact of related drilling protocols on primary stability in different bone
619 densities: an in vitro comparison study. *Int J Oral Maxillofac Implants.* **2015**, 30, 564–568. doi:
620 10.11607/jomi.3903.
- 621 49. Gehrke, S.A.; da Silva, U.T.; Del Fabbro, M. Does Implant Design Affect Implant Primary
622 Stability? A Resonance Frequency Analysis-Based Randomized Split-Mouth Clinical Trial. *J*
623 *Oral Implantol.* **2015**, 41, 281–286. doi: 10.1563/aaid-joi-D-13-00294
- 624 50. Degidi, M.; Piattelli, A.; Iezzi, G.; Carinci, F. Do longer implants improve clinical outcome in
625 immediate loading? *Int J Oral Maxillofac Surg.* **2007**, 36, 1172–1176.
626 DOI:10.1016/j.ijom.2007.05.014
- 627 51. Balleri, P.; Cozzolino, A.; Ghelli, L.; Momicchioli, G.; Varriale, A. Stability measurements of
628 osseointegrated implants using Osstell in partially edentulous jaws after 1 year of loading: a
629 pilot study. *Clin Implant Dent Relat Res.* **2002**, 4, 128–132. DOI:
630 10.1111/j.1708-8208.2002.tb00162.x
- 631 52. Ostman, P.O.; Hellman, M.; Wendelhag, I.; Sennerby, L. Resonance frequency analysis
632 measurements of implants at placement surgery. *Int J Prosthodont.* **2006**, 19, 77–83.
- 633 53. O'Sullivan, D.; Sennerby, L.; Meredith, N. Measurements comparing the initial stability of five
634 designs of dental implants: a human cadaver study. *Clin Implant Dent Relat Res.* **2000**, 2, 85–92.
635 DOI: 10.1111/j.1708-8208.2000.tb00110.x
- 636 54. Romanos, G.E.; Ciornei, G.; Jucan, A.; Malmstrom, H.; Gupta, B. In vitro assessment of primary
637 stability of Straumann® implant designs. *Clin Implant Dent Relat Res.* **2014**, 16, 89–95. doi:
638 10.1111/j.1708-8208.2012.00464.x
- 639 55. Jensen, S.S.; Aaboe, M.; Janner, S.F.; Saulacic, N.; Bornstein, M.M.; Bosshardt, D.D.; Buser, D.
640 Influence of particle size of deproteinized bovine bone mineral on new bone formation and
641 implant stability after simultaneous sinus floor elevation: a histomorphometric study in
642 minipigs. *Clin Implant Dent Relat Res.* **2015**, 17, 274–85. doi: 10.1111/cid.12101
- 643 56. Browaeys, H.; Bouvry, P.; De Bruyn, H. A literature review on biomaterials in sinus
644 augmentation procedures. *Clin Implant Dent Relat Res.* **2007**, 9, 166–177. doi:
645 10.1111/j.1708-8208.2007.00050.x
- 646 57. Degidi, M.; Daprile, G.; Piattelli, A. RFA values of implants placed in sinus grafted and
647 nongrafted sites after 6 and 12 months. *Clin Implant Dent Relat Res.* **2009**, 11, 178–182. doi:
648 10.1111/j.1708-8208.2008.00113.x.
- 649 58. Jensen, O.T.; Sennerby, L. Histologic analysis of clinically retrieved titanium microimplants
650 placed in conjunction with maxillary sinus floor augmentation. *Int J Oral Maxillofac Implants.*
651 **1998**, 13, 513–521.
- 652 59. Lai, H.C.; Zhang, Z.Y.; Wang, F.; Zhuang, L.F.; Liu, X. Resonance frequency analysis of stability
653 on ITI implants with osteotome sinus floor elevation technique without grafting: a 5-month
654 prospective study. *Clin Oral Implants Res.* **2008**, 19, 469–475. doi:
655 10.1111/j.1600-0501.2007.01501.x.

656

© 2017 by the authors. Submitted for possible open access publication under the terms and conditions of the



Creative Commons Attribution (CC BY) license
(<http://creativecommons.org/licenses/by/4.0/>).





